INVESTIGATION OF NOVEL RECESSIVE CAUSATIVE GENES AND GENE/ALLELE FREQUENCY FOR CMT DISEASE IN TURKEY

by

Ayşe Candayan

B.S., Molecular Biology and Genetics, Boğaziçi University, 2013

Submitted to the Institute for Graduate Studies in
Science and Engineering in partial fulfillment of
the requirements for the degree of
Doctor of Philosophy

Graduate Program in Molecular Biology and Genetics
Boğaziçi University
2021

ACKNOWLEDGEMENTS

The PhD journey is a great one, although it could be troubling at times. I am glad that I did not have to go through it all by myself. I was lucky enough to have a wonderful mentor: Prof. Esra Battaloğlu. I could not express enough how thankful I am for the invaluable support, both academic and personal, she has provided me, I will be grateful for a lifetime.

I would also like to thank my thesis progress committee members, Prof. Müge Türet and Prof. Yeşim Parman, for their constructive feedback throughout my studies. I am also thankful to additional committee members, Prof. Z. Oya Uyguner and Dr. Ş. Anıl Doğan, for taking their time to evaluate this thesis.

I am grateful to Prof. Albena Jordanova for providing me the opportunity and the tools to conduct part of this study at her laboratory. Members of her research team, Dr. Derek Atkinson, Dr. Paulius Palaima and Els de Vriendt have become dear friends to me, and I am thankful for their constant support.

I am thankful to all the families participating in this study and the clinicians who have provided us with the clinical data and tissue samples. I would also like to thank TUBITAK, Boğaziçi University BAP and Turkish Neurological Society for their financial support for this study. I am also sincerely grateful to Darüşşafaka Society and all its benefactors, not only for their financial support during my undergraduate and graduate years, but mainly because they made me part of this beautiful family and molded me into the person I am today.

I also truly loved being part of the MBG community at Boğaziçi University. I feel very lucky to have known Dr. Stefan Fuss for he told me that I have "scientist material" and boosted my confidence along the way even though he has a peculiar way of doing so. I am grateful to Ümit Bayraktar, Aslı Gündoğdu, and Cenan Özbakır.

They solved all my problems throughout these years without complaining even once. I have learned so much from Dr. Burçak Özeş and Dr. Aslı Uğurlu and I cannot thank them enough for their candid friendship and mentoring. I also made great friends along the way, some of them I found really early on, but some I found at the last minute and I wish I could spend more time with each one of them: Nazmiye Özkan, Seden Tezel, Dr. Mahmut Can Hız, Dr. Burak Bali, Dr. Ece Terzioğlu Kara, Zeynep Dokuzluoğlu, Ezgi Şenoğlu, Tayfun Hazar Eyyuboğlu, Ecenaz Kıvanç, Aysu Alkiraz, Yiğit Kocagöz, Barış Can Mandacı, Sinay Mollamustafaoğlu, and Şiran Şireci.

I would like to share my gratitude for my lifelong friends, Simge Başmak, Sıla Ön, Ahmet Karakaş, Mehmet Bayrak, Güneş Kahraman and Dr. Lotte Keulen for they have carried all the weight I had put on them without a flinch during all these years. I am in so many ways thankful to Dr. Olga Nehir Öztel, she cheered for me at times I did not even know I needed and that kept me going.

I would like to express my greatest appreciation for my brother, Mesut Koca, for he has been my rock since I was a silent little kid. He put in my head the idea of having a "Dr." title in front of my name, although he had something else in mind. Still, everything I accomplish is for -and because of- him.

Last, but not least, my warmest feelings go to my dear fiancé, Harun Niron. His loving, caring, supportive attitude changed the way I see the world, he constantly reminded me that I matter, he comforted me during the toughest of times and he always encouraged me to seek what is best for my peace of mind. I am looking forward to turning life into an adventure with you.

ABSTRACT

INVESTIGATION OF NOVEL RECESSIVE CAUSATIVE GENES AND GENE/ALLELE FREQUENCY FOR CMT DISEASE IN TURKEY

Inherited peripheral neuropathies are a group of genetic disorders of the peripheral nervous system. The most common type is called Charcot-Marie-Tooth (CMT) disease that constitutes an interesting research focus due to its clinical and genetic heterogeneity. Mutations in more than 90 genes and loci are associated with CMT that presents with autosomal dominant (AD), autosomal recessive (AR), X-linked, or mitochondrial inheritance. Despite the advances in genetic testing, approximately 35% of all CMT cases worldwide remain without a molecular diagnosis. The diagnostic rate is even lower for ARCMT due to the presence of many individually rare genes. This diagnostic gap points to the presence of yet unidentified causative genes, as well as potential non-Mendelian features of the disease. In order to identify novel genes/alleles causing ARCMT and determine the frequency for known genes in Turkey, we have analyzed 56 consanguineous families diagnosed with CMT who present with early onset polyneuropathy with additional symptoms. Through the screening of patients for *GDAP1* mutations, and subsequent whole-exome sequencing and homozygosity mapping, we have identified 22 recurrent and 13 novel alleles in known CMT genes achieving a potential diagnosis rate of 62,5%. Moreover, we identified *FXN* as a candidate gene for a novel disease in the spectrum between CMT and Friedreich's ataxia, *ATP8B3* for ARCMT2, and *SEPT11* for AR-cerebellar ataxia with axonal neuropathy. This study paints the genetic landscape of the Turkish ARCMT population, reports candidate genes that might enlighten new disease mechanisms, and can serve as a reference for diagnosis strategies specific to populations with similar genetic backgrounds.

ÖZET

ÇEKİNİK CMT HASTALIĞI İÇİN YENİ GENLERİN ARAŞTIRILMASI VE TÜRKİYE'DE CMT YAPICI GEN/ALEL SIKLIĞI İNCELEMESİ

Kalıtsal periferik nöropatiler, periferik sinir sistemini etkileyen genetik bir hastalıklar grubudur. En yaygın türü, klinik ve genetik çeşitliliği sebebiyle ilginç bir araştırma odağı oluşturan Charcot-Marie-Tooth (CMT) hastalığıdır. CMT ile ilişkilendirilmiş 90'dan fazla gen ve gen bölgesi otozomal baskın, otozomal çekinik, X'e bağlı ve mitokondriyal olarak kalıtılabilmektedir. Genetik tarama testlerinin gelişmişliğine rağmen, dünya çapında tüm CMT hastalarının yaklaşık %35'i moleküler tanı alamamaktadır. Otozomal çekinik CMT'de (OÇCMT) genetik tanı başarısı, çok sayıda nadir genin varlığı nedeniyle daha da düşüktür. Bu tanısal boşluk, henüz tanımlanmamış hastalık yapıcı genlerin varlığına ve Mendel-dışı kalıtım olasılığına işaret etmektedir. OÇCMT'ye sebep olan yeni gen/aleller tanımlamak ve bilinen hastalık yapıcı genlerin ülkemizdeki sıklığını belirlemek amacıyla, ebeveynleri akraba evliliği yapmış, erken başlangıçlı polinöropati ile ek klinik bulguları bulunan 56 CMT hastasını genetik açıdan analiz ettik. Tüm hastalarda *GDAP1* geni taramasını takiben, tüm ekzom dizileme ve homozigotluk haritalaması yöntemlerini kullanarak 22 tekrarlayan, 13 yeni allel belirledik ve %62,5 oranında potansiyel genetik tanı oranı yakaladık. Ek olarak, *FXN* genini CMT ve Friedreich ataksi arasındaki spektrumda yer alan yeni bir hastalık, *ATP8B3* genini OÇCMT2 ve *SEPT11* genini aksonal polinöropatiyle seyreden serebellar ataksi için hastalık yapıcı aday genler olarak belirledik. Bu çalışma, Türkiye OÇCMT popülasyonunun genetik çerçevesini çizmekte ve yeni hastalık mekanizmalarını aydınlatmaya yardımcı olabilecek genler rapor etmektedir. Ayrıca, benzer genetik arka plana sahip toplumlara özgü genetik tanı stratejileri için bir referans ortaya koymuştur.

TABLE OF CONTENTS

LIST OF FIGURES

LIST OF TABLES

LIST OF SYMBOLS

A	Adenine
C	Cytosine
G	Guanine
T	Thymine
v	Volume
w	Weight
X	Stop codon
α	Alpha/Anti
μg	Microgram
μl	Microliter

LIST OF ACRONYMS/ABBREVIATIONS

Aa/aa	Amino acid
AARS	Alanyl-tRNA synthetase
AD	Autosomal dominant
$AgNO_3$	Silver nitrate
Ala	Alanine
ALS	Amyotrophic lateral sclerosis
AMEM	Minimum essential medium, alpha modification
APS	Ammonium persulfate
AR	Autosomal recessive
ARCMT	Autosomal recessive Charcot-Marie-Tooth disease
Arg	Arginine
ARSACS	Autosomal recessive spastic ataxia of Charlevoix-Saguenay
Asn	Asparagine
Asp	Aspartic acid
ATP	Adenosine triphosphate
BSA	Bovine serum albumin
$CaCl_2$	Calcium chloride
cDNA	Complementary DNA
CMT	Charcot-Marie-Tooth disease
CNS	Central nervous system
CO_2	Carbon dioxide
Cq	Quantitation cycle
Cys	Cysteine
DAPI	4′,6-diamidino-2-phenylindole
del	Deletion
dHMN	Distal hereditary motor neuropathy
DI	Dominant intermediate
DMEM	Dulbecco's modified Eagle medium

DMM	Delayed motor milestones
DMSO	Dimethyl sulfoxide
DNA	Deoxyribonucleic acid
dNTP	Deoxyribonucleotide triphosphate
EDTA	Ethylenediaminetetraacetic acid
EMG	Electromyography
EtBr	Ethidium bromide
FBS	Fetal bovine serum
fs	Frameshift
Gln	Glutamine
Glu	Glutamic acid
Gly	Glycine
HCl	Hydrochloric acid
HEPES	4-(2-hydroxyethyl)-1-piperazineethanesulfonic acid
Het	Heterozygous
His	Histidine
HMSN	Hereditary motor and sensory neuropathy
HNPP	Hereditary neuropathy with liability to pressure palsy
Hom	Homozygous
HSP	Hereditary spastic paraplegia
IE	Inexcitable
Ile	Isoleucine
IPN	Inherited peripheral neuropathy
KCl	Potassium chloride
kDa	kilodalton
LB	Luria broth
Leu	Leucine
Lys	Lysine
Mb	Megabase
Met	Methionine
mg	Milligram

$MgCl_2$	Magnesium chloride
ml	Milliliter
mM	Millimolar
mRNA	Messenger RNA
NaCl	Sodium chloride
NaOH	Sodium hydroxide
NCV	Nerve conduction velocity
ng	Nanogram
NGS	Next-generation sequencing
nm	Nanometer
PBS	Phosphate buffered saline
PCR	Polymerase chain reaction
PFA	Paraformaldehyde
Phe	Phenylalanine
PNS	Peripheral nervous system
Pro	Proline
PVDF	Polyvinylidene fluoride
RMSD	Root mean square deviation
RNA	Ribonucleic acid
rpm	Rotations per minute
SDS	Sodium dodecyl sulfate
Ser	Serine
TBS	Tris buffered saline
TE	Tris-EDTA
TEMED	Tetramethylethylenediamine
Thr	Threonine
tRNA	Transfer RNA
Trp	Tryptophan
Tyr	Tyrosine
Val	Valine

1. INTRODUCTION

1.1. Inherited Peripheral Neuropathies

Inherited peripheral neuropathies (IPNs) are a diverse group of disorders of the peripheral nervous system (PNS) that can be broadly classified into two groups. The first group consists of disorders in which neuropathy is the only or the most predominant clinical feature, such as Charcot-Marie-Tooth disease and related neuropathies including hereditary neuropathy with liability to pressure palsies, hereditary sensory neuropathy, hereditary motor neuropathy, and hereditary neuralgic amyotrophy. The second group consists of disorders in which the neuropathy is part of a multisystem disorder, such as familial amyloid polyneuropathy, hereditary ataxias, and neuropathy associated with mitochondrial diseases [1,2]. IPNs are clinically and genetically heterogeneous disorders [2]; therefore, they constitute an interesting research field for human geneticists.

1.2. Charcot-Marie-Tooth Disease and Related Neuropathies

The most common type of IPN is Hereditary Motor and Sensory Neuropathy (HMSN), more commonly referred to as Charcot-Marie-Tooth (CMT) disease to honor the three clinicians who originally reported the clinical features simultaneously in 1886: French neurologist Jean-Martin Charcot, his student Pierre Marie, and British neurologist Howard Henry Tooth [1, 3, 4]. CMT is a type of neuropathy that affects both motor and sensory nerves, while hereditary motor neuropathy (HMN) predominantly affects motor neurons and hereditary sensory/autonomic neuropathy (HSN or HSAN) predominantly affects sensory and autonomic nerves [1, 3, 5]. These three disorders are collectively called CMT and related neuropathies and they represent a phenotypic continuum [1, 6].

CMT is a clinically and genetically heterogeneous group of neurological disorders. Age of onset may vary from birth to late adulthood, while the severity of the symptoms may encompass a wide range of phenotypes [7]. The hallmark of the disease is slowly progressive, length-dependent, symmetrical nerve degeneration, which results in chronic muscle weakness and wasting starting at distal limbs [5, 7]. Foot deformities such as high arch of the foot, called pes cavus, are also commonly observed. The defects in the neurons may cause skeletal deformities, gait disorder, wheelchair dependence, and sensory disturbances [3, 5, 7, 8].

The initial step in clinical diagnosis of CMT and related disorders is to investigate the symptoms of neuropathy in the patient. It is usually quite obvious since most patients present with length-dependent muscle weakness and sensory loss starting at feet and slowly ascending to knees and hands [2, 5]. Still, the findings should be confirmed with nerve conduction studies as in some congenital cases, collateral sprouting may cause normal compound muscle action potentials, and in such cases neuropathy may only be diagnosed using electromyography [2, 3]. In the clinical examination of the patient, it is essential to question the developmental history of the individual, such as presence of contractures at birth, delayed motor milestones, poor performance in sports at school, and difficulty of shoe-fitting during childhood [1, 2].

The true prevalence of CMT is difficult to pinpoint since widespread population analyses are limited. The early estimates reported that one in 2500 individuals worldwide are affected [4], however, most current prevalence reports are generally from certain regions in the world and there are discrepancies among them. For instance, a retrospective, population study from Japan suggests 10,8 cases in 100.000 individuals [9] and another study from Egypt reports a prevalence of 12 cases in 100.000 individuals [10]. The prevalence was reported to be 11,8 in 100.000 in a study from northern England [11]. Another report, this time from Sweden, suggests a prevalence of 20,1 in 100.000 individuals [12]. To gather and analyze data from different prevalence studies Barreto *et al.* [13] systematically reviewed 802 studies and suggested CMT prevalence to be between 9,7-82,3 in 100.000 individuals worldwide with no ethnic predisposition.

The study also reports that most such studies were from European countries, perhaps due to the presence of major European centers for CMT diagnosis [13]. This prevalence classifies CMT as a rare disease, but makes it the most common inherited disorder of the human peripheral nervous system [5, 14].

1.2.1. Classification of CMT disease

As a group of multiple related disorders, the need for classification of CMT was prominent from the beginning of its research. Historically, CMT is classified into two broad groups based on the clinical features of the patients according to nerve conduction studies. In the clinical setting, CMT type 1 (CMT1) is the demyelinating type of the disease affecting the Schwann cells, whereas CMT type 2 (CMT2) is the axonal type of the disease as it primarily affects the axons [7]. A decrease in nerve conduction velocity generally suggests myelin dysfunction and is interpreted as demyelination or hypomyelination of the nerves [15]. A reduction in the amplitudes of compound muscle action potential, on the other hand, will suggest axonal damage and/or loss of neuronal fibers [16]. Thus, the patients are diagnosed with demyelinating neuropathy when their upper limb motor nerve conduction velocity (mNCV) is less than 38 m/s, while the diagnosis is axonal CMT if the upper limb motor nerve conduction velocity is over 38 m/s, but the amplitudes of compound muscle action potential is reduced [17]. Later, a new subtype was defined for individuals with an upper limb mNCV between 25 m/s and 45 m/s as "intermediate CMT" (also called CMT-I) [18]. Still, it should be kept in mind that, both axonal and demyelinating CMT will eventually result in axonal loss in the later stages of the disease [16].

As the field advanced and the genes that cause the pathology have begun to be identified, a further sub-classification was introduced based on a combination of electrophysiological findings, the causative gene, and inheritance pattern [19]. This current classification uses different numbers and letters to define different CMT subtypes. However, as the gene discovery rate accelerated due to advancements in next-generation sequencing (NGS) technologies, the classification have become less straightforward.

Additionally, the issue became more complicated as it was shown that different mutations in the same causative gene may cause different CMT phenotypes or may have different inheritance patterns [20–23]. More recently, a new classification system was proposed that uses abbreviations for inheritance type, phenotypical form of the disease, and the genetic cause [24,25]. For instance, according to this new proposal, when a patient is diagnosed with demyelinating CMT due to a biallelic mutation in the *GDAP1* gene, the clinical diagnosis should be AR-CMTde-GDAP1, instead of CMT4A, while for another patient with axonal CMT due to a dominant mutation in *GDAP1*, the diagnosis will be AD-CMTax-GDAP1, instead of CMT2K. The proposed classification is also extended to cover CMT-related neuropathies, such as hereditary motor neuropathy (HMN) and hereditary sensory and autonomic neuropathy (HSAN) [25]. However, this new classification system is still not fully implemented to the field. Figure 1.1 gives an overview of the current, most commonly used classification of the disease.

1.2.2. Genetics of CMT disease

The first CMT-causing genetic locus was identified in 1982 [26], followed by others identifying new causative loci. The discovery of a 1.4-Mb duplication in the region of chromosome 17 that contains the *PMP22* gene as the cause of CMT1A, was the pioneering report for an individual causative gene [27, 28]. In preliminary studies, investigation of causative genes was performed by genetic linkage analyses in large pedigrees, positional cloning or candidate gene studies. Human Genome Project and subsequent advances in NGS technologies at the turn of the century have led to a great acceleration in the number of CMT causing genes and mutations [7, 29]. At the time of writing, more than 90 distinct causative genes have been reported [1, 7, 30]. These reported genes indicate that CMT can be inherited through autosomal dominant, autosomal recessive, X-linked, and maternal inheritance. A significant number of isolated cases are observed due to *de novo* mutations in CMT genes [7, 19].

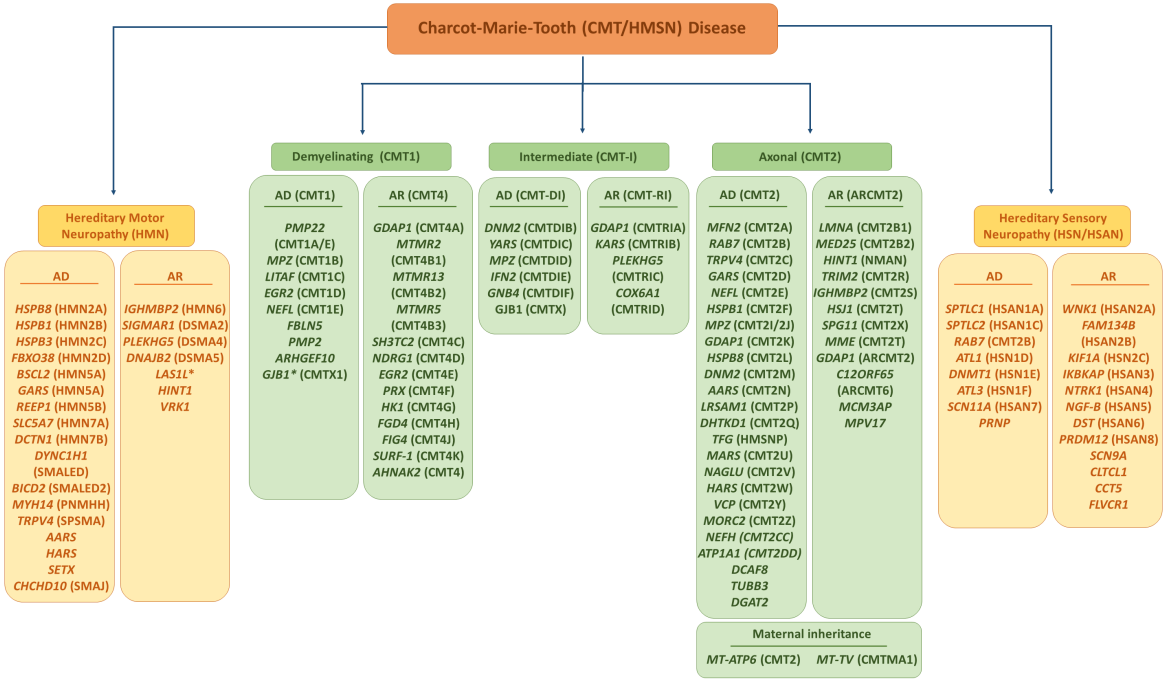

Figure 1.1. An overview of subtype classification of CMT and related neuropathies based on electrophysiological findings, inheritance pattern and causative gene. Abbreviations in italics indicate gene names, abbreviations in parentheses indicate CMT subtype. * indicates X-linked inheritance.

Different mutations in the same causative gene may present with different clinical phenotypes such as demyelinating or axonal types of the disease, whereas mutations in different causative genes may present with similar clinical phenotypes. These features underline the complexity of genotype/phenotype correlation in CMT disease [29].

1.2.2.1. Charcot-Marie-Tooth Disease Type 1 (CMT1). Demyelinating CMT due to mutations inherited in an autosomal dominant manner is termed as CMT1. In this type of CMT, the pathology arises due to mutations in genes maintaining Schwann cell function and myelin sheath formation [1, 7]. The most common type of CMT1 is CMT1A that is caused by a 1.4 Mb tandem duplication of chromosome 17p11.2 including the *Peripheral Myelin Protein 22* (*PMP22*) gene [27, 28]. Nearly 70% of all diagnosed demyelinating cases and about 40% of all CMT cases are CMT1A cases [1,31]. Point mutations in *PMP22* gene are also disease-causing, but these only make up about 1-5% of demyelinating cases. This type of disease is called CMT1E [1,2]. Deletion of the same 1.4 Mb region on chromosome 17p11.2 that is duplicated in CMT1A, results in a different disorder called Hereditary Neuropathy with Liability to Pressure Palsies (HNPP) [32]. The PMP22 protein is a major component of myelin making up 2-5% of all proteins in the peripheral nervous system myelin [33, 34]. Since this gene is duplicated, but not disrupted in CMT1A patients, it is suggested that a gene dosage effect could be in place, at least partially, for CMT1A pathology [35]. Other commonly mutated genes in CMT1 include *Gap Junction Protein Beta-1* (*GJB1*) linked to the X-chromosome (Xq13.1) and *Myelin Protein Zero* (*MPZ*) linked to chromosome 1q23.3. *GJB1* encodes for a connexin protein in Schwann cells that forms channels to facilitate transfer of ions and small molecules that are essential for communication between the Schwann cells and the neurons [36]. Pathogenic mutations in this gene cause CMTX1 with a prevalence of nearly 10% of all demyelinating CMT cases [37, 38]. Males are more severely affected in CMTX1 than females possibly due to random X-inactivation [39]. *MPZ*, on the other hand, encodes for one of the most important proteins in myelin sheath production and compaction, and pathogenic mutations in this gene are observed in almost 5% of all CMT cases [2,40]. *MPZ* gene encodes for a transmembrane protein that constitutes over 50% of all the proteins purified from myelin sheaths [41].

The protein is exclusively expressed from the Schwann cells in the peripheral nervous system and is essential for myelin compaction [42–44]. The pathology that arises due to mutations in *MPZ* is referred as CMT1B and the patients have severely hypomyelinated axons [45]. Other genes that cause dominant demyelinating CMT include *LITAF* (CMT1C), *EGR2* (CMT1D), *NEFL* (CMT1F), *FBLN5*, and *PMP2* (CMT1G) [46].

1.2.2.2. Charcot-Marie-Tooth Disease Type 2 (CMT2). Axonal form of the disease inherited in autosomal dominant fashion is called CMT2. The genes mutated in this CMT subtype are generally related to neuron function, metabolism and maintenance, and pathogenic mutations in these genes cause axonal degeneration [1,7]. It is distinguished from demyelinating CMT using nerve conduction studies: In the axonal form the nerve conduction velocities are normal or higher (over 38 m/s), but there is a decrease in compound muscle action potentials [2,5]. CMT2 is less common than CMT1 [13]. Autosomal dominant as well as autosomal recessive forms of axonal CMT, are caused by many different genes that typically affect only several families [47]. The most common cause of CMT2 is mutations in *Mitofusin 2* (*MFN2*) gene on chromosome 1p36.22 with a prevalence of about 20% among all axonal cases [48]. The size of mitochondria differs greatly with cell type and physiological condition and this arrangement is determined by a critical balance between mitochondrial fusion and fission. Mitofusin proteins (Mfn1 and Mfn2) mediate the fusion of mitochondria [49]. CMT disease type 2A2A (CMT2A2A) is caused by heterozygous mutations in the *MFN2* gene [48], while rare homozygous or compound heterozygous mutations in *MFN2* cause a more severe form of the disease with earlier age of onset, called CMT2A2B [50]. Other genes that cause CMT2 due to dominant mutations include *RAB7* (CMT2B), *TRPV4* (CMT2C), *GARS* (CMT2D), *NEFL* (CMT2E), *HSPB1* (CMT2F), *GDAP1* (CMT2K), *HSPB8* (CMT2L), *DNM2* (CMT2M), and *AARS* (CMT2N) [46].

1.2.2.3. Charcot-Marie-Tooth Disease Type 4 (CMT4). Demyelinating CMT disease due to autosomal recessive mutations is termed as CMT4. This type of disease is extremely rare, genetically highly diverse, and is caused by many different genes.

These mutations typically affect a handful of families [2, 47, 51]. Still, patients with CMT4 almost always have early onset of symptoms and have more severe clinical phenotypes than the dominant types of the disease [3, 52]. The most common cause of CMT4 is biallelic mutations in *Ganglioside-induced Differentiation-Associated Protein 1* (*GDAP1*), designated CMT4A, followed by mutations in *SH3 Domain and Tetratricopeptide Repeat Domain 2* (*SH3TC2*), designated CMT4C [1, 21, 47, 53, 54]. Expressed both in neurons and Schwann cells, *GDAP1* encodes for a protein that is crucial for mitochondrial fragmentation, counterbalancing the activity of mitochondrial fusion proteins; Mfn1 and Mfn2 [55]. The tight balance in mitochondrial dynamics is essential for myelinated neuron function and, therefore, underlines a common disease mechanism for *GDAP1* and *MFN2* mutations [55, 56]. *SH3TC2*, on the other hand, encodes for a protein abundant in several components of the endocytotic pathway. The impairment of endocytotic and membrane trafficking pathways due to pathogenic mutations in this gene likely disrupts the communication between the Schwann cell and the axon; thus, cause abnormal myelin formation [57]. Other genes causative for CMT4 include *MTMR2* (CMT4B1), *MTMR13/SBF2* (CMT4B2), *MTMR5/SBF1* (CMT4B3), *NDRG1* (CMT4D), *EGR2* (CMT4E), *PRX* (CMT4F), *HK1* (CMT2G), *FGD4* (CMT4H), and *FIG4* (CMT4J) [46].

1.2.2.4. Autosomal Recessive Axonal Charcot-Marie-Tooth Disease (ARCMT2). Axonal CMT disease due to autosomal recessive mutations are very rare and are designated ARCMT2 [1]. The most common cause of recessive axonal neuropathy is *Histidine Triad Nucleotide Binding Protein 1* (*HINT1*), accounting for around 10% of all recessive CMT cases. About 80% of individuals with axonal neuropathy presenting with neuromyotonia have mutations in this gene [54, 58, 59]. *HINT1* encodes for an enzyme that hydrolyses aminoacyl adenylates, which are intermediate products in charging of tRNAs with their relevant amino acids and help aminoacyl-tRNA synthetases [60–62]. ARCMT2-causative mutations in *HINT1* cause loss of function of the gene with unclear disease pathomechanism, however, it is suggested that the enzymatic function of the *HINT1* protein is likely to underlie the disease mechanism since catalytically inactive but stable versions of HINT1 are capable of causing the disease [58].

Other genes that are causative for ARCMT2 include *LMNA* (CMT2B1), *MED25* (CMT2B2), *TRIM2* (CMT2R), *IGHMBP2* (CMT2S), *HSJ1* (CMT2T), *SPG11*, *MME*, *GDAP1*, and *C12ORF65* [46].

1.2.2.5. Intermediate CMT (CMT-I). Intermediate CMT or CMT-I is a relatively new term used to describe inherited motor and sensory neuropathy cases with motor nerve conduction velocities between 25-45 m/s [18]. In these patients, mNCV values can differ among different nerves in the same patient or among affected family members [1]. Inheritance of CMT-I genes could be dominant or recessive. The most common causes of intermediate CMT are dominant mutations in *MPZ* and *GJB1* genes [16]. Other genes that may cause CMT-I include *DNM2* (CMTDIB), *YARS* (CMTDIC), *IFN2* (CMTDIE), *GNB4* (CMTDIF), *GDAP1* (CMTRIA), *KARS* (CMTRIB), *PLEKHG5* (CMTRIC), and *COX6A1* (CMTRID) [46].

1.2.3. Molecular mechanisms causing CMT disease

The clinical distinction between demyelinating and axonal forms of the disease is eminent, but it is also recognized that there is a final common pathway in disease presentation. The pathology either begins with demyelination of the nerves or with defects in nerve function. The demyelinating forms of the disease are caused by defects in Schwann cells that cause failure to make or maintain myelin sheaths, which in turn causes failure to maintain axonal integrity. In axonal forms of the disease, pathogenic mutations in different genes cause defects in axonal integrity even in the presence of normal myelin. Both these pathologies eventually converge into a final common pathway that results in progressive axonal loss and subsequent muscle denervation [63]. The progression of disease pathology is summarized in Figure 1.2.

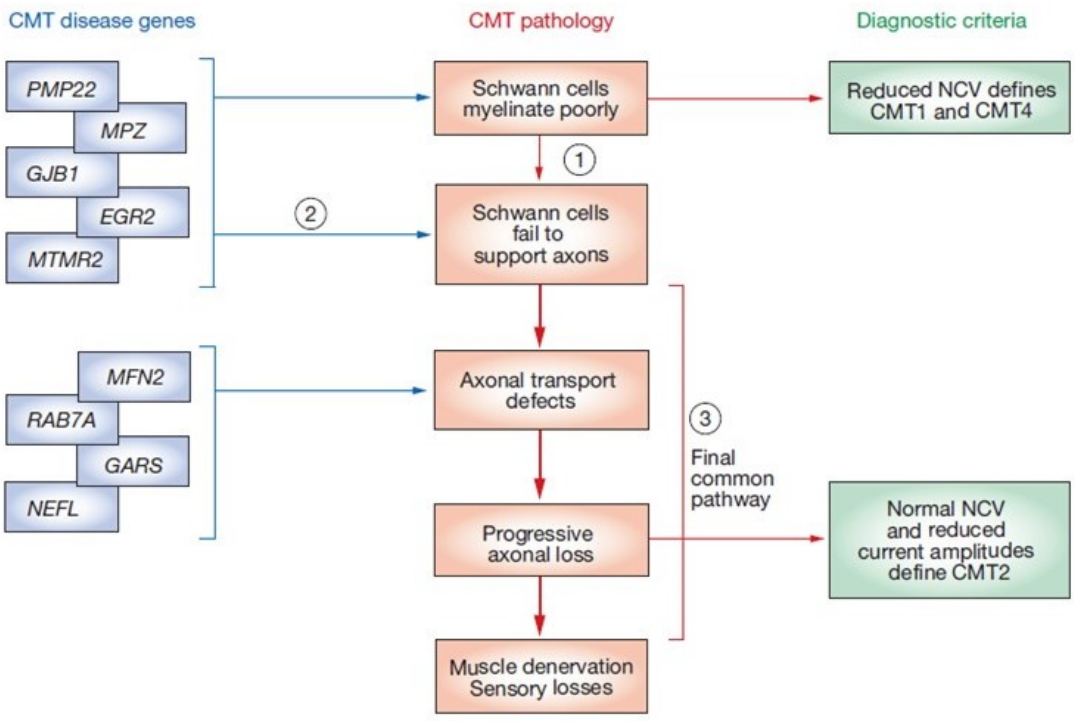

Figure 1.2. Representation of CMT disease progression in terms of cellular pathology (adapted from [63]).

The mechanisms of how each distinct gene result in the common cellular pathology is another focus of CMT research. CMT-causative genes belong to a myriad of functional classes such as structural, cytoskeletal or signaling proteins, proteins involved in mitochondrial dynamics and axonal transport, etc. Understanding the alterations in the molecular mechanisms due to pathogenic mutations in these genes will help us identify molecular targets for therapeutic approaches. A summary of known CMT-causative genes and the pathways these genes are involved in are given in Figure 1.3.

Historically, CMT1A was the leading subject in experimental CMT research since it is the commonest form [63]. After the discovery of chromosome 17p11.2 duplication and deletion causing CMT1A and HNPP respectively, it was clear that a gene dosage mechanism was in action. *PMP22* is located in this locus and produces *Peripheral myelin protein 22*, a small integral membrane protein expressed in Schwann cells [32,64].

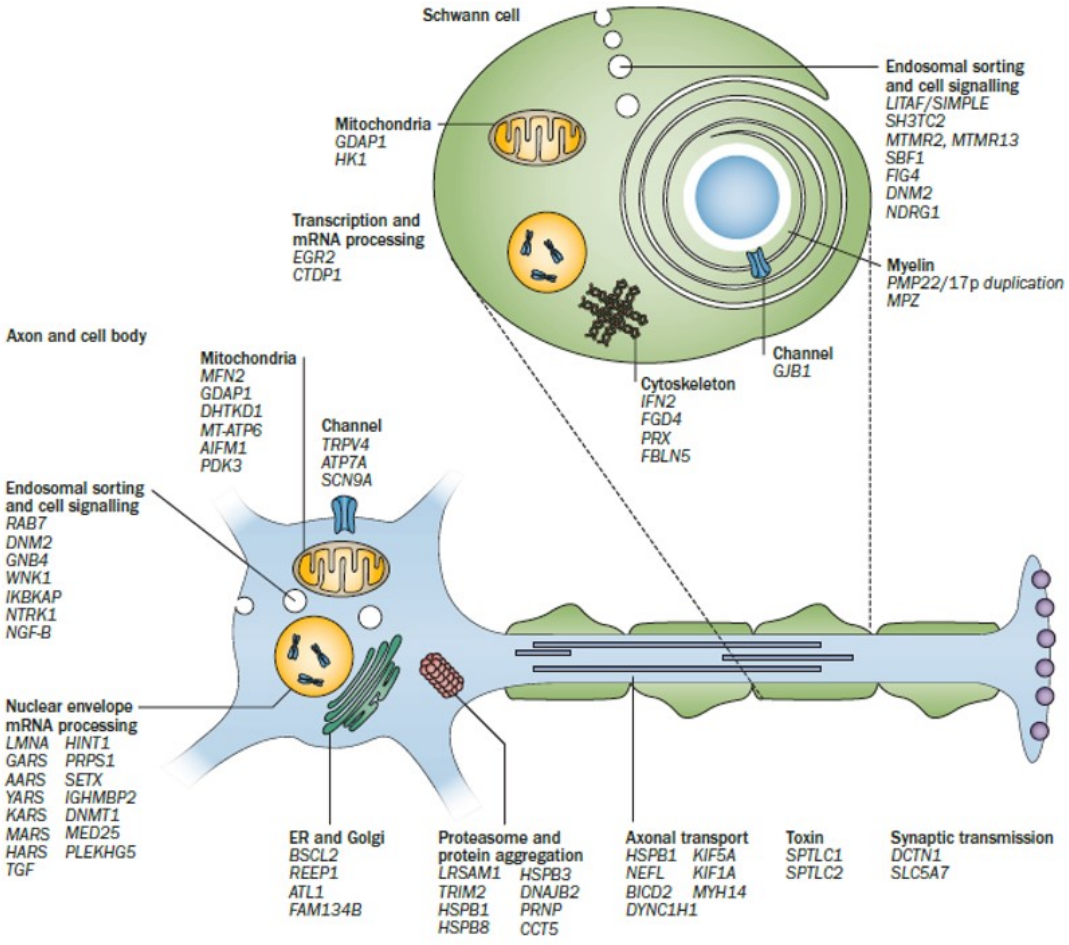

Figure 1.3. Summary of known causative genes and proposed pathomechanisms in CMT and related neuropathies (adapted from [31]).

Patients with a heterozygous duplication in this locus have 1.5-fold overexpression of this myelin protein and present with CMT1A pathology. Patients with decreased *PMP22* gene dosage have haploinsufficiency and they present with HNPP [63]. It has been reported that *PMP22-null* mutation does not actually prevent myelination *in vivo*, however numerous sausage-shaped swellings of the myelin sheath, termed tomacula, were observed in nerve biopsy samples from null mice [65]. PMP22 has also been shown to interact with *Myelin protein zero*, the gene product of *MPZ*, and it has been suggested that myelin is destabilized when the ratio between these two proteins is altered [66]. A striking observation is that, when PMP22 is overexpressed in cell cultures or *in vivo*, the excess protein forms ubiquitinated aggregates in late endosomes [67,68].

This, in turn, was suggested to be a cellular response to excess misfolded proteins and might overload protein degradation machinery in Schwann cells, subsequently perturbing Schwann cell function [69].

The causative gene for CMT1B, *MPZ*, encodes for *myelin protein zero*, which is the main membrane protein of the peripheral myelin that acts as a cell adhesion molecule [42, 43]. It was shown in *null* mutant mice that MPZ was essential for myelination and membrane compaction [42, 44]. Mutations in *MPZ* could cause a clinical phenotype either through toxicity of misfolded proteins or haploinsufficiency in protein levels [63]. The *MPZ* gene is exclusively expressed in Schwann cells, however, mutations in different domains in the protein may cause demyelinating or axonal forms of the disease, the mechanisms of the latter being poorly understood [63]. Investigation of CMT1B mouse models made a breakthrough in our understanding of disease pathomechanism. It was shown that cells of the immune system (T-cells and macrophages, in particular) were involved in the demyelination process in the progression of pathology, probably in an attempt to repair defects in myelin caused due to *MPZ* mutations. Similar findings were later reported in CMT1A and CMTX mouse models [70, 71].

Healthy mitochondria are an important indicator of healthy neurons. Mitochondria dysfunction is known to be involved in the pathogenesis of many neurodegenerative disorders, including Alzheimer's disease, Parkinson's disease, and neuromuscular disorders [72]. Since peripheral neurons have exceptionally long axons with special energy and transport requirements, proper mitochondrial function is essential for these cells. Mitochondrial fusion and fission, collectively termed mitochondrial dynamics, are fundamental for proper distribution of these organelles along the axons of peripheral nerves [73]. Timely and balanced fragmentation of these organelles is required for regulating the shape, size and number of mitochondria, their proper transport along axons, and functionality [73]. A significant number of CMT cases are caused by genes regulating mitochondrial dynamics, such as *MFN2* and *GDAP1*. Both these nuclear genes are expressed in the outer mitochondrial membranes of Schwann cells and neurons [48, 55].

MFN2, together with *MFN1*, is required for mitochondrial fusion, while *GDAP1* is required for mitochondrial fission [55, 74]. Pathogenic mutations in these genes, thus, perturb routine mitochondrial dynamics, leading to improper distribution of these organelles along axons and/or formation of abnormally shaped mitochondria [73]. These organelles with altered morphologies are likely incapable of performing fundamental tasks; causing increased oxidative stress and altered cytosolic calcium balance [75], which ultimately leads to axonal degeneration and neuronal death [73, 76].

Axonal transport of vesicles, mitochondria and other organelles along microtubules is especially important for neuron function, and thus, emerges as a molecular target in many neuronal pathologies [72]. An intact cytoskeleton is essential for proper intracellular trafficking of cargo in extended axons. Indeed, mutations in important members of the neurofilament family (*NEFL* and *NEFH* genes) were shown to be associated with axonal neuropathy [77, 78]. Mutations in *RAB7*, a protein localized to late endosomes and acts as vesicular transport regulator, were also found to be causative for axonal CMT [79]. Similarly, *DNM2* gene, which encodes for a large protein suggested to be involved in receptor-mediated endocytosis, membrane trafficking from the late endosomes, and actin assembly, was reported to underlie an intermediate CMT phenotype [80–82]. Mutations in the heavy chain of dynein motor protein (*DYNC1H1*) have been associated with CMT2 [83], while mutations in *DCTN1*, which encodes part of a multi-subunit complex protein that binds to the motor protein *Dynein* have been associated with distal HMN [84]. Both of these proteins are critical for microtubule-mediated axonal transport [85]. Mutations in small heat shock proteins (*HSPB1*, *HSPB3*, and *HSPB8*) were also shown to be causative for axonal CMT and distal HMN. These proteins act as molecular chaperons and have been suggested to regulate assembly of actin and intermediate filaments [86–88]. The discovery of many causative genes involved in cytoskeletal function further implies axonal transport as a common mechanism in many neuronal diseases [89].

1.2.4. Molecular diagnosis strategies in CMT disease

Genetic testing in CMT is often performed for the purpose of family planning, such as in predictive or preimplantation assessment [31, 90]. One of the most important requirements for correct genetic diagnosis is the active communication between the geneticist and the clinician. Once a clinical diagnosis is established according to neurological examination and electrophysiological findings, the next step is to provide evidence for its genetic origin. This could be relatively easy in large families with multiple affected individuals, however, it is more challenging in adopted individuals or small families with isolated cases [2, 52]. A detailed family history should be obtained with specific questions regarding the developmental milestones of the patient or their sports performance in school. Using clinical markers such as asymmetrical weakness, cerebrospinal fluid (CSF) protein level, and MRI imaging generally helps distinguishing acquired neuropathy from genetic neuropathy [2]. If a patient is suspected to have a genetic basis for neuropathy, then they should be referred to molecular diagnosis.

Multiple diagnostic tools and strategies are available for genetic testing of CMT disease. One should address several issues in order to define the clinical phenotype and to correctly choose a strategy for molecular diagnosis. The first step is to determine the likely mode of inheritance: If there is consanguinity between the parents of the affected individual and/or are multiple affected individuals in the same generation, autosomal recessive inheritance is more likely. If there is male to male transmission, then X-linked inheritance is excluded. If the mode of inheritance is not obvious such as in small families and sporadic cases, autosomal dominant or *de novo* dominant inheritance is more likely in Northern Europe and North America, while autosomal recessive inheritance is still likely in countries with high consanguinity rates [2, 31], such as in Turkey. Strict maternal transmission with axonal pathology likely indicates a causative mutation in mitochondrial DNA [2, 91, 92]. The next issue is to determine whether the patient has a demyelinating or axonal pathology since these different types may indicate different genes and different inheritance patterns. Similarly, the clinician should also determine if the neuropathy is predominantly motor, sensory or both.

Nerve conduction studies are essential for this purpose, since sensory involvement may have minimal clinical signs but will be revealed by neurophysiological studies [2]. Once the clinical phenotype and the inheritance pattern of the patient are established, the geneticist could then proceed to determine the causative gene.

1.2.4.1. Sequential screening of recurrent genes. Multiple studies have suggested strategies for genetic testing that generally reflect mutation frequency [52]. These studies are based on careful phenotypical screening of clinical symptoms and sequential screening of most likely causative genes [19,38,52,93,94]. Sequential screening of causative genes is generally an economical and high yield strategy since certain mutations are responsible for a great number of patients [19]. For instance, *PMP22* duplication is responsible for approximately 40% of all CMT cases, making this locus a reasonable first target for testing [38, 94]. If the patient has a demyelinating pathology and tests negative for *PMP22* duplication, then, they could be tested for *MPZ* mutations and subsequently *GJB1* mutations if there is no male-to-male transmission in the family. For axonal CMT cases, the patient could be screened for mutations in the *MFN2* gene [38]. In retrospective studies with large patient cohorts, it has been shown that four genes (*PMP22*, *MPZ*, *GJB1*, and *MFN2*) were responsible for over 90% of all diagnosed CMT cases [90,95,96]. Thus, it is suggested that these four genes should be screened first before further genetic testing with more advanced tools [96]. Additionally, some distinct clinical findings may direct the geneticist to consider certain genes. For instance, 80% of recessive axonal neuropathy patients with neuromyotonia have causative mutations in the *HINT1* gene [58]. Likewise, scoliosis or kyphoscoliosis in patients with recessive demyelinating neuropathy is a frequent sign of *SH3TC2* mutations [97]. Vocal cord paresis and diaphragmatic dysfunction are very frequent in patients with *GDAP1* mutations [98]. Therefore, patients with relevant clinical features and likely inheritance may be subjected to screening in these genes.

1.2.4.2. Next-generation sequencing. Sequential screening may be time and cost effective for CMT1, however the procedure could become very expensive and overwhelming in CMT2 due to a great number of individually rare causative genes [2]. Following the publication of Human Genome Project and subsequent advancements in next-generation sequencing technologies, the trend for genetic diagnosis strategies has shifted. Next-generation sequencing, or high-throughput DNA sequencing, describes massively parallel sequencing of DNA fragments which has rapidly evolved and been commercialized since early 2010s [99, 100]. NGS technology is an advancement to the first generation of DNA sequencing methodology (Sanger sequencing), and the most common sequencers generally use a method called "sequencing by synthesis". The basic steps include random shearing of genomic DNA, capture of fragments in separate chambers or through adaptors, amplification of fragments using modified nucleotides, and detection of incorporated nucleotides on each round of synthesis to allow parallel sequencing of fragments [100, 101].

NGS technologies can be used to sequence the whole genome of an organism; termed whole-genome sequencing/WGS, or used to allow targeted sequencing of certain regions of the genome; such as a certain number of genes (gene panels) or only the protein coding 2% of the genome (whole-exome sequencing/WES) [2, 6]. The choice of NGS technology depends on the purpose of the analysis: Using gene panels, a small set of genes can be screened with good read-depth and genetic diagnosis could easily be achieved if the person has a pathogenic mutation in one of the known genes; while with whole-exome sequencing a large set of genes could be screened with relatively less read-depth, and novel causative genes may be identified if the person in analysis does not have a mutation in known genes [2, 6, 7].

The current practice in large diagnostic centers is to use gene panels that utilize capture kits to target and sequence known causative genes for genetic diagnosis of CMT disease [6, 30, 102–104]. Gene panels provide excellent coverage of known causative genes and high read depths, but, the use of panels limited to specific subtypes, is increasingly discouraged due to phenotypic overlap between various disorders.

These include different CMT subtypes, inherited ataxias, distal myopathies and hereditary spastic paraplegias [6]. Still, the generation of large gene panels that include all known CMT-causative genes will radically reduce sequencing costs and help better characterize genotype-phenotype correlation in CMT. Gene panels are also expected to unveil digenic and other less common inheritance patterns [7]. Currently, the gene panels do not have full coverage of all sequences of interest, and they are not widely commercially available. Still, this technology is soon expected to replace sequential Sanger sequencing completely [7].

WES, on the other hand, has been an exceedingly popular tool for identification of novel CMT causative genes in the past decade since it allows unbiased sequencing of all protein coding genes [6]. Although WES provides near complete coverage of protein coding regions with high read-depth, the analysis and interpretation of nearly 20.000 single nucleotide variants and small indels for each patient limits its widespread use in the clinical setting [6]. It has been previously suggested that 85% of all mutations causative for Mendelian disorders reside in the protein-coding sequences which makes up about 2% of the human genome [105]. Therefore, WES is a great technology for identification of novel causative alleles or genes. In the meantime, some research centers utilize whole-genome sequencing (WGS) for families that remain undiagnosed following WES analysis, however, WGS still seems less efficient and more expensive compared to WES in identification of novel genes [106].

Third-generation sequencing is the term for currently the most advanced sequencing technology. It is also called large fragment single molecule sequencing [100]. This technology aims to sequence extremely long DNA/RNA sequences (up to 30-50 kb) in a single run. The commercial leader in the field uses an engineered DNA polymerase bound to the DNA to be sequenced in a micro-chamber. The DNA polymerase uses the DNA it is bound to as a template and incorporates correct nucleotides labeled with different fluorophores to the new sequence. The technology allows detection of incorporated nucleotides at the bottom of the micro-chamber on the millisecond time scale. This reaction simultaneously occurs in parallel in up to one million chambers [100].

The use of this technology is not common yet mostly due to high cost and novelty of the methodology. Though, it is expected to identify novel genes/mutations causative for CMT disease, especially those that are poorly covered in NGS technologies, such as large repeat sequences, large deletions/insertions, translocations, and inversions. This is expected because it allows sequencing of much longer reads at a time comparable to WES and WGS [107].

The rate of identification of novel CMT-causative genes had decreased in the beginning of 2000's due to shortage of large families, but the development of high-throughput genomic sequencing technologies has led to re-acceleration [7]. With novel genes being identified, genetic diagnosis rates in CMT have increased greatly. Several studies using CMT gene panels report diagnostic rates ranging from 18% to 31% [102–104,108]. Studies utilizing WES, on the other hand, report diagnosis rates between 45-60% [5,20,38,94,109,110]. However, there is a great diagnostic gap between CMT1 and CMT2. For instance, the study published by Inherited Neuropathy Consortium (INC) reviewed 1652 patients from 13 INC centers and found that 60.4% of these patients received a genetic diagnosis: The diagnosis rate in CMT1 was 91,4%, while only 42% of CMT2 cases received a genetic diagnosis [111]. Similarly, another study testing 1206 patients from Germany reported genetic diagnosis in 56% of CMT1 cases and only 17% in CMT2 cases [93]. These findings suggest that there are CMT-causative genes yet to be identified, especially in axonal CMT, and that non-Mendelian aspects of CMT disease, such as multigenic inheritance and modifier genes, will be uncovered in the future [7, 51].

2. PURPOSE

Charcot-Marie-Tooth (CMT) disease is a critical research focus for human geneticists due to its clinical and genetic heterogeneity. Despite advances in diagnosis strategies, the genetic diagnosis rate in CMT disease generally does not exceed 65%, while for autosomal recessive or axonal types, this rate is far more reduced. This diagnostic gap suggests that there are yet unidentified causative genes, disease mechanisms or non-Mendelian inheritance patterns responsible for this disorder.

To uncover the underlying reasons of this gap, the first aim of this study was to identify and characterize novel genes and/or alleles causative for autosomal recessive CMT disease. Identification of novel causative genes may enlighten underlying disease mechanisms and shed light on potential therapeutic targets. For this purpose, we have screened 56 consanguineous Turkish CMT patients with early onset polyneuropathy and severe additional clinical symptoms using next-generation sequencing technologies in combination with homozygosity mapping based on NGS data. Additionally, we have cultured patient primary fibroblasts to investigate molecular characteristics of the novel candidate genes we have identified.

The second aim was to investigate gene/allele frequency of recurrent genes in the Turkish autosomal recessive CMT population. By surveying all patients who received a genetic diagnosis and analyzing gene frequency in the cohort, we wanted to provide a reference for diagnostic strategies that might be developed specific to populations with similar genetic backgrounds. Relevant diagnostic strategies/tools specific to populations increase genetic diagnosis rate, while decreasing diagnostic costs.

3. MATERIALS

3.1. Patient Cohort

A total of 180 individuals including affected and unaffected individuals from 56 families have been analyzed in this study. The index patients from each family were evaluated by expert neurologists and were initially diagnosed with CMT. Among these 56 families, 27 had family history with more than one affected individual born to consanguineous parents, while 29 families had a single affected individual in each family born to consanguineous parents. Age of onset was in childhood in 52 index patients and in adulthood in four families. 66% of index patients studied here had a severe phenotype with additional clinical symptoms to distal muscle weakness such as scoliosis, vocal cord involvement, hearing loss, intellectual disability etc. Acquired neuropathy probability was excluded for all patients in the clinical setting. Therefore, the patients studied here most likely represented an autosomal recessive CMT cohort. The study was approved by the Ethics Committee of Istanbul University and Boğaziçi University Human Research Ethics Committees and informed consent was obtained from all families enrolled in the study. The clinical features of the patients are given in Table 3.1.

Table 3.1. Clinical findings of the patients enrolled in the study.

Nr.	**Patient ID**	**Family history**	**Age of onset**	**mNCV (m/s)**	**Additional findings**
1	P77	Isolated	11-20	36,9	pes cavus, scoliosis, hammer toe
2	P165	Isolated	DMM	60	N/A
3	P241	Isolated	2-10	38,7	pes cavus, tremor
4	P265	2 affected	21-40	44,8	pes cavus, tremor
5	P294	Isolated	2-10	IE	pes cavus, scoliosis, wheelchair-confined

mNCV: motor nerve conduction velocity, DMM: delayed motor milestones, IE: inexcitable, N/A: not applicable/unknown, CSF: cerebrospinal fluid, HSP: hereditary spastic paraplegia

Table 3.1. Clinical findings of the patients enrolled in the study. (cont.)

Nr.	Patient ID	Family history	Age of onset	mNCV (m/s)	Additional findings
6	P300	Isolated	2-10	IE	pes cavus, hammer toe
7	P322	2 affected	2-10	22	pes cavus, scoliosis, sensory ataxia
8	P431	Isolated	11-20	50	neuromyotonia
9	P448	Isolated	2-10	IE	pes cavus, tremor, sensory ataxia
10	P470	2 affected	over 40	38,8	pes cavus, hammer toe, sensory ataxia
11	P492	Isolated	at birth	16,7	pes cavus, wheelchair use, claw hands, tremor
12	P555	Isolated	2-10	>38	pes cavus
13	P567	3 affected	2-10	55	pes cavus, wheelchair-confined
14	P581	Isolated	at birth	IE	pes planus
15	P629	Isolated	at birth	26,6	pes cavus, scoliosis, mild tremor at hands
16	P639	2 affected	20	32	pes cavus
17	P711	4 affected	21-40	29	pes cavus
18	P774	Isolated	2-10	19,8	pes cavus, hammer toes
19	P809	4 affected	11-20	57,8	pes cavus
20	P811	2 affected	at birth	IE	pes cavus, scoliosis, sensory ataxia, hearing loss, cerebellar dysfunction
21	P854	Isolated	DMM	16	pes cavus, hammer toe, abnormal CSF protein
22	P954	2 affected	11-20	19	pes cavus, tremor
23	P963	Isolated	2-10	11,7	pes planus
24	P966	3 affected	DMM	IE	scoliosis, nystagmus, wheelchair-confined
25	P969	2 affected	DMM	IE	pes cavus, scoliosis, hammer toe

mNCV: motor nerve conduction velocity, DMM: delayed motor milestones, IE: inexcitable, N/A: not applicable/unknown, CSF: cerebrospinal fluid, HSP: hereditary spastic paraplegia

Table 3.1. Clinical findings of the patients enrolled in the study. (cont.)

Nr.	Patient ID	Family history	Age of onset	mNCV (m/s)	Additional findings
26	P987	2 affected	at birth	IE	scoliosis, wheelchair-confined, hoarseness
27	P991	5 affected	11-20	IE	hearing loss, abnormal CSF protein
28	P1025	Isolated	DMM	13,3	pes cavus, hammer toe, kyphoscoliosis, vocal cord involvement, tremor, sensory ataxia
29	P1041	Isolated	2-10	44	mild spasticity
30	P1130	2 affected	at birth	N/A	N/A
31	P1142	Isolated	2-10	51,9	pes cavus, hammer toes, pyramidal signs
32	P1148	2 affected	11-20	56	pes cavus
33	P1150	Isolated	DMM	42,2	pes cavus, hammer toes, sensory ataxia
34	P1152	3 affected	2-10	32,8	N/A
35	P1154	Isolated	DMM	26,8	pes cavus, tremor, hammer toes
36	P1180-4	2 affected	2-10	<38	N/A
37	P1188	Isolated	DMM	14	tremor
38	P1220	2 affected	2-10	<38	N/A
39	P1251	Isolated	2-10	47.1	cerebellar ataxia, cardiomyopathy
40	P1255	Isolated	DMM	4	sensory ataxia
41	P1258-1	3 affected	2-10	>38	pes cavus
42	P1262	2 affected	DMM	IE	pes cavus, wheelchair-confined
43	P1267-1	3 affected	DMM	14,7	scoliosis
44	P1282	2 affected	2-10	50,6	scoliosis
45	P1289-3	2 affected	DMM	13,3	scoliosis

mNCV: motor nerve conduction velocity, DMM: delayed motor milestones, IE: inexcitable, N/A: not applicable/unknown, CSF: cerebrospinal fluid, HSP: hereditary spastic paraplegia

Table 3.1. Clinical findings of the patients enrolled in the study. (cont.)

Nr.	**Patient ID**	**Family history**	**Age of onset**	**mNCV (m/s)**	**Additional findings**
46	P1291	Isolated	at birth	30	pes cavus, tremor, hammer toes, mild spasticity, pyramidal signs, cerebellar ataxia
47	P1302	Isolated	2-10	N/A	sensory ataxia
48	P1306	Isolated	11-20	>38	pes cavus
49	P1319	Isolated	11-20	48	pes cavus, neuromyotonia, intellectual disability
50	P1325	2 affected	2-10	46	pes cavus
51	P1330	10 affected	2-10	36,6	pes cavus, hammer toes
52	P1331	Isolated	2-10	IE	pes cavus
53	P1333	Isolated	2-10	IE	pes cavus
54	P1336	Isolated	21-40	29,6	pes cavus, short stature
55	P1350	Others with HSP	2-10	4.	visual impairment, multicranial <38
56	P1353	Isolated	2-10	15,9	N/A

mNCV: motor nerve conduction velocity, DMM: delayed motor milestones, IE: inexcitable, N/A: not applicable/unknown, CSF: cerebrospinal fluid, HSP: hereditary spastic paraplegia

3.2. Primers

Primers used for variant verification were designed using Primer3 software. Primers used for elimination of CMT1A duplication/HNPP deletion in STR analysis are given in Table 3.2.

Table 3.2. Primers for STR markers used in the analysis of CMT1A locus.

Primer name	**Sequence 5'→3'**	**Tm°C**	**Product size (bp)**
4A_F	CTACTTGCATATGCACTTTC	55.6	118
4A_R	GCACTAAAGTAGCTTGTAAC	51.6	
9A_F	CAACCATCAGTGATTTGATGGTTTA	60.9	167
9A_R	CTGTTCTTCTTAATCCTTAACCAGT	56.5	
9B_F	TCTCAGTCCTGATTTCTTGATTTTG	60.9	115
9B_R	CCAGAGCTAACACCACATTCA	58.8	
20_F	CCTCAGTCATCTTTCTCCTTCT	56.7	302
20_R	TTGGGCAACAGAGCAAAATCC	64.5	
26_F	GCATTCTTGTCTCAGTCCTG	60.6	121
26_R	GTGTCTTCCAGAGCTAACACCACA	62.8	

Primers used for identification of variants in the *GDAP1* gene are given in Table 3.3.

Table 3.3. Primers used for identification of *GDAP1* variants.

Primer name	**Sequence 5'→3'**	**Tm°C**	**Product size (bp)**
GDAP1_1F2	AGCAACCCTCAGTATCTTGG	56.9	618
GDAP1_1R2	CACTGGAGGCGGATTTCTAG	59.8	
GDAP1_F2	GGCTGCTTAGCGGTGTCCA	64.8	330
GDAP1_R2	GGGAACACATAGTTGTGTTG	53.8	
GDAP1_F3	GCTTTTGAGTGTAACAACTCATG	56.7	317
GDAP1_R3	GACCATGAGACATGCTAGGTC	57.2	
GDAP1_F4	CAGGGTAAGCCCAAGGCAGAG	63.4	288
GDAP1_R4	GTAGAACATTTACTCCGTGCA	55.5	
GDAP1_F5	GGCTGAACTCTGTAAGAGTTT	53.0	281
GDAP1_R5	GACCTAAGAATGTTCCCATG	54.5	
GDAP1_F6	CCACTGATACCAGCTGG	52.9	526
GDAP1_R6	CAGAGAGCCACGGGCAATCAC	62.5	

Primers used for disease-causing candidate variant identification and verification in genes analyzed in the study are listed in Table 3.4.

Table 3.4. Primers used for analysis of candidate variants.

Primer name	**Sequence 5'→3'**	**Tm°C**	**Product size (bp)**
AARS_20_F	CTTTCCCTGCATTCCTCCCT	62.7	391
AARS_20_R	GACTGCTCCCAAGTGTGTT	62.1	
AARS_18_F	AGTTGTGGCCCAGATTGAG	60.7	200
AARS_18_R	CCTAGGAAACACTCTGGCC	60.2	
ABCA8_F	TTTATTCGCAAAGGACATG	60.7	325
ABCA8_R	GAAACCAGTGATTACCCGCC	61.6	
ABCD1_7_F	CGATGTGAGCGTGTGGATG	62.4	236
ABCD1_7_R	GTGCACGACGTCCAGGAT	60.7	
ABHD12_1F	GAACTAGAGAGGAGGTGGCC	57.9	377
ABHD12_1R	CTCGGTCCGCTTCCTCATC	63.2	
ADCY4_F1	AGTTCCTGGGTCCTAGTGGG	60.4	213
ADCY4_R1	TCAGGTGGGCAAAAGGCT	61.8	
ADCY4_F2	TCACAACCTGTCCTGAAGAGG	60.3	285
ADCY4_R2	GCCCAAATCCAGGGGTT	60.7	
AHNAK_nF	GCTGGATAGTGCGCATCTG	60.5	382
AHNAK_nR	TATTTCGGGGCCCTTGAG	60.9	
AP4M1_10F	TCCCAAAACAGGAGTCAGGA	60.6	250
AP4M1_10R	GAGAGACCAGAGAGCAACAAG	60.6	
AP4M1_6F	TTGGCTTGGTCAGTAGAGGG	60.2	230
AP4M1_6R	GATCCCAGAGCAAAACCAGA	60.2	
AP5Z1_12F	CCCTGCAAAGCCACCTCTA	61.3	600
AP5Z1_12R	ATGTGGGCAGCAGAGAGAG	59.1	
AP5Z1_17F	GCTGAAGATGCCTAGCGTG	59.7	243
AP5Z1_17R	GCCCTCCTGAGCTCCTATC	58.9	
ARGFX_F	TCACCCACAAAGTACCAGGT	57.9	240
ARGFX_R	ACAAGAGGCAAGAAGACCACT	58.1	
ARSA_3U_F	TCTGCTGTCATCCTGGCTG	61.2	300
ARSA_3U_R	TGGCTGGGTGATCTTGTACA	60.1	
ASAH1_1F	CCAGAGGGCAGGATTTCC	60.6	395
ASAH1_1R	AGGGACAAGGAGCAGTTGAG	59.4	

Table 3.4. Primers used for analysis of candidate variants. (cont.)

Primer name	**Sequence 5'→3'**	**Tm°C**	**Product size (bp)**
ASAH1_5nF	ACTCTCGTTCCTGCCTTCTC	58.6	585
ASAH1_5nR	GGCTCTTCCGTATCTTGATCTG	60.2	
ATL3_ex1_F	ACCCGTCCCTCTCCTCTG	60.2	247
ATL3_ex1_R	GAAACCGAGTGACCCCG	60	
ATL3_ex6_F	GTGGGATGTGAGCAGGGAAT	62.3	298
ATL3_ex6_R	GCTGTAGTTTGCCAATCTGTG	60.3	
ATL3_ex8_F	GTTGTCCCTAGTGAAGAAAAA	59.6	362
ATL3_ex8_R	GTCTCAGTAAGTCAGGAGCA	57.8	
ATP7A_2_2F	ACGGCGTCACTGACTT	58.3	379
ATP7A_2_2R	ACAGACACCTAAGCCTTACA	57.2	
ATP8B3_F	CGGCCAGTTCTGCTTCCT	61.5	249
ATP8B3_R	TTCTCAGTGCGTCCAGGG	61	
ATXN1_F	CCACCACTCCATCCCAGC	62.6	344
ATXN1_R	GTGTGGGATCATCGTCTGGT	60.8	
ATXN2_1nF	GTGCGAGCCGGTGTATG	59.8	481
ATXN2_1nR	ACAGGCCTGACAATCCCAG	61.1	
ATXN7_10F	CACAATGTGGAGTCAGCTAT	57	297
ATXN7_10R	AAGACTCCTTGGGCCTCAA	59.8	
BICD2_ex5_F	AAGCTCTCGGGGTCCATAG	59.2	239
BICD2_ex5_R	GTCCTTCTCGTTGTCCAGG	58.2	
BSCL2_ex1_F	CCTCCTCCTTTCCTCCCTCT	61.1	408
BSCL2_ex1_R	CGGGCGTGGGAAGTAATCTA	62.2	
C10orf113_nF	TGTGACACTGGCTTGAGAGG	60	488
C10orf113_nR	ATCCATGCTTCCCTTTGGTT	60.7	
C12orf49_F	CATAATCAGCCCATCCCGT	60.7	235
C12orf49_R	GTTGGAGATGAGCGAGGAGA	60.5	
C12orf61_F	CCTTGTCCATTCTGTGCAGT	58.7	161
C12orf61_R	TGAGGTTTAAAAGCCAGGAG	58	
C12orf65_F	CCTCGGTAACAGATGGGTCA	60.9	492
C12orf65_R	ATCTCTGGAGGCTGTGGAAC	59.3	
CAPN13_F	CCATCTGGGGCTCACATTT	60.9	236
CAPN13_R	GCTGCAGGGAATGTCTCATC	60.8	

Table 3.4. Primers used for analysis of candidate variants. (cont.)

Primer name	**Sequence 5'→3'**	**Tm°C**	**Product size (bp)**
CBS_nF	ATGGTGCACAAGGAAGAAGC	60.3	589
CBS_nR	CAGAGAGGAAGGGACAGGAG	59	
CDC88C_15F	AGCAGCAGCCACAAGACG	61.4	252
CDC88C_15R	GGCAGTGCTATCGTCCAAGAC	62.1	
CEP290_F	GCCTATGCGTGCTTTTGAAA	61.3	286
CEP290_R	TGTCTCTAGTTGTAGCAATTC	60.3	
COL12A1_F	TGCATGTGGGTGAAGAACAA	61.1	250
COL12A1_R	AGACACAAGAGCAGCAATGAA	59.7	
COQ9_F	GTCCAGAGGGCCAGATGTAT	59	371
COQ9_R	CAAAAGGGAGCAAGACCAG	58.4	
CTDP1_8F	GAAAAGAGGCCGGCAGAAG	62.3	249
CTDP1_8R	AGCTCGCTGTTCTGTGACTCG	63.2	
CYP2U1_2_2F	TGGTTTTATGTCACGAGGCC	60.9	373
CYP2U1_2_2R	ACCTTGTACATCGGGGTTCA	60.2	
CYP2U1_3F	CTGAACTGCCAACTGACCAG	59.5	351
CYP2U1_3R	CCTCACCTCAACTACCCTGG	59.6	
CYP7B1_4F	AGCACATCATTTAGGCTTTCT	58.6	280
CYP7B1_4R	CAGCTATGAGTGATAAACCGA	57.6	
DCTN1_3F	TCTGGTTGGGAGAGTGGAAG	60.2	369
DCTN1_3R	GGGAATATGGTAGTGACGGAA	61.2	
DCTN1_6F	TCTGTCTCCTTCCCTTGCC	60.3	399
DCTN1_6R	CCAAGTTCTAGGTCTTTGCCA	59.4	
DIXDC1_7F	CATGAACTGTACTCCCTCTTTT	59.7	293
DIXDC1_7R	CCTCATTCAGTTCTGACCTCC	59.7	
DMD_ex49_F	CCTTATGTACCAGGCAGAAAT	59.9	300
DMD_ex49_R	GTCAATGGCAAATGTACAACA	61.5	
DNM2_11F	CCGCATTTTCTACCTGTGTG	59.2	334
DNM2_11R	CAGCATGATAGGGACAGGGA	61	
DNM2_2F	GCTGAGGTCGCCCAAATTG	64	290
DNM2_2R	TCCAATGACAGCCCAGGAC	62.1	
DNM2_3nF	CAGCCTGGGTCATTACTTTCA	60.1	372
DNM2_3R	CAACTGTTTGTGAATGGGCA	60.6	

Table 3.4. Primers used for analysis of candidate variants. (cont.)

Primer name	**Sequence 5'→3'**	**Tm°C**	**Product size (bp)**
DNMT1_11F	AGCTTGTGTCAGCCCTTAGG	59.5	274
DNMT1_11R	TGGACTTGAACCCAGAGCC	61.2	
DNMT1_26F	GCCCTAGATGAAAACTGAAAA	60.5	287
DNMT1_26R	GGGGCTTTGTAGATGACTTT	60.5	
DNMT1_32F	CCTGAGTTAACAAGGCGCTT	59.5	486
DNMT1_32R	GGACTACAGGCACACACCA	58	
DNMT1_37F	CCCCACACTCTTTCAGGACA	61.1	292
DNMT1_37R	TCCAGGTTCACAGGCCAA	61.3	
DNMT1_4F	AGCTGTCCTCATTGCCTGAT	59.8	340
DNMT1_4R	TAGCCTCTCCATCGGACTTG	60.4	
DRP2_19F	CAGAGACGAGGACCAGTACC	57.3	247
DRP2_19R	TTGCTCAAGGTCAGACAGCT	58.8	
DST_ex1_F	TGCCACTTTTCACCGTTAGAA	60.7	339
DST_ex1_R	CAAAGAGCTCACCATTCCTGA	60.4	
DST_ex34_F	AGCCATTCTGATCCCGCA	62.8	520
DST_ex34_R	TATACCACCGCCATCGTTTT	60.2	
EGR2_2_F4	AAGTACCCCAACAGACCCAG	58.9	247
EGR2_2_R4	ACTTTCGGCCACAGTAGTCA	58.4	
FBLN5_ex1_F	ATCTGAACCAGCTGTGTCCA	59.3	385
FBLN5_ex1_R	AGAAAGAAAAGTCCAGCGCC	60.9	
FBXO38_15F	ATGGAGGGTACGACATGGAA	60.2	397
FBXO38_15R	ATCGGCTTTGATCTGCTCAC	60.4	
FECH_ex2_F	GCGAGCACTTTAATTTTGTCA	61.5	246
FECH_ex2_R	TTTTCCCAGCACCTTTCCTC	61.5	
FXN_F	GGCAGCATTTGTGGAATCAG	61.6	249
FXN_R	GTCCTTAAAACGGGGCTGG	61.7	
GALC_ex1_F	CCTGCCCGTATCTATCGTGG	62.7	371
GALC_ex1_R	GAGTGGAGCCGGTGGAAA	62.2	
GALC_ex9_F	GGCATGATTCGTCTTCTGG	59.2	444
GALC_ex9_R	GGGAGTGAGAGATGGAACTGA	59.2	
GAN_ex9_F	CCTTGCTGTTCACTGGGTCT	60.3	392
GAN_ex9_R	CGACTGAAAGCACAAAGAA	59.6	

Table 3.4. Primers used for analysis of candidate variants. (cont.)

Primer name	**Sequence 5'→3'**	**Tm°C**	**Product size (bp)**
GCHFR_1F	GCCAGAGCCGGAGTAACG	61.9	231
GCHFR_1R	AGGAGGGAGGCATGAAGGT	61	
GJB3_end_F	TCTTCCTCTACCTGCTGCAC	58.2	492
GJB3_end_R	TAGTGAACTCAGAGTGGGGTC	56.2	
GJB3_st_F	CCTCTAATTCTCTCAGGTAGG	59.8	289
GJB3_st_R	AAGATGAGCTGCAGGGCC	61.5	
GNB4_ex1_F	CTCCTCCATCCTCTGATCATGT	60.5	450
GNB4_ex1_R	TCTTACTTCGCCATGTGAGAG	58.1	
GTF3C5_7F	CCAACTCCCATCTCCAGTGT	60	202
GTF3C5_7R	ACTCATGACCCACAAAAGGC	60	
HINT1_1F	CCGAGATGGCAGATGAGATT	60.2	336
HINT1_1R	CGGGGCAGATAACGAGTAAC	59.6	
HINT1_3F	TGCTCTGTTGGGATTAAGAGTT	58	424
HINT1_3R	TGAATCTCTCCATACACAGGC	57.8	
HK1_ex11_F	GTGGAGAAAGAAAGGGTGGC	61	498
HK1_ex11_R	AAATCGTGCATCACCAGTGT	59	
HK1_ex19_F	GGGGCTGTCTGTGCTTTG	60.4	363
HK1_ex19_R	GGATTTTGCTTTCCTCCCC	60.8	
HSPB1_F1	AAACGGGTCATTGCCATTAA	60.2	538
HSPB1_nR1	CACTGCGACCACTCCTCC	60.4	
HSPB1_F2	CTACCAGCCTGCAGTCCTG	59.6	605
HSPB1_R2	ACAGGTGGTTGCTTTGAACTT	60.1	
HSPD1_ex8_F	TGATGATTCTCTTGCATGGTG	60.5	387
HSPD1_ex8_R	TCATTCTTGGACTCAGAACCC	61.9	
IKBKAP_8F	CCGAGAGACAAGGGACACAT	60.1	299
IKBKAP_8R	GGCACTTACCTTAACCTCATC	59.2	
IKBKAP_9F	GATGAGCTCAGGTAGTGGGA	57.8	300
IKBKAP_9R	GGACTAAGTAGAAGGGATGA	57.5	
INF2_ex17_F	CCTTGTCAGAGACCACCGT	58.7	389
INF2_ex17_R	CCGACGAAAGGTGCCTCT	61.4	
ITPR1_51F	GTGAGAGAACCCTGTTTTGTC	60	236
ITPR1_51R	AAAACAGTGGCAAGGAAGGT	58.7	

Table 3.4. Primers used for analysis of candidate variants. (cont.)

Primer name	**Sequence 5'→3'**	**Tm°C**	**Product size (bp)**
KANSL2_F	GTGTGTTCTTTTGTGGGTCTA	57.2	214
KANSL2_R	ACTAGCACAGAGATTCCCACT	56.8	
KARS_ex9_F	ACTCATCGGGTGGTTGGTAT	59.1	398
KARS_ex9_R	TTAGGGCAGGAGACATCACA	59.2	
KIAA1524_F	CAGTGGCACTTTGAGGGAA	59.8	376
KIAA1524_R	CACAATGCACACTAGACTGAG	59.1	
KIF1B_23F	ACATTAAACAGTGGGAGCAAC	57.8	413
KIF1B_23R	GCAGTGGTTGTGAGTGGATA	57.1	
KIF1B_28F	GCCCAACTCCCTCCTCTT	59.2	395
KIF1B_28R	GGTTTCTGGTTCTCACTCCC	58.6	
KIF5A_26F	TGTGGCCATGTTTGTTTTCC	61.7	355
KIF5A_26R	TTTTATTTGAAGCCTTGGCAC	61.8	
LAS1L_2F	CATTACCGTGTCTCCTCCCA	60.9	400
LAS1L_2R	GAGGTACACGCAGGGTTTTG	60.6	
LRSAM_4F	TCTGGGAGAGCAAGATGGT	58.3	361
LRSAM_4R	ACACACAGCCCACAGAAGTA	56.7	
LRSAM_22F	AGTTGAAACAGCCCCCTCTT	60.1	362
LRSAM_22R	CTCATTTGGCTCAGCAGGTC	60.9	
LRSAM_25F	TCACTTGGGGTCAGGAGTTC	60.09	437
LRSAM_25R	TCAGCTGCTGTGGTAGATGC	60.17	
MARS_17F	GCATGTTGAGAGCCTCCTTG	60.9	366
MARS_17R	CTGGATTGTGGCACTAACCG	61.5	
MARS_20F	GCCGCTTCCTCACTTACAGT	59.5	366
MARS_20R	GTGCTTTCAGTTCTCGGACA	59	
MAT1A_F	CTCCCTTCTCAGCAGTCCTC	59.1	208
MAT1A_R	ATCCACCGGTCCATTCAT	58.5	
MFN2_2F	TTCAATCCCCACCTCCAGAC	62.2	258
MFN2_2R	ATTCTGAAGCATGTCCCTGC	60.2	
MFN2_17F	GTAAGGGTGTGTGTCAAGCG	59.2	234
MFN2_17R	CACATGGCACTTAGGGCTG	60.3	
MFN2_6F	GACGGTAACTCCTCCTCTGC	58.9	397
MFN2_6R	GGATGGGAGAGGGGAAAGA	61.3	

Table 3.4. Primers used for analysis of candidate variants. (cont.)

Primer name	**Sequence 5'→3'**	**Tm°C**	**Product size (bp)**
MFN2_9F	CCTCTGTGTGTTCCAGGAGT	57.7	173
MFN2_9R	GCTCTCTCCACCTATCTGCA	58.1	
MGRN1_4F	GTCCACATAGCCACCTCCAC	60.4	385
MGRN1_4R	CGTGGTAAAGTCCTGGGAGT	59.4	
MME_ex5_F	TGGTGCCAAACTATGCCTAGA	60.6	273
MME_ex5_R	GTCCAAGAAGCACCTAAAGCA	59.5	
MME_ex7_F	GGTCACCCCATAAACAGCAA	60.8	322
MME_ex7_R	TGTGTGATTTTAAGTCCCTGT	59.5	
MORC2_11F	GTCCTGGAGCCTACACACAAC	59.6	242
MORC2_11R	CCCAGAACTTGATGATTCCCC	62.8	
MORC2_4F	GCTTCCCTTAAAGTGCCTGC	61.2	299
MORC2_4R	ACAGAAATCTTTTGTCCTGC	61	
MPV17_2F	AGTGGAGGTCAGCAGATGTC	57.8	246
MPV17_2R	ACCACTGTTGAGTCCACTGA	56.5	
MPV17_nF	TGCTCAATGCAAAGTTCCTGG	63.5	452
MPV17_nR	TGTGAGAGTCCAAGGGAAGC	60.4	
MPZ_3F	AGCTGTGTTCTCATTAGGGTCC	59.6	432
MPZ_3R	GCATTGAGGATGTAGGACTCC	65.3	
MROH8_1F	CGAGTGAAATGAATGAGGCC	60.6	445
MROH8_1R	TAGAACTCATCCTGGCCCG	61.2	
MTMR2_13F	AAGTCAAAATTCAGCCTGCAA	61.1	390
MTMR2_13R	ATGGGGAAGGTCATGTTTCAT	60.4	
MTMR2_15F	AAGGTGCCATTGGTTCCAAC	62.1	368
MTMR2_15R	GATGGGTTCTAAATTCCGAAG	60.2	
MYBPH_5F	TGGAGTTAAGGAGGTGTGGG	60	285
MYBPH_5R	CACTGTTCCCCTGGCTCC	61.7	
MYH14_10F	GTTAAGACCACACATCGGGG	60.2	245
MYH14_10R	GATGCTCTCTACGTGGGACA	58.8	
MYH14_7F	GGGTTTGGGCTGTTGTTCA	61.9	214
MYH14_7R	GTGCTTTCCATACTCAGTGCTG	59.9	
NDRG1_4F	TCCCTTGCCCCATGAAAC	61.8	578
NDRG1_4R	GTGACGGCTGCACAACAAT	60.8	

Table 3.4. Primers used for analysis of candidate variants. (cont.)

Primer name	**Sequence 5'→3'**	**Tm°C**	**Product size (bp)**
NEB_F1	AAACAGTATTCCCCGACCCC	62.2	483
NEB_R1	CATCAGGCAAAGCAATGGG	62.5	
NEB_F2	CTGGCCCTCTGGAGTGTTTA	60.2	279
NEB_R2	GACATCCTTGCAGCAGACG	60.6	
NEFH_4F	AAAATCCCCAGCCGAAGT	59.5	685
NEFH_4R	GGCTTCTGGAGACTTCACATC	58.9	
NEFL_1F_end	CTGAGGAATGGTTCAAGAGCC	61.1	301
NEFL_1R_end	CCCCTGGTCTCCACTTTCTG	62	
NEFL_ex1_1F	CCCGGCGTATAAATAGGGGT	62	496
NEFL_ex1_1R	GGCTTCCAGGACCTTGTTCT	60.6	
NTRK1_5U_F	TGGTTCCAGAGCCCATTCT	60.6	380
NTRK1_5U_R	CAATGACCCAACTCAGCACA	60.7	
NTRK1_15F	CTGTTCCGCTCCTCCATC	59.3	493
NTRK1_15R	GCTCTCAGTGGTCTTGGGAT	59.3	
NTRK1_6F	TGGGCTCCAGGTCATTGAG	62.2	298
NTRK1_6R	GCTCTGCCTGGACCTCTTG	61.1	
OPTN_ex2_F	TGGTTCATCAGATCAAGTCCA	60	391
OPTN_ex2_R	CAGGCAAAACACCAATCCA	60.5	
OPTN_ex7_F	GGTTCAGCCTGTTTTCTCCT	58.4	367
OPTN_ex7_R	TGCTCACACATTAACTGGAAC	59.2	
OR2C1_F	CCTCTTCTCCTATTTGCTGAC	59.4	267
OR2C1_R	AATGCCATCACCACCAGC	60.5	
OR5K1_F	CCACTGCAGTACCACATCATG	60	352
OR5K1_R	AAAAGTGGGATGCACAGGTA	58.1	
PDCD6IP_F	GGGTGCTAACTCCATTGCTG	60.7	288
PDCD6IP_R	GGATTTCTCTATTTCGTTGC	58.8	
PDE11A_F	GAGCCAGAGAAGGAAGGGG	61.3	243
PDE11A_R	CAAACAACTCTGGGTGCCTG	61.7	
PDK3_ex2_F	TAGTAACCGTGCTACCGTGG	58.7	288
PDK3_ex2_R	TCTCGCTGCCAAATGTTCAC	62.3	
PIK3IP1_nF	GGGGCTTCTTTTCCTCACAG	61.1	597
PIK3IP1_nR	TAGCCTCACCCCAGCCTC	61.3	

Table 3.4. Primers used for analysis of candidate variants. (cont.)

Primer name	**Sequence 5'→3'**	**Tm°C**	**Product size (bp)**
PLCG2_F	GCTCAAAGGCCTAAACTTGG	59	257
PLCG2_R	GACAGGCGTATTCTCAGAGCT	58.7	
PLEC_ex32_F	TTTGCTTTGAGGGCCTGC	62.4	396
PLEC_ex32_R	CTGTCACAGCCTTCTCGGC	62.1	
PMEL_F	CTTCTTCCTTGCTTTTCATTC	59.4	244
PMEL_R	CTGCCTTCTCTTGCCCTACA	60.5	
PMP2_ex2_F	TGGCTATGCTCTCTTGGTCA	59.5	280
PMP2_ex2_R	TTCCTCTCTCTCAAGCAGCC	59.8	
PMP22_5UF	CTGCCCTCCCTCTCTCCTG	62.4	323
PMP22_5UR	CTCACTGGAAGATGCCCACA	62.3	
PMP22_1F	AAAGATGTTCCGTTGCAGGC	62.5	515
PMP22_1R	CTCAAAGCAACTGGAAGGGG	62.1	
PMP22_2F	GCCTTTCTCCTTCCCCTT	58.2	279
PMP22_2R	AACGACATTCTGGCTTGTGT	58.2	
PMP22_3F	CTTCTGCTGCCTGTGAGG	58.1	409
PMP22_3R	AAGCACCCACCCTCACTT	58.1	
PMP22_4F	GCCATGGACTCTCCGTC	57.5	267
PMP22_4R	TTTTCCCTTCCTCCCTTC	56.6	
POLN_ex3_F	TCAAGAGGCTTCAGTTCTACA	59.7	476
POLN_ex3_R	CACTTACCACTGGAGGGGAA	60	
POLQ_F	AGTCTGGCTGCAAATGTGAG	59	236
POLQ_R	GCATACCCTCTCGATGACC	58	
PPFIBP2_F	GCAAAAGAGGAAGCACAGTG	60.6	228
PPFIBP2_R	AAAGGAAAGTGGGTCAAGCC	60.5	
PRNP_ex1_F	CTGGTTCTCTTTGTGGCCAC	60.7	396
PRNP_ex1_R	ATGTATGATGGGCCTGCTCA	61.4	
PRX_4F_end	CTCAGGCAAGGTAGAGGTGG	59.9	386
PRX_4R_end	CGGCTGTGGACACCTTCA	61.9	
PRX_4F_st	GAAGGGGCTGTGTCGGTAG	60.7	289
PRX_4R_st	CTACAACTTCAGGAGCAGCG	58.8	
PSME4_nF	CCTGGCTGGGTTTCGTATTT	61.2	593
PSME4_nR	CTGTGGTGGGTGCTCTGTAG	59.3	

Table 3.4. Primers used for analysis of candidate variants. (cont.)

Primer name	**Sequence 5'→3'**	**Tm°C**	**Product size (bp)**
RBM20_F	ACATGATCGCAAACACCACC	61.8	240
RBM20_R	GCCTCGTCTTTCCTCCTGG	62.2	
RBM6_F	GAGAAGAATCCACACATGACCA	60	289
RBM6_R	ACATCACGGTACTCCATGCTT	59.5	
RFC1_3F	ACTGACAGTGTTTTTGCCTGT	57.4	253
RFC1_3R	GGCTGAGGCAGGAGATTCAC	62,3	
RNF170_1F	GAGCAAGAGACTCCATCCAAA	59.4	334
RNF170_1R	CTGACCACAACTGCCACAAG	60.3	
RNF170_4F	AAGGGTTGGCTGGATGAAGT	60.9	354
RNF170_4R	GGTGACATCAAAGAAGATTTG	60.3	
RNF170_5F	GCTTGTTGACACTTTAGTTGC	59	401
RNF170_5R	CCAAACAAGGCTTCAGGTACA	60.2	
RTN2_ex6_F	GGAAAGGGAGGTGAGGAGAC	60.1	280
RTN2_ex6_R	TTCTCACTGGAAAGGGTTGG	60.1	
SACS_8_F	ATGATGATTGCTGTTCCTTTCC	60.3	362
SACS_8_R	GTTGACTACACCATCACACCA	57.3	
SACS_9_F1	ATACTGCCAAACTCCCAGCA	60.7	288
SACS_9_R1	CCATCTGTTCCTGTGATATCT	60.7	
SACS_9_F2	GCAGCAGTTGTTACAGTTTGC	58.6	491
SACS_9_R2	ACGTCGTTATGTTGCATATGT	58.5	
SACS_9_F3	GCAGTCAGGACAAAGAGAGC	61.5	214
SACS_9_R3	CCACAAAGCAGGTCCATGAC	61.5	
SBF2_ex21_F	TGCTGGGTCATAATGGTAATT	59.8	299
SBF2_ex21_R	ACATCCTTTCCTGGCACACA	61.5	
SCN11A_10F	CTCTCAGGTCGGGGTCATTT	61.4	390
SCN11A_10R	TGGATGCATGAAAGTATGTGC	59.6	
SCN11A_14F	GCGATCTGATGGCTATGTTCA	61.2	595
SCN11A_14R	TGCATTTGAGAGGCATGTAGG	61.2	
SCN11A_21F	AGAGATCAAGCCCTGCACAT	59.8	557
SCN11A_21R	TGAGGCTCAGCAGTCAATGA	60.7	
SCN11A_6F	CATAGGCTAGGCTGGAGTCC	58.9	429
SCN11A_6R	AGTCCTCCCTTGCTGCTAAG	58.7	

Table 3.4. Primers used for analysis of candidate variants. (cont.)

Primer name	**Sequence 5'→3'**	**Tm°C**	**Product size (bp)**
SCN9A_12F	AGCCATAATTTGAACCCAGCA	61.7	542
SCN9A_12R	AGATCACCCAACATCTGTCTTT	60.4	
SCN9A_20F	TCCTGTTGAGTTGCTTTTAGT	57.2	351
SCN9A_20R	ACACACACATACATAAACAGC	56.3	
SEC23B_nF	AGTAAATTGCTAAGTACTGGG	55.7	494
SEC23B_nR	TGATGCCTCAAATGCTTTCTG	63	
SELO_F	TTTTCACAAGGGGCTGGG	62	246
SELO_R	CACTGACCTCCCGGAAGAA	61.2	
SEPT11_F	GGACACTTTGTTCAACACCAA	59.9	240
SEPT11_R	GGCCTTTAAATTTACCTGGGA	59.3	
SEPT9_ex1_F	GGGTTCTATGCGCATCTC	56.7	350
SEPT9_ex1_R	GAACTCGACCTGCAGTGTG	57.9	
SEPT9_ex3_F	ATGAAGGACGGGAAGAGACC	60.5	250
SEPT9_ex3_R	TGGAATTTCTGGGTGGAGCT	61.9	
SEPT9_ex7_F	TCAGCAAGCCAGACCTCC	60.1	256
SEPT9_ex7_R	GGGATGAAGTAGAGGCAGCA	60.4	
SETX_ex20_F	CCCACATCACCACACAGAAA	56.2	298
SETX_ex20_R	TGACACTAGGCAGAGAGATGT	55	
SETX_ex3_F	CAGAATAGCCCAAGGAGCCT	60.7	376
SETX_ex3_R	CCTACCCTCTGAGATCCCCT	59.5	
SETX_ex8_F	CTTGACAAGAGAACAGGCCC	59.8	347
SETX_ex8_R	CTGTTGAAACGTGCTGCTCT	59.2	
SH3TC2_11F	CCTGCAGGCTGTACGACTCT	60.6	692
SH3TC2_11R	CTTCCTTTGGCTGATGAGGA	60.3	
SH3TC2_11_3F	TAGGTCCTCAAATGCTCC	59.6	237
SH3TC2_11_3R	GATAGGTCCTCAAATGCTCCA	59.1	
SH3TC2_11_2F	GCCTATCTCTTAGCCAGCCA	59.6	368
SH3TC2_11_2R	GCCAACCAGAGAAACACCTG	60.7	
SH3TC2_11_1F	GGCTTTTCTGGATCATGAGGG	63.1	897
SH3TC2_11_1R	TGCTCGAGGTACACTTTGGA	59.4	
SH3TC2_ex14F	GGGGGACTTTAGCAGAGGAT	59.5	331
SH3TC2_ex14R	AGGAGAAGAGGGACTCAGGC	60	

Table 3.4. Primers used for analysis of candidate variants. (cont.)

Primer name	**Sequence 5'→3'**	**Tm°C**	**Product size (bp)**
SH3TC2_ex15F	GCTTCTGTTCCTAGGCTGGA	59.09	244
SH3TC2_ex15R	TGCGGTGTTATTGCTTTGCT	59.04	
SH3TC2_ex2F	TCCATGCCACTAATCCTGGA	61.4	241
SH3TC2_ex2R	AGGGCTTGTCTTTGGCATTT	61	
SH3TC2_int10F	CCCATCCTGACCTAACACCA	60.8	383
SH3TC2_int10R	TCCGGGTCATCAAGGTCAT	61.3	
SHROOM3_F1	GAATGGATCTGGCAGGCC	61.6	217
SHROOM3_R1	GTGGGTGCTCTTTCTCTCATT	61.2	
SHROOM3_F2	GCCACCTCCTTTCGACG	60.3	348
SHROOM3_R2	GCTGCTCTCCGGGAAAC	59.4	
SLC26A6_F	GGGATGCCTTCACTGTGTC	59	179
SLC26A6_R	GTGGGTCCTAGGTGCTGAG	58.2	
SLC5A7_1F	CTGGTTTATTCCTGGCTGCC	61.9	399
SLC5A7_1R	GACCAACATTTGCTTTGTCAC	60.9	
SMKR1_2F	GGCAAGTCTCATGGGAAGAAA	61.5	209
SMKR1_2R	CCCAGGTCCTGTTGTCTGTAA	58.6	
SPG11_10F	AGGACAAGAAAAGGAAAGGGT	58.3	487
SPG11_10R	AACCTTTGCCAAACATTCTG	57.7	
SPG11_12F	CACTACCACATACTCTTCTCAA	57.3	378
SPG11_12R	TTCCCTACATTAAATGCCCTC	58.1	
SPG7.4AF	AAGCTCTGGATGTCGCCCGT	66	379
SPG7.4AR	AGGAAATGCTGCCTCCGCTG	62.8	
SPINK8_F	TCCTGGTCAGTGAGGGATCT	59.6	250
SPINK8_R	GAACAGCACTTCCACTTCCA	58.9	
SPTBN_18F	CCTTGAGTCCAGAAGCCAG	58.5	298
SPTBN_18R	AGGCTGAGAAAGGGTCATCT	57.9	
SPTLC1_6F	AGAAGTTGTATGGGCCTAGAA	57.5	586
SPTLC1_6R	CCACAGAGCTGCACAAAGAA	60.2	
SPTLC1_9F	TTCAAATTCTTCACTGCTCTG	59.6	462
SPTLC1_9R	ACACCAAAGTTTCGTGACCC	59.9	
SPTLC2_1F4	TACTTTTCCCTGGGCTCCG	62.4	965
SPTLC2_1R4	TCAGGGGTTTGAGAAGGGAC	61.4	

Table 3.4. Primers used for analysis of candidate variants. (cont.)

Primer name	**Sequence 5'→3'**	**Tm°C**	**Product size (bp)**
STARD_23F	AGGCTTGGTCCCATCAACTA	59.6	248
STARD_23R	ATGGACATCAGTGGGCTCTC	30.1	
SULT1B1_F	ACTTAGATCTCCATGTGCGC	57.9	290
SULT1B1_R	TCACAATGTCATCTGGTCTGC	59.7	
SYNE2_F	TGTTTGACTGTGGGCAAGTC	59.7	235
SYNE2_R	TTTGTAACGTCTTCACAGCTA	59.5	
TAF1A_6F	ACCCATCAGTAAACTTATGCT	57.82	393
TAF1A_6R	CTGGAGCCAACTTTCTCTGT	57.44	
TBP_2nF	CAGCCAGCCTAACCTGTTTT	59.4	376
TBP_2nR	GGTGCAGTTGTGAGAGTCTG	56.9	
TBP_F	CACAGCCTATTCAGAACACCA	58.8	253
TBP_R	GAGTGGAAGAGCTGTGGTG	56.8	
TFG_ex1_F	TGTTGCCTCCAGACCATTT	59.1	498
TFG_ex1_R	GAGTTTGAGGTGACACTGAGC	57.5	
TGM6_10F	CAGGGTCCCGGAAAGAGAG	62.1	288
TGM6_10R	TGCGGGTATAGAGGATGGTG	60.9	
TMEM216_F	CCACTCAGGGAAGATACTCTC	62.5	238
TMEM216_R	TTCTCAGGACAACTTGCCCC	62.5	
TMX4_4F	GTTCAGATGGCGTTCAGATGT	60.1	364
TMX4_4R	TGGCCATGAGTAATCTGGGTA	60.3	
TOX2_nF	TAGACCTACAACGGCCAGAG	58	388
TOX2_nR	CAACTCCAAGCAACCAGGTA	58.8	
TPBGL_F3	TCGACCTCAGCCACAACC	60.8	840
TPBGL_R3	TGTCTCATCTCCACGGCTTC	61.4	
TRPV4_1_1F	TCATTACAACGGTGGCTTTGA	61.4	368
TRPV4_1_1R	CTGGAACTTCATGCGCAGAT	61.3	
TRPV4_8F	GAGAGTGAAGGAGGAGGCTC	58.1	379
TRPV4_8R	AGAACGTGGGATTGGAGG	58.4	
TTN_F2	GTTGTGAAAGTGCTTGGTAAG	58.9	502
TTN_R2	GGTCCAGGAGTTTCTAAAGCA	58.4	
USP47_F	TGTTACTGGGCTTAGCTATTC	60.2	485
USP47_R	AATAATGTTGCTGTGGATGTCC	58.8	

Table 3.4. Primers used for analysis of candidate variants. (cont.)

Primer name	**Sequence 5'→3'**	**Tm°C**	**Product size (bp)**
USP8_14F	GCCAACATGTTATCCTAAAGC	60	300
USP8_14R	GCAGCAGAAAACTAATGGACT	58.7	
USP8_F1	CTGCACAGTTCGTTTCTTAGA	57.9	472
USP8_R1	CCATGCTCTTAACCATTATTG	58.7	
USP8_F2	AGCCTGGAAGTTCACATTTTC	59.3	281
USP8_R2	TCAGTGGTCCCATTCTCTCA	59.2	
VAPB_4F	GCAGCAAGACTTCAGGGTT	59.5	476
VAPB_4R	GCTGATTTCATAAAGGCCCA	60.8	
VWA2_F	GGCCACATACAGCAGGGA	60.7	232
VWA2_R	AACCTCATCCTCGGAGTGTG	60.1	
WDR76_F	TAAACCCGGCCTGATCCT	61.2	276
WDR76_R	CAGATGTCTAATGTATGCACTG	60.2	
WNK1_F1	AGACAGATACCAGAGAGTAACC	55	391
WNK1_R1	GAACTGGGTCATTGGTTATAAC	55.2	
WNK1_F2	ACTGTCTTTCTGCCCTTTTACA	58.1	284
WNK1_R2	ACCAATGCTCCTCAGTTATCAA	58.7	
ZNF595_4F	CAGAATGTGGCAGATCGTTTT	60.1	453
ZNF595_4R	GGCTCCTGGACTGTCTAAAGG	60.3	
ZNF814_F	TTCACGCCGGAGAAAGAC	59.9	910
ZNF814_R	CAGAATGTAGAGCTGTGGGT	57.1	

Primers used for quantitative PCR (qPCR) analysis of gene expression of candidate genes were designed using NCBI Primer Blast tool. The sequences of primers used for qPCR analyses are listed in Table 3.5.

Table 3.5. Primers used for qPCR analyses.

Primer name	**Sequence 5'→3'**	**Tm°C**	**Product size (bp)**
ACO1q_F	CTGCAGGACTTTACGGGTGT	59.97	107
ACO1q_R	GCAGGGCAGACAGGGTTTAT	60.03	

Table 3.5. Primers used for qPCR analyses. (cont.)

Primer name	**Sequence 5'→3'**	**Tm°C**	**Product size (bp)**
ACTBq_F	GTTGCTATCCAGGCTGTGCT	60.39	107
ACTBq_R	TACCCCTCGTAGATGGGCAC	60.76	
AIFM1q_F	AATGGCTAGCTCTGGTGCAT	59.45	192
AIFM1q_R	GCAGATAACGCGGCCTTTTT	59.83	
APTXq_F	CACACTGTGGGGGAAAAGGT	60.11	121
APTXq_R	AATCCTGGCTGATCACATGAAG	59.8	
ATP8A1_qF_n	GGGAAACTCTCAGTCGTCACT	59.39	177
ATP8A1_qnR	GAGGAGAAACCCGACAGCAA	59.97	
ATP8A2_qnF	GAGATGCTGAACGGCGCA	60.82	223
ATP8A2_qnR	TGATCTGGTTGTCGCGGAAT	59.75	
ATP8B2_qnF	CAACACCGTTGTGCCCATTT	59.9	149
ATP8B2_qR_n	CCAGCTCCTCGTTTAGGGTG	60.11	
ATP8B3_qF_1	ACGACCCGACCTAAGGAGAA	59.96	199
ATP8B3_qR_1	GGTACAACAGCTGGTCTGGG	60.32	
ATP8B3_qF_2	ACTTCGGCTACGTGTTCCTG	60.04	198
ATP8B3_qR_2	GCAAGCGTTCGAAGATGACC	59.9	
ATP8B3_qF_3	CCCTGGTCAAGAAGTACCACC	60	144
ATP8B3_qR_3	GCACGAAGTCGCTGTTCTGA	60.94	
ATP8B3_qF_4	ACGGTGCCAACGACATCAA	60.23	101
ATP8B3_qR_4	GCACGAAGTCGCTGTTCTGA	60.94	
CHCHD4q_F	GCAGGAAGGGAAGGATCGAA	59.46	101
CHCHD4q_R	CCTCGTATGGATCGTTGGGG	59.97	
EXOC3_qF	ATCGTGAGCCTCTTGACGTG	60.11	179
EXOC3_qR	AGCCAGGCGATGATGTTTGA	60.04	
EXOC4_qF	GCAAAAGCAAAGACCCCTCG	60.04	187
EXOC4_qR	TGGTATGTGCGAATGGCTGT	60.04	
FXNq_F	ACGTGGCCTCAACCAGATTT	59.89	136
FXNq_R	GTCCAGCGTTTCCTCTGCTA	59.75	
GAPDHq_F	ATTCCATGGCACCGTCAAGG	60.68	102
GAPDHq_R	TCGCCCCACTTGATTTTGGA	59.89	
NFU1q_F	CGCAGGCGGTTCTGTCATA	60.15	99
NFU1q_R	GGCTGCAGGTAGTGGGAAAA	60.25	

Table 3.5. Primers used for qPCR analyses. (cont.)

Primer name	**Sequence 5'→3'**	**Tm°C**	**Product size (bp)**
SACSq_F	GGCCGCGAGTTATCTGACTG	60.8	119
SACSq_R	GGCGTTGTCTGACCAAATCG	59.8	
SDHAq_F	AGCACCTGAAGACGTTCGAC	60.32	114
SDHAq_R	GTGCCTCTGCTCCGTAGATG	60.25	
SEPT10q_4nF	TGTGAATACAGTGGGATTTGGT	57.62	159
SEPT10q_4nR	AGACACACATGGATGCGAGAA	59.72	
SEPT10q_F	TTCTCTGTGTGGGGGAAACTG	59.86	99
SEPT10q_R	TTGGGCAAAAATGTGAGGATTCA	59.35	
SEPT11q_CtF	AGGCAGAGAAAGAGCTTCACG	60.34	158
SEPT11q_CtR	CTGGGCCTGGGACTGTAGTA	60.33	
SEPT11q_3F	TGTTGGTGAGACAGGCATTGG	60.82	112
SEPT11q_3R	TCTGGCTTTTAACCGAACACCT	60.16	
SEPT11q_4F	TGCCCCTACTGGACATTCAC	59.38	107
SEPT11q_4R	TGGCAATGGTGTCAGCTTTTG	59.93	
SEPT11q_F	AACTGGTCAGCAATGGGGTC	60.25	106
SEPT11q_R	CCAACCACTGCAAATGGGAG	59.4	
SEPT12q_F	CATCATGGTGGTGGGGCAAA	60.9	140
SEPT12q_R	CATGGGTCAGTGAATGCAGC	59.55	
SEPT14q_5nF	CTGCTCAAGCGAACTCCTCA	60.04	95
SEPT14q_5nR	TAGTGACGGCCTCTGACCAT	60.04	
SEPT14q_F	ATGCCCACACAAATACCTGCT	60.27	111
SEPT14q_R	GCTCACCAACTGATTGGGCA	60.9	
SEPT1q_F	GATGGAGCTACAGTGGGACT	58.51	134
SEPT1q_R	TTGTCCATGACTCCGCCAG	59.7	
SEPT2q_F	GTTGAAATTGAAGAGCGAGGG	57.52	96
SEPT2q_R	TGTCTTAAAACAATCTCTGCAGTT	57.06	
SEPT3q_3nF	TCGGCATCGACACCATCATC	60.25	116
SEPT3q_3nR	CGTGTTGACCAGCGTTGATT	59.41	
SEPT3q_F	AATCAACGCTGGTCAACACG	59.41	109
SEPT3q_R	TGCCCGATAGCTTTGATCTCC	59.93	
SEPT4q_2nF	CCCAGTCCTCTGACAACCAG	59.68	139
SEPT4q_2nR	AGGGTTGCAAAGCCCACATA	59.89	

Table 3.5. Primers used for qPCR analyses. (cont.)

Primer name	**Sequence 5'→3'**	**Tm°C**	**Product size (bp)**
SEPT4q_F	TTCTCAGGAAATGCGAGCTG	58.27	102
SEPT4q_R	ATCATCATAGAGGTCCGGGG	58.06	
SEPT5q_7nF	CGCCAAAGCTGACTGTCTTG	59.76	122
SEPT5q_7nR	CATCCTCGTCCGAGTCACAC	60.18	
SEPT5q_F	GCATCAGCCAGACGGTAGAG	60.25	82
SEPT5q_R	TCCACGATGGTGAGCTTCAG	59.75	
SEPT6q_7nF	GACCCTGACAGCAAACCCTT	60.18	118
SEPT6q_7R	TGACTCGCTGGACGAACATC	60.11	
SEPT6q_F	AAATTCGAAGGGGAGCCAGC	60.68	104
SEPT6q_R	ACGATCGTGAGCTTTAGCCT	59.18	
SEPT7q_F	GAACACACATGCAGGACTTGAA	59.38	139
SEPT7q_R	GCCAGAGGGCTCTTAGTCA	58.4	
SEPT8q_F	GCCTCTACTTCATCACGCCC	60.53	126
SEPT8q_R	CGCTCTTGGAGATGGTGTCA	59.75	
SEPT9q_F	GGCTACGTGGGGATTGACTC	60.18	112
SEPT9q_R	AGGTGGATTTACCCAAGCCG	60.03	

Primers used for Gateway cloning of candidate disease-causing gene *SEPT11* into donor vector pDONR207 are given in Table 3.6.

Table 3.6. Primers used for Gateway cloning of *SEPT11* gene into pDONR207 vector.

Primer name	**Sequence 5'→3'**
Sept11_GW_F	GGGGACAAGTTTGTACAAAAAAGC AGGCTTCATGGCCGTGGCCGTG
Sept11_GW_WT_R	GGGGACCACTTTGTACAAGAAAGC TGGGTCTGTGAAGCTTGCATT
Sept11_GW_P1251_R	GGGGACCACTTTGTACAAGAAAGC TGGGTCACAATGGTTAACTTCAGC

3.3. Antibodies

Primary and secondary antibodies used in Western-blotting and immunofluorescence assays are listed in Table 3.7.

Table 3.7. Antibodies used throughout the study.

Antibody type	Antibody name	Application	Host	Dilution	Supplier	Product number
Primary	α-β-actin	WB	Goat	1:1000	Santa Cruz	sc-47778
Primary	α-ATP8B3	WB	Rabbit	1:1000	Thermo Fisher	PA5-49285
Primary	α-F-actin	IF	Mouse	1:200	Abcam	ab205
Primary	α-FXN	WB	Mouse	1:500	Abcam	ab110328
Primary	α-GFP	IF	Mouse	1:1000	Santa Cruz	sc-9996
Primary	α-NFU1	WB	Rabbit	1:1000	Thermo-Fisher	PA5-77130
Primary	α-SEPT9	WB, IF	Rat	1:500, 1:200	Sigma	SAB4200191
Primary	α-SEPT11	WB	Rabbit	1:1000	Abcam	ab183537
Primary	α-vinculin	WB	Sheep	1:1000	R&D Systems	AF6896
Secondary	α-ms-488	IF	Donkey	1:500	Invitro-gen	A21202
Secondary	α-ms-555	IF	Goat	1:500	Invitro-gen	A21424
Secondary	α-ms-647	IF	Goat	1:500	Invitro-gen	A21235
Secondary	α-ms-HRP	WB	Goat	1:1000	Cell Signaling	7076
Secondary	α-rb-488	IF	Goat	1:500	Invitro-gen	A11034
Secondary	α-rb-HRP	WB	Goat	1:5000	Santa Cruz	sc-2004

WB: Western-blotting, IF: Immunofluorescence assay, ms: mouse, rb: rabbit

Table 3.7. Antibodies used throughout the study. (cont.)

Antibody type	**Antibody name**	**Application**	**Host**	**Dilution**	**Supplier**	**Product number**
Secondary	α-rat-555	IF	Goat	1:500	Invitrogen	A21434
Secondary	α-rat-HRP	WB	Goat	1:5000	Novus Bio	NB7115
Secondary	α-shp-HRP	WB	Donkey	1:5000	R&D Systems	HAF-016

WB: Western-blotting, IF: Immunofluorescence assay, ms: mouse, rb: rabbit

3.4. Cell Culture Mediums

Mediums used for maintenance and cryopreservation of cell lines are given in Table 3.8.

Table 3.8. Cell culture mediums and their ingredients used in this study.

Medium	**Content**
Complete AMEM culture medium	Minimum Essential Medium Alpha (AMEM) 1% penicillin/streptomycin 10% fetal bovine serum
Complete DMEM culture medium	Dulbecco's Minimum Essential Medium (DMEM) 1% penicillin/streptomycin 10% fetal bovine serum
Freezing medium	Minimum Essential Medium (MEM) 10% DMSO 20% fetal bovine serum

3.5. Buffers and Solutions

Buffers and solutions used in STR analysis, Western-blotting and IF assays are listed in Table 3.9.

Table 3.9. Buffers and solutions used in the study.

Buffer or Solution	Recipe	Application
2x Protein Sample Buffer	100 mM Tris-HCl (pH 6.8) 4% SDS 0.2% bromophenol blue 20% glycerol 200 mM β-mercaptoethanol	Western Blotting
6X Protein Sample Buffer	300 mM Tris-HCl (pH 6.8) 12 mM EDTA 60% glycerol 12% SDS 6% β-mercaptoethanol 0.04% bromophenol blue	Western Blotting
30% Acryl:Bis Solution	29% Acrylamide 1% N,N'-methylenebisacrylamide	Western Blotting
$AgNO_3$ Solution	0.1% $AgNo_3$	Silver Staining
Ammonium Persulfate	10% APS (w/v) in dH_2O	Western Blotting
Blocking Buffer	1-5% skim milk powder or BSA in TBS-T	Western Blotting
Blocking Solution	1% BSA 0.05% Triton-X dissolved in PBS	IF Assay
Cell Lysis Buffer	20 mM Tris-HCl (pH 7.5) 150 mM NaCl 1 mM EDTA 1% Triton-X	Western Blotting
Developing Buffer	1.5% NaOH 0.015% formaldehyde	Silver Staining
Fixation Solution	4% PFA (pH 7.4) in PBS	IF Assay

Table 3.9. Buffers and solutions used in the study. (cont.)

Buffer or Solution	**Recipe**	**Application**
HEPES-buffered Saline (2X)	50 mM HEPES 280 mM NaCl 12 mM dextrose (D-glucose) 10 mM KCl 1.5 mM $Na_2HPO_4.2H_2O$ 10 M NaOH for pH 7.05	Transfection
Nuclei Lysis Buffer	400 mM NaCl 2 mM EDTA (pH 7.4) 10 mM Tris-HCl (pH 8.0)	DNA Isolation
Permeabilization Solution	0.5% Triton X-100 in PBS	IF Assay
RBC Lysis Buffer	155 mM NH_4Cl 10 mM $KHCO_3$ 1 mM EDTA (pH 7.4)	DNA Isolation
Running Buffer	25 mM Tris 250 mM glycine 0.2% SDS	Western Blotting
Stripping Solution	62.5 mM Tris-HCl (pH 6.8) 2% SDS 0.7% β-mercaptoethanol	Western Blotting
Tris Buffered Saline (TBS)	20 mM Tris-HCl (pH 8.0) 150 mM NaCl	Western Blotting
Transfer Buffer	25 mM Tris 200 mM Glycine 20% Methanol	Western Blotting
TBE Buffer (10X)	20 mM EDTA (pH 8.3) 0.89 M Tris-Base 0.89 M Boric Acid	Electrophoresis

The recipes for all the gels used throughout the study are given in Table 3.10.

Table 3.10. Gels used in the study.

Gel Type	**Recipe**
Agarose Gel for separation of DNA (1%)	1% (w/v) agarose in 0.5X TBE Buffer 0.2 μg/ml Ethidium Bromide
Polyacrylamide Gel for separation of DNA (10%)	30% Acrylamide:Bisacrylamide (29:1) 12% 5X TBE Buffer 1% TEMED 0.1% APS
Polyacrylamide Gel for Western Blotting (10% Running Gel)	10% Acrylamide:Bisacrylamide (37.5:1) 375 mM Tris-HCl (pH 8.8) 0.1% TEMED 0.1% SDS 0.1% APS
Polyacrylamide Gel for Western Blotting (4.5% Stacking Gel)	4.5% Acrylamide:Bisacrylamide (37.5:1) 125 mM Tris-HCl (pH 6.8) 0.1% TEMED 0.1% SDS 0.1% APS

3.6. Vectors

Maps of the vectors used in Gateway cloning of human *SEPT11* gene are obtained from SnapGene Plasmid Database. The vector map of the donor vector (pDONR207) is given in Figure 3.1.

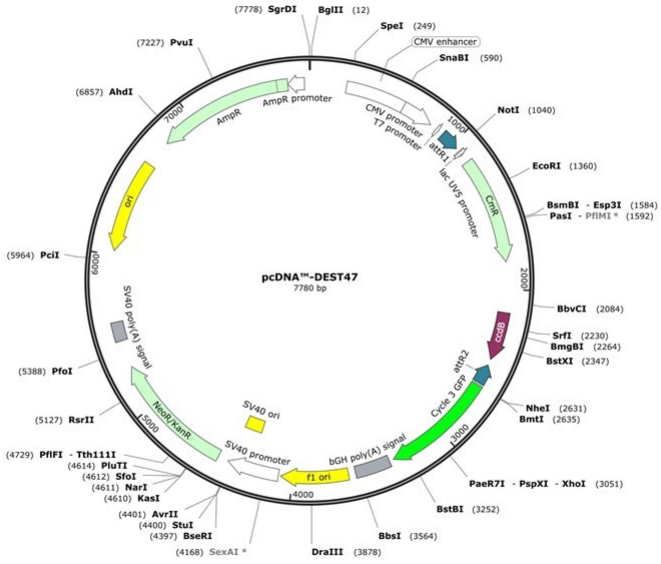

Figure 3.1. Vector map of Gateway donor vector pDONR207.

The vector map of the destination vector (pcDNA-DEST47) is given in Figure 3.2.

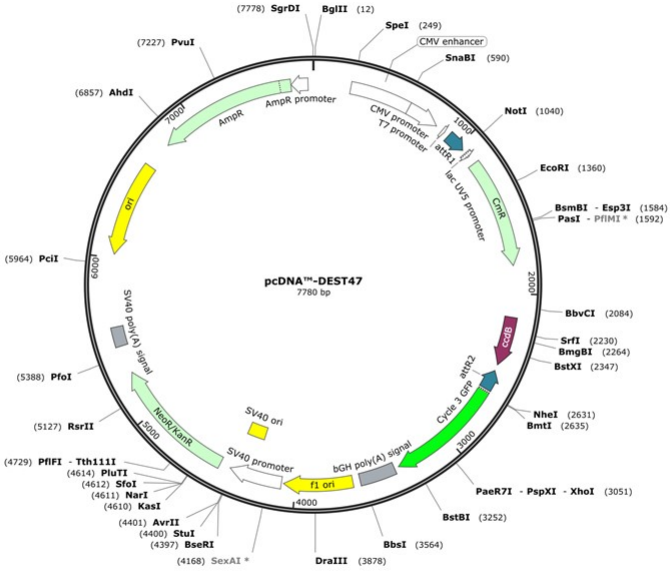

Figure 3.2. Vector map of Gateway destination vector pcDNA-DEST47.

3.7. Chemicals

Chemicals used throughout the study are listed in Table 3.11.

Table 3.11. Chemicals used in the study.

Chemical	Supplier	Product Number
100bp DNA ladder	Grisp	GL041.0050
1kb DNA ladder	Grisp	GL051.0050
2-Mercaptoethanol	Merck Millipore	805740
Acrylamide	Sigma	A3553
Alpha MEM Eagle medium	PAN Biotech	P04-21050
Ammonium persulphate	Fluka	9914
BCA protein assay kit	ThermoFisher	23225
Boric Acid	Sigma-Aldrich	B6768
Bovine Serum Albumin	Sigma-Aldrich	A2153
Bromophenol Blue (BPB)	Sigma-Aldrich	B5525
Collagenase Type-II NB4	Biological Industries	SE1745402
DAPI	Roche	10236276001
Dimethylsulfoxide (DMSO)	Sigma-Aldrich	M81802
DMEM	Gibco	1858686
EDTA	Riedel-de Haen	34549
EDTA blood collection tubes	BD Vacutainer	367525
Ethanol	ISO-LAB	920-026-2500-2.5L
Ethidium Bromide	ThermoFisher	15585011
Fetal Bovine Serum (FBS)	PAN Biotech	P30-3306
Formaldehyde	Sigma-Aldrich	15512
Glucose	Sigma-Aldrich	G8270
Glycerol	Sigma-Aldrich	G5516
Glycine	Sigma-Aldrich	G8898
HEPES	Sigma-Aldrich	H3375

Table 3.11. Chemicals used in the study. (cont.)

Chemical	**Supplier**	**Product Number**
HCl	Merck	1003172500
Magnesium Chloride	Grisp	GE01.0500C1
Methanol	Merck Millipore	1.06007.2500
N,N'-Methylenebisacrylamide	Sigma-Aldrich	M7279
Nucleoside triphosphate mix	ThermoFisher	10297018
PageRuler Prestained Protein Ladder	ThermoFisher	26616
Paraformaldehyde (PFA)	Sigma-Aldrich	15812-7
PCR Purification Kit (QIAQuick)	QIAGEN	28104
Penicillin-Streptomycin	Merck Millipore	TMS-AB2-C
Phosphatase inhibitor cocktail tablets	Roche	4906837001
Phosphate Buffered Saline	PAN Biotech	P04-36500
Phusion High-Fidelity DNA Polymerase	Thermo Scientific	F-530S
Plasmid MidiPrep Kit	Omega	D6904-03
Plasmid MiniPrep Kit	Macherey-Nagel	740588.5
Poly-D-lysine (PDL)	Sigma-Aldrich	P7280
Potassium Chloride	Sigma-Aldrich	P9541
Protease inhibitor cocktail tablets	Roche	11873580001
RNA MiniPrep Kit	Zymo Research	R1054
SensiFAST SYBR No-ROX Kit	Bioline	BIO-98005
Silver Nitrate	Merck Millipore	101512
Skim milk powder	Sigma-Aldrich	70166
Sodium chloride	Merck Millipore	106404

Table 3.11. Chemicals used in the study. (cont.)

Chemical	Supplier	Product Number
Sodium deoxycholate	Merck	6504
Sodium dodecyl sulphate	Sigma-Aldrich	L3771
Sodium hydroxide	Sigma-Aldrich	6203
SuperSignal West Femto Sensitivity Substrate	Thermo Scientific	34095
Taq polymerase	Grisp	GE01.0500
TEMED	Sigma-Aldrich	T7024
Transcriptor First Strand cDNA Synthesis Kit	Roche	4379012001
Trizma base	Sigma-Aldrich	T1503
Triton X-100	Sigma-Aldrich	T8787
Trypsin-EDTA	PAN Biotech	P10-0231SP
Tween-20	Riedel-de Haen	63158
Western blotting luminol reagent	Expedeon	ECLP0250
Xylene Cyanol	Sigma-Aldrich	X4126

3.8. Disposables

Disposables used throughout the study are listed in Table 3.12.

Table 3.12. Disposable materials used in the study.

Product	Supplier	Product Number
12-well plates	TPP	92012
4-well plates	Thermo Fisher	144444
6-well plates	TPP	92006

Table 3.12. Disposable materials used in the study. (cont.)

Product	**Supplier**	**Product Number**
Cell scraper	TPP	99003
Centrifuge tubes, 15 ml	CAPP-Denmark	5100015C
Centrifuge tubes, 50 ml	CAPP-Denmark	5100050C
Coverslips (18-mm)	Merck	CLS284518-2000EA
MagnaLyzer Green Beads	Roche	3358941001
Microcentrifuge tubes, 0.2 ml	Axygen Scientific	PCR-02-L-C
Microcentrifuge tubes, 1.5 ml	Axygen Scientific	MCT-150-A
Microcentrifuge tubes, 2 ml	Axygen Scientific	MCT-200-C
Microscope slides	Thermo Scientific	J1800AMNZ
Pasteur pipettes	ISOLAB	084.02.001
Pipette tips (1000μl)	Axygen Scientific	T1000-B
Pipette tips (200μl)	Axygen Scientific	T205-WB-C
Pipette tips (10μl)	Axygen Scientific	T300
PVDF Western Blotting Membranes	Roche	3010040001
Serological pipettes (25ml)	CAPP-Denmark	SP-25-C
Serological pipettes (10ml)	CAPP-Denmark	SP-10-C
Serological pipettes (2ml)	CAPP-Denmark	SP-2-C
Sterile Scalpel Blades Nr.10	Beybi	197
T150 tissue culture flasks	TPP	90875
T175 tissue culture flasks	TPP	90850

3.9. Equipment

All equipment used in the study are listed in Table 3.13.

Table 3.13. Equipment used in the study.

Equipment	**Supplier**
Autoclave	Astell Scientific
Balance	Gec Avery
Blotting Apparatus	Mini Trans-Blot Cell, Bio-Rad
Centrifuge	Spectrafuge 16 M, Labnet
Confocal Microscopy System	Leica Sp5 Microsystems
Deep Freezers	Arçelik
Desktop Computer	HP
Documentation System	Bio-Rad SynGene
Electrophoresis System	Mini-Protean III Cell, Bio-Rad
Fluorescence Microscopy	Leica Microsystems
Heat Blocks	Techne
Hemocytometer	Merck
Homogenizer	Roche MagnaLyser
Incubators	Nüve
Magnetic Stirrer	Hanna Instruments
Microcentrifuge	Centrifuge 5415-R, Eppendorf
Micropipettes	Gilson, Rainin
Microwave Oven	Arçelik
Power Supplies	Bio-Rad
qPCR Machine	Thermo PikoReal
Refrigerator	Arçelik
Shaker	SL 350 Nüve

4. METHODS

4.1. Patient Selection

Patient selection was performed by analyzing the pedigrees and files of the patients in our CMT cohort at Bogazici University CMT Lab. All individuals selected for analysis were pre-diagnosed with a CMT-like disease by expert neurologists. The selected individuals all had high probability of autosomal recessive disease segregation in their family with multiple affected individuals in the same generation or isolated patients born to consanguineous parents. The inclusion criteria included early onset of disease symptoms in patients (such as delayed motor milestones or disease onset before 20 years of age) and additional symptoms that increase severity of the phenotype (such as scoliosis, vocal cord involvement, hearing loss etc.). Acquired neuropathy probability was excluded for all patients in the clinical setting. All patient information was recorded in a computer environment with anonymous barcoding. Accordingly, 56 families were included in this study among which 27 have multiple affected individuals and 29 had single isolated affected individuals. The primary analyses were performed for the index patients and DNA samples from additional family members were requested when required. A total of 180 individuals were analyzed throughout the study.

4.2. DNA Isolation From Peripheral Blood

DNA extraction was performed from peripheral blood samples obtained from patients and their affected/unaffected family members. 10 ml blood sample at 4°C was transferred to 50 ml centrifuge tubes and 30 ml RBC lysis buffer was added. The mixture was vortexed every 10 minutes and incubated at 4°C for 30 minutes to lyse erythrocyte membranes. The tubes were then centrifuged at 5000 rpm at 4°C for 10 minutes. The supernatant was discarded, and the pellet was resuspended in 10 ml RBC lysis buffer. The tubes were centrifuged at 5000 rpm for 10 minutes at 4°C again.

The supernatant was discarded, the pellet was resuspended in 5 ml nuclei lysis buffer, 40 μl proteinase K, and 50 μl 10% SDS by gentle pipetting. The tubes were incubated overnight at 37°C to degrade cellular proteins. The next day, 10 ml 2.5M NaCl solution was added into the tubes. The tubes were mixed and centrifuged at 5000 rpm at room temperature for 30 minutes. The supernatant containing DNA was transferred into a fresh tube and two volumes of absolute ethanol at -20°C was added to the samples to precipitate DNA. The precipitated DNA samples were fished out from the Falcon tubes and transferred into fresh 1.5 ml microcentrifuge tubes. Following air drying of samples, DNA was dissolved in 100-300 μl TE buffer. DNA concentration and purity measurements were performed using the NanoDrop device. Genomic DNA extracted from peripheral blood samples of selected patients were barcoded anonymously with a unique family identifier and kept refrigerated until further use.

4.3. STR Analysis

CMT1A duplication/HNPP deletion was excluded for all patients included in the study using short tandem repeats (STR) assay using STR markers described previously [112]. For this, primers designed by Latour *et al.* that amplify DNA sequences that span the STR markers 4A, 9A, 9B, 20 and 26 were used in polymerase chain reaction.

4.3.1. Polymerase Chain Reaction

PCR reactions were performed in 0.2 ml microcentrifuge tubes containing 100 ng DNA, 5 μl 10X Taq polymerase buffer, 2-2.5 mM $MgCl_2$, 0.4 mM of forward and reverse primers, 0.2 mM dNTPs and 1 U Taq polymerase. $MgCl_2$ concentration was optimized for different primer pairs. The reaction was performed in a thermal cycler following an initial denaturation at 95°C for 5 minutes, 25-35 cycles of 30 seconds at 95°C, 30 seconds at annealing temperature optimized according to primers, 30 seconds at 72°C, and a final elongation step at 72°C for 10 minutes. The tubes were stored at 4°C until further use. PCR products were run on 1% agarose gel with 6X agarose loading dye in order to check for their size and specificity using an appropriate DNA marker.

4.3.2. Polyacrylamide Gel Analysis

A 10% polyacrylamide gel was prepared by mixing 33 ml dH2O, 7,2 ml 5X TBE buffer, 19,5 ml 29:1 acrylamide:bisacrylamide solution, 600 μl 10% APS, and 60 μl TEMED. The PCR products were then run on this gel by mixing with an equal amount of 2X polyacrylamide loading dye for 16 hours at 90V.

4.3.3. Silver Staining

In order to visualize PCR products on the polyacrylamide gel, silver staining method was used. The gels were incubated in 0,1% $AgNO_3$ solution for 10 minutes. Next, the solution was removed, the gels were rinsed with dH_2O and incubated in developing buffer containing NaOH and formaldehyde until DNA bands become visible. Then, DNA bands were analyzed for each STR marker to identify if the patient carries single, double or multiple bands for the markers, suggesting deletion, wild-type allele, or duplication in the *PMP22* locus respectively.

4.4. Sanger Sequencing

Sanger sequencing was performed for sequence analysis of amplicons produced by PCR using the appropriate primers. The sequencing reactions were outsourced to Macrogen Inc.(Netherlands). The chromatograms were received as ab1 files and were analyzed using ApE or SnapGene Viewer tools.

4.5. Screening of Patient Samples for *GDAP1* Mutations

GDAP1 gene mutations are known to be responsible for about 10% of autosomal recessive CMT cases. Based on this knowledge, all patients in the study were initially screened for *GDAP1* mutations using PCR and Sanger sequencing. This way, cost of whole-exome sequencing for identification of causative genes was reduced. Primers spanning six exons of *GDAP1* were designed and optimized for PCR procedure.

All exons of *GDAP1* were amplified in all patients and Sanger sequencing was outsourced to Macrogen Inc. (Netherlands). Chromatograms showing the sequences of PCR products were analyzed and the variants in patients were compared to the reference sequence of *GDAP1* transcript NM_018972. The variants observed in the patients were tested for *in silico* prediction of pathogenicity using MutationTaster database and the recurrent mutations in the gene were found in the Human Gene Mutation Database as well as in the publications they were originally reported in. Patients carrying recurrent mutations in this gene and their clinicians were informed and these patients were excluded from further analyses of the current study.

4.6. Whole-Exome Sequencing

Whole-exome sequencing (WES) was performed in 50 patients out of 56, excluding the six patients shown to have recurrent mutations in *GDAP1*. WES procedure was outsourced to DNA Lab company (Turkey). Illumina NextSeq 500 device and Illumina Nextera rapid capture kit were used for the procedure. The company provided BAM, VCF, FASTQ and Excel files for each patient individually and confirmed data quality by combining paired-end and single-end BAM files, excluding repetitions and excluding variants with a coverage less than 50X. An average of 20.000 different variants were observed in each patient as a result of WES. In order to decrease this number, a structured filtering was performed.

Initially, every patient was screened for a dataset of known inherited peripheral neuropathy (IPN) causative genes and variants in these genes were filtered: synonymous and intronic variants and variants with alternative allele frequency over 5% in the general population were filtered out. Recurrent disease-causing mutations identified in patients using this approach were verified in index cases using Sanger sequencing. Additionally, a number of patients were identified to have variants in known disease-causing genes that were previously not reported in databases as disease-causing. For these patients, the variants were verified in the proband and their available affected/unaffected family members using Sanger sequencing for segregation analysis.

For the variants that fit the inheritance pattern in the family, the referring clinician was contacted to provide feedback on whether the identified gene could explain the clinical phenotype of the respective patient. When the clinical phenotype was explicable in the light of the genetic findings, the variants were considered for possible genetic diagnoses. The patients for which the causative gene could not be identified by this procedure were further analyzed for disease-causing gene discovery.

4.7. HOMWES Analysis

For candidate disease-causing gene discovery, WES data of the patients were analyzed in the light of HOMWES (Homozygosity mapping based on whole-exome sequencing analysis) program. This publicly available software was utilized to determine the homozygous regions in patient exomes as previously described [113]. This software uses variants identified in WES and screens a sliding window of 20 variants at a time along a chromosome to create a map of homozygous regions throughout the sequence data. WES data of all 50 available patients were analyzed with this software using reference genome hg19 with a density parameter at 200 (allowing one SNP every 200 bases) and gap parameter at 4000 bp (limiting the length between two SNPs to 4000 bases). Homozygous regions larger than 6 Mb were considered very good for studying, regions in 5-6 Mb in length were considered relatively large, while homozygous regions up to 4 Mb were not considered significant.

In order to test the reliability and effectiveness of the parameters of HOMWES data, we have initially analyzed the homozygous regions identified by the software in patients with recurrent CMT mutations and confirmed that the homozygous regions identified by the software includes the locus of the recurrent homozygous mutations observed in our patients. WES data variants that reside in large homozygous regions of the genome identified by HOMWES were prioritized for the search of novel candidate genes. Variant filtering was performed with stricter parameters: Variants with read depth less than 30 and alternative allele frequency over 1%, and variants that were predicted to be benign/tolerated by both SIFT and PolyPhen2 algorithms were excluded.

The segregation pattern of the remaining candidate variants were verified with Sanger sequencing in the proband and their affected or unaffected family members.

4.8. Prioritization of Candidate Genes

Whenever multiple candidate disease-causing genes were identified through WES and HOMWES they were prioritized using ToppGene and Endeavour algorithms. All genetic variants identified in this study were described according to the ACMG criteria and classified according to this guideline [114].

4.9. Molecular Assays

To provide further evidence for the pathogenicity of the candidate disease-causing genes and their variants identified in the study, cellular and molecular analyses were performed on fibroblast cell cultures generated from patient skin punch biopsy samples. The effect of candidate variants on the corresponding mRNA and protein levels, as well as its protein localization were analyzed.

4.9.1. Generation and culturing of fibroblast cell lines

To show the effect of candidate variants at cellular level, patient fibroblast cell cultures were generated obtained from skin punch biopsy samples. The biopsy samples were obtained from the hip of the patients under local anesthesia using a 5 mm round biopsy scalpel by an expert neurologist at the Department of Neurology in Istanbul University Istanbul Medical Faculty. All individuals who donated skin samples, or their legal guardians when needed, signed a written informed consent form.

Biopsy samples were brought to the laboratory in ice-cold AMEM solution containing 1% penicillin-streptomycin and 10% fetal bovine serum (FBS). The tissue samples were cut into 1 mm pieces with a sharp scalpel, dissolved in 5 ml of type-II collagenase solution and incubated at 37°C in a shaking water bath for 1 hour until the tissue was dissolved completely. Then, 1 volume PBS was added into the mixture and the tubes were centrifuged at 500g for 10 minutes. The supernatant was removed, the pellet was resuspended by tapping the tubes gently. Five ml complete AMEM solution at 37°C was then added to the resuspension. The mixture was transferred to a T175 cell culture flask. The flask was filled with 20 ml full AMEM solution and incubated at 37°C for 72 hours without moving. After 72 hours, the cell culture medium was changed with 25 ml fresh AMEM containing 10% FBS and 1% penicillin-streptomycin. Colonies were observed 7-9 days after initial seeding. The cells were initially passaged on days 12-14 after seeding by trypsinization. Following the first passage, the cells were passaged when the flasks were 80% confluent and cell culture medium was changed with fresh medium every 72 hours for maintenance. During each passage, a portion of the cells were stored in DMSO containing cell freezing medium at -80°C for cryopreservation. The cells were harvested on second, third and fourth passages for RNA isolation, cell extract preparation and immunofluorescence assays and continuous culture was terminated after the fourth passage.

4.9.2. Total RNA Isolation

Quantitative real-time PCR (qPCR) analysis was used to investigate expression of candidate genes at mRNA level in control and patient primary fibroblasts. For this purpose, total RNA was purified from these cell lines using the Zymo Quick-RNA MiniPrep (R1054) kit following manufacturer's instructions. Briefly, cell culture medium was removed from the flask and the cells were pelleted by trypsinization. Then, 300 μl RNA lysis buffer was added to the tubes and the pellets were resuspended by brief vortexing. The lysates were cleared by centrifugation at 10.000g for 1 minute. The supernatant was transferred into a Spin-Away filter in a collection tube and centrifuged at 10.000g.

One volume absolute ethanol was added into the flow-through, mixed and transferred into a Zymo-Spin IIICG column in a collection tube. The mixture was centrifuged for 30 seconds and the flow-through was discarded. The column was pre-washed with 400μl RNA wash buffer and centrifuged for 30 seconds. The columns were incubated with 80μl DNAse I reaction mix at room temperature for 15 minutes and centrifuged for 30 seconds. 400 μl RNA Prep buffer was added to the column and centrifuged for 30 seconds. They were subsequently washed twice with RNA wash buffer and centrifuged for 2 minutes to ensure complete removal of ethanol and the wash buffer. The columns were then transferred into fresh RNase-free microcentrifuge tubes. 50-100 μl DNAse/RNase-free water was used to elute RNA depending on the confluency of the cells in the beginning. Ten μl of the isolated sample was aliquoted to be used for concentration, purity, and integrity measurements.

The concentration and purity measurements of the purified RNA samples were performed using NanoDrop device. The samples were also run on 2% agarose gel to observe prominent 18S and 28S rRNA bands on gel.

4.9.3. cDNA Synthesis

Once the concentration, purity and the integrity of the RNA samples were shown to be sufficient for further analyses, cDNA synthesis was performed from isolated total RNA samples using the Roche Transcriptor First Strand cDNA Synthesis kit (REF 04379012001) following manufacturer instructions. For this purpose, 1μg RNA was mixed with 2.5 μM anchored-oligo$(dT)_{18}$ primer and PCR grade water to reach a total volume of 13μl. This template-primer mixture was incubated at 65°C for 10 minutes to denature RNA secondary structures. Next, 4 μl of 5X Transcriptor Reverse Transcriptase Reaction Buffer, 20 U Protector RNase Inhibitor, 1 mM of each Deoxynucleotide Mix and 10 U of Transcriptor Reverse Transcriptase was added into the mixture. The tubes were incubated at 55°C for 30 minutes in a lid-heated thermal cycler and the reaction was inactivated at 85°C for 5 minutes. The cDNA samples synthesized in this way were stored at -80°C until further use.

4.9.4. Quantitative PCR (qPCR) Analysis

For qPCR procedure, appropriate primers were designed using NCBI Primer Blast tool. The primers were selected specific to the gene of interest to amplify the possible largest number of different transcripts of the gene. The primers spanned exon-exon boundaries when possible; otherwise, they were selected so that forward primer was on one exon, while the reverse was on the neighboring exon to ensure amplification of cDNA samples. Synthesized cDNA samples were diluted to 5ng/μl and were used in qPCR protocol with Bioline SensiFAST SYBR No-ROX Kit (Cat. No. BIO-98005). In the qPCR setting, for each gene analyzed; one no-template control (without cDNA/RNA template), three copies of cDNA samples from fibroblast cell lines (replicas), and one no-RT control (only RNA template) were used. The same qPCR setup was repeated three times with templates isolated from cells of different passages in order to employ statistical analyses. *ACTB*, *SDHA* and *GAPDH* genes were used as reference genes for relative comparison in qPCR analysis. The qPCR program was performed using the Thermo PikoReal Real-Time PCR System with initial denaturation at 95°C for 2 minutes, 40 cycles of denaturation at 95°C for 5 seconds, annealing and extension at 60°C for 30 seconds followed by fluorescent data acquisition. Melting curve analysis was performed between 70-95°C with a hold time of 1 second and temperature increment of 0,2°C after each hold.

For the analysis of qPCR data, $\Delta\Delta$CT method was used. Accordingly, the threshold cycle (CT), which is the number of cycles during which the studied cDNA molecules start amplifying logarithmically, is used for each experimental gene to compare to reference genes, in order to obtain data on the relative expression level of the gene of interest. Fold-change calculation was achieved with the formula $2^{-\Delta\Delta CT}$ and this number in the base of log2 is given as log2-fold change.

4.9.5. Preparation of Total Cell Extracts

Total cell extracts were prepared from control and patient fibroblasts to be used in Western-blotting (WB) technique. For this, total cell extracts were prepared from control and patient fibroblasts by trypsinizing the cells at 37°C, pelleting the cells by centrifugation, dissolving the pellet in 500 μl cell lysis buffer, and lysing the cells using MagnaLyser at 6500 rpm for 60 seconds. Protein concentration for each sample was measured with Bradford assay by relative comparison to different concentrations of BSA standard solution.

4.9.6. Western-Blotting Procedure

In order to determine the level of gene expression at protein level, Western-blotting (WB) technique was used. Following cell extract preparation and concentration measurements, the samples were mixed with 6X protein sample buffer in appropriate amounts according to sample concentration and incubated at 95°C for 5 minutes for denaturation. The samples were placed on ice immediately afterwards and loaded on 10% polyacrylamide gel inside a Western-blot tank filled with fresh Running Buffer. The samples were run on the gel next to a pre-stained protein marker until the dye reaches the end of the gel. Next, the gel was removed from the apparatus and transferred into a PVDF membrane in a transfer tank filled with fresh Transfer Buffer containing methanol. The membrane was incubated in a blocking solution appropriate for the antibody to be used (1-5% skim milk or BSA dissolved in TBS-T) for 1 hour at room temperature. Then, the membrane was incubated in primary antibody solution at 4°C overnight. The next day, primary antibody solution was recovered, the membranes were washed three times with TBS-T and incubated in secondary antibody solution for 1 hour at room temperature. The membranes were washed with TBS-T to remove excess antibody solution and visualized using a luminol working solution with SynGene device. The antibodies used for WB protocol are listed in Table 3.7.

4.9.7. Immunofluorescence Assay

Immunofluorescence (IF) assay was used for studying cellular localization of the proteins of interest. For this purpose, the cells were seeded onto PDL-coated coverslips in 4- or 6-well plates. The next day, cells were fixed with 4% paraformaldehyde at 37°C for 30 minutes. The cells were washed with PBS three times and permeabilized with 0.5% Triton-X in PBS at room temperature for 30 minutes. Then, they were incubated in the blocking solution containing 1% BSA in 0.05% Triton-X in PBS for 1 hour at room temperature. Next, they were incubated in primary antibody in blocking solution overnight at 4°C, washed three times with PBS, and incubated in an appropriate secondary antibody solution in a dark room for 1 hour at room temperature. The cells were then washed three times with PBS, stained with DAPI working solution for 3 minutes, and briefly rinsed with PBS. The coverslips were then mounted onto a microscope slide by using FluoroMount (Diagnostic Biosystems, K024) mounting medium. The cells were visualized using Leica Sp5 confocal microscopy system. The antibodies used for IF assay are listed in Table 3.7.

4.10. Gateway Cloning

To provide further evidence on the impact of candidate gene variants at cellular level, the wild-type and mutated versions of one of our candidate genes were cloned into an expression vector and overexpressed in Human Embryonic Kidney (HEK293) cells. Gateway cloning system was used for the cloning procedure. For this purpose, primers that amplify and add flanking attB sides to both ends of the wild-type and mutated versions of the coding sequence of the gene of interest (*SEPT11*) were designed using the Primer3 tool. The primers were designed so that the stop codon was excluded from the sequence. These primers are given in Table 3.6.

4.10.1. PCR Amplification of the Insert DNA

The designed primers were used for PCR amplification of the gene using cDNA of control and patient fibroblasts as template DNA. PCR reaction was performed using a high-fidelity Taq polymerase enzyme. PCR products were run on agarose gel for verification of DNA bands, and then purified using QIAquick PCR Purification Kit (Cat. No: 28104) following manufacturer instructions. DNA concentration and purity were measured using a NanoDrop device.

4.10.2. BP-Reaction

In order to ligate PCR products with the donor vector, 100 ng of the products were used in BP reaction together with 150 ng/μl donor vector (pDONR207) and TE buffer to make total volume 8 μl. 2 μl BP Clonase enzyme was added on top, mixed briefly by vortexing, and microcentrifuged to spin all components down. The reaction was incubated at 25°C for 1 hour. After addition of 1 μl proteinase K the tube was incubated at 37°C for 10 minutes to terminate the reaction.

4.10.3. Transformation

The competent *E. coli* cells were transformed with the ligation products. For this purpose, the bacteria were incubated together with the ligated product on ice for 30 minutes. Heat shock was achieved at 42°C for 1 minute and the cells were placed back on ice. LB was added to the tubes and the cells were incubated at 37°C on a shaker for 1 hour to recover and start gene expression from the vector. Following the incubation, the cells were plated on LB agar plates containing gentamycin and incubated at 37°C overnight for selection of colonies that contain the plasmid DNA.

4.10.4. Verification of Insert DNA

The next day following transformation, colonies grown on the plates were used for colony PCR in order to verify the presence of the insert DNA inside the plasmid. For this, whole colonies were removed from the plate by the tip of a micropipette, dissolved in 50 μl dH_2O, and 10 μl of this mixture was used as a template together with insert-specific primers for colony PCR. For further verification of the presence of the insert, the colonies from the plates were grown overnight at 37°C in liquid LB. Plasmids were isolated using NucleoSpin Plasmid Miniprep Kit (REF 740588.50) following manufacturer instructions. The isolated plasmids were subjected to diagnostic restriction digestion by using two restriction enzymes: one inside the vector and one on the insert DNA sequence. Additionally, the isolated plasmids were outsourced for Sanger sequencing to Macrogen Inc. (Netherlands).

4.10.5. LR-Reaction

Once the donor vectors were verified to contain the insert DNA, the insert was transferred from the entry clone to the destination vector (pcDNA-DEST47) using LR reaction. For this 50-150 ng entry clone, 150 ng/μl of pcDNA-DEST47 destination vector and TE buffer to make the mixture volume 8 μl were mixed in a 1.5 ml tube at room temperature. Then, 2 μl of LR Clonase II enzyme mix was added to the reaction and mixed well by brief vortexing and centrifuged down. The reactions were incubated at 25°C for 1 hour. To terminate the reaction, 1 μl proteinase K solution was added to each sample and the tubes were incubated at 37°C for 10 minutes. The ligation products were then transformed into *E. coli* and the cells were plated into ampicillin containing LB plates as described previously. The colonies were then inoculated into ampicillin containing liquid LB and grown overnight. The next day, the expression vectors were isolated from the cultures using Omega Plasmid DNA Midi kit (D6904-03) according to manufacturer instructions.

4.11. Transfection into HEK293 cells

The destination vectors constructed using Gateway cloning were used for overexpression of the candidate gene in HEK293 cells in order to observe potential differences between cells that express wild-type and mutated copies of the gene of interest. For this purpose, 10.000 HEK293 cells per well were seeded onto 18-mm coverslips inside 12-well cell culture plates. The cells were incubated at 37°C overnight for settling inside the wells. The next day, the transfection mixture was prepared by mixing 500 ng destination vector, dH2O to make the volume 43,8 μl and 6,2 μl ice-cold 2M $CaCl_2$, respectively. The mixture was incubated at room temperature for 5 minutes. Then, 50 μl ice-cold 2X HBS solution was added on top drop by drop. The tubes were rubbed against a rack to form bubbles inside the solution. The mixture was incubated at room temperature for 10 minutes. It was then resuspended gently and 100 μl of it was added drop by drop onto the cells. The cells were fixed 24 hours later and stained by anti-GFP antibody and DAPI using the IF protocol described above and visualized using the Leica Sp5 confocal system.

5. RESULTS

With the aim to find out gene/allele frequency of autosomal recessive CMT-causative genes in the Turkish population and identify novel CMT-causative genes, 56 patients clinically diagnosed with CMT disease were selected from our cohort. The selection was based on pedigree analyses and phenotypic severity in order to reflect a pure autosomal recessive CMT cohort. Initially, these patients were screened for mutations in the *GDAP1* gene. Next, whole-exome sequencing (WES) and homozygosity mapping was performed on the patients for whom mutations in *GDAP1* were excluded. Once the variants in known CMT/peripheral neuropathy genes were determined in the WES data, segregation analysis was performed to confirm their responsibility for the disease phenotype. To verify the pathogenicity of the novel genes, one the other hand, cell culture-based molecular analyses was used. The results are given in the chronological order of methods and analyses performed to help the reader in the follow up.

5.1. Screening of Patients for *GDAP1* Gene Mutations

Mutations in the *GDAP1* gene make up the most common cause of autosomal recessive CMT cases with a mutation frequency of 5-10% [54]. Thus, all patients included in the study were initially screened for *GDAP1* mutations using PCR and Sanger sequencing. The cost of whole-exome sequencing that would be later used to determine the causative CMT genes was reduced in this way by excluding patients with recurrent *GDAP1* mutations. Accordingly, the variants observed in patients were compared to the reference sequence of *GDAP1* transcript NM_018972 and were tested for *in silico* prediction of pathogenicity using MutationTaster database. When a recurrent mutation in the *GDAP1* gene was found in a patient, the mutation was searched in the Human Gene Mutation Database, as well as in the publications they were originally reported in. The phenotypes of the patients reported in the databases were compared to that of our patients.

Six patients out of 56 in the study were found to carry homozygous recurrent *GDAP1* mutations. These patients and the positions of the mutations relative to the coding sequence of NM_018972 transcript of *GDAP1* are given in Table 5.1 together with the publications these mutations were first reported in. These six patients were given genetic diagnosis and were excluded from further analyses in the study.

Table 5.1. Mutations observed in *GDAP1* among 56 patients included in the study.

Patient ID	**Clinical findings**	**Variant**	**HGMD ID**	**Initial report**
P294	Childhood onset, NCV: IE, pes cavus, scoliosis	c.786del p.Phe263Leufs*22, homozygous	CD023843	[21]
P448	Childhood onset, NCV: IE, pes cavus, sensory ataxia	c.174_176delinsTGTG p.Pro59Valfs*4, homozygous	CX083408	[115]
P555	Childhood onset, axonal PNP, pes cavus	c.786del p.Phe263Leufs*22, homozygous	CD023843	[21]
P987	Onset at birth, NCV: IE, scoliosis, vocal cord paresis	c.786del p.Phe263Leufs*22, homozygous	CD023843	[21]
P1262	DMM, NCV: IE, pes cavus	c.786del p.Phe263Leufs*22, homozygous	CD023843	[21]
P1325	Childhood onset, NCV: 46 m/s, pes cavus	c.458C>T p.Phe263Leufs*22, homozygous	CM077286	[116]

ID: identifier, NCV: nerve conduction velocity, IE: inexcitable, PNP: polyneuropathy, DMM: delayed motor milestones.

Sanger chromatograms showing the *GDAP1* coding sequences of the patients with recurrent mutations in the gene are given in Figure 5.1 together with control sequences for comparison.

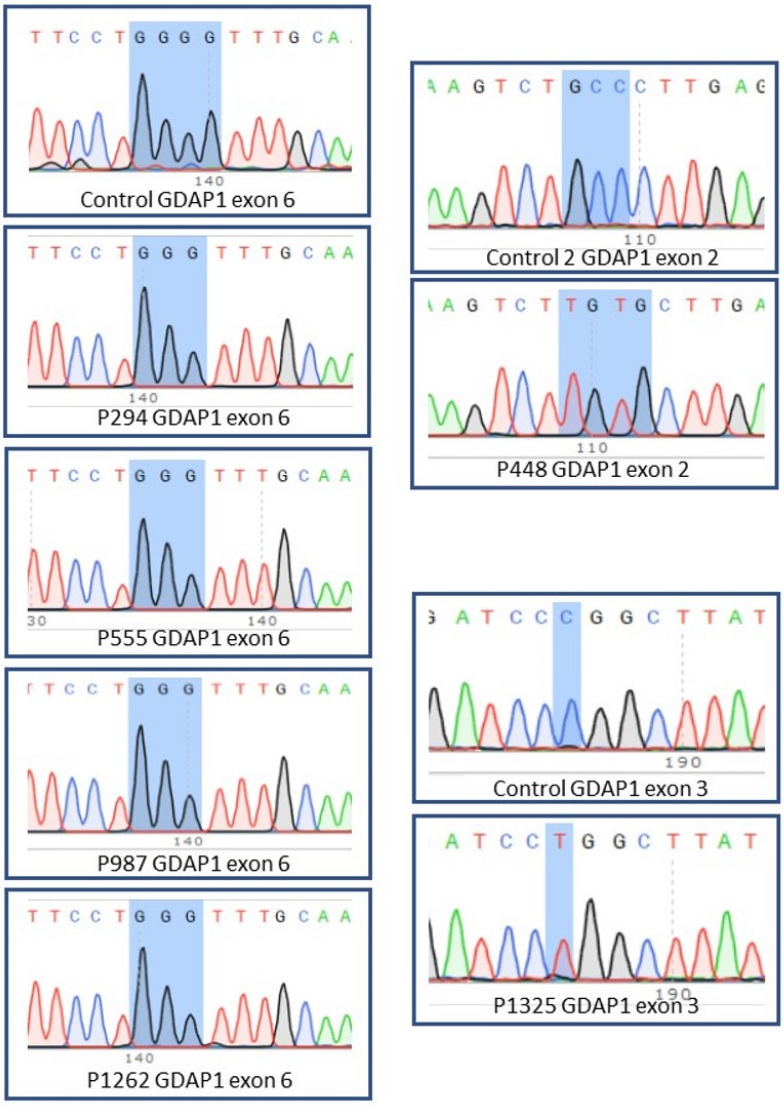

Figure 5.1. Sanger chromatograms of patients with recurrent mutations in the *GDAP1* gene compared to the sequences of an unaffected individual (control). Changes in nucleotide sequences are indicated with blue boxes.

5.2. Whole-Exome Sequencing

Whole-exome sequencing (WES) was performed in 50 patients out of 56, excluding six patients who were shown to have recurrent mutations in *GDAP1*. The variants observed in WES data of the patients were initially screened for known peripheral neuropathy-causing genes as described previously in section 4.6.

5.2.1. Screening of Variants in Known Peripheral Neuropathy Genes

During the initial analysis of WES data, focus was given onto recurrent mutations in known peripheral neuropathy genes. Using this approach, 16 out of 50 patients with whole-exome sequencing data were shown to have recurrent mutations in known inherited neuropathy genes. List of patients with recurrent mutations, names of the genes and the mutations observed in these genes, as well as HGMD or dbSNP identifier for the mutations and the research articles that had initially reported these mutations are given in Table 5.2. All variants were verified using Sanger sequencing in the index patients and were shown to be true variants, not false positives. The familial segregation analyses were performed whenever DNA samples from additional family members were available.

Table 5.2. List of patients with recurrent mutations in known IPN genes.

Patient ID	**Gene name, Transcript**	**Variant**	**HGMD/ dnSNP ID**	**Initial report**
P300	MFN2, NM_014874.3	c.1090C>T, p.Arg364Trp, heterozygous	CM060340	[72]
P581	EGR2 NM_000399.3	c.1142G>A, p.Arg381His heterozygous	CM004043	[117]

†Compound heterozygosity is observed in the family. HGMD: The Human Gene Mutation Database, dbSNP: The Single Nucleotide Polymorphism Database.

Table 5.2. List of patients with recurrent mutations in known IPN genes. (cont.)

Patient ID	**Gene name, Transcript**	**Variant**	**HGMD/ dnSNP ID**	**Initial report**
P639	SH3TC2, NM_024577.3	c.2642A>G, p.Asn881Ser, heterozygous/ c.1586G>A, p.Arg529His, heterozygous	CM064263/ rs80338923	[97], [53]
P711	GJB1 NM_001097642.2	c.47A>T, p.His16Leu, heterozygous	CM095432	[118]
P811-1	PRX, NM_181882.2	c.1102C>T, p.Arg368Ter, homozygous	CM011005	[119]
P991	SH3TC2, NM_024577.3	c.1178-1G>A, homozygous	CS064451	[97]
P1148	MFN2, NM_014874.3	c.1085C>T, p.Thr362Met, heterozygous	CM062856	[120]
P1152	SH3TC2, NM_024577.3	c.1894_1897delinsAAA, p.Glu632Lysfs*13, homozygous	CX117975	[121]
P1255	PRX, NM_181882.2	c.3208C>T, p.Arg1070Ter, homozygous	CM044034	[122]
P1289-3	SH3TC2, NM_024577.3	c.1894_1897delinsAAA, p.Glu632Lysfs*13, homozygous	CX117975	[121]
P1291	SACS, NM_014393.4	c.2182C>T, p.Arg728Ter, homozygous	CM087685	[123]

†Compound heterozygosity is observed in the family. HGMD: The Human Gene Mutation Database, dbSNP: The Single Nucleotide Polymorphism Database.

Table 5.2. List of patients with recurrent mutations in known IPN genes. (cont.)

Patient ID	**Gene name, Transcript**	**Variant**	**HGMD/ dnSNP ID**	**Initial report**
P1306	MPV17, NM_002437.4	c.122G>A, p.Arg41Gln, homozygous	rs140992482	[124]
P1319	HINT1, NM_005340.5	c.368G>A, p.Trp123Ter, homozygous	CM128652	[59]
P1330	GJB1, NM_001097642.2	c.518G>T, p.Cys173Phe, hemizygous	CM070941	[125]
P1331	MFN2, NM_014874.3	c.1090C>T, p.Arg364Trp, heterozygous	CM060340	[72]
P1333	MFN2, NM_014874.3	c.310C>T, p.Arg104Trp, heterozygous	CM083543	[126]

†Compound heterozygosity is observed in the family. HGMD: The Human Gene Mutation Database, dbSNP: The Single Nucleotide Polymorphism Database.

Since these variants have been previously reported as disease-causing, the genetic findings have been determined as definitive diagnoses in the corresponding patients. The patients from Table 5.2 and/or their clinicians were informed, and the patients received genetic counseling when requested. For these 16 patients who received a definitive genetic diagnosis, mutations in the corresponding genes were shown with Sanger chromatograms on pedigrees in Appendix A.

Almost half of the patients with recurrent mutations (7/16 patients) were shown to have mutations in autosomal dominant CMT genes such as *MFN2*, *GJB1*, and *EGR2*. Although parental consanguinity criterion was satisfied for all patients, probability of autosomal dominant segregation was also considered in the remaining analyses in the project.

Recurrent mutations in known neuropathy-related genes were not observed for the remaining 34 patients; however, further evaluation of WES data disclosed a total of around 120 novel variants in known inherited neuropathy genes with an alternative allele frequency of less than 5%. These novel variants were analyzed using PCR and Sanger sequencing in index patients and their family members to observe if the variant was segregating with disease status in the pedigree. With this approach we have identified novel candidate disease-causing variants in 13 patients shown in Table 5.3.

Table 5.3. List of patients with novel variants in IPN genes.

Patient ID	**Gene name. Transcript**	**Variant**	**AAF (%)**	**ACMG criteria**	**Outcome**
P265	MME, NM_000902.3	c.531delA, p.Lys177Asnfs*15,	NP	PVS1, PM2, PM4, PP4 PP5	Pathogenic
P322	SH3TC2, NM_024577.3	c.1586G>A, p.Arg529His,	0.00283	PM1, PM2 PM5, PP4, PP5	Likely pathogenic
P431	HINT1, NM_005340.5	c.99delT, p.Phe33Leufs*22, homozygous	NP	PVS1, PM2, PM4, PP4	Pathogenic
P492	MFN2, NM_014874.3	c.271G>T, p.Val91Leu, homozygous	NP	PM2, PM5 PP1, PP4	Likely pathogenic
P629	SPG7, NM_003119.2	c.454A>G, p.Met152Val, homozygous	0.006721	PM2, PP1, PP4	VUS
P963	NDRG1, NM_006096.4	c.237C>A, p.Tyr79Ter, homozygous	NP	PVS1, PM2, PM4, PP1 PP4	Pathogenic
P969	NEFL, NM_006158.3	c.54C>A, p.Tyr18Ter, homozygous	0.0004363	PM1, PM2, PM4, PP1, PP4	Likely pathogenic

AAF: Alternative Allele Frequency, ACMG: American College of Medical Genetics, NP: Not present in databases, VUS: Variant of Unknown Significance.

Table 5.3. List of patients with novel variants in IPN genes. (cont.)

Patient ID	**Gene name. Transcript**	**Variant**	**AAF (%)**	**ACMG criteria**	**Outcome**
P1041	AP5Z1, NM_014855.2	c.1568G>A, p.Arg523His, homozygous	0.0038	PM2, PP1 PP2	VUS
P1130	GDAP1, NM_018972.2	c.112C>T, p.Gln38Ter, homozygous	NP	PVS1, PM2, PM4, PP1, PP4	Pathogenic
P1142	C12ORF65, NM_152269.4	c.18_21delATTT, p.Leu6PhefsTer7, homozygous	NP	PM2, PM4 PP1, PP4	Likely pathogenic
P1180-4	SH3TC2, NM_024577.3	c.54dupT, p.Lys19Ter, homozygous	NP	PVS1, PM2, PM4, PP1, PP4	Pathogenic
P1188	SBF2, NM_0,30962.3	c.2549T>C, p.Met850Thr, homozygous	NP	PM2, PP1, PP4	VUS
P1267-3	MPZ, NM_000530.6	c.362A>G, p.Asp121Gly, heterozygous	NP	PM1, PM2	VUS

AAF: Alternative Allele Frequency, ACMG: American College of Medical Genetics, NP: Not present in databases, VUS: Variant of Unknown Significance.

Segregation analyses were performed in 10 families out of 13 and the variants were shown to fit the segregation of disease status in the pedigrees. In three patients, DNA samples from additional family members were not available, therefore the variants were only verified in index patients. Additionally, for all 13 cases, the referring clinicians stated that the corresponding genes could explain the clinical presentation in each patient. Seven of these 13 patients carried homozygous termination or frameshift mutations in causative genes indicating that they were highly likely to be causative due to loss-of-function. Other novel variants were homozygous missense mutations for which pathogenicity cannot be assessed solely by familial segregation or clinical phenotype.

Nevertheless, nine out of these 13 candidate variants were classified as pathogenic or likely pathogenic variants according to ACMG criteria [114], and therefore suggested definitive genetic diagnoses for the corresponding families. The remaining four were classified as variants of unknown significance and are suggested as potential genetic diagnoses.

All variants reported here are novel disease-causing alleles, and they will be reported in literature for the first time by this study. These variants are shown with Sanger chromatograms on pedigrees in Appendix A.

Unfortunately, the novel variants identified in families P265, P322, and P431 could only be verified in the index patients using Sanger sequencing: familial segregation could not be performed since DNA samples were not available from additional family members. The variant observed in patient P265 was a homozygous variant in *MME* (c.531delA, p.Lys177Asnfs*15). It causes a frameshift and introduces an early stop codon in the protein sequence (Table 5.3). Higuchi *et al.* (2016) reported 10 families diagnosed with late onset CMT that have homozygous or compound heterozygous mutations in the *MME* gene and determined that loss-of-function mutations in this gene are disease-causing for CMT [127]. Our patient P265 has similar clinical features with the previously reported families and the mutation in the *MME* gene likely causes loss-of-function. Furthermore, the ACMG classification for this variant was "pathogenic", therefore, this mutation was suggested as a definitive diagnosis for this patient even though segregation analysis could not be performed in family members.

The second novel variant that could only be verified in the index patient was identified in family P322. The patient was homozygous for c.1586G>A, p.Arg529His mutation in the *SH3TC2* gene. The alternative allele frequency of this variant was reported to be 0.0000283 in the gnomAD database; however, this variant has never been observed in homozygous state in more than 140.000 individuals analyzed in the database. Moreover, a pathogenic mutation in the same codon (p.Arg529Gln) has been reported to be caussative for CMT4C in two Turkish families previously [53].

The clinical phenotype of the index patient P322 was very similar to other patients with CMT4C. Additionally, according to the ACMG criteria, this variant should be classified as "likely pathogenic". Therefore, this mutation was listed as a definitive genetic diagnosis for family P322, although a familial segregation analyses could not be completed.

In family P431, homozygous c.99delT, p.Phe33Leufs*22 mutation in the *HINT1* gene was confirmed only in the index patient, as for families P265 and P322. Loss-of-function mutations in the HINT1 gene are known to cause a distinct CMT representation with neuromyotonia [59]. The clinical findings of the patient P431 were found to be compatible with the clinical findings seen in other patients with pathogenic *HINT1* mutations and the mutation is likely to cause loss-of-function in the protein as it causes a frameshift with an early stop codon in the protein sequence. The suggested ACMG criteria for the variant was pathogenic; therefore, the mutation in the *HINT1* gene was evaluated to be the disease-causing mutation in family P431.

In family P492, a homozygous c.271G>T, p.Val91Leu variant in CMT-causative *MFN2* gene was found to be segregating in the family with disease. This particular variant has never been reported in databases; but in the same position, a mutation in which the valine amino acid is converted into glutamic acid (p.Val91Glu) was reported in the HGMD database ID:CM117904), and this mutation was reported to be associated with CMT2A2 [128]. In the variant shown in patient P492, the valine amino acid having a hydrophobic side chain is replaced with leucine which has a longer hydrophobic side chain that could affect protein stability or function. Additionally, *MFN2* mutations, responsible for autosomal dominant CMT2, are rarely observed in homozygosity and are known to cause relatively severe clinical findings [50]. Because the patient P492 had clinical findings at birth and had to use a wheelchair early in her life, and that the ACMG classification for the variant was "likely pathogenic", the mutation responsible for the disease in this family was evaluated to be this biallelic *MFN2* variant.

In patient P629, none of the variants in CMT-causative genes were shown to segregate in the family. However, when the genes that cause other hereditary neuropathies were examined, a homozygous c.454A>G, p.Met152Val variant in the HSP-causative *SPG7* gene was observed. This variant, having an allele frequency of 0,00006721 in the gnomAD database, was shown to segregate with the disease in the pedigree. For this reason, the patient was re-evaluated in the clinical setting and her differential diagnosis was provided as hereditary spastic paraplegia. The variant observed in patient P629 causes sulfur-containing methionine amino acid to be converted into valine in the protein sequence. Although both of these amino acids are in the hydrophobic side chain-containing amino acids group, it can be suggested that loss of methionine can be associated with loss of sulfur bridge in the mature protein and cause changes in protein folding. In another patient (P1188), the methionine amino acid was replaced with a threonine residue due to a homozygous c.2539T>C, p.Met850Thr variant in the *SBF2* gene. The mutation was segregating with the disease status in the pedigree. This variant has never been reported in ExAc, 1000G and gnomAD databases previously and is predicted to be disease-causing by SIFT, PolyPhen2 and MutationTaster algorithms. Threonine contains a polar uncharged side chain and its addition with an extra -OH group suggests that an additional chemical bond can be made in this region, which may alter protein function. Besides, due to the mutation in this patient the AUG codon is converted to ACG, which encodes for threonine and is a minor codon in the human genome as shown by Park *et al.* (2017) [129]. It is known that minor codons can affect co-translational protein folding. Because the reservoir of tRNAs containing the minor codons is limited in the cell, it has been shown that during translation the ribosomes stall in regions of minor codons on mRNA molecules and this causes a change in co-translational protein folding [129]. In the light of this knowledge, it can be suggested that Sbf2 protein folding might be significantly different in patient P1188, which cannot be determined by *in silico* tools.

Patient P1041 had a homozygous c.1568G>A, p.Arg523His variant in the *AP5Z1* gene which is known to cause HSP. The allele had a reported frequency of 0.000038 in gnomAD and had not been observed in homozygous state in general population.

SIFT, PolyPhen2, and MutationTaster algorithms suggested that the variant is damaging. The variant replaces an arginine residue; a positively charged amino acid, with a histidine residue; an amino acid with an aromatic ring, possibly affecting 3D structure or folding of the protein. The unaffected parents and siblings of the index patient were all heterozygous for the variant, while the index patient was homozygous. A detailed clinical examination of the index patient has also suggested clinical features compatible with HSP, rather than CMT. Although *in silico* findings, familial segregation and clinical examination of the patient supports pathogenicity of the variant, the ACMG criteria for this variant are not sufficient enough to report this finding as "pathogenic" or "likely pathogenic". Therefore, the homozygous variant (c.1568G>A, p.Arg523His) in the *AP5Z1* gene in this family only makes up a potential genetic diagnosis for the index patient.

In patient P1267-3, a heterozygous *MPZ* gene variant (c.362A>G, p.Asp121Gly) was observed. *MPZ* is known to cause dominant CMT. The mother and son of the patient were also affected and they both carry the mutation in heterozygous state. This variant has never been reported in ExAc, 1000G and gnomAD databases previously and is predicted to be disease-causing by PolyPhen2 and MutationTaster algorithms. The variant in this family causes a change in the protein sequence where the negatively charged aspartic acid residue is replaced with glycine, a short chain amino acid. Since the variant is predicted to cause a significant change in the protein folding and function, it can be suggested that this variant might be disease-causing, however additional molecular analyses are required to seek further proof.

In the last four families (P629, P1041, P1188, and P1267) that have been just described, the novel missense variants could not be classified as pathogenic/likely pathogenic based on ACMG criteria. Though, they were all in known neuropathy-related genes with low allele frequency in the healthy population and the variant segregation fitted the disease status in each pedigree. Additionally, the clinicians of these families agreed that the corresponding genes could explain the clinical phenotype in the patients. Still, these variants were classified as "variant of unknown significance".

In order for them to be classified as pathogenic and let the families receive a definitive genetic diagnosis, further molecular analyses are required to prove their pathogenicity.

In summary, initial screening of *GDAP1* gene proved to be the correct method of choice since it allowed exclusion of six patients with *GDAP1* mutations from further studies. WES analysis allowed identification of another 16 patients with recurrent mutations in known neuropathy-related genes. Thirteen patients were shown to have novel variants in known causative genes; nine of which were classified as pathogenic or likely pathogenic according to ACMG criteria. In conclusion, 35 patients out of 56 (62,5%) have received genetic diagnoses, 31 of these being definitive genetic diagnoses, while in four cases the variants of unknown significance must be investigated further for molecular evidence of pathogenicity.

5.2.2. Incidental Findings

Most whole-exome sequencing studies report several incidental findings. Similarly, there was one incidental finding in this study. We have observed a homozygous c.941A>T, p.Gln314Leu mutation in the *OPTN* gene in patient P969. This mutation was reported to cause amyotrophic lateral sclerosis (ALS) in heterozygous state [130]. Familial segregation analysis of this mutation in P969 family showed that the index patient was homozygous, while his unaffected mother and affected sister were both heterozygous for the mutation. Figure 5.2 shows the inheritance of the c.941A>T, p.Gln314Leu mutation in the *OPTN* gene in family P969.

Thus, the c.941A>T, p.Gln314Leu mutation that was reported to cause ALS by Del Bo *et al.* (2011) did not segregate with disease status in family P969. Additionally, the index patient had clinical findings of frequent falling, abnormal mobility, distal weakness in upper and lower limbs, pes cavus, hammer toe, hypoactive deep tendon reflex, sensory loss and scoliosis. NCV study suggested sensory and motor neuropathy with primary myelin defects. There was no clinical finding suggesting ALS diagnosis.

This finding suggests that *OPTN* c.941A>T, p.Gln314Leu mutation which was reported only in one patient in the literature, is not a causative variant, at least in the genetic background of our family. In addition to that, in family P969, a novel homozygous c.54C>A, p.Tyr18Ter mutation was observed in the known CMT-causative *NEFL* gene. The patient's clinical findings were similar to the clinical findings of patients with *NEFL* gene mutations and the variant segregated with disease status in the pedigree. Therefore, the *NEFL* variant was the causative one rather than the *OPTN* variant, in the family.

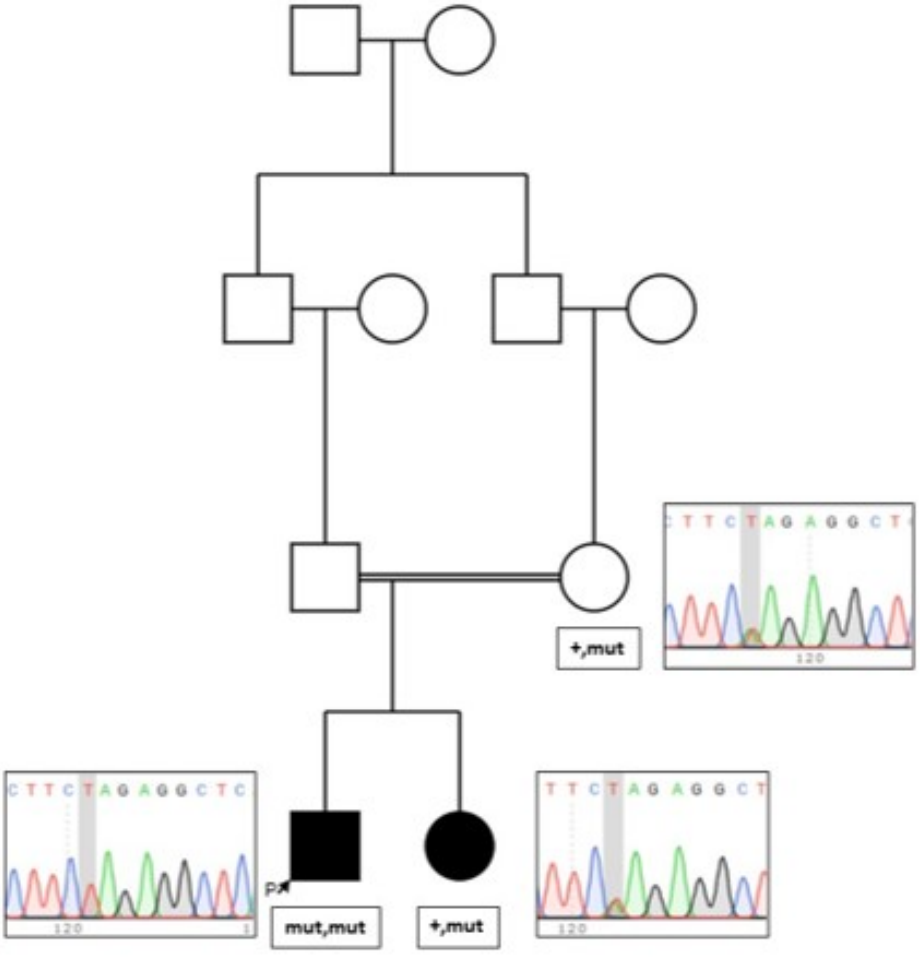

Figure 5.2. Sanger chromatograms of *OPTN*, c.941A>T, p.Gln314Leu mutation in family P969. Variant position is shown with grey boxes.

5.3. Homozygosity Mapping

Similar studies use whole-genome SNP analysis in combination with whole-exome sequencing in order to identify novel genes/alleles, however, we have decided to use publicly available "homozygosity mapping based on whole-exome sequencing analysis" (HOMWES) software to determine homozygous regions in patient exomes. This software uses variants identified in WES, screens a sliding window of 20 variants at a time along a chromosome, allowing one heterozygous variant each time to create a map of homozygous regions throughout the genome. The confirmation and optimization of this software have been completed by Prof. Albena Jordanova's research group in Belgium [113]. We have used the HOMWES software with the same parameters to identify homozygous regions in 50 patients for which we have WES data.

In order to test the reliability of the parameters of the HOMWES data, we analyzed the homozygous regions identified by the software in patients with recurrent CMT mutations and confirmed that the homozygous regions identified by the software includes the locus of the recurrent homozygous mutations observed in our patients. The representation of homozygous regions of patient P811-1 for which we had previously shown to carry a homozygous recurrent PRX mutation (c.1102C>T, p.Arg368Ter) is given as an example for this preliminary study in Figure 5.3.

According to Figure 5.3, patient P811-1 has homozygous regions larger than 1Mb on chromosomes 1, 2, 4, 5, 6, 7, 9, 10, 11, 12, 14, 16, 19 and 21. The multitude and length of these homozygous regions along the genome confirms parental consanguinity in this patient. It can be observed on Figure 5.3 that the *PRX* causative variant resides in one of the homozygous regions found in the exome of this patient (chromosome 19, shown in gold color). Similar analyses performed in patients with homozygous recurrent mutations also confirmed the parameters applied by the software are successful in determining the homozygous regions using WES data and can lead us to candidate genes. Starting from this point, homozygous regions in the genome of 50 patients with WES data were determined and candidate genes were sought based on this data.

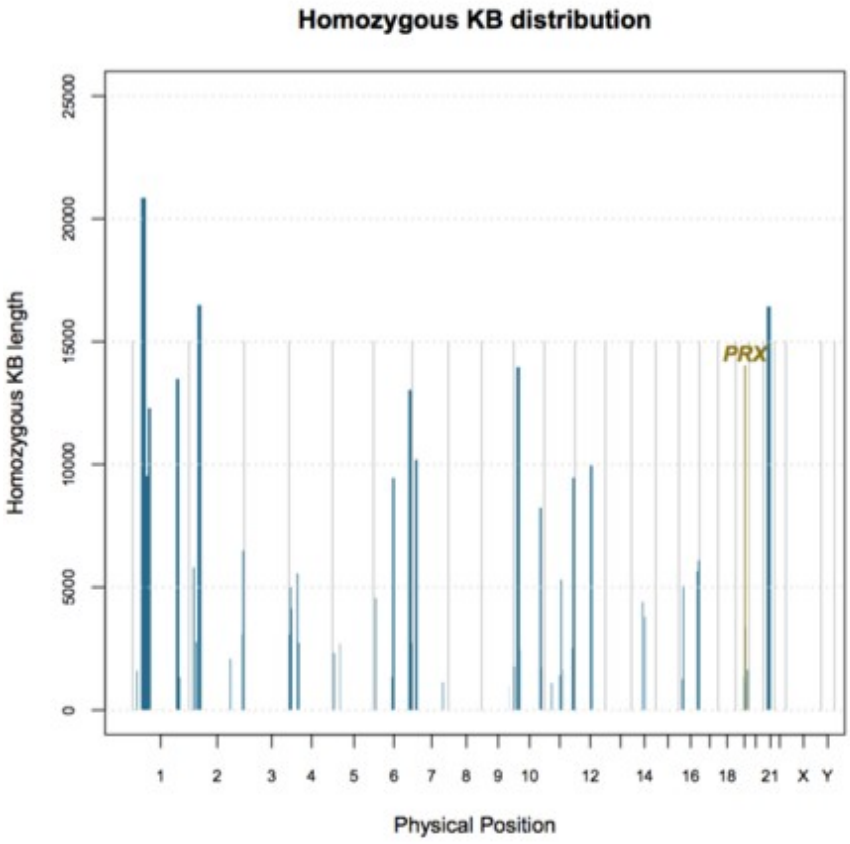

Figure 5.3. Representation of homozygous regions over 1Mb on different chromosomes of patient P811-1. The homozygous region where *PRX* gene resides on chromosome 19 is shown in gold color.

5.4. Candidate Gene Search

In order to search for candidate genes for patients without a genetic diagnosis so far, we focused on the variants in the WES data that reside in the large homozygous regions determined by HOMWES. Using a sorting algorithm, we have compared the HOMWES and WES data for each of these patients and filtered variants as described previously. We, then checked the segregation of the candidate variants in the corresponding families. Using this technique, we have managed to identify one novel gene-CMT disease relationship and two additional candidate IPN genes.

5.4.1. Family P966

In family P966, the initial analysis of WES data for known CMT-related genes did not reveal a pathogenic variant. When the genes that cause phenotypically overlapping neurological diseases were screened, a biallelic c.493C>T, p.Arg165Cys mutation in the *FXN* gene was identified with true familial segregation. *FXN* mutations are known to cause Friedreich's ataxia (FRDA). It is also known that approximately 98% of FRDA patients have an expansion in the number of GAA triplet repeats in the first intron of the *FXN* gene [131]. Rare point mutations in the *FXN* gene are also reported in compound heterozygosity with the GAA triplet repeat expansion in 2% of the cases [132, 133]. The point mutation (p.Arg165Cys) seen in patient P966 is one of the mutations that has been reported in FRDA patients in compound heterozygosity with the GAA triplet repeat expansion. Homozygous point mutations in *FXN* gene are thought to be embryonic lethal since they have never been reported before. Interestingly, three affected siblings in the family P966 all have the same homozygous point mutation, while the unaffected parents and the unaffected siblings are heterozygous carriers (Figure 5.5a). Since point mutations in *FXN* gene have always been reported in compound heterozygous state with the GAA triplet repeat expansion, the number of GAA repeats was also examined in NDAL Laboratory in Koç University. The test is performed with double blind experiments and it was determined that the number of repeats are not in pathological level in any individuals in the family (Figure 5.4).

Since *FXN* has not been reported as a CMT-causative gene but is the only known causative gene for Friedreich's ataxia, a detailed neurological re-evaluation of the family was performed. The patient was reported to have muscle weakness and atrophy in lower limbs with bilateral steppage gait, as well as optic nerve atrophy and dysarthria. He also had pes planus, scoliosis, retained upper limb reflexes and hyperactive Patellar reflex. The clinical manifestation of the patient was not compatible with FRDA but was more suggestive of CMT with an atypical phenotype. The demonstration of homozygous *FXN* point mutation in this family suggests that this mutation causes a CMT-like disease and does not cause embryonic lethality.

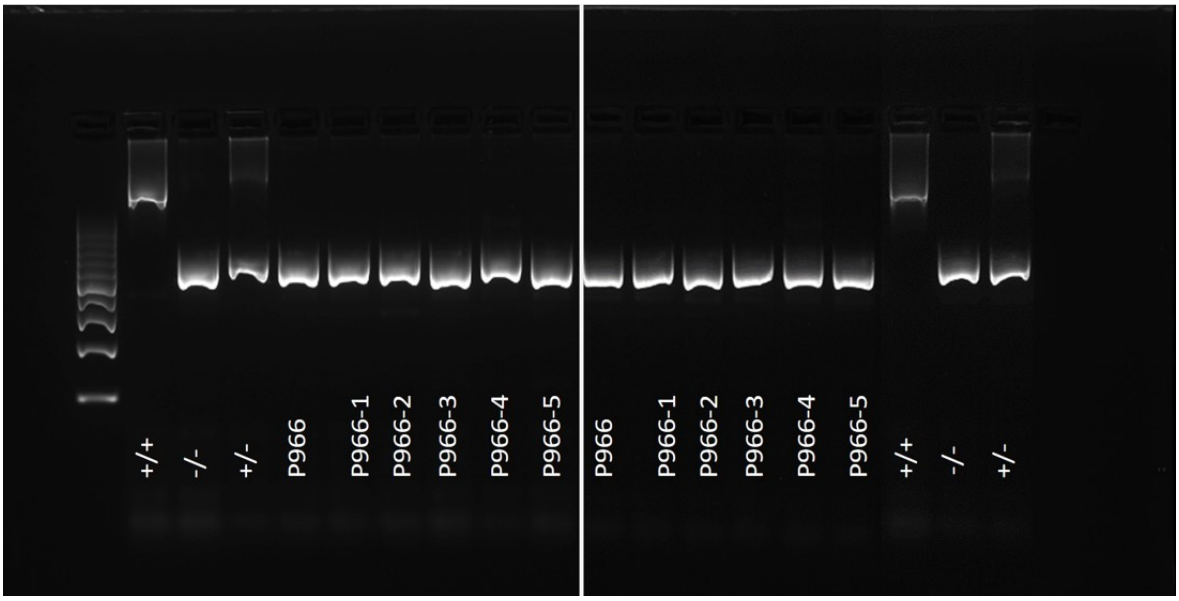

Figure 5.4. Gel image of long-range PCR for *FXN* pathological allele. +/+ refers to a positive control with pathological levels of GAA repeat expansion, -/- refers to a negative control, and +/- refers to a heterozygous carrier.

We have analyzed primary fibroblast cell lines generated from skin punch biopsy samples of the index patient, his heterozygous mother and a healthy volunteer to shed light into the molecular impact of this mutation. When the mRNA levels of these different cell lines were evaluated, we have observed no significant difference in *FXN* mRNA levels in family members or controls, as well as mRNA levels of *NFU1*, *AIFM1*, *APTX*, and *ACO1* genes (Figure 5.5B) which were shown to change dramatically in FRDA patient transcriptomes [134]. Similarly, no significant change in *FXN* and *NFU1* protein expression was observed in the patients, his heterozygous mother and the healthy control (Figure 5.5C). Our findings suggest that even though the *FXN* expression is not altered in the patient, the functioning of the protein must be perturbed by the mutation, which in turn causes the phenotype.

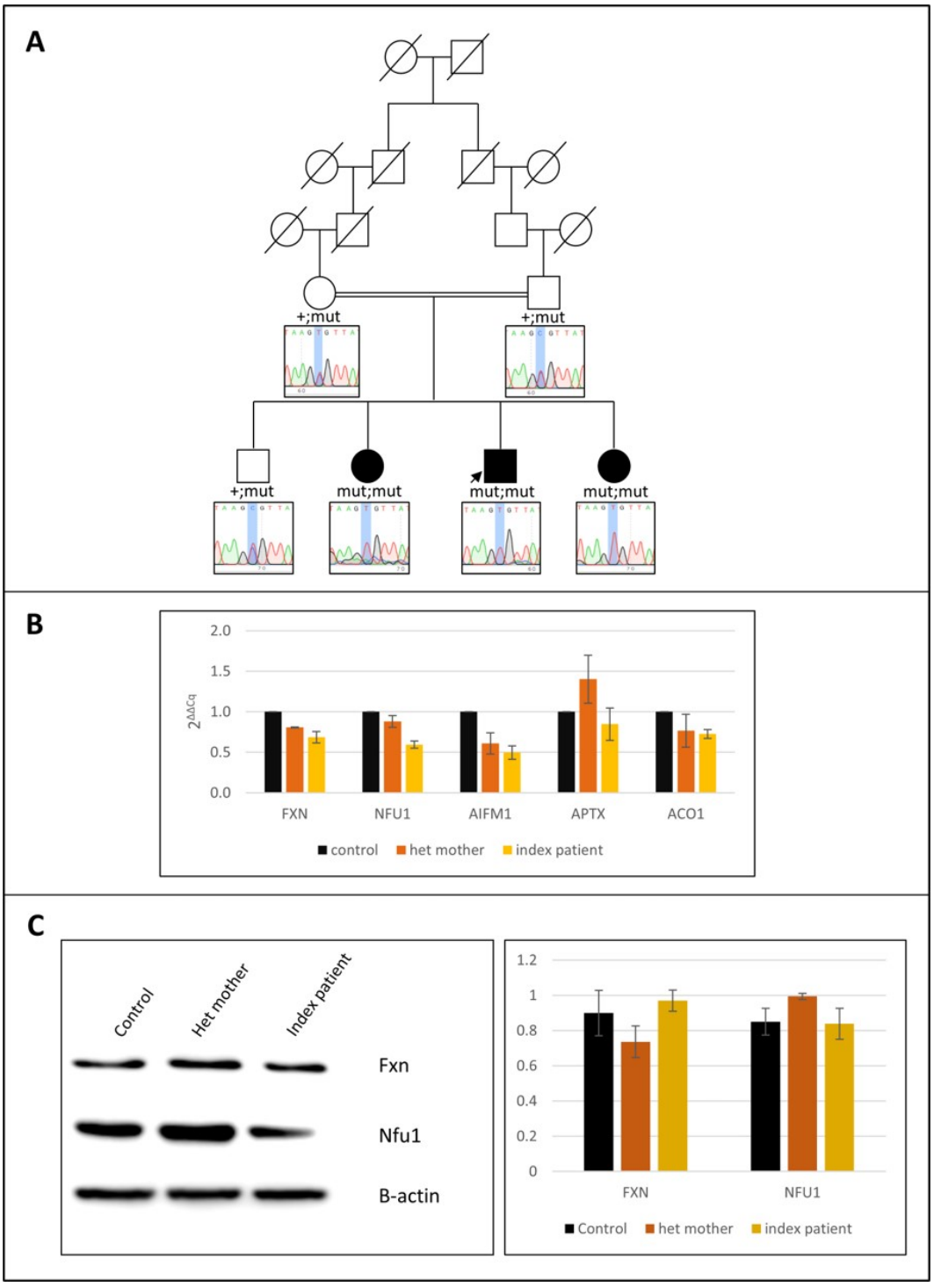

Figure 5.5. Genetic and molecular findings for family P966. A) Individual electropherograms showing the mutation in the *FXN* gene. B) Relative mRNA levels in primary fibroblasts. C) Relative protein levels in primary fibroblasts.

5.4.2. Family P1258

Family P1258 had three affected siblings diagnosed with mild axonal peripheral neuropathy. The variants in known IPN-causative genes were initially examined in the WES data of the index patient. It was seen that the proband does not have a recurrent mutation that have been reported as pathogenic previously; however, she had novel variants in genes *TRK-Fused Gene* (*TFG*), *WASH Complex Subunit 5* (*WASHC5*), *Inverted Formin 2* (*INF2*), *Septin 9* (*SEPT9*), and *TATA-Box Binding Protein* (*TBP*). Pathogenic variants in these genes are known to cause spastic paraplegia 57, spastic paraplegia 8, DI-CMT-E, hereditary neuralgic amyotrophy, and spinocerebellar ataxia 17, respectively. The segregation analyses in the family showed that none of these variants segregated with the disease in the pedigree and therefore are excluded from disease-causing candidate variants. The results of the segregation analysis showing the genotypes of these individuals are given in Table 5.4.

Table 5.4. Genotypes of individuals from family P1258 for variants in known IPN-causative genes. Two alleles are shown for each variant. "var" indicates the allele contains the variant, while "+" indicates the allele is wild type.

Gene name and variant	***P1258-1***	***P1258-2***	***P1258-3***	***P1258-4***	***P1258-5***	***P1258-6***	***P1258-7***	***P1258-8***	***P1258-9***
TFG: c.68G>A, p.Arg23Gln	+,var	+,+	+,var	+,var	ND	+,var	+,var	ND	+,+
WASHC5: c.332+4T>C	+,var	+,var	+,var	+,+	ND	+,+	+,var	ND	+,+
INF2: c.2630G>A, p.Arg877Gln	+,+	+,+	+,+	+,var	ND	+,var	+,+	ND	+,var
SEPT9: c.1726A>G, p.Met576Val	+,+	+,+	+,+	+,+	ND	+,+	ND	ND	+,+
TBP: c.222_223insG, p.Gln75Alafs*103	+,var	+,+	+,+	+,var	ND	ND	ND	ND	ND

*Affected individuals are indicated with shaded columns. ND: Not done.

Once all candidate variants in neuropathy-related genes were excluded, WES data of the index patient was further analyzed in comparison with the HOMWES data. Figure 5.6 5.6 shows the homozygous regions larger than 1Mb throughout the exome of the index patient P1258-1. According to HOMWES data, the patient had large homozygous regions along chromosomes 1, 2, 3, 4, 6, 7, 8, 9, 10, 11, 14, 16, 17, 18, 19 and 22, some of which are extremely large (more than 5 Mb).

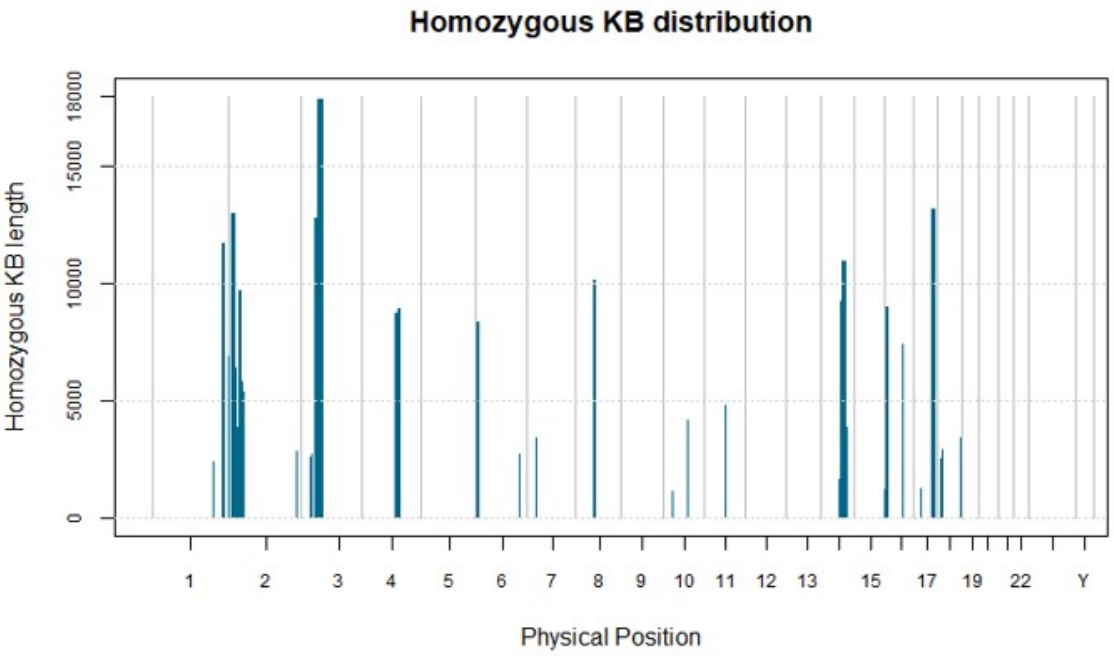

Figure 5.6. Homozygous regions over 1Mb on different chromosomes of patient P1258-1.

When the filtering criteria were applied to the WES variants found in these homozygous regions, 10 candidate variants previously not associated with any neurological condition were determined. The results of the segregation analyses of these candidate variants are given in Table 5.5.

Table 5.5. Genotypes of individuals from family P1258 for candidate variants. Two alleles are given for each variant. "var" indicates the allele contains the variant, "+" indicates the allele is wild-type.

Gene name and variant	**P1258-1**	**P1258-2**	**P1258-3**	**P1258-4**	**P1258-5**	**P1258-6**	**P1258-7**	**P1258-8**	**P1258-9**
ATP8B3: c.3056G>A, p.Gly1019Asp	var,var	var,var	var,var	+,var	+,var	+,+	+,+	+,+	+,var
CAPN13: c.60C>A, p.Asp20Glu	var,var	var,var	var,var	+,var	+,var	+,var	+,var	var,var	+,var
PIK3IP1: c.193G>A, p.Gly65Ser	var,var	var,+	var,var	var,var	var,var	var,var	var,+	var,var	var,var
C2ORF61: c.452A>T, p.Lys151Ile	var,var	var,var	var,var	var,var	ND	ND	ND	ND	ND
SPINK8: c.2T>C, p.Met1?	var,var	var,var	var,var	+,var	+,var	+,var	+,var	var,var	+,var
SLC26A6: c.67G>C, p.Asp23His	var,var	var,var	var,var	+,var	+,var	+,var	+,var	var,var	+,var
PSME4: c.1504-4A>G	var,var	var,var	var,var	var,var	ND	ND	ND	ND	ND
ZNF814: c.1789G>A, p.Val597Ile	var,var	var,var	var,var	+,var	+,+	var,var	+,var	+,var	var,var
ABCA8: c.1826C>G, p.Pro609Arg	var,var	var,var	var,var	+,var	+,+	+,+	+,var	var,var	+,var
MAT1A: c.-78_-73dup	var,var	var,var	var,var	+,var	var,var	var,var	var,var	var,var	var,var

*Affected individuals are indicated with shaded columns. ND: Not done.

As can be observed from Table 5.5, only the variant in *ATP8B3* gene segregated with disease status in the pedigree. The global alternative allele frequency of this variant was reported as 0,003094 in gnomAD. SIFT predicted the variant to be deleterious (score: 0) and PolyPhen2 predicted it to be probably damaging (score: 0,929). This missense variant causes a change in the amino acid sequence; it replaces a codon encoding a glycine residue into a codon encoding an aspartic acid residue, which has a negatively charged side chain.

ATP8B3 is a member of type-4 P-type ATPase protein subfamily that are transmembrane proteins that transport phospholipid molecules in exchange of ATP [135–137]. Also called P4-ATPases, these proteins contribute to asymmetric distribution of phospholipids in biological membranes; hence, pathogenic mutations in these genes may have severe consequences in cell and organelle morphology, cell movement, division, signal transduction, and vesicle biogenesis and transport [136, 138–140]. In fact, loss of function mutations in several P4-ATPases have been shown to cause neurodegeneration and sensory impairment in mice [141–143]. *ATP8B3* has been suggested to actively transport phosphatidylserine and have a role in male mouse fertility [144, 145]. More recently, a study investigating genetic variants in sporadic ALS cases reported an individual with two compound heterozygous variants in *ATP8B3* [146], one of which is the same variant as in our family P1258 (p.Gly1019Asp).

The genetic findings in the family and the findings in literature suggested the homozygous variant in the *ATP8B3* gene might be disease-causing in family P1258. Therefore, we have sought to further investigate the pathogenicity of this variant. Unfortunately, during the study period the index patient passed away due to an unrelated disease; thus, we obtained skin biopsy samples from one of her affected siblings (P1258-2) and her heterozygous mother. Using the fibroblast cell line generated from biopsy samples, we have tried to analyze mRNA expression levels of different P4-ATPases and *CDC50A*, *CDC50B*, and *CDC50C*, since they were shown to be critical interactors of P4-ATPases [147]. Unfortunately, we could not detect *ATP8B3* mRNA using qPCR although we tried different primers for the assay (data not shown).

On the other hand, when we have prepared cell extracts from fibroblast lines and performed Western blotting to investigate Atp8b3 protein expression, we could detect protein bands in both control and patient fibroblasts, although there was no difference in the expression levels of Atp8b3 protein between primary fibroblasts of the patient, her heterozygous mother and a healthy control individual (Figure 5.7).

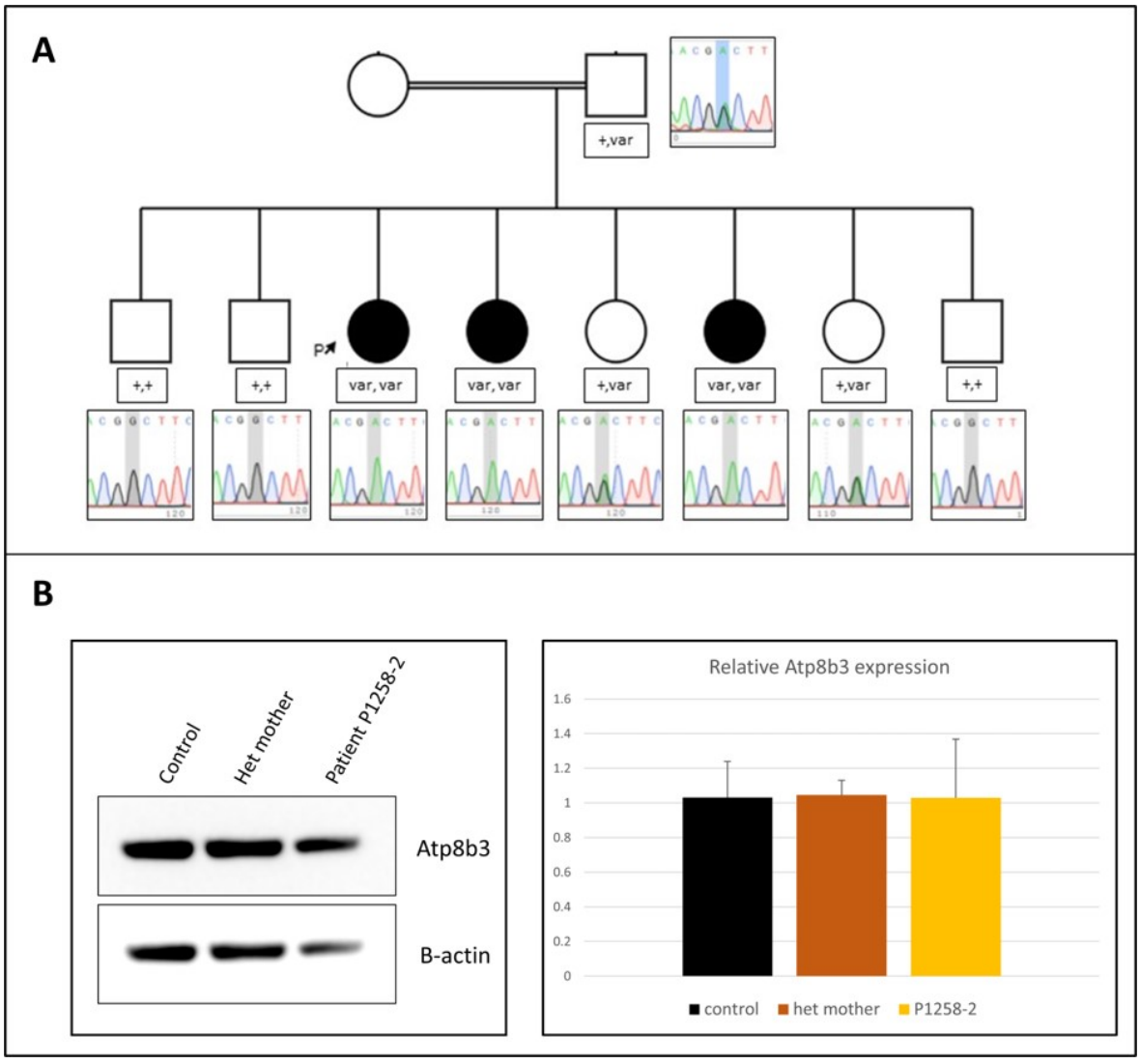

Figure 5.7. Genetic and molecular findings for family P1258. A) Individual electropherograms showing the variant in the *ATP8B3* gene. B) Relative Atp8b3 protein levels in primary fibroblasts.

The molecular analyses in this family did not reveal a distinct phenotype in patient cells. We, then, collaborated with another research group in order to analyze the effect of the variant on the protein using molecular dynamics simulations. Since the crystal structure of *ATP8B3* was missing in the literature, SWISS-MODEL tool was used to predict 3D structure of the protein [148,149]. Next, Visual Molecular Dynamics (VMD) software was used to model the movement of the wild-type and mutant protein structure under normal cellular conditions [150]. Figure 5.8 shows the radius of gyration (Rg) graph for wild-type and mutant *ATP8B3*. Rg is the root-mean-square (RMSD) distance of each atom in the protein structure from the center of mass of the protein and it is an indicator of compactness of a protein [151]. In Figure 5.8A, there is a significant difference between Rg of the wild-type and mutant protein. The simulation of the protein movements for 50ns under normal cellular conditions shows that the mutant protein is significantly more compact than the wild-type protein, suggesting the backbone of the mutant protein is less mobile.

The 3D model of the protein showed that the 1019th residue resided in a loop connecting two alpha helices, one of which extends to a Mg^{+} binding pocket in the protein. Using the VMD tool, we have then measured the distances between important amino acid residues in the protein that may coordinate the Mg^{+} ion in the binding pocket and the Mg^{+} ion in this pocket. Figure 5.8B shows the distance between the Mg^{+} ion and the tyrosine amino acid at 497th residue in wild-type and mutant protein. It can be observed here that this distance is significantly increased in the mutant protein, suggesting that the variant observed in family P1258 might reduce the ability of Mg^{+} coordination of the protein. Additional analyses of different residues that interact with the Mg^{+} ion obtained with VMD simulations are in accordance with this finding and are given in Appendix B. Our findings suggest that the variant in family P1258 might have a significant impact on Atp8b3 molecular dynamics that might affect normal protein function and cause a neurological pathology.

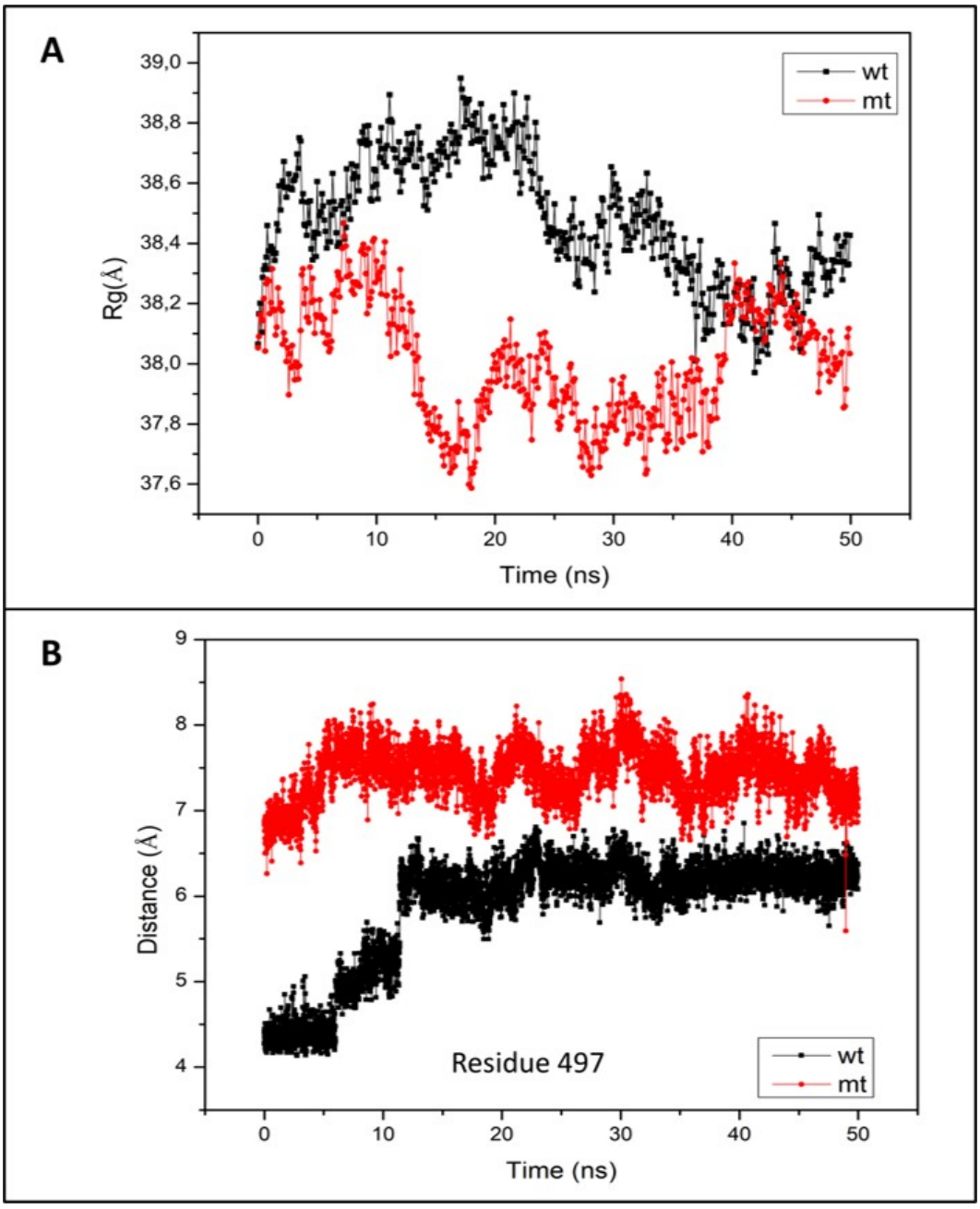

Figure 5.8. *In silico* findings for the variant observed in the *ATP8B3* gene. A) Radius of gyration for wild-type and mutant Atp8b3. B) The distance of the tyrosine amino acid at residue 497 to the Mg^{+} ion in the binding pocket.

5.4.3. Family P1251

In family P1251, the symptoms of the index patient started at eight years of age and the neurological examination identified cerebellar ataxia with sensory and motor axonal neuropathy. The index case had no pathogenic variants in any CMT genes, , however she had novel variants in genes *DNA Methyltransferase 1* (*DNMT1*), *Cytochrome P450 Family 2 Subfamily U Polypeptide 1* (*CYP2U1*), *Vesicle-Associated Membrane Protein-Associated Protein B* (*VAPB*), *Ataxin 7* (*ATXN7*), *Calcium Channel Voltage-Dependent P/Q Type Alpha 1A Subunit* (*CACNA1A*), *Coiled-Coil Domain-Containing Protein 88C* (*CCDC88C*) and *Plectin* (*PLEC*) that are known to cause hereditary sensory neuropathy, hereditary spastic paraplegia, amyotrophic lateral sclerosis, spinocerebellar ataxia 7, spinocerebellar ataxia 6, spinocerebellar ataxia 10 and muscular dystrophy 17, respectively. The segregation analyses showed that none of these variants segregated with the disease in the pedigree and therefore are excluded from disease-causing candidate variants. The genotypes of the family members for these variants are given in Table 5.6.

Table 5.6. Genotypes of individuals from family P1251 for variants in known IPN-causative genes. Two alleles are given for each variant. "var" indicates the allele contains the variant, while "+" indicates the allele is wild-type.

Gene name and variant	**P1251-1**	**P1251-2**	**P1251-3**	**P1251-4**	**P1251-5**
CYP2U1: c.992A>G, p.Asn331Ser	+,+	+,var	+,var	+,var	+,+
DNMT1: c.2382-4C>T	+,+	+,var	+,var	+,+	+,var
VAPB: c.390T>G, p.Asp130Glu	+,var	+,+	+,var	+,var	+,var
ATXN7: c.1901C>T, p.Ala634Val	+,+	+,var	+,var	+,+	+,var
CACNA1A: c.2204A>C, p.Glu735Ala	+,var	+,+	+,var	+,var	+,+
CACNA1A: c.6991_6993dupCAG, p.Gln2331dup	+,var	+,var	+,var	+,+	+,var
CCDC88C: c.2429A>G, p.Asn810Ser	+,var	+,var	+,var	var,var	+,var
PLEC: c.9512C>T, p.Ala3171Val	+,var	+,+	+,var	ND	+,+

*The affected individual is indicated with shaded columns. ND: Not done.

Once all candidate variants in neuropathy-related genes were excluded, WES data of the index patient was further analyzed in comparison with HOMWES data. Figure 5.9 shows the homozygous regions larger than 1Mb throughout the exome of the index patient P1251-3. According to HOMWES data, the patient had large homozygous regions along chromosomes 3, 4, 5, 9, 11, 14, 15, 16 and 19. The largest homozygous regions reside on chromosomes 3 and 4 of the patient exome.

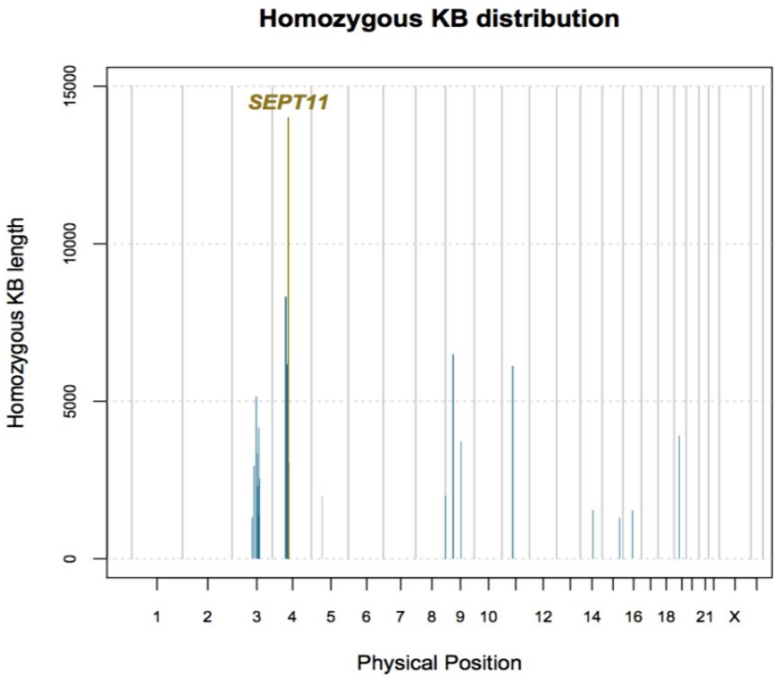

Figure 5.9. Homozygous regions over 1Mb on different chromosomes of index patient P1251-3. The homozygous region on chromosome 4 where *SEPT11* gene is located is shown in gold color.

When the filtering criteria were applied to the WES variants found in these homozygous regions, seven candidate variants in six genes previously not associated with any neurological condition were determined. All these genes were located on chromosomes 3 and 4. Chromatograms of the variants in neuropathy-related genes and candidate variants found in family P1251 are given in Appendix A, while genotypes of the individuals for the candidate variants are given in Table 5.7.

Table 5.7. Genotypes of individuals from family P1251 for candidate variants. Two alleles are given for each variant. "var" indicates the allele contains the variant, "+" indicates the allele is wild-type.

Gene name and variant	**P1251-1**	**P1251-2**	**P1251-3**	**P1251-4**	**P1251-5**
ARGFX: c.863C>T, p.Thr288Ile	var,+	var,+	var,var	var,+	ND
KIAA1524: c.173G>T, p.Cys58Phe	var,+	var,+	var,var	var,+	+,+
POLQ: c.7393G>A, p.Glu2465Lys	var,+	var,+	var,var	var,+	+,+
SEPT11: c.263_264insG, p.Glu89GlyfsTer12	var,+	var,+	var,var	var,+	+,+
SHROOM3: c.1691A>C, p.Glu564Ala	var,var	var,var	var,var	var,var	var,var
SHROOM3: c.3035C>A, p.Thr1012Asn	var,var	var,var	var,var	var,var	var,var
SULT1B1: c.-9G>T	var,var	var,+	var,var	var,var	+,var

*The affected individual is indicated with shaded columns. ND: Not done.

As can be seen in Table 5.7, only the variants in *ARGFX*, *KIAA1524*, *POLQ* and *SEPT11* segregated with disease in the pedigree. Thus, *SHROOM3* and *SULT1B1* were excluded as candidate disease-causing genes in this family. To prioritize one of these candidate genes, we have utilized two *in silico* tools, ToppGene and Endeavour, using autosomal recessive CMT-causative genes as training genes. In both tools, *ARGFX* was ranked the last and *POLQ* was ranked third. On the other hand, *SEPT11* was ranked first in Endeavour, while *KIAA1524* was ranked first in ToppGene. Data generated by Endeavour and ToppGene is given in the Appendix C. Taking the nature of the variants into consideration, we have decided that *SEPT11* should be the main candidate gene since it was the only one among the candidates to cause a frameshift in the protein sequence that generates a premature stop codon. This variant was not reported in population databases including ExAc, 1000g and gnomAD, and MutationTaster algorithm predicted the variant to cause nonsense-mediated mRNA decay.

SEPT11 is a member of the septin family of GTP-binding proteins that are known to polymerize into three-dimensional structures such as filaments and rings [152].

These proteins have been shown to function in various cellular processes including cytokinesis, intracellular vesicle trafficking and scaffold-forming [153–155]. It was also reported that some septins localize at the base of dendritic spines in the hippocampal neurons and knock-down of *SEPT7* or *SEPT11* reduces dendritic branching and spine density [152, 156–158]. Moreover, it was shown that different septins are expressed during oligodendrocyte and Schwann cells development, and *SEPT11* expression, as well as septins 2, 3, 5, 6, 7, 8, 9 and 10, is increased during the highest myelination period in the sciatic nerve [159].

SEPT11 protein has been shown to be highly expressed in fibroblasts [153]; therefore, we have obtained patient fibroblasts to show the impact of *SEPT11* mutation at a molecular level. It has been known that septin protein family members frequently interact with each other [160]. Besides, Hall and Russell (2004) suggested that RNAi-mediated knock-down of a septin in a complex could alter the expression of other components in that complex [161]. Martinez *et al.* (2004) have shown that cellular repertoire of human septins is important for specific cellular locations of individual septins [162]. Thus, it can be suggested that depletion of SEPT11 may alter the expression, localization or bundling of other septins. To elaborate on this matter, we have analyzed mRNA expression of all septin family members that are readily expressed in fibroblasts. The Cq values obtained from the qPCR analysis and the calculations done using the $\Delta\Delta$Cq method are given in Appendix D. Figure 5.10B shows the $\log_2$-fold change of different septin mRNAs in patient fibroblasts compared to control cells. Accordingly, *SEPT5* and *SEPT6* mRNA levels were significantly increased in P1251 fibroblasts, while *SEPT11* mRNA levels were significantly decreased. The decrease in *SEPT11* mRNA levels in P1251 fibroblasts indicates that the variant seen in WES data of the patient causes a real change in the cell. Besides, the increase in *SEPT5* mRNA levels might support the presence of a SEPT5/7/11 complex suggested by Xie *et al.* (2007) [156]. Because SEPT7 is an essential component of all other septin complexes [163], it might be suggested that its expression is not affected by the expression levels of other septins. In addition, SEPT11, which is the closest homolog of SEPT6, was found to be increased in the myelin membranes of SEPT6-null mouse [159, 164].

Our findings also suggest a compensation mechanism between SEPT6 and SEPT11 in consensus with these studies.

Figure 5.10C shows relative SEPT9 and SEPT11 protein expression in P1251 fibroblasts. In patient cell extracts, although protein bands were observed on blots targeting SEPT9, vinculin and actin, no bands were observed in blots targeting SEPT11, even when high amounts of cell extracts were used for Western blotting. The anti-SEPT11 antibody (ab183537) recognizes the C-terminal of the major SEPT11 transcript (Q9NVA2) with the immunogen being a synthetic peptide of amino acids 379-429 in SEPT11 transcript Q9NVA2. The recognition sequence only differs in the last four and six amino acids with alternative Sept11 transcripts H0Y9G8 and H0Y961, respectively. It is possible that the antibody does not recognize the products of H0Y961 and H0Y9G8 transcripts due to the difference in the last amino acid sequences if these amino acids change 3D structure of the protein and cause a change in the epitope that is recognized by the antibody. It is also possible that these alternative transcripts are not expressed in fibroblasts. Still, it is obvious from the results that the major Sept11 protein transcript is not expressed in patient fibroblasts. On the other hand, there is no significant difference in SEPT9 protein expression between patient and control fibroblasts. The representation of alternative transcripts of SEPT11 protein is shown in Figure 5.11 together with the positions of the variant observed in the patient, the primers used for qPCR analysis and the immunogen used for the production of the antibody that recognizes the C-terminal of Sept11 protein.

We have also performed immunofluorescence assays to check the localization of SEPT9 and SEPT11 proteins in primary fibroblasts. Figure 5.12 shows confocal microscopy images of control and P1251 primary fibroblasts after antibody staining for SEPT9 and F-actin. We did not encounter a significant difference in anti-SEPT9 staining of the control and P1251 cells. In both cell types, SEPT9 protein localizes to the cytoplasm and there seems to be no significant difference in the amount of SEPT9 protein, which was also previously shown using Western blotting. Additional confocal microscopy images are given in Appendix E.

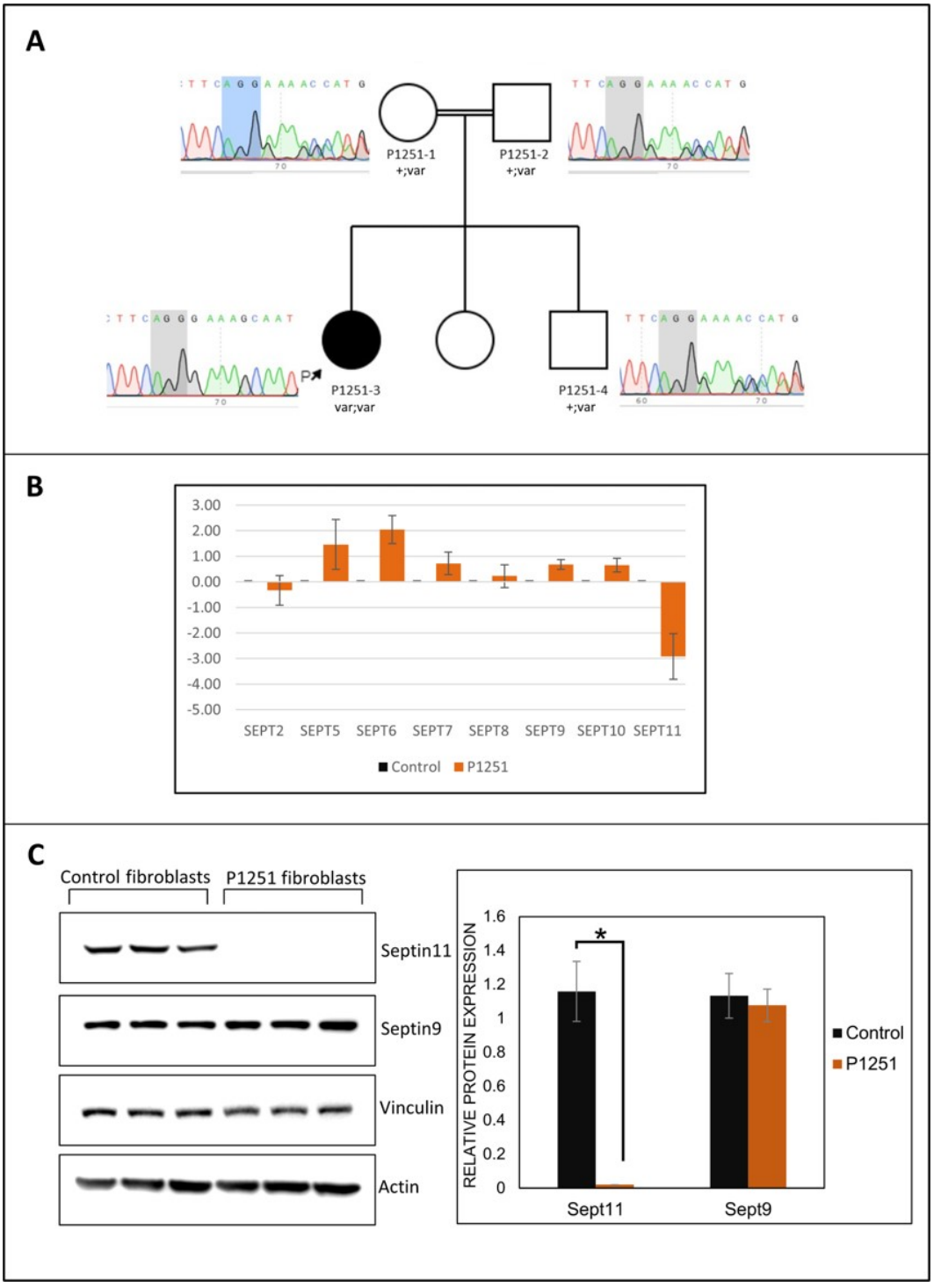

Figure 5.10. Genetic and molecular findings for family P1251. A) Individual electropherograms showing the variant in the *SEPT11* gene. B) Relative mRNA levels in primary fibroblasts. C) Relative protein levels in primary fibroblasts.

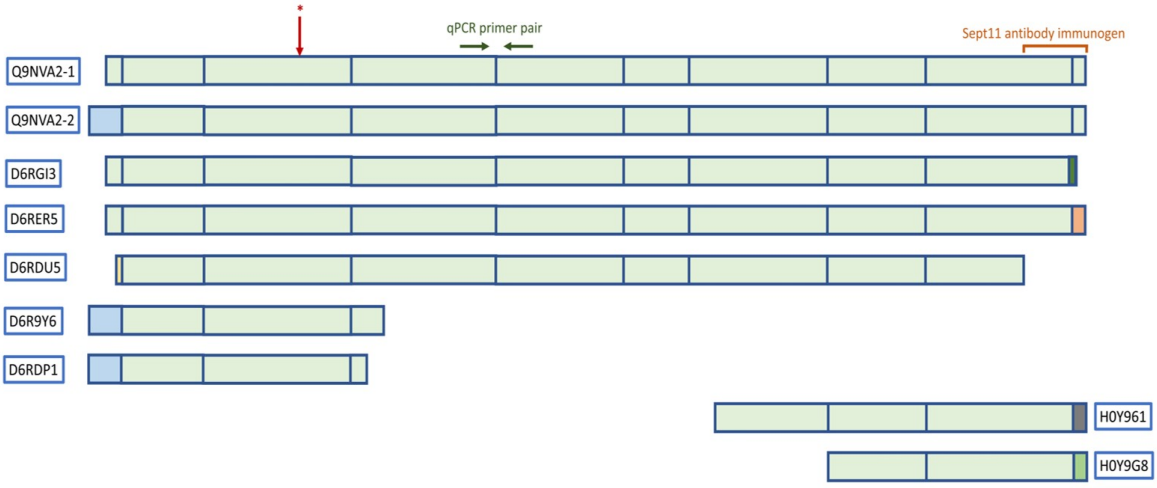

Figure 5.11. Representation of alternative SEPT11 transcripts in the UniProtKB database. The position of the P1251 variant is indicated with a red asterisk.

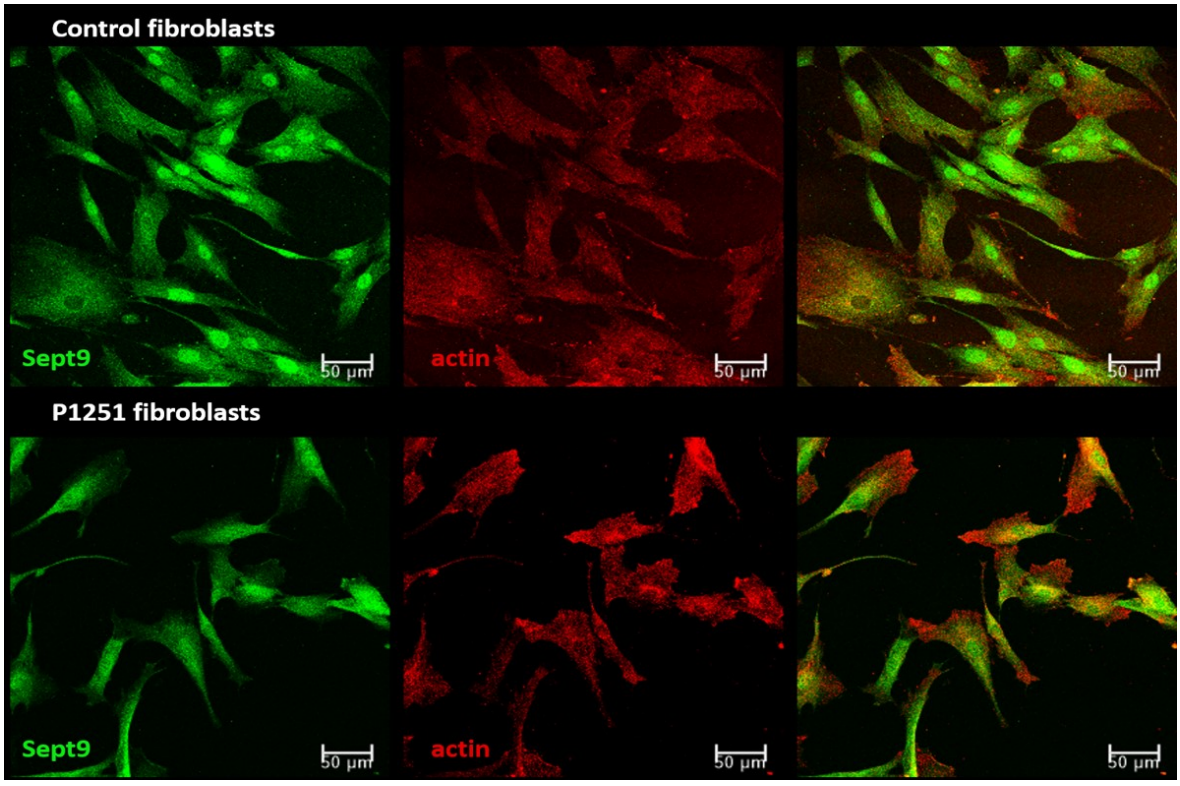

Figure 5.12. Confocal microscopy images of control and P1251 fibroblasts after antibody staining of SEPT9 and F-actin.

We tested SEPT11 C-terminal antibody (ab183537) in immunofluorescence assay, even though the antibody was not tested nor guaranteed to work in immunofluorescence assays by the manufacturer. Figure 5.13 shows the confocal microscopy images of control and P1251 fibroblasts after antibody staining for SEPT11 and F-actin.

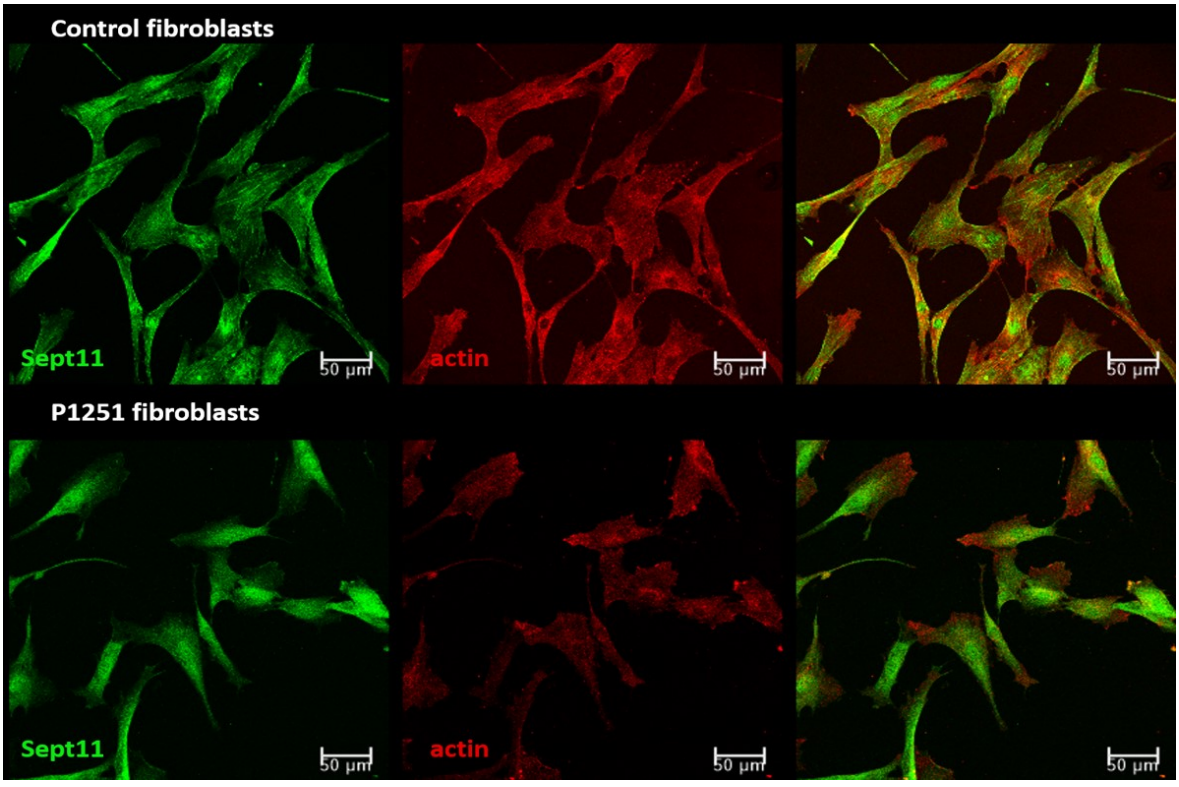

Figure 5.13. Confocal microscopy images of control and P1251 fibroblasts after antibody staining of SEPT11 and F-actin.

It can be observed in Figure 5.13 that both control and P1251 fibroblasts were positive for staining with anti-SEPT11 antibody (green panel). This is quite interesting since the Western blotting results implied there was no SEPT11 protein expression, at least for the major transcript, in the patient fibroblasts. During Western-blotting, the cell extracts are mixed with Laemmli buffer containing β-mercaptoethanol, heated to 95°C and run on a resolving gel containing SDS. In this technique, the proteins are denatured so that they can be separated on gel based on their sizes. Then, the gel is blotted onto a membrane and the membrane is incubated in a specific antibody solution.

However, in the IF assay, the cells are fixed with paraformaldehyde and then incubated in a specific antibody solution. In the IF procedure, the proteins are fixed in the cells in their native conformations. As shown in Figure 5.11, the variant observed in patient P1251 seems to disrupt the major transcript and most alternative transcripts of SEPT11 protein, except for transcripts H0Y961 and H0Y9G8. Thus, we may expect to observe these smaller transcripts on the Western-blotting membranes if they are normally expressed in fibroblasts, but there were no protein bands recognized with this antibody in patient cell extracts at all. There is a possibility that the antibody does not recognize the products of alternative transcripts in denatured form as in Western blotting but recognizes the epitope in its native form in IF assay. Perhaps, the signal we get from SEPT11 antibody in the IF assay reflects the presence of alternative transcripts (H0Y961 and H0Y9G8) of SEPT11 protein in patient fibroblasts.

Another striking observation is the difference in the staining pattern for SEPT11 in control and patient fibroblasts. In control cells, SEPT11 seem to form filament-like structures, while patient fibroblasts lack this fibrous pattern. This can suggest that the variant in *SEPT11* gene disrupts the protein structure, as well as expression, and prevent septin bundling in the cell.

We, then cloned the major transcript (Q9NAV2) of wild-type and mutant *SEPT11* into mammalian expression vectors containing a GFP signal using Gateway cloning and overexpressed these proteins in HEK293 cells to check for protein localization (Figure 5.14). It is also clear in these overexpression cell models that the mutant protein is unable to form filaments when compared to wild-type SEPT11.

Based on the findings that the variant in *SEPT11* gene in family P1251 segregates in the family, causes a frameshift mutation, significantly decreases mRNA and protein levels and diminishes the ability of SEPT11 major transcript to form filaments, we have determined this gene as a novel disease-causing gene for autosomal recessive cerebellar ataxia with axonal peripheral neuropathy according to the prominent clinical features of our index patient in this family.

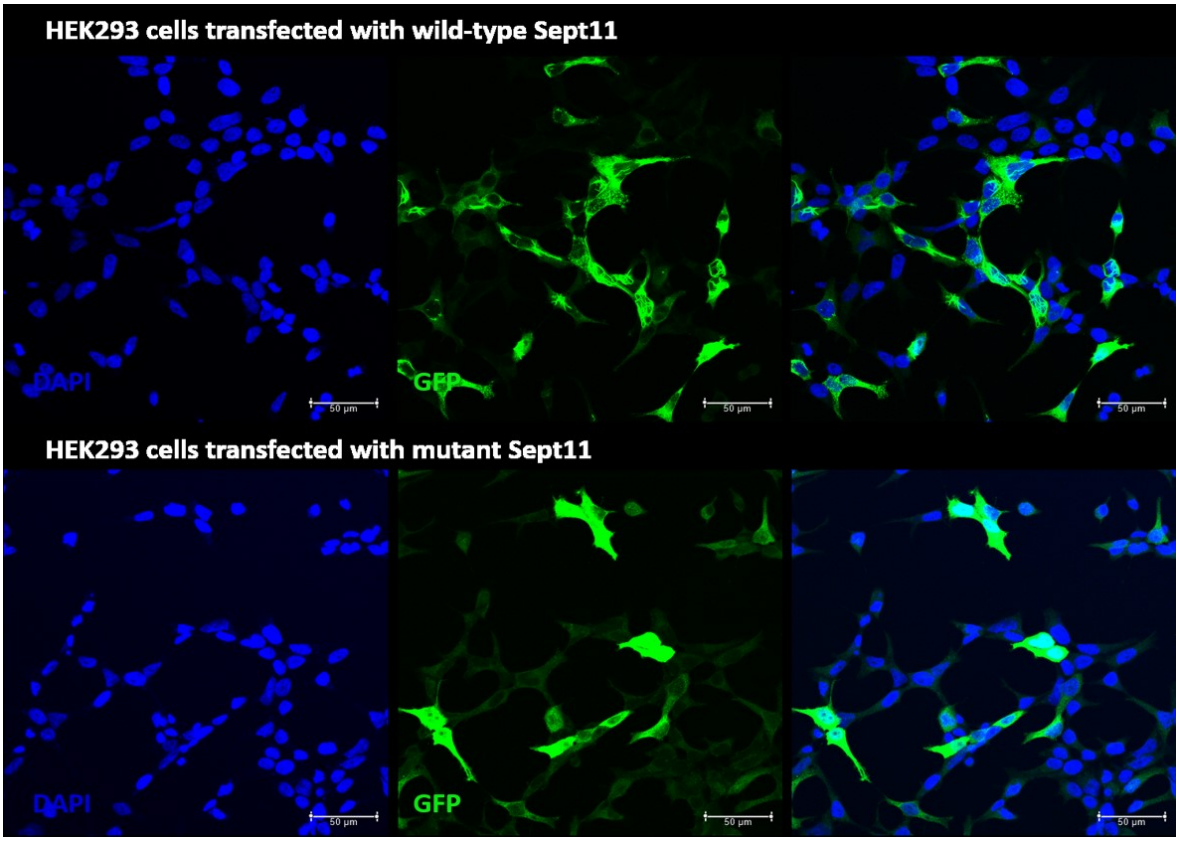

Figure 5.14. Confocal microscopy images of HEK293 cells overexpressing wild-type and mutant SEPT11 with a GFP tag at the C-terminal.

5.5. Undiagnosed Cases

Initially, 56 families were enrolled in the study and throughout the study, six patients were shown to have recurrent disease-causing mutations in the *GDAP1* gene, 16 were found to have recurrent mutations in various known inherited neuropathy-related genes, 13 were found to have novel variants in known inherited neuropathy genes. Moreover, in one family we have identified a novel gene-disease relationship (*FXN* in P966 family) and in two families, we have identified candidate disease-causing genes (*ATP8B3* and *SEPT11*). In addition to that, two families who were initially willing to take part in the study, retracted their consents (patients P470 and P567). Therefore, analyses were finalized in 40 patients in total.

Even with the use of NGS technology, 16 families remained to be genetically undiagnosed. No recurrent/novel variants in known neuropathy-related genes or novel candidate genes were determined in patients P77, P954, P1282, and P1350-3 that match the filtering criteria. This is mainly because the number and/or the length of the homozygous regions in these patients were too small. Although parental consanguinity criterion was provided for all patients, the lack of homozygous regions in these four patients suggests an autosomal dominant segregation rather than recessive. If we exclude the homozygosity criteria during filtration of the WES data, about 2000 variants are found that satisfy other filtering criteria. Segregation analysis of all of these variants in families is extremely costly and requires an irredeemable amount of time, therefore the analyses were terminated for these four patients.

For the eight undiagnosed patients (P165, P241, P774, P854, P1150, P1154, P1302, and P1353), 170 candidate variants satisfying the filtering criteria were determined. However, DNA samples from family members were unavailable; therefore, segregation analyses could not be performed and the analyses were terminated.

For the last four families (P809, P1025, P1220, and P1336), candidate variants that meet the filtering criteria in the large homozygous regions are given in Table 5.8. All variants listed in the table have been checked for segregation with DNA samples from available family members. The segregating variants remain to be candidate genes, however, as can be seen in Table 5.8, there are multiple candidate genes for each family. Due to time and funding constraints, these variants have not been investigated further for pathogenicity using cellular/molecular tools. Instead, we have uploaded our genetic findings to GeneMatcher and GENESIS databases, which are platforms that facilitate data sharing among different institutions conducting genetic research. These tools allow researchers to contact each other and collaborate if they have families with matching genetic findings. In fact, we have been contacted with another research group for the *TAF1A* gene variant in family P809 who have an additional family with a variant in the same gene and a similar phenotype and are willing to perform functional analyses for these variants.

Table 5.8. Candidate variants that satisfy the filtering criteria and reside in the homozygous regions of patients with no recurrent mutations in known genes.

Family ID	Gene name	Reference transcript transcript	Change in the coding sequence	Change in the protein sequence	Hom/ Het
P809	GCHFR	NM_005258.2	c.-42G>T	-	Hom
	HNF4G	NM_004133.4	c.703+6_703+7delTT	-	Hom
	MACROD2	NM_080676.5	c.163+7T>C	-	Hom
	MGRN1	NM_015246.3	c.385C>T	p.Arg129Cys	Hom
	MROH8	NM_152503.4	c.93_94insAGTG CCGGCCGCGGGG CCCTGTCTATAAG	p.Pro32Serfs*1022	Hom
	NEBL	NM_001010896.2	c.184C>T	p.Arg62Trp	Hom
	OR2C1	NM_012368.2	c.245T>C	p.Leu82Pro	Hom
	PLCG2	NM_002661.3	c.1444T>C	p.Tyr482His	Hom
	PMEL	NM_001200054.1	c.575G>A	p.Arg192Gln	Hom
	POLN	NM_181808.2	c.670A>G	p.Thr224Ala	Hom
	SELO	NM_031454.1	c.832G>A	p.Asp278Asn	Hom
	SPTBN5	NM_016642.2	c.3698G>A	p.Arg1233Gln	Hom
	TAF1A	NM_005681.4	c.869G>C	p.Arg290Thr	Hom
	TOX2	NM_001098797.1	c.370C>A	p.Leu124Ile	Hom
	TMX4	NM_021156.2	c.362G>A	p.Arg121His	Het
	WDR76	NM_024908.3	c.1603C>T	p.Leu535Phe	Hom
P1025	COQ9	NM_020312.3	c.826C>T	p.Arg276Trp	Hom
	PDE11A	NM_016953.3	c.-46A>G	-	Hom
	PPFIBP2	NM_003621.3	c.1601C>G	p.Ala534Gly	Hom
	RBM20	NM_001134363.1	c.2262C>A	p.Ser754Arg	Hom
P1220	USP47	NM_017944.3	c.76G>C	p.Asp26His	Hom
	CBS	NM_000071.2	c.1145+7C>T	-	Hom
P1336	ADCY4	NM_001198568.1	c.1991T>C	p.Ile664Thr	Hom
	ADCY4	NM_001198568.1	c.1391T>C	p.Leu464Pro	Hom
	PDCD6IP	NM_013374.5	c.1300G>A	p.Asp434Asn	Hom
	RBM6	NM_005777.2	c.1058C>T	p.Ser353Phe	Hom

Hom: Homozygous variant, Het: Heterozygous variant. Variants that remain as candidates after familial segregation analyses are shown in shaded rows.

5.6. Diagnostic Outcome of the Analyses

The initial screening of the patients for recurrent *GDAP1* mutations in our cohort identified six families with *GDAP1* mutations. WES analysis identified the causative gene/variant for 29 additional cases. Among these, 16 had recurrent and 13 had novel variants in known inherited neuropathy-related genes. This approach of screening known disease-causing genes allowed genetic diagnosis for 62,5% (35/56) of families in our cohort. Nine of the novel variants met the ACMG variant classification and are classified as "likely pathogenic" or "pathogenic". The other four novel variants in known neuropathy-related genes are not considered definitive diagnoses since these missense variants are classified as "variants of uncertain significance/VUS" according to ACMG criteria. Excluding these three families with VUS, the definitive genetic diagnosis rate was 55,35%. We have also identified a novel gene-disease relationship and presented highly potent *in silico*/*in vitro* findings for two additional candidate genes to be considered as disease-causing. The summary of all genetic findings for all the families enrolled in the study are listed in Table 5.9.

Table 5.9. Summary of genetic findings of the study cohort.

Nr.	**ID**	**Family history**	**Age of onset**	**mNCV (m/s)**	**Molecular finding**	**Gene**	**Variant**	**AAF (%)**	**HGMD/ dbSNP ID**	**ACMG outcome**
1	P77	no	11-20 years	36.9	Unsolved	-	-	-	-	-
2	P165	no	DMM	60	Unsolved	-	-	-	-	-
3	P241	no	2-10 years	3.7	Unsolved	-	-	-	-	-
4	P265	yes	21-40 years	44.8	Novel allele in known gene	MME (NM_000902.3)	homozygous; c.531delA; p.Lys177Asnfs*15	NP	-	pathogenic
5	P294	no	2-10 years	IE	Recurrent mutation	GDAP1 (NM_018972.2)	homozygous; c.786delG; p.Phe263Leufs*22	NP	CD023843	pathogenic
6	P300	no	2-10 years	IE	Recurrent mutation	MFN2 (NM_014874.3)	heterozygous; c.1090C>T; p.Arg364Trp	NP	CM060340	pathogenic
7	P322	yes	2-10 years	22	Novel allele in known gene	SH3TC2 (NM_024577.3)	homozygous; c.1586G>A; p.Arg529His	0.00283	rs80338923	likely pathogenic
8	P431	no	11-20 years	50	Novel allele in known gene	HINT1 (NM_005340.5)	homozygous; c.99delT; p.Phe33Leufs*22	NP	-	pathogenic

mNCV: Motor nerve conduction velocity, AAF: Alternative allele frequency, IE: inexcitable, DMM: Delayed motor milestones, NP: Not present.

Table 5.9. Summary of genetic findings for the study cohort. (cont.)

Nr.	**ID**	**Family history**	**Age of onset**	**mNCV (m/s)**	**Molecular finding**	**Gene**	**Variant**	**AAF (%)**	**HGMD/ dbSNP ID**	**ACMG outcome**
9	P448	no	2-10 years	IE	Recurrent mutation	GDAP1 (NM_018972.2)	homozygous; c.174_176delinsTGTG; p.Pro59Valfs*4	NP	CX083408	pathogenic
10	P470	yes	>40 years	38,8	Unsolved	-	-	-	-	-
11	P492	no	at birth	16,7	Novel allele in known gene	MFN2 (NM_014874.3)	homozygous; c.271G>T; p.Val91Leu	NP	-	likely pathogenic
12	P555	no	2-10 years	>38	Recurrent mutation	GDAP1 (NM_018972.2)	homozygous; c.786delG; p.Phe263Leufs*22	NP	CD023843	pathogenic
13	P567	yes	2-10 years	55	Unsolved	-	-	-	-	-
14	P581	no	at birth	IE	Recurrent mutation	EGR2 (NM_000399.3)	heterozygous; c.1142G>A; p.Arg381His	NP	CM004043	pathogenic
15	P629	no	at birth	26.6	Novel allele in known gene	SPG7 (NM_003119.2)	homozygous; c.454A>G; p.Met152Val	0.006721	rs146186857	VUS

mNCV: Motor nerve conduction velocity, AAF: Alternative allele frequency, IE: inexcitable, DMM: Delayed motor milestones, NP: Not present.

Table 5.9. Summary of genetic findings for the study cohort. (cont.)

Nr.	**ID**	**Family history**	**Age of onset**	**mNCV (m/s)**	**Molecular finding**	**Gene**	**Variant**	**AAF (%)**	**HGMD/ dbSNP ID**	**ACMG outcome**
16	P639	yes	20 years	32	Recurrent mutation	SH3TC2 (NM_024577.3)	compound heterozygous; c.2642A¿G; p.Asn881Ser and c.1586G>A; p.Arg529His	0.002123 and 0.002830	CM064263 and rs80338923	likely pathogenic
17	P711	yes	21-40 years	29	Recurrent mutation	GJB1 (NM_001097642.2)	heterozygous; c.47A>T; p.His16Leu	NP	CM095432	pathogenic
18	P774	no	2-10 years	19.8	Unsolved	-	-	-	-	-
19	P809	yes	11-20 years	57.8	Unsolved	-	-	-	-	-
20	P811	yes	at birth	IE	Recurrent mutation	PRX (NM_181882.2)	homozygous; c.1102C>T; p.Arg368Ter	NP	CM011005	pathogenic
21	P854	no	DMM	16	Unsolved	-	-	-	-	-
22	P954	yes	11-20 years	19	Unsolved	-	-	-	-	-
23	P963	no	2-10 years	11.7	Novel allele in known gene	NDRG1 (NM_001135242.1)	homozygous; c.237C>A; p.Tyr79Ter	NP	rs199928197	pathogenic

mNCV: Motor nerve conduction velocity, AAF: Alternative allele frequency, IE: inexcitable, DMM: Delayed motor milestones, NP: Not present.

Table 5.9. Summary of genetic findings for the study cohort. (cont.)

Nr.	**ID**	**Family history**	**Age of onset**	**mNCV (m/s)**	**Molecular finding**	**Gene**	**Variant**	**AAF (%)**	**HGMD/ dbSNP ID**	**ACMG outcome**
24	P966	yes	DMM	IE	Candidate gene	FXN (NM_000144.4)	homozygous; c.493C>T; p.Arg165Cys	NP	rs138034837	pathogenic
25	P969	yes	DMM	IE	Novel allele in known gene	NEFL (NM_006158.3)	homozygous; c.54C>A; p.Tyr18Ter	0.0004363	-	likely pathogenic
26	P987	yes	at birth	IE	Recurrent mutation	GDAP1 (NM_018972.2)	homozygous; c.786delG; p.Phe263Leufs*22	NP	CD023843	pathogenic
27	P991	yes	11-20 years	IE	Recurrent mutation	SH3TC2 (NM_024577.3)	homozygous; c.1178-1G>A	NP	CS064451	pathogenic
28	P1025	no	DMM	13.3	Unsolved	-	-	-	-	-
29	P1041	no	2-10 years	44	Novel allele in known gene	AP5Z1 (NM_014855.2)	c.1568G>A, p.Arg523His, homozygous	0.0038	-	VUS
30	P1130	yes	at birth	N/A	Novel allele in known gene	GDAP1 (NM_018972.2)	homozygous; c.112C>T; p.Gln38Ter	NP	-	pathogenic

mNCV: Motor nerve conduction velocity, AAF: Alternative allele frequency, IE: inexcitable, DMM: Delayed motor milestones, NP: Not present.

Table 5.9. Summary of genetic findings for the study cohort. (cont.)

Nr.	**ID**	**Family history**	**Age of onset**	**mNCV (m/s)**	**Molecular finding**	**Gene**	**Variant**	**AAF (%)**	**HGMD/ dbSNP ID**	**ACMG outcome**
31	P1142	no	2-10 years	51.9	Novel allele in known gene	C12ORF65 (NM_152269.4)	homozygous; c.18_21delATTT; Leu6Phefs*7	NP	-	likely pathogenic
32	P1148	yes	11-20 years	56	Recurrent mutation	MFN2 (NM_014874.3)	heterozygous; c.1085C>T; p.Thr362Met	0.003181	CM062856	pathogenic
33	P1150	no	DMM	42.2	Unsolved	-	-	-	-	-
34	P1152	yes	2-10 years	32.8	Recurrent mutation	SH3TC2 (NM_024577.3)	homozygous; c.1894_1897delinsAAA; p.Glu632Lysfs*13	NP	CX117975	pathogenic
35	P1154	no	DMM	26.8	Unsolved	-	-	-	-	-
36	P1180-4	yes	2-10 years	<38	Novel allele in known gene	SH3TC2 (NM_024577.3)	homozygous; c.54dupT; p.Lys19Ter	NP	-	pathogenic
37	P1188	no	DMM	14	Novel allele in known gene	SBF2 (NM_030962.3)	homozygous; c.2549T>C; p.Met850Thr	NP	-	VUS
38	P1220	yes	2-10 years	<38	Unsolved	-	-	-	-	-

mNCV: Motor nerve conduction velocity, AAF: Alternative allele frequency, IE: inexcitable, DMM: Delayed motor milestones, NP: Not present.

Table 5.9. Summary of genetic findings for the study cohort. (cont.)

Nr.	ID	Family history	Age of onset	mNCV (m/s)	Molecular finding	Gene	Variant	AAF (%)	HGMD/ dbSNP ID	ACMG outcome
39	P1251	no	2-10 years	>38	Candidate gene	SEPT11 (NM_018243.2)	homozygous; c.263_264insG; p.Glu89Glyfs*12	NP	-	GUS
40	P1255	no	DMM	4	Recurrent mutation	PRX (NM_181882.2)	homozygous; c.3208C>T; p.Arg1070Ter	0.0007958	CM044034	pathogenic
41	P1258-1	yes	2-10 years	>38	Candidate gene	ATP8B3 (NM_138813.3)	homozygous; c.3056G>A; p.Gly1019Asp	0.3094	rs202137046	GUS
42	P1262	yes	DMM	IE	Recurrent mutation	GDAP1 (NM_018972.2)	homozygous; c.786delG; p.Phe263Leufs*22	NP	CD023843	pathogenic
43	P1267-1	yes	DMM	14.7	Novel allele in known gene	MPZ (NM_000530.6)	heterozygous; c.362A>G; p.Asp121Gly	NP	-	VUS
44	P1282	yes	2-10 years	5.6	Unsolved	-	-	-	-	-
45	P1289-3	yes	DMM	13.3	Recurrent mutation	SH3TC2 (NM_024577.3)	homozygous; c.1894_1897delinsAAA; p.Glu632Lysfs*13	NP	CX117975	pathogenic

mNCV: Motor nerve conduction velocity, AAF: Alternative allele frequency, IE: inexcitable, DMM: Delayed motor milestones, NP: Not present.

Table 5.9. Summary of genetic findings for the study cohort. (cont.)

Nr.	**ID**	**Family history**	**Age of onset**	**mNCV (m/s)**	**Molecular finding**	**Gene**	**Variant**	**AAF (%)**	**HGMD/ dbSNP ID**	**ACMG outcome**
46	P1291	no	at birth	30	Recurrent mutation	SACS (NM_014363.4)	homozygous; c.2182C>T; p.Arg728Ter	0.001597	CM087685	pathogenic
47	P1302	no	2-10 years	N/A	Unsolved	-	-	-	-	-
48	P1306	no	11-20 years	>38	Recurrent mutation	MPV17 (NM_002437.4)	homozygous; c.122G>A; p.Arg41Gln	0.002475	CM1510714	pathogenic
49	P1319	no	11-20 years	48	Recurrent mutation	HINT1 (NM_005340.5)	homozygous; c.368G>A; p.Trp123Ter	NP	CM128652	pathogenic
50	P1325	yes	2-10 years	46	Recurrent mutation	GDAP1 (NM_018972.2)	homozygous; c.458C>T; p.Pro153Leu	0.001591	CM077286	pathogenic
51	P1330	yes	2-10 years	36.6	Recurrent mutation	GJB1 (NM_001097642.2)	hemizygous; c.518G>T; p.Cys173Phe	NP	CM070941	pathogenic
52	P1331	no	2-10 years	IE	Recurrent mutation	MFN2 (NM_014874.3)	heterozygous; c.1090C>T; p.Arg364Trp	NP	CM060340	pathogenic

mNCV: Motor nerve conduction velocity, AAF: Alternative allele frequency, IE: inexcitable, DMM: Delayed motor milestones, NP: Not present.

Table 5.9. Summary of genetic findings for the study cohort. (cont.)

Nr.	**ID**	**Family history**	**Age of onset**	**mNCV (m/s)**	**Molecular finding**	**Gene**	**Variant**	**AAF (%)**	**HGMD/ dbSNP ID**	**ACMG outcome**
53	P1333	no	2-10 years	IE	Recurrent mutation	MFN2 (NM_014874.3)	heterozygous; c.310C>T; p.Arg104Trp	NP	CM083543	pathogenic
54	P1336	yes	21-40 years	29.6	Unsolved	-	-	-	-	-
55	P1350	yes	2-10 years	<38	Unsolved	-	-	-	-	-
56	P1353	no	2-10 years	15.9	Unsolved	-	-	-	-	-

mNCV: Motor nerve conduction velocity, AAF: Alternative allele frequency, IE: inexcitable, DMM: Delayed motor milestones, NP: Not present.

6. DISCUSSION

This thesis study aimed to perform a genetic survey in a cohort of inherited peripheral neuropathy cases from Turkey to unravel mutational frequency in the population and identify novel genes/alleles responsible for autosomal recessive subtypes of CMT disease. A further aim was to unravel the effects of these candidate disease-causing genes on cellular mechanisms that lead to CMT phenotype. Accordingly, 56 index patients with inherited peripheral neuropathy were preliminarily screened for recurrent GDAP1 mutations and 10,7% of the patients were shown to carry homozygous pathogenic mutations in this gene. Next, WES analysis was performed on the rest of the patients. This approach helped identification of causative variants in known CMT and related neurological disease genes in 29 additional patients, 13 out of which were carrying novel variants. We have also identified a new gene-disease relationship between *FXN* and ARCMT and two candidate disease causing genes: *ATP8B3* for ARCMT and *SEPT11* for autosomal recessive cerebellar ataxia with axonal sensorimotor polyneuropathy.

Mutations in *GDAP1* gene are known to make up the most common cause of autosomal recessive CMT cases with a mutation frequency of 5-10% [54]. With this in mind, we have initially screened all patients included in the study for mutations in *GDAP1*. This approach also helped to decrease next-generation sequencing costs. This direct sequencing approach allowed exclusion of six patients with *GDAP1* mutations from further analysis. Among these, families P294, P555, P987 and P1262 were all shown to carry the same biallelic frameshift mutation in *GDAP1* (c.786delG, p.Phe263Leufs*22) and the clinical findings of these patients were very similar (Table 5.1). This mutation, registered as CD023843 in HGMD, has been suggested to be a founder mutation previously in the Turkish population [21]. Observing the same mutation in four unrelated families in our cohort provided further evidence for this suggestion.

The patients who were shown to carry homozygous recurrent mutations in *GDAP1* were provided with genetic diagnosis and multilocus inheritance was not considered in these patients. This type of inheritance refers to situations where contribution from multiple loci is required to cause disease, instead of a single allele in a single locus [165]. Multilocus inheritance has been previously documented in neurological disorders including CMT [166–168]. Several studies have reported unrelated CMT families with digenic inheritance having pathogenic mutations in two known disease genes or loci [169–172]. The common observation in these cohorts is that patients with digenic/multilocus inheritance have more severe phenotypes with earlier age of onset. These patients also had clinical features generally atypical for the known disease gene which is termed "phenotypic expansion" [169]. Karaca *et al.* (2018) examined a large neurodevelopmental phenotype cohort and reported multilocus inheritance in 31,6% of families with phenotypic expansion, while only 2.3% of families without phenotypic expansion were shown to have multilocus variation [173]. Based on this, it is generally not advisable to finalize genetic diagnosis based on targeted sequencing of a single locus, especially in patients with phenotypic expansion. We have chosen to exclude patients that have recurrent homozygous *GDAP1* mutations from further analyses in the study since none of these patients had clinical features beyond those reported for *GDAP1* mutations (Table 5.1). Even though multilocus inheritance is known to be very rare in the absence of additional severe symptoms, we still acknowledge the risk of missing additional pathogenic mutations in our patients with *GDAP1* mutations.

We have, then, performed WES on 50 patients and initially investigated variants in known IPN-related genes. This approach successfully identified 16 patients with recurrent mutations in known IPN genes. Furthermore, 13 patients were shown to have novel variants in known genes that are being reported here for the first time. Although most of these neuropathy-related genes have been known to be disease-causing for a long time, more than one-third of genetically diagnosed patients in our cohort exhibited novel mutations in these genes, suggesting a high genetic diversity in the Turkish population. This also signifies the need for similar genetic surveys to serve as reference for genetic diagnosis strategies specific to populations with similar genetic backgrounds.

Among 56 index patients surveyed, mutations in the *GDAP1* gene were observed most commonly with a frequency of 12,5% (seven families), followed by mutations in *SH3TC2* in 10,7% (six families) and mutations in *MFN2* in 8,9% (five families). Pathogenic mutations in *HINT1*, *PRX*, and *GJB1* were observed in two families each (3,6% each), while pathogenic mutations in each of the *AP5Z1*, *C12ORF65*, *EGR2*, *MME*, *MPV17*, *MPZ*, *NDRG1*, *NEFL*, *SACS*, *SBF2*, and *SPG7* genes were observed in single families. Similar studies investigating ARCMT cases report *GDAP1* mutation rates around 10-15%, followed by *SH3TC2* mutations with a rate of 7,5% [21,54]. Our data is in correlation with these previously reported population frequencies, however the frequency of *SH3TC2* mutations is slightly higher in our cohort. Therefore, we suggest prior screening of *GDAP1* and *SH3TC2* genes in possible autosomal recessive CMT cases to reduce NGS costs in the genetic diagnosis of patients in similar cohorts.

In our study cohort, three families were found to have mutations in genes that are not causative for CMT, although all patients were referred to our laboratory with an initial clinical diagnosis of CMT. In patient P1291, a known mutation in the *SACS* gene that causes Charlevoix-Saguenay-type spastic ataxia (ARSACS) has been observed. Even though the typical clinical findings in ARSACS include pyramidal signs, spastic ataxia and neuropathy, in some cases neuropathy might develop prior to other symptoms causing misdiagnosis. It is thought that such cases prevent the understanding of true prevalence of ARSACS [123]. Similar to the instances reported by Vermeer *et al.* (2008), in patient P1291, neuropathy was the predominant symptom in initial examination at an early age, but mild spasticity and Babinski sign was recognized at a second detailed examination following genetic testing. Thus, his differential diagnosis was determined as ARSACS, instead of CMT. As can be seen here, it should be noted that the characteristic features of ARSACS could become prominent later as the disease progresses and the correct early diagnosis may only be provided with genetic testing in such cases. In patients P629 and P1041, novel homozygous point mutations were discovered in *SPG7* and *AP5Z1* genes, respectively, both of which were reported to be causative for hereditary spastic paraplegia (HSP). These patients were also reevaluated in the clinical setting and the differential diagnosis was reported to be HSP for both.

Identification of causative mutations in genes responsible for related neurological disorders supports the idea that it might not always be sufficient to analyze WES data based on primary clinical diagnosis, especially in neurological disorders which generally have overlapping clinical and genetic features.

Even though we aimed to investigate autosomal recessive cases and selected our study cohort accordingly, we have also found deleterious variants in dominant CMT genes. Families P300, P1148, P1331, and P1333 were shown to have recurrent heterozygous mutations in the *MFN2* gene, while Family P1267 was shown to have a novel heterozygous variant in the *MPZ* gene. Families P711 and P1330, on the other hand, carried recurrent hemizygous mutations in the *GJB1* gene which is linked to the X chromosome. In the literature, it has been suggested that mutations in the *MFN2* gene could occur *de novo* and expressivity could be low in some individuals [50], whereas mutations in the *GJB1* gene may cause mild clinical features in females due to random X-inactivation [39]. For instance, in Family P300, both the index case and his unaffected father carried the same heterozygous recurrent mutation in the *MFN2* gene, however only the index patient had clinical symptoms suggesting polyneuropathy. These findings could be explained by the effect of modifier genes that cause phenotypic diversity or reduced expressivity in these families. Given the identification of patients with dominant mutations in disease-causing genes in our cohort, we suggest considering dominant segregation too, especially in isolated cases, even if there is familial consanguinity in the pedigree. In our WES data analysis, we have initially focused on known disease genes without using homozygosity as an inclusion criterion and managed to identify these patients with dominant disease-causing mutations in known genes.

Considering all 35 variants that fit disease segregation in the pedigrees and correlate well with disease phenotype, the study yielded a "potential" genetic diagnosis rate of 62,5% (35/56 families). When variants of unknown molecular significance were excluded and only the variants that can be classified as "pathogenic" or "likely pathogenic" according to ACMG criteria were considered, the "definitive" genetic diagnosis rate was calculated to be 55,35% (31/56 families).

The genetic diagnosis rate is in accordance with the rates of 45-60% reported for CMT disease in previous studies [5, 7, 38, 109, 110]. We believe our high rate of variant identification is partly due to the initial use of relaxed filtering criteria. In general, the filtering criteria of WES data include the change caused by the variant, allele frequency, and pathogenicity scores predicted by *in silico* tools such as SIFT and PolyPhen2 [174]. Read depth is sometimes used to exclude false positive results from the data. In our study, during the initial analysis of WES data for variants in known IPN genes, read depth and pathogenicity predictions were not used as exclusion criteria, while alternative allele frequency criterion was set to a rather wide range of less than 5%. Our raw WES data was initially filtered for variants with a coverage of less than 50X, therefore, we did not encounter a high number of false positive results. The initial use of relaxed filtering allowed us to reach a relatively high molecular diagnosis success. Furthermore, even though the patients enrolled in the study were referred to our laboratory with a clinical diagnosis of CMT disease, genetic findings revealed different neurological disorders with overlapping clinical features for some patients. Therefore, investigation of the causative genes for related neurological disorders with similar clinical phenotypes to CMT in data analysis also improved our genetic diagnosis rate.

The definitive diagnosis rate of this study is one of the highest reported in literature [38, 54, 93, 175]. Unfortunately, we failed to provide genetic diagnosis for 32% of our patients. This could be attributed to several reasons, mostly due to the nature of WES analysis. WES provides sequence data on protein coding regions and exon-intron junctions in the genome covering ˜2% of human genome [176, 177]. Even though it is estimated that ˜85% of disease-causing mutations reside in the protein coding regions, especially in Mendelian diseases, this leaves out pathogenic variants that reside in regulatory regions or deep within introns [105, 174, 176, 177]. Another disadvantage is the restricted type of identified mutations in WES. NGS technologies generally produce sequence data through sequence capture by hybridization techniques generating short reads that are later aligned to the reference genome for variant calling [107, 174, 176].

It is well established that this process causes low coverage of some parts of the exome, especially GC-rich first exons, and misses copy-neutral rearrangements such as inversions, copy number variations, and large deletion/duplications [11, 174, 176]. This causes WES to capture single nucleotide variations more effectively, while performing poorly in determining large deletions, duplications, copy number variations or structural rearrangements. Besides, the filtering process after variant calling greatly affects genetic diagnosis outcome and should be performed according to consensus guidelines for effective identification and reporting [114, 178]. Nevertheless, the genetic diagnosis rate in CMT generally does not exceed 60% even with more advanced diagnostic tools. This underlines the genetic heterogeneity of peripheral neuropathies and may point to the presence of yet undiscovered causative genes in these disorders [7]. Taking a step further, this might also mean that CMT may also have a complex genetic aspect; in some instances, instead of monogenic inheritance, the disease may present as a result of combined effect of multiple alleles. Non-Mendelian characteristics of CMT disease such as reduced penetrance, modifier genes, and multilocus inheritance are currently being investigated by large research groups overseen by the CMT Consortium [51].

NGS studies generally discover incidental findings. Similarly, in our study, we have shown that the index patient in Family P969 had a biallelic mutation in the *OPTN* gene (c.941A>T, p.Gln314Leu) that was reported to cause ALS in heterozygous state [130]. Through direct sequencing, it was shown that this variant does not fit disease segregation in this pedigree (Figure 5.2). Besides, detailed clinical examination of the index patient revealed clinical findings such as frequent falling, abnormal mobility, significant distal weakness in upper and lower extremities, pes cavus, hammer toe, hypoactive deep tendon reflex, sensory loss, and scoliosis. NCV study was characteristic for sensory and motor neuropathy with primary myelin defects. The detailed clinical examination did not suggest ALS diagnosis. Furthermore, WES data of the index case revealed a novel biallelic mutation (c.54C>A, p.Tyr18Ter) in the *NEFL* gene which segregates with disease status in the pedigree and the clinical findings of the patient were similar to those of the reported patients with mutations in *NEFL* gene.

Therefore, we agreed that the *NEFL* variant was the causative one, rather than the *OPTN* variant in this family. Based on these findings, it could be suggested that the *OPTN* c.941A>T, p.Gln314Leu mutation which was reported only in one patient in the literature, is not a causative variant, at least in the genetic background of our family. This conflict was overcome by regular and effective communication between genetic and clinical researchers and genetic diagnosis was provided to the family in accordance with clinical findings. This is an example for the importance of clinical input required both before and after genetic testing [179]. It also underlines the importance of training genetic researchers for correct interpretation of findings.

The "diagnostic odyssey" that patients with genetic disorders go through, is extensively discussed in literature [176,177,179–183]. Several reports in Europe and USA show that about one third of patients with a rare disease wait for up to five years for an accurate diagnosis, while about 15% of the patients remain undiagnosed for six or more years. Furthermore, a survey reports that one fourth of patients with a rare disease took 5-30 years after initial symptom onset for a correct diagnosis, while 40% of these were initially misdiagnosed causing them to receive ineffective medical treatment and even unnecessary surgery (reviewed in [177]). During this period, patients make multiple visits to different specialists and go through invasive and expensive tests such as repeated imaging studies, unnecessary biopsy operations, lumbar punctures, nerve conduction studies, needle electromyograms, and/or electroencephalograms, most of which can be avoided with an accurate molecular diagnosis [177]. It is possible to generate strategies to facilitate genetic diagnosis and decrease unnecessary diagnostic and treatment costs in patients. The first and the most evident step in CMT molecular diagnosis is to exclude CMT1A duplication/deletion locus that is observed in 70% of demyelinating CMT cases [95]. Based on the findings of this study and other findings in literature, it can be advised to screen *GDAP1* mutations in patients with likely autosomal recessive inheritance prior to further NGS-based screening. Our findings also indicate advantages for screening *SH3TC2* mutations in patients with likely autosomal recessive inheritance in Turkish patients and cohorts with similar genetic backgrounds.

Patients could also be referred to targeted sequencing of certain genes based on distinct clinical phenotypes. For instance, patients with nonsense mutations in *SBF2* present with juvenile-onset glaucoma in addition to demyelinating neuropathy [184]; while mutations in *HINT1* generally present with neuromyotonia accompanying axonal neuropathy [58]. Patients with such distinct phenotypes could be candidates for screening of certain genes that cause relevant clinical features. After initial screening for common genes, undiagnosed patients could be referred to NGS-based gene panels or whole-exome or -genome sequencing studies in qualified laboratories.

One of the main objectives of this study was to identify new candidate genes that cause autosomal recessive CMT to shed light to disease mechanisms. In accordance with this, we have identified a new gene-disease relationship in Family P966 and two additional candidate genes in families P1258 and P1251.

In Family P966, we have shown that a biallelic missense mutation in the *FXN* gene (c.493C>T, p.Arg165Cys) causes a CMT-like phenotype with unusual clinical features, instead of Friedreich's ataxia (FRDA). The family we identified (P966) had three affected individuals born to consanguineous parents. Our index patient had prominent optic nerve atrophy, dysarthria, muscle weakness and atrophy in lower limbs which led the clinician to consider CMT initially. The patient also had rotatory nystagmus, retained upper limb reflexes and hyperactive Patellar reflex, pes planus and scoliosis. Since the gene we identified in these patients were reported to cause FRDA, the affected individuals were reexamined clinically. However, some clinical features such as optic nerve atrophy, distal rapidly progressive muscle weakness with retained deep tendon reflexes, and sensorimotor axonal polyneuropathy were considered not to be compatible with the FRDA phenotype. The p.Arg165Cys mutation in the *FXN* gene has been previously reported in two other patients in compound heterozygous state with the common pathogenic triplet repeat expansion [185, 186]. Two additional studies reported five patients with p.Arg165Pro mutation in this gene, again in compound heterozygous state with the repeat expansion [187, 188]. All patients reported in literature, including ours, show involvement of both peripheral and central nervous systems.

This suggests a continuous clinical spectrum comprising CMT and FRDA when atypical symptoms and overlapping features are considered. Biallelic point mutations in the *FXN* gene have never been reported before and thus, are suggested to cause embryonic lethality [133]. The mutation we identified in the *FXN* gene results in a full-length protein but replaces a charged hydrophilic amino acid residue with an uncharged hydrophobic one in a highly conserved structural domain [185]. Our cellular analyses in primary fibroblasts obtained from the index patient suggest that mRNA and protein levels of *FXN*, as well as mRNA levels of *NFU1*, *AIFM1*, *APTX* and *ACO1* which were shown to change dramatically in FRDA patient transcriptomes [134], were comparable to the levels in primary fibroblasts of the heterozygous mother of the affected siblings and a healthy control (Figure 5.5). The homozygous GAA triplet repeat expansion is known to cause reduced *FXN* levels, leading to deficiency in Fe-S cluster enzymes, increased iron levels in mitochondria, and hypersensitivity to oxidative stress [189]. It was previously reported that the p.Arg165Cys mutant *FXN* protein colocalizes to mitochondria and has comparable protein expression levels to wild-type *FXN in vitro* [190]; however, p.Arg165Cys protein was shown to be a dysfunctional mutation that causes decreased binding of *FXN* protein to the Fe-S cluster assembly complex in mitochondria [191]. Concordantly, our findings suggest that *FXN* expression is not altered in our patient, but perhaps the function of the protein is perturbed. Therefore, it can be suggested that the homozygous p.Arg165Cys mutation in this patient, probably due to its residual activity, leads to a less severe phenotype than FRDA, but causes a novel disease in the clinical spectrum between CMT and FRDA. Since, a dysregulation in mitochondrial function is a known disease mechanism in neurodegenerative diseases [72, 73], one can argue that the biallelic p.Arg165Cys mutation might be causing peripheral nerve pathology due to dysregulation in iron metabolism of mitochondria. Homozygous truncation/termination mutations in this gene, on the other hand, may cause a more severe phenotype and/or lethality due to complete loss of function of the protein. Our finding also challenges the long-established prediction that point mutations in this gene causes lethality and provides the first genetic insight on the potential link between FRDA and CMT paving the way to further unravel pathomechanisms leading to both diseases [192].

We identified a candidate gene in Family P1258 with three affected siblings having early onset axonal polyneuropathy as suggested by nerve conduction studies. The index patient presented with frequent falls, distal weakness in upper and lower limbs, steppage gait with ataxia, missing deep tendon reflexes, normal plantar reflexes, decreased vibration sense, positive Romberg's sign, and mild dysmetria in lower limbs. In this family, we have identified a biallelic missense variant (c.3056G>A, p.Gly1019Asp) in *ATP8B3* as a candidate gene for autosomal recessive axonal CMT. The genetic findings in the family and the findings in literature suggested the hpmozygous variant in this gene might be disease-causing in family P1258. Unfortunately, during the study period, the index patient passed away due to an unrelated cause; therefore, we obtained skin biopsy samples from one of her affected siblings (P1258-2) and her heterozygous mother to study mRNA and protein levels of the gene of interest. However, we could not detect *ATP8B3* mRNA using qPCR, while ATP8B3 protein levels in patient fibroblasts were comparable to that of healthy controls (Figure 5.7). Due to limitations in resources, we could not perform further molecular analyses in this family; therefore, we collaborated with Dr. Aslı Yenenler-Kutlu to analyze the potential effects of the variant on the protein using virtual molecular dynamics simulations. These studies showed that the backbone of the mutant protein was less mobile, and that the variant observed in family P1258 might reduce the ability of Mg^{+} coordination of the important residues in the protein (Figure 5.8). These findings suggest that the variant in family P1258 might have a significant impact on ATP8B3 molecular dynamics that might affect normal protein function and cause a neurological pathology. *ATP8B3* is a member of type-4 P-type ATPase protein subfamily which transports phosphatidylserine across different leaflets of plasma membrane [135, 193]. The members of type-4 P-type ATPase protein subfamily contribute to asymmetric distribution of phospholipids in biological membranes; therefore, pathogenic mutations in these genes may cause severe phenotypes in cell and organelle morphology, cell movement, division, signal transduction, and vesicle biogenesis and transport [136, 138–140]. In fact, loss of function mutations in *ATP8B1* have been shown to cause sensory impairment, while mutations in *ATP8A2* were shown to cause axon degeneration and neurodegenerative disease in mice [141,142].

More recently, a study investigating genetic variants in sporadic ALS cases reported an individual with two compound heterozygous variants in *ATP8B3* [146], one of which is the same variant as in our family P1258 (p.Gly1019Asp). Based on our findings and information in the literature, we have listed *ATP8B3* as a novel candidate gene for axonal autosomal recessive CMT disease. It has been suggested that cytosolic leaflets of recycling endosomes are rich in phosphatidylserine and members of the P4-ATPase family are required for this asymmetrical distribution of phosphatidylserine in these membranes, supporting vesicular trafficking [194]. Since axonal transport of vesicles is a cumbersome process in lengthy axons of the peripheral nerves, alterations in vesicular trafficking also appear as a common disease mechanism [72]. It can be speculated that mutations that cause the expression of dysfunctional ATP8B3 protein creates alterations in vesicular trafficking in axons, leading to an axonal pathology.

The third family in which we identified a candidate gene was Family P1251. There was an isolated case in this family born to consanguineous parents. The symptoms of the index case started with walking difficulty at the age of seven. Prominent findings during clinical examination included dysmetria, dysdiadochokinesia, cerebellar ataxia, axonal sensorimotor polyneuropathy in the lower extremities, hypertrophic cardiomyopathy, and bilateral symmetrical prolonged latency in visual evoked potential. Our genetic studies showed that the isolated patient in this family had a biallelic frameshift variant (c.263_264insG; p.Glu89Glyfs*12) in the *SEPT11* gene. *SEPT11* is a member of the septin family of GTP-binding proteins which are components of the cytoskeletal proteins that are known to polymerize into filaments or ring structures [152]. Septin proteins have been shown to function in various cellular processes; including cytokinesis, intracellular vesicle trafficking and scaffold-forming [153–155]. Therefore, their expression and regulation is highly likely to be important for these cellular processes. Septin protein family members have been associated with cancer and infectious diseases for a long time. Reciprocal translocations were reported between *MLL* gene and *SEPT5*, *SEPT6*, *SEPT9* and *SEPT11* in leukemia [161]. Additionally, there are multiple studies that report the manipulation of septin proteins by pathogens such as *Listeria monocytogenes*, Shigella and Rickettsia to alter cytoskeleton for entry into the cell [195–197].

More recently, septin protein family members have also been shown to be associated with neurological disorders. For instance, *SEPT5* has been shown to be important in pathogenesis of Parkinson's disease and Down Syndrome [198], whereas *SEPT9* is the only known causative gene for hereditary neuralgic amyotrophy [199]. *SEPT5* has been identified as a biomarker for autoimmune cerebellar ataxia quite recently [200]. Another study has identified aberrant SEPT11 protein accumulation in brain tissues of patients with frontotemporal lobar degeneration and suggested a role for this protein in neurodegeneration [201]. It has also been shown that many septins localize at the base of dendritic spines in the hippocampal neurons and knock-down of *SEPT7* or *SEPT11* reduced dendritic branching and spine density in mice [152, 156–158]. We were convinced that the clinical features of our patient could be explained by reduced dendritic branching of the neurons in the cerebellum by reduced expression of SEPT11 due to the biallelic frameshift mutation in this gene. Our molecular assays confirmed that the patient fibroblasts have significant reduction in mRNA and protein levels of *SEPT11* compared to control cells (Figure 5.10). Besides, immunofluorescence assays on both primary fibroblasts and SEPT11-overexpressing HEK293 cells suggested that the mutant protein lacks the ability to form filaments which might be causing impaired intracellular vesicle trafficking or impaired compartmentalization of cells and can be the disease pathomechanism in this case (Figure 5.13 and Figure 5.14). Unfortunately, we were not able to find additional families with similar clinical features and genetic findings in this gene using matchmaking tools; however, both our findings and findings from the literature [157] are quite convincing in suggesting that the reduced expression of *SEPT11* due to loss of function mutations in this gene could be causative for autosomal recessive cerebellar ataxia with axonal sensorimotor polyneuropathy.

Unfortunately we could not find any additional families with similar clinical features with a loss of function mutation in *SEPT11*, thus we decided to generate an animal model to provide evidence for its pathogenicity. Mouse models of septin knockouts have been broadly studied. Röseler *et al.* (2011) generated SEPT11-null mice, which developed normally until day 11,5, however these mice have developmental retardation from this time point onwards until they die on day 13,5 post coitum [202].

Ono *et al.* (2005) generated Sept6 deficient mice and showed that they have a normal lifespan with no obvious phenotype [164]. Buser *et al.* (2009) studied these Sept6-null mice in the context of myelination in CNS and PNS and observed that there is no aberrant phenotype; however, Sept11, the closest homolog of Sept6, was more abundant in myelin membranes purified from these mice, suggesting a compensation mechanism among septins [159]. Since it is more cost-effective and easier to study, we are currently collaborating with Prof. Arzu Çelik at Boğaziçi University to develop *Drosophila melanogaster* models to further study *SEPT11* in the context of nervous system. In the near future, we will perform behavioral and phenotypic assays using the flies expressing human Sept11 and mutant flies that lack Drosophila homolog of Sept11.

In conclusion, we have surveyed a cohort of 180 individuals from 56 consanguineous Turkish families with likely autosomal recessive peripheral neuropathy. We have succeeded providing potential genetic diagnoses to 62,5% (35/56 cases) among which 55,35% (31/56 cases) received definitive genetic diagnoses as these genetic findings were classified as "pathogenic" or "likely pathogenic" according to ACMG criteria (Table 5.9). Our genetic diagnosis rate is one of the highest rates reported in literature and this success is likely attributed to our pipeline in WES data analysis. Our analyses identified 22 families with 17 distinct recurrent mutations, as well as 13 families with 13 distinct novel alleles in known IPN-related genes, suggesting a rather high heterogeneity in this cohort. We have also identified a new gene-disease relationship (*FXN*-CMT) and two novel candidate genes: one causative for autosomal recessive axonal CMT (*ATP8B3*) and one for autosomal recessive cerebellar ataxia with axonal sensorimotor polyneuropathy (*SEPT11*). We suggest *FXN*, *ATP8B3* and *SEPT11* genes should also be screened in patients with relevant clinical features when more common causative genes are excluded in genetic diagnosis (Figure 6.1). Our study paints the genetic landscape of autosomal recessive peripheral neuropathy population in Turkey and provides a reference point for genetic diagnosis strategies for populations with similar genetic backgrounds, as well as contributing to enlightenment of the pathomechanisms leading to peripheral neuropathy by identifying novel candidate genes.

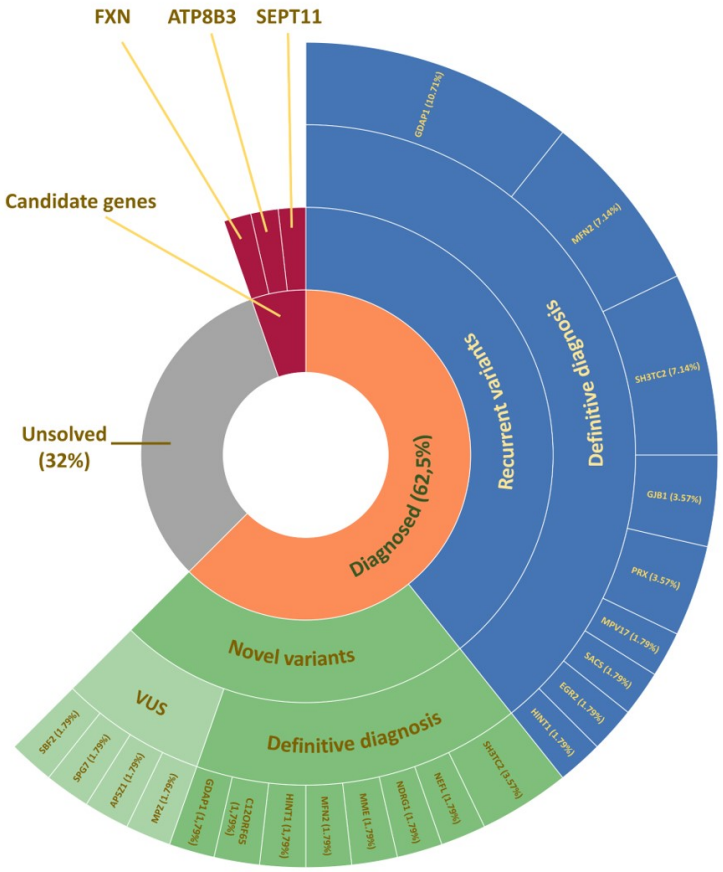

Finding	Gene name	Total number of cases	Percentage
Diagnosed	GDAP1	7	12.50%
	SH3TC2	6	10.71%
	MFN2	5	8.92%
	HINT1	2	3.57%
	PRX	2	3.57%
	GJB1	2	3.57%
	EGR2	1	1.79%
	SACS	1	1.79%
	MPV17	1	1.79%
	C12ORF65	1	1.79%
	MME	1	1.79%
	NDRG1	1	1.79%
	NEFL	1	1.79%
	SBF2	1	1.79%
	AP5Z1	1	1.79%
	MPZ	1	1.79%
Candidate genes	FXN	1	1.79%
	ATP8B3	1	1.79%
	SEPT11	1	1.79%
Unsolved		18	32.14%

Figure 6.1. Summary of genetic findings of the study.

REFERENCES

1. Pisciotta, C. and M. E. Shy, "Chapter 42: Neuropathy", *Handbook of Clinical Neurology*, Vol. 148, pp. 653–665, 2018.

2. Rossor, A. M., M. R. Evans and M. M. Reilly, "A Practical Approach to the Genetic Neuropathies", *Practical Neurology*, Vol. 15, No. 3, pp. 187–198, 2015.

3. De Jonghe, P., V. Timmerman, E. Nelis, J.-J. Martin and C. Van Broeckhoven, "Charcot-Marie-Tooth Disease and Related Peripheral Neuropathies", *Journal of the Peripheral Nervous System*, Vol. 2, No. 4, pp. 370–387, 1997.

4. Skre, H., "Genetic and Clinical Aspects of Charcot-Marie-Tooth's Disease", *Clinical Genetics*, Vol. 6, No. 2, pp. 98–118, 1974.

5. Reilly, M. M., S. M. Murphy and M. Laurá, "Charcot-Marie-Tooth Disease", *Journal of the Peripheral Nervous System*, Vol. 16, No. 1, pp. 1–14, 2011.

6. Pipis, M., A. M. Rossor, M. Laura and M. M. Reilly, "Next-Generation Sequencing in Charcot–Marie–Tooth Disease: Opportunities and Challenges", *Nature Reviews Neurology*, Vol. 15, No. 11, pp. 644–656, 2019.

7. Timmerman, V., A. V. Strickland and S. Züchner, "Genetics of Charcot-Marie-Tooth (CMT) Disease Within the Frame of the Human Genome Project Success", *Genes*, Vol. 5, No. 1, pp. 13–32, 2014.

8. Parman, Y. and E. Battaloğlu, "Recessively Transmitted Predominantly Motor Neuropathies", *Handbook of Clinical Neurology*, Vol. 115, pp. 847–861, 2013.

9. Kurihara, S., Y. Adachi, K. Wada, E. Awaki, H. Harada and K. Nakashima, "An Epidemiological Genetic Study of Charcot-Marie-Tooth Disease in Western Japan", *Neuroepidemiology*, Vol. 21, No. 5, pp. 246–250, 2002.

10. Kandil, M. R., E. S. Darwish, E. M. Khedr, M. M. Sabry and M. A. Abdulah, "A Community-Based Epidemiological Study of Peripheral Neuropathies in Assiut, Egypt", *Neurological Research*, Vol. 34, No. 10, pp. 960–966, 2012.

11. Foley, C., I. Schofield, G. Eglon, G. Bailey, P. F. Chinnery and R. Horvath, "Charcot-Marie-Tooth Disease in Northern England", *Journal of Neurology, Neurosurgery and Psychiatry*, Vol. 83, No. 5, pp. 572–573, 2012.

12. Holmberg, B. H., G. Holmgren, E. Nelis, C. Van Broeckhoven and B. Westerberg, "Charcot-Marie-Tooth Disease in Northern Sweden: Pedigree Analysis and the Presence of the Duplication in Chromosome 17p11.2", *Journal of Medical Genetics*, Vol. 31, No. 6, pp. 435–441, 1994.

13. Barreto, L. C. L. S., F. S. Oliveira, P. S. Nunes, I. M. P. De França Costa, C. A. Garcez, G. M. Goes, E. L. A. Neves, J. De Souza Siqueira Quintans and A. A. De Souza Araújo, "Epidemiologic Study of Charcot-Marie-Tooth Disease: A Systematic Review", *Neuroepidemiology*, Vol. 46, No. 3, pp. 157–165, 2016.

14. Kazamel, M. and C. J. Boes, "Charcot Marie Tooth Disease (CMT): Historical Perspectives and Evolution", *Journal of Neurology*, Vol. 262, No. 4, pp. 801–805, 2015.

15. Capasso, M., A. Di Muzio, M. Ferrarini, M. V. De Angelis, C. M. Caporale, S. Lupo, T. Cavallaro, G. M. Fabrizi and A. Uncini, "Inter-Nerves and Intra-Nerve Conduction Heterogeneity in CMTX with Arg(15)Gln Mutation", *Clinical Neurophysiology*, Vol. 115, No. 1, pp. 64–70, 2004.

16. Pareyson, D., Scaioli and M. Laurà, "Clinical and Electrophysiological Aspects of Charcot-Marie-Tooth Disease", *NeuroMolecular Medicine*, Vol. 8, pp. 3–22, 2006.

17. Harding, A. and P. Thomas, "The Clinical Features of Hereditary Motor and Sensory Neuropathy Types I and II", *Brain*, Vol. 103, No. 2, pp. 259–280, 1980.

18. Davis, C., W. Bradley and R. Madrid, "The Peroneal Muscular Atrophy Syndrome: Clinical, Genetic, Electrophysiological and Nerve Biopsy Studies. I. Clinical, Genetic and Electrophysiological Findings and Classification", *Journal de Genetique Humaine*, Vol. 26, No. 4, pp. 311–349, 1978.

19. Siskind, C. E., S. Panchal, C. O. Smith, S. M. Feely, J. C. Dalton, A. B. Schindler and K. M. Krajewski, "A Review of Genetic Counseling for Charcot Marie Tooth Disease (CMT)", *Journal of Genetic Counseling*, Vol. 22, No. 4, pp. 422–436, 2013.

20. Brennan, K. M., Y. Bai and M. E. Shy, "Demyelinating CMT – What's Known, What's New and What's In Store?", *Neuroscience Letters*, Vol. 2, No. 596, pp. 14–26, 2015.

21. Nelis, E., S. Erdem, P. Van den Bergh, M. C. Belpaire-Dethiou, C. Ceuterick, V. Van Gerwen, A. Cuesta, L. Pedrola, F. Palau, A. A. Gabreëls-Festen, C. Verellen, E. Tan, M. Demirci, C. Van Broeckhoven, P. De Jonghe, H. Topaloglu and V. Timmerman, "Mutations in GDAP1: Autosomal Recessive CMT with Demyelination and Axonopathy", *Neurology*, Vol. 59, No. 12, pp. 1865–1872, 2002.

22. Niemann, A., K. M. Wagner, M. Ruegg and U. Suter, "GDAP1 Mutations Differ in Their Effects on Mitochondrial Dynamics and Apoptosis Depending on the Mode of Inheritance", *Neurobiology of Disease*, Vol. 36, No. 3, pp. 509–520, 2009.

23. Tazir, M., M. Bellatache, S. Nouioua and J.-M. Vallat, "Autosomal Recessive Charcot-Marie-Tooth Disease: From Genes to Phenotypes", *Journal of the Peripheral Nervous System*, Vol. 18, No. 2, pp. 113–129, 2013.

24. Magy, L., S. Mathis, G. Le Masson, C. Goizet, M. Tazir and J.-M. Vallat, "Updating the Classification of Inherited Neuropathies", *Neurology*, Vol. 90, No. 10, pp. e870–e876, 2018.

25. Mathis, S., C. Goizet, M. Tazir, C. Magdelaine, A. S. Lia, L. Magy and J. M. Vallat, "Charcot-Marie-Tooth Diseases: An Update and Some New Proposals for the Classification", *Journal of Medical Genetics*, Vol. 52, No. 10, pp. 681–690, 2015.

26. Bird, T. D., J. Ott and E. R. Giblett, "Evidence for Linkage of Charcot-Marie-Tooth Neuropathy to the Duffy Locus on Chromosome 1", *American Journal of Human Genetics*, Vol. 34, No. 3, pp. 388–394, 1982.

27. Lupski, J. R., R. M. de Oca-Luna, S. Slaugenhaupt, L. Pentao, V. Guzzetta, B. J. Trask, O. Saucedo-Cardenas, D. F. Barker, J. M. Killian, C. A. Garcia, A. Chakravarti and P. I. Patel, "DNA Duplication Associated with Charcot-Marie-Tooth Disease Type 1A", *Cell*, Vol. 66, No. 2, pp. 219–232, 1991.

28. Raeymaekers, P., V. Timmerman, E. Nelis, P. De Jonghe, J. E. Hoogenduk, F. Baas, D. F. Barker, J. J. Martin, M. De Visser, P. A. Bolhuis and C. Van Broeckhoven, "Duplication in Chromosome 17p11.2 in Charcot-Marie-Tooth Neuropathy Type 1a (CMT 1a)", *Neuromuscular Disorders*, Vol. 1, No. 2, pp. 93–97, 1991.

29. Pang, S. Y. Y., K. C. Teo, J. S. Hsu, R. S. K. Chang, M. Li, P. C. Sham and S. L. Ho, "The Role of Gene Variants in the Pathogenesis of Neurodegenerative Disorders as Revealed by Next Generation Sequencing Studies: A Review", *Translational Neurodegeneration*, Vol. 6, No. 1, pp. 1–11, 2017.

30. Cortese, A., J. E. Wilcox, J. M. Polke, R. Poh, M. Skorupinska, A. M. Rossor, M. Laura, P. J. Tomaselli, H. Houlden, M. E. Shy and M. M. Reilly, "Targeted Next-Generation Sequencing Panels in the Diagnosis of Charcot-Marie-Tooth Disease", *Neurology*, Vol. 94, No. 1, pp. e51–e61, 2020.

31. Rossor, A. M., J. M. Polke, H. Houlden and M. M. Reilly, "Clinical Implications of Genetic Advances in Charcot-Marie-Tooth Disease", *Nature Reviews Neurology*,

Vol. 9, No. 10, pp. 562–571, 2013.

32. Chance, P. F., M. K. Alderson, K. A. Leppig, M. W. Lensch, N. Matsunami, B. Smith, P. D. Swanson, S. J. Odelberg, C. M. Disteche and T. D. Bird, "DNA Deletion Associated with Hereditary Neuropathy with Liability to Pressure Palsies", *Cell*, Vol. 72, No. 1, pp. 143–151, 1993.

33. Snipes, G. J., U. Suter, A. A. Welcher and E. M. Shooter, "Characterization of a Novel Peripheral Nervous System Myelin Protein (PMP-22/SR13)", *Journal of Cell Biology*, Vol. 117, No. 1, pp. 225–238, 1992.

34. Spreyer, P., G. Kuhn, C. O. Hanemann, C. Gillen, H. Schaal, R. Kuhn and G. H. Lemke Muller, "Axon-Regulated Expression of a Schwann Cell Transcript That Is Homologous to a "Growth Arrest-Specific" Gene", *EMBO Journal*, Vol. 10, No. 12, pp. 3661–3668, 1991.

35. Patel, P. I., B. B. Roa, A. A. Welcher, R. Schoener-Scott, B. J. Trask, L. Pentao, G. J. Snipes, C. A. Garcia, U. Francke, E. M. Shooter, J. R. Lupski and U. Suter, "The Gene for the Peripheral Myelin Protein PMP–22 Is A Candidate for Charcot–Marie–Tooth Disease Type 1A", *Nature Genetics*, Vol. 1, No. 3, pp. 159–165, 1992.

36. Bergoffen, J., S. S. Scherer, S. Wang, M. Oronzi Scott, L. J. Bone, D. L. Paul, K. Chen, M. W. Lensch, P. F. Chance and K. H. Fischbeck, "Connexin Mutations in X-Linked Charcot-Marie-Tooth Disease", *Science*, Vol. 262, No. 5142, pp. 2039–2042, 1993.

37. Boerkoel, C. F., H. Takashima, C. A. Garcia, R. K. Olney, J. Johnson, K. Berry, P. Russo, S. Kennedy, A. S. Teebi, M. Scavina, L. L. Williams, P. Mancias, I. J. Butler, K. Krajewski, M. Shy and J. R. Lupski, "Charcot-Marie-Tooth Disease and Related Neuropathies: Mutation Distribution and Genotype-Phenotype Correlation", *Annals of Neurology*, Vol. 51, No. 2, pp. 190–201, 2002.

38. Murphy, S. M., M. Laura, K. Fawcett, A. Pandraud, Y. T. Liu, G. L. Davidson, A. M. Rossor, J. M. Polke, V. Castleman, H. Manji, M. P. Lunn, K. Bull, G. Ramdharry, M. Davis, J. C. Blake, H. Houlden and M. M. Reilly, "Charcot-Marie-Tooth Disease: Frequency of Genetic Subtypes and Guidelines for Genetic Testing", *Journal of Neurology, Neurosurgery and Psychiatry*, Vol. 83, No. 7, pp. 706–710, 2012.

39. Kleopa, K. A., "The Role of Gap Junctions in Charcot-Marie-Tooth Disease", *Journal of Neuroscience*, Vol. 31, No. 49, pp. 17753–17760, 2011.

40. Sanmaneechai, O., S. Feely, S. S. Scherer, D. N. Herrmann, J. Burns, F. Muntoni, J. Li, C. E. Siskind, J. W. Day, M. Laura, C. J. Sumner, T. E. Lloyd, S. Ramchandren, R. R. Shy, T. Grider, C. Bacon, R. S. Finkel, S. W. Yum, I. Moroni, G. Piscosquito, D. Pareyson, M. M. Reilly and M. E. Shy, "Genotype-Phenotype Characteristics and Baseline Natural History of Heritable Neuropathies Caused by Mutations in the MPZ Gene", *Brain*, Vol. 138, No. 11, pp. 3180–3192, 2015.

41. Greenfield, S., S. Brostoff, E. H. Eylar and P. Morell, "Protein Composition of Myelin of the Peripheral Nervous System", *Journal of Neurochemistry*, Vol. 20, No. 4, pp. 1207–1216, 1973.

42. Giese, K. P., R. Martini, G. Lemke, P. Soriano and M. Schachner, "Mouse P0 Gene Disruption Leads to Hypomyelination, Abnormal Expression of Recognition Molecules, and Degeneration of Myelin and Axons", *Cell*, Vol. 71, No. 4, pp. 565–576, 1992.

43. Lemke, G. and R. Axel, "Isolation and Sequence of a cDNA Encoding the Major Structural Protein of Peripheral Myelin", *Cell*, Vol. 40, No. 3, pp. 501–508, 1985.

44. Martini, R., J. Zielasek, K. V. Toyka, K. P. Giese and M. Schachner, "Protein Zero (P0)-Deficient Mice Show Myelin Degeneration in Peripheral Nerves Characteristic of Inherited Human Neuropathies", *Nature Genetics*, Vol. 11, No. 3, pp.

281–286, 1995.

45. Shy, M. E., A. Jáni, K. Krajewski, M. Grandis, R. A. Lewis, J. Li, R. R. Shy, J. Balsamo, J. Lilien, J. Y. Garbern and J. Kamholz, "Phenotypic Clustering in MPZ Mutations", *Brain*, Vol. 127, No. 2, pp. 371–384, 2004.

46. Laurá, M., M. Pipis, A. M. Rossor and M. M. Reilly, "Charcot-Marie-Tooth Disease and Related Disorders: An Evolving Landscape", *Current Opinion in Neurology*, Vol. 32, No. 5, pp. 641–650, 2019.

47. Tazir, M., T. Hamadouche, S. Nouioua, S. Mathis and J. M. Vallat, "Hereditary Motor and Sensory Neuropathies or Charcot-Marie-Tooth Diseases: An Update", , 2014.

48. Züchner, S., I. V. Mersiyanova, M. Muglia, N. Bissar-Tadmouri, J. Rochelle, E. L. Dadali, M. Zappia, E. Nelis, A. Patitucci, J. Senderek, Y. Parman, O. Evgrafov, P. De Jonghe, Y. Takahashi, S. Tsuji, M. A. Pericak-Vance, A. Quattrone, E. Battologlu, A. V. Polyakov, V. Timmerman, J. M. Schröder and J. M. Vance, "Mutations in the Mitochondrial GTPase Mitofusin 2 Cause Charcot-Marie-Tooth Neuropathy Type 2A", *Nature Genetics*, Vol. 36, No. 5, pp. 449–451, 2004.

49. Santel, A. and M. T. Fuller, "Control of Mitochondrial Morphology by a Human Mitofusin", *Journal of Cell Science*, Vol. 114, No. 5, pp. 867–874, 2001.

50. Nicholson, G. A., C. Magdelaine, D. Zhu, S. Grew, M. M. Ryan, F. Sturtz, J. M. Vallat and R. A. Ouvrier, "Severe Early-Onset Axonal Neuropathy with Homozygous and Compound Heterozygous Mfn2 Mutations", *Neurology*, Vol. 70, No. 19, pp. 1678–1681, 2008.

51. Bis-Brewer, D. M., S. Fazal and S. Züchner, "Genetic Modifiers and Non-Mendelian Aspects of CMT", *Brain Research*, Vol. 1726, No. September 2019, 2020.

52. Pareyson, D., "Diagnosis of Hereditary Neuropathies in Adult Patients", *Journal of Neurology*, Vol. 250, pp. 148–160, 2003.

53. Senderek, J., C. Bergmann, C. Stendel, J. Kirfel, N. Verpoorten, P. De Jonghe, V. Timmerman, R. Chrast, M. H. Verheijen, G. Lemke, E. Battaloglu, Y. Parman, S. Erdem, E. Tan, H. Topaloglu, A. Hahn, W. Müller-Felber, N. Rizzuto, G. M. Fabrizi, M. Stuhrmann, S. Rudnik-Schöneborn, S. Züchner, J. M. Schröder, E. Buchheim, V. Straub, J. Klepper, K. Huehne, B. Rautenstrauss, R. Büttner, E. Nelis and K. Zerres, "Mutations in a Gene Encoding a Novel SH3/TPR Domain Protein Cause Autosomal Recessive Charcot-Marie-Tooth Type 4C Neuropathy", *American Journal of Human Genetics*, Vol. 73, No. 5, pp. 1106–1119, 2003.

54. Zimoń, M., E. Battaloğlu, Y. Parman, S. Erdem, J. Baets, E. De Vriendt, D. Atkinson, L. Almeida-Souza, T. Deconinck, B. Ozes, D. Goossens, S. Cirak, P. Van Damme, M. Shboul, T. Voit, L. Van Maldergem, B. Dan, M. S. El-Khateeb, V. Guergueltcheva, E. Lopez-Laso, N. Goemans, A. Masri, S. Züchner, V. Timmerman, H. Topaloğlu, P. De Jonghe and A. Jordanova, "Unraveling the Genetic Landscape of Autosomal Recessive Charcot-Marie-Tooth Neuropathies Using a Homozygosity Mapping Approach", *Neurogenetics*, Vol. 16, No. 1, pp. 33–42, 2014.

55. Niemann, A., M. Ruegg, V. La Padula, A. Schenone and U. Suter, "Ganglioside-Induced Differentiation Associated Protein 1 Is A Regulator of the Mitochondrial Network: New Implications for Charcot-Marie-Tooth Disease", *Journal of Cell Biology*, Vol. 170, No. 7, pp. 1067–1078, 2005.

56. Niemann, A., P. Berger and U. Suter, "Pathomechanisms of Mutant Proteins in Charcot-Marie-Tooth Disease", *NeuroMolecular Medicine*, Vol. 8, No. 1-2, pp. 217–241, 2006.

57. Lupo, V., M. I. Galindo, D. Martinez-Rubio, T. Sevilla, J. J. Vilchez, F. Palau and C. Espinos, "Missense Mutations in the SH3TC2 Protein Causing Charcot-

Marie-Tooth Disease Type 4C Affect Its Localization in the Plasma Membrane and Endocytic Pathway", *Human Molecular Genetics*, Vol. 18, No. 23, pp. 4603–4614, 2009.

58. Peeters, K., T. Chamova, I. Tournev and A. Jordanova, "Axonal Neuropathy with Neuromyotonia: There Is A HINT", *Brain*, Vol. 140, No. 4, pp. 868–877, 2017.

59. Zimoń, M., J. Baets, L. Almeida-Souza, E. De Vriendt, J. Nikodinovic, Y. Parman, E. Battaloğlu, Z. Matur, V. Guergueltcheva, I. Tournev, M. Auer-Grumbach, P. De Rijk, B. S. Petersen, T. Müller, E. Fransen, P. Van Damme, W. N. Löscher, N. Bariši, Z. Mitrovic, S. C. Previtali, H. Topaloğlu, G. Bernert, A. Beleza-Meireles, S. Todorovic, D. Savic-Pavicevic, B. Ishpekova, S. Lechner, K. Peeters, T. Ooms, A. F. Hahn, S. Züchner, V. Timmerman, P. Van Dijck, V. M. Rasic, A. R. Janecke, P. De Jonghe and A. Jordanova, "Loss-of-function Mutations in HINT1 Cause Axonal Neuropathy with Neuromyotonia", *Nature Genetics*, Vol. 44, No. 10, pp. 1080–1083, 2012.

60. Brenner, C., P. Garrison, J. Gilmour, D. Peisach, D. Ringe, G. A. Petsko and J. M. Lowenstein, "Crystal Structures of Hint Demonstrate that Histidine Triad Proteins are GalT-Related Nucleotide-Binding Proteins", *Nature Structural Biology*, Vol. 4, No. 3, pp. 231–238, 1997.

61. Lee, Y.-N. and E. Razin, "Nonconventional Involvement of LysRS in the Molecular Mechanism of USF2 Transcriptional Activity in FcϵRI-Activated Mast Cells", *Molecular and Cellular Biology*, Vol. 25, No. 20, pp. 8904–8912, 2005.

62. Lee, Y. N., H. Nechushtan, N. Figov and E. Razin, "The Function of Lysyl-tRNA Synthetase and Ap4A as Signaling Regulators of MITF Activity in FcϵRI-Activated Mast Cells", *Immunity*, Vol. 20, No. 2, pp. 145–151, 2004.

63. Nave, K. A., M. W. Sereda and H. Ehrenreich, "Mechanisms of Disease: Inherited Demyelinating Neuropathies - From Basic to Clinical Research", *Nature Clinical*

Practice Neurology, Vol. 3, No. 8, pp. 453–464, 2007.

64. Timmerman, V., E. Nelis, W. Van Hul, B. W. Nieuwenhuijsen, K. L. Chen, S. Wang, K. B. Othman, B. Cullen, R. J. Leach, C. O. Hanemann, P. De Jonghe, P. Raeymaekers, G. J. van Ommen, J. J. Martin, H. W. Müller, J. M. Vance, K. H. Fischbeck and C. Van Broeckhoven, "The Peripheral Myelin Protein Gene PMP–22 Is Contained Within the Charcot–Marie–Tooth Disease Type 1A Duplication", *Nature Genetics*, Vol. 1, No. 3, pp. 171–175, 1992.

65. Adlkofer, K., R. Martini, A. Aguzzi, J. Zielasek, K. V. Toyka and U. Suter, "Hypermyelination and Demyelinating Peripheral Neuropathy in Pmp22-Deficient Mice", *Nature Genetics*, Vol. 11, pp. 274–280, 1995.

66. D'Urso, D., P. Ehrhardt and H. W. Müller, "Peripheral Myelin Protein 22 and Protein Zero: A Novel Association in Peripheral Nervous System Myelin", *Journal of Neuroscience*, Vol. 19, No. 9, pp. 3396–3403, 1999.

67. Fortun, J., J. C. Go, J. Li, S. A. Amici, W. A. Dunn and L. Notterpek, "Alterations in Degradative Pathways and Protein Aggregation in a Neuropathy Model Based on PMP22 Overexpression", *Neurobiology of Disease*, Vol. 22, No. 1, pp. 153–164, 2006.

68. Notterpek, L., M. C. Ryan, A. R. Tobler and E. M. Shooter, "PMP22 Accumulation in Aggresomes: Implications for CMT1A Pathology", *Neurobiology of Disease*, Vol. 6, No. 5, pp. 450–460, 1999.

69. Johnston, J. A., C. L. Ward and R. R. Kopito, "Aggresomes: A Cellular Response to Misfolded Proteins", *Journal of Cell Biology*, Vol. 143, No. 7, pp. 1883–1898, 1998.

70. Ip, C. W., A. Kroner, S. Fischer, M. Berghoff, I. Kobsar, M. Mäurer and R. Martini, "Role of Immune Cells in Animal Models for Inherited Peripheral Neu-

ropathies", *NeuroMolecular Medicine*, Vol. 8, No. 1-2, pp. 175–189, 2006.

71. Mäurer, M., I. Kobsar, M. Berghoff, C. D. Schmid, S. Carenini and R. Martini, "Role of Immune Cells in Animal Models for Inherited Peripheral Neuropathies: Facts and Visions", *Journal of Anatomy*, Vol. 200, No. 4, pp. 405–414, 2002.

72. Züchner, S. and J. M. Vance, "Mechanisms of Disease: A Molecular Genetic Update on Hereditary Axonal Neuropathies", *Nature Clinical Practice Neurology*, Vol. 2, No. 1, pp. 45–53, 2006.

73. Pareyson, D., P. Saveri, A. Sagnelli and G. Piscosquito, "Mitochondrial Dynamics and Inherited Peripheral Nerve Diseases", *Neuroscience Letters*, Vol. 596, pp. 66–77, 2015.

74. Cartoni, R. and J. C. Martinou, "Role of Mitofusin 2 Mutations in the Physiopathology of Charcot-Marie-Tooth Disease Type 2A", *Experimental Neurology*, Vol. 218, No. 2, pp. 268–273, 2009.

75. Barneo-Muñoz, M., P. Juárez, A. Civera-Tregón, L. Yndriago, D. Pla-Martin, J. Zenker, C. Cuevas-Martín, A. Estela, M. Sánchez-Aragó, J. Forteza-Vila, J. M. Cuezva, R. Chrast and F. Palau, "Lack of GDAP1 Induces Neuronal Calcium and Mitochondrial Defects in a Knockout Mouse Model of Charcot-Marie-Tooth Neuropathy", *PLoS Genetics*, Vol. 11, No. 4, pp. 1–27, 2015.

76. Espinós, C., M. I. Galindo, M. A. García-Gimeno, J. S. Ibáñez-Cabellos, D. Martínez-Rubio, J. M. Millán, R. Rodrigo, P. Sanz, M. Seco-Cervera, T. Sevilla, A. Tapia and F. V. Pallardó, "Oxidative Stress, A Crossroad Between Rare Diseases and Neurodegeneration", *Antioxidants*, Vol. 9, No. 4, pp. 1–26, 2020.

77. Mersiyanova, I. V., A. V. Perepelov, A. V. Polyakov, V. F. Sitnikov, E. L. Dadali, R. B. Oparin, A. N. Petrin and O. V. Evgrafov, "A New Variant of Charcot-Marie-

Tooth Disease Type 2 Is Probably the Result of a Mutation in the Neurofilament-Light Gene", *American Journal of Human Genetics*, Vol. 67, No. 1, pp. 37–46, 2000.

78. Rebelo, A. P., A. J. Abrams, E. Cottenie, A. Horga, M. Gonzalez, D. M. Bis, A. Sanchez-Mejias, M. Pinto, E. Buglo, K. Markel, J. Prince, M. Laura, H. Houlden, J. Blake, C. Woodward, M. G. Sweeney, J. L. Holton, M. Hanna, J. E. Dallman, M. Auer-Grumbach, M. M. Reilly and S. Zuchner, "Cryptic Amyloidogenic Elements in the 3′ UTRs of Neurofilament Genes Trigger Axonal Neuropathy", *American Journal of Human Genetics*, Vol. 98, No. 4, pp. 597–614, 2016.

79. Verhoeven, K., P. De Jonghe, K. Coen, N. Verpoorten, M. Auer-Grumbach, J. M. Kwon, D. FitzPatrick, E. Schmedding, E. De Vriendt, A. Jacobs, V. Van Gerwen, K. Wagner, H. P. Hartung and V. Timmerman, "Mutations in the Small GTP-ase Late Endosomal Protein RAB7 Cause Charcot-Marie-Tooth Type 2B Neuropathy", *American Journal of Human Genetics*, Vol. 72, No. 3, pp. 722–727, 2003.

80. Hinshaw, J. E., "Dynamin and Its Role in Membrane Fission", *Annual Review of Cellular and Developmental Biology*, Vol. 16, pp. 483–519, 2000.

81. Schafer, D. A., S. A. Weed, D. Binns, A. V. Karginov, J. T. Parsons and J. A. Cooper, "Dynamin2 and Cortactin Regulate Actin Assembly and Filament Organization", *Current Biology*, Vol. 12, No. 21, pp. 1852–1857, 2002.

82. Züchner, S., M. Noureddine, M. Kennerson, K. Verhoeven, K. Claeys, P. De Jonghe, J. Merory, S. A. Oliveira, M. C. Speer, J. E. Stenger, G. Walizada, D. Zhu, M. A. Pericak-Vance, G. Nicholson, V. Timmerman and J. M. Vance, "Mutations in the Pleckstrin Homology Domain of Dynamin 2 Cause Dominant Intermediate Charcot-Marie-Tooth Disease", *Nature Genetics*, Vol. 37, No. 3, pp. 289–294, 2005.

83. Weedon, M. N., R. Hastings, R. Caswell, W. Xie, K. Paszkiewicz, T. Antoniadi, M. Williams, C. King, L. Greenhalgh, R. Newbury-Ecob and S. Ellard, "Exome Sequencing Identifies a DYNC1H1 Mutation in a Large Pedigree with Dominant Axonal Charcot-Marie-Tooth Disease", *American Journal of Human Genetics*, Vol. 89, No. 2, pp. 308–312, 2011.

84. Puls, I., C. Jonnakuty, B. H. LaMonte, E. L. Holzbaur, M. Tokito, E. Mann, M. K. Floeter, K. Bidus, D. Drayna, S. J. Oh, R. H. Brown, C. L. Ludlow and K. H. Fischbeck, "Mutant Dynactin in Motor Neuron Disease", *Nature Genetics*, Vol. 33, No. 4, pp. 455–456, 2003.

85. De Vos, K. J., A. J. Grierson, S. Ackerley and C. C. Miller, "Role of Axonal Transport in Neurodegenerative Diseases", *Annual Review of Neuroscience*, Vol. 31, pp. 151–173, 2008.

86. Evgrafov, O. V., I. Mersiyanova, J. Irobi, L. V. Van Den Bosch, I. Dierick, C. L. Leung, O. Schagina, N. Verpoorten, K. Van Impe, V. Fedotov, E. Dadali, M. Auer-Grumbach, C. Windpassinger, K. Wagner, Z. Mitrovic, D. Hilton-Jones, K. Talbot, J. J. Martin, N. Vasserman, S. Tverskaya, A. Polyakov, R. K. Liem, J. Gettemans, W. Robberecht, P. De Jonghe and V. Timmerman, "Mutant Small Heat-Shock Protein 27 Causes Axonal Charcot-Marie-Tooth Disease and Distal Hereditary Motor Neuropathy", *Nature Genetics*, Vol. 36, No. 6, pp. 602–606, 2004.

87. Irobi, J., K. Van Impe, P. Seeman, A. Jordanova, I. Dierick, N. Verpoorten, A. Michalik, E. De Vriendt, A. Jacobs, V. Van Gerwen, K. Vennekens, R. Mazanec, I. Tournev, D. Hilton-Jones, K. Talbot, I. Kremensky, L. Van Den Bosch, W. Robberecht, J. Vandekerckhove, C. Van Broeckhoven, J. Gettemans, P. De Jonghe and V. Timmerman, "Hot-Spot Residue in Small Heat-Shock Protein 22 Causes Distal Motor Neuropathy", *Nature Genetics*, Vol. 36, No. 6, pp. 597–601, 2004.

88. Kolb, S. J., P. J. Snyder, E. J. Poi, E. A. Renard, A. Bartlett, S. Gu, S. Sutton, W. D. Arnold, M. L. Freimer, V. H. Lawson, J. T. Kissel and T. W. Prior, "Mutant Small Heat Shock Protein B3 Causes Motor Neuropathy: Utility of a Candidate Gene Approach", *Neurology*, Vol. 74, No. 6, pp. 502–506, 2010.

89. D'Ydewalle, C., V. Benoy and L. Van Den Bosch, "Charcot-Marie-Tooth Disease: Emerging Mechanisms and Therapies", *International Journal of Biochemistry and Cell Biology*, Vol. 44, No. 8, pp. 1299–1304, 2012.

90. Miller, L. J., A. S. Saporta, S. L. Sottile, C. E. Siskind, S. M. Feely and M. E. Shy, "Strategy for Genetic Testing in Charcot-Marie-Tooth Disease", *Acta Myologica*, Vol. 30, pp. 109–116, 2011.

91. Fay, A., Y. Garcia, M. Margeta, S. Maharjan, C. Jürgensen, J. Briceño, M. Garcia, S. Yin, L. Bassaganyas, T. McMahon, Y. M. Hou, Y. H. Fu and L. J. Ptáček, "A Mitochondrial tRNA Mutation Causes Axonal CMT in a Large Venezuelan Family", *Annals of Neurology*, Vol. 88, No. 4, pp. 830–842, 2020.

92. Pitceathly, R. D., S. M. Murphy, E. Cottenie, A. Chalasani, M. G. Sweeney, C. Woodward, E. E. Mudanohwo, I. Hargreaves, S. Heales, J. Land, J. L. Holton, H. Houlden, J. Blake, M. Champion, F. Flinter, S. A. Robb, R. Page, M. Rose, J. Palace, C. Crowe, C. Longman, M. P. Lunn, S. Rahman, M. M. Reilly and M. G. Hanna, "Genetic Dysfunction of MT-ATP6 Causes Axonal Charcot-Marie-Tooth Disease", *Neurology*, Vol. 79, No. 11, pp. 1145–1154, 2012.

93. Rudnik-Schöneborn, S., D. Tölle, J. Senderek, K. Eggermann, M. Elbracht, U. Kornak, M. von der Hagen, J. Kirschner, B. Leube, W. Müller-Felber, U. Schara, K. von Au, D. Wieczorek, C. Bußmann and K. Zerres, "Diagnostic Algorithms in Charcot-Marie-Tooth Neuropathies: Experiences From a German Genetic Laboratory on the Basis of 1206 Index Patients", *Clinical Genetics*, Vol. 89, No. 1, pp. 34–43, 2016.

94. Saporta, A. S., S. L. Sottile, L. J. Miller, S. M. Feely, C. E. Siskind and M. E. Shy, "Charcot-Marie-Tooth Disease Subtypes and Genetic Testing Strategies", *Annals of Neurology*, Vol. 69, No. 1, pp. 22–33, 2011.

95. DiVincenzo, C., C. D. Elzinga, A. C. Medeiros, I. Karbassi, J. R. Jones, M. C. Evans, C. D. Braastad, C. M. Bishop, M. Jaremko, Z. Wang, K. Liaquat, C. A. Hoffman, M. D. York, S. D. Batish, J. R. Lupski and J. J. Higgins, "The Allelic Spectrum of Charcot-Marie-Tooth Disease in Over 17,000 Individuals With Neuropathy", *Molecular Genetics & Genomic Medicine*, Vol. 2, No. 6, pp. 522–529, 2014.

96. Østern, R., T. Fagerheim, H. Hjellnes, B. Nygård, S. I. Mellgren and Ø. Nilssen, "Diagnostic Laboratory Testing for Charcot Marie Tooth Disease (CMT): The Spectrum of Gene Defects in Norwegian Patients With CMT and Its Implications for Future Genetic Test Strategies", *BMC Medical Genetics*, Vol. 14, No. 1, 2013.

97. Azzedine, H., N. Ravise, C. Verny, A. Gabreels-Festen, M. Lammens, D. Grid, J.-M. Vallat, G. Durosier, J. Senderek, S. Nouioua, T. Hamadouche, A. Bouhouche, A. Guilbot, C. Stendel, M. Ruberg, A. Brice, N. Birouk, O. Dubourg, M. Tazir and E. Leguern, "Spine Deformities in Charcot-Marie-Tooth 4C Caused by SH3TC2 Gene Mutations", *Neurology*, Vol. 67, No. 4, pp. 602–606, 2006.

98. Sevilla, T., T. Jaijo, D. Nauffal, D. Collado, M. J. Chumillas, J. J. Vilchez, N. Muelas, L. Bataller, R. Domenech, C. Espinós and F. Palau, "Vocal Cord Paresis and Diaphragmatic Dysfunction Are Severe and Frequent Symptoms of GDAP1-Associated Neuropathy", *Brain*, Vol. 131, No. 11, pp. 3051–3061, 2008.

99. Behjati, S. and P. S. Tarpey, "What Is Next Generation Sequencing?", *Archives of Disease in Childhood: Education & Practice*, Vol. 98, pp. 236–238, 2013.

100. Slatko, B. E., A. F. Gardner and F. M. Ausubel, "Overview of Next-Generation Sequencing Technologies", *Current Protocols in Molecular Biology*, Vol. 122,

No. 1, p. e59, 2018.

101. Bamshad, M. J., S. B. Ng, A. W. Bigham, H. K. Tabor, M. J. Emond, D. A. Nickerson and J. Shendure, "Exome Sequencing as a Tool for Mendelian Disease Gene Discovery", *Nature Reviews Genetics*, Vol. 12, No. 11, pp. 745–755, 2011.

102. Lupo, V., F. García-García, P. Sancho, C. Tello, M. García-Romero, L. Villarreal, A. Alberti, R. Sivera, J. Dopazo, S. I. Pascual-Pascual, C. Márquez-Infante, C. Casasnovas, T. Sevilla and C. Espinós, "Assessment of Targeted Next-Generation Sequencing as a Tool for the Diagnosis of Charcot-Marie-Tooth Disease and Hereditary Motor Neuropathy", *Journal of Molecular Diagnostics*, Vol. 18, No. 2, pp. 225–234, 2016.

103. Nam, S. H., Y. B. Hong, Y. S. Hyun, D. E. Nam, G. Kwak, S. H. Hwang, B.-O. Choi and K. W. Chung, "Identification of Genetic Causes of Inherited Peripheral Neuropathies by Targeted Gene Panel Sequencing", *Molecules and Cells*, Vol. 39, No. 5, pp. 382–388, 2016.

104. Wang, W., C. Wang, D. B. Dawson, E. C. Thorland, P. A. Lundquist, B. W. Eckloff, Y. Wu, S. Baheti, J. M. Evans, S. S. Scherer, P. J. Dyck and C. J. Klein, "Target-Enrichment Sequencing and Copy Number Evaluation in Inherited Polyneuropathy", *Neurology*, Vol. 86, No. 19, pp. 1762–1771, 2016.

105. Botstein, D. and N. Risch, "Discovering Genotypes Underlying Human Phenotypes: Past Successes for Mendelian Disease, Future Approaches for Complex Disease", *Nature Genetics*, Vol. 33, No. 3S, pp. 228–237, 2003.

106. Choi, B. O., S. K. Koo, M. H. Park, H. Rhee, S. J. Yang, K. G. Choi, S. C. Jung, H. S. Kim, Y. S. Hyun, K. Nakhro, H. J. Lee, H. M. Woo and K. W. Chung, "Exome Sequencing Is An Efficient Tool for Genetic Screening of Charcot-Marie-Tooth Disease", *Human Mutation*, Vol. 33, No. 11, pp. 1610–1615, 2012.

107. Xiao, T. and W. Zhou, "The Third Generation Sequencing: The Advanced Approach to Genetic Diseases", *Translational Pediatrics*, Vol. 9, No. 2, pp. 163–173, 2020.

108. Yoshimura, A., J. H. Yuan, A. Hashiguchi, M. Ando, Y. Higuchi, T. Nakamura, Y. Okamoto, M. Nakagawa and H. Takashima, "Genetic Profile and Onset Features of 1005 Patients With Charcot-Marie-Tooth Disease in Japan", *Journal of Neurology, Neurosurgery and Psychiatry*, Vol. 90, No. 2, pp. 195–202, 2019.

109. Baets, J., T. Deconinck, E. De Vriendt, M. Zimoń, L. Yperzeele, K. Van Hoorenbeeck, K. Peeters, R. Spiegel, Y. Parman, B. Ceulemans, P. Van Bogaert, A. Pou-Serradell, G. Bernert, A. Dinopoulos, M. Auer-Grumbach, S. L. Sallinen, G. M. Fabrizi, F. Pauly, P. Van Den Bergh, B. Bilir, E. Battaloglu, R. E. Madrid, D. Kabzińska, A. Kochanski, H. Topaloglu, G. Miller, A. Jordanova, V. Timmerman and P. De Jonghe, "Genetic Spectrum of Hereditary Neuropathies With Onset in the First Year of Life", *Brain*, Vol. 134, No. 9, pp. 2664–2676, 2011.

110. Pareyson, D. and C. Marchesi, "Diagnosis, Natural History, and Management of Charcot-Marie-Tooth Disease", *The Lancet Neurology*, Vol. 8, No. 7, pp. 654–667, 2009.

111. Fridman, V., B. Bundy, M. M. Reilly, D. Pareyson, C. Bacon, J. Burns, J. Day, S. Feely, R. S. Finkel, T. Grider, C. A. Kirk, D. N. Herrmann, M. Laurá, J. Li, T. Lloyd, C. J. Sumner, F. Muntoni, G. Piscosquito, S. Ramchandren, R. Shy, C. E. Siskind, S. W. Yum, I. Moroni, E. Pagliano, S. Zuchner, S. S. Scherer, M. E. Shy and o. b. o. t. I. N. Consurtium, "CMT Subtypes and Disease Burden in Patients Enrolled in the Inherited Neuropathies Consortium Natural History Study: A Cross-Sectional Analysis", *Journal of Neurology Neurosurgery and Psychiatry*, Vol. 86, No. 8, pp. 873–878, 2015.

112. Latour, P., L. Boutrand, N. Levy, R. Bernard, A. Boyer, F. Claustrat, G. Chazot, M. Boucherat and A. Vandenberghe, "Polymorphic Short Tandem Repeats

for Diagnosis of the Charcot-Marie-Tooth 1A Duplication", *Clinical Chemistry*, Vol. 47, No. 5, pp. 829–837, 2001.

113. Kancheva, D., D. Atkinson, P. De Rijk, M. Zimon, T. Chamova, V. Mitev, A. Yaramis, G. Maria Fabrizi, H. Topaloglu, I. Tournev, Y. Parma, E. Battaloglu, A. Estrada-Cuzcano and A. Jordanova, "Novel Mutations in Genes Causing Hereditary Spastic Paraplegia and Charcot-Marie-Tooth Neuropathy Identified by an Optimized Protocol for Homozygosity Mapping Based on Whole-Exome Sequencing", *Genetics in Medicine*, Vol. 18, No. 6, pp. 600–607, 2016.

114. Richards, S., N. Aziz, S. Bale, D. Bick, S. Das, J. Gastier-Foster, W. W. Grody, M. Hegde, E. Lyon, E. Spector, K. Voelkerding and H. L. Rehm, "Standards and Guidelines for the Interpretation of Sequence Variants: A Joint Consensus Recommendation of the American College of Medical Genetics and Genomics and the Association for Molecular Pathology", *Genetics in Medicine*, Vol. 17, No. 5, pp. 405–424, 2015.

115. Auer-Grumbach, M., C. Fischer, L. Papić, E. John, B. Plecko, R. E. Bittner, G. Bernert, T. R. Pieber, G. Miltenberger, R. Schwarz, C. Windpassinger, F. Grill, V. Timmerman, M. R. Speicher and A. R. Janecke, "Two Novel Mutations in the GDAP1 and PRX Genes in Early Onset Charcot-Marie-Tooth Syndrome", *Neuropediatrics*, Vol. 39, No. 1, pp. 33–38, 2008.

116. Kabzińska, D., G. M. Saifi, H. Drac, K. Rowińska-Marcińska, I. Hausmanowa-Petrusewicz, A. Kochański and J. R. Lupski, "Charcot-Marie-Tooth Disease Type 4C4 Caused by a Novel Pro153Leu Substitution in the GDAP1 Gene", *Acta Myologica*, Vol. 26, No. OCT., pp. 108–111, 2007.

117. Pareyson, D., F. Taroni, S. Botti, M. Morbin, S. Baratta, G. Lauria, C. Ciano and A. Sghirlanzoni, "Cranial Nerve Involvement in CMT Disease Type 1 Due to Early Growth Response 2 Gene Mutation", *Neurology*, Vol. 54, No. 8, pp. 1696–1698, 2000.

118. Keckarevic-Markovic, M., V. Milic-Rasic, J. Mladenovic, J. Dackovic, M. Kecmanovic, D. Keckarevic, D. Savic-Pavicevic and S. Romac, "Mutational Analysis of GJB1, MPZ, PMP22, EGR2, and LITAF/SIMPLE in Serbian Charcot-Marie-Tooth Patients", *Journal of the Peripheral Nervous System*, Vol. 14, No. 2, pp. 125–136, 2009.

119. Boerkoel, C. F., H. Takashima, P. Stankiewicz, C. A. Garcia, S. M. Leber, L. Rhee-Morris and J. R. Lupski, "Periaxin Mutations Cause Recessive Dejerine-Sottas Neuropathy", *American Journal of Human Genetics*, Vol. 68, No. 2, pp. 325–333, 2001.

120. Chung, K. W., S. B. Kim, K. D. Park, K. G. Choi, J. H. Lee, H. W. Eun, J. S. Suh, J. H. Hwang, W. K. Kim, B. C. Seo, S. H. Kim, I. H. Son, S. M. Kim, I. N. Sunwoo and B. O. Choi, "Early Onset Severe and Late-Onset Mild Charcot-Marie-Tooth Disease With Mitofusin 2 (MFN2) Mutations", *Brain*, Vol. 129, No. 8, pp. 2103–2118, 2006.

121. Fischer, C., S. Trajanoski, L. Papić, C. Windpassinger, G. Bernert, M. Freilinger, M. Schabhüttl, M. Arslan-Kirchner, P. Javaher-Haghighi, B. Plecko, J. Senderek, C. Rauscher, W. N. Löscher, T. R. Pieber, A. R. Janecke and M. Auer-Grumbach, "SNP Array-Based Whole Genome Homozygosity Mapping as the First Step to a Molecular Diagnosis in Patients with Charcot-Marie-Tooth Disease", *Journal of Neurology*, Vol. 259, No. 3, pp. 515–523, 2012.

122. Kijima, K., C. Numakura, E. Shirahata, Y. Sawaishi, M. Shimohata, S. Igarashi, T. Tanaka and K. Hayasaka, "Periaxin Mutation Causes Early-Onset but Slow-Progressive Charcot-Marie-Tooth Disease", *Journal of Human Genetics*, Vol. 49, No. 7, pp. 376–379, 2004.

123. Vermeer, S., R. P. P. Meijer, B. J. Pijl, J. Timmermans, J. R. M. Cruysberg, M. M. Bos, H. J. Schelhaas, B. P. C. Van De Warrenburg, N. V. A. M. Knoers, H. Scheffer and B. Kremer, "ARSACS in the Dutch Population: A Frequent

Cause of Early-Onset Cerebellar Ataxia", *Neurogenetics*, Vol. 9, No. 3, pp. 207–214, 2008.

124. Choi, Y. R., Y. B. Hong, S. C. Jung, J. H. Lee, Y. J. Kim, H. J. Park, J. Lee, H. Koo, J. S. Lee, D. H. Jwa, N. Jung, S. Y. Woo, S. B. Kim, K. W. Chung and B. O. Choi, "A Novel Homozygous MPV17 Mutation in Two Families With Axonal Sensorimotor Polyneuropathy", *BMC Neurology*, Vol. 15, No. 1, pp. 1–10, 2015.

125. Shy, M. E., C. Siskind, E. R. Swan, K. M. Krajewski, T. Doherty, D. R. Fuerst, P. J. Ainsworth, R. A. Lewis, S. S. Scherer and A. F. Hahn, "CMT1X Phenotypes Represent Loss of GJB1 Gene Function", *Neurology*, Vol. 68, No. 11, pp. 849–855, 2007.

126. Brockmann, K., S. Dreha-Kulaczewski, P. Dechent, C. Bönnemann, G. Helms, M. Kyllerman, W. Brück, J. Frahm, K. Huehne, J. Gärtner and B. Rautenstrauss, "Cerebral Involvement in Axonal Charcot-Marie-Tooth Neuropathy Caused by Mitofusin2 Mutations", *Journal of Neurology*, Vol. 255, No. 7, pp. 1049–1058, 2008.

127. Higuchi, Y., A. Hashiguchi, J. Yuan, A. Yoshimura, J. Mitsui, H. Ishiura, M. Tanaka, S. Ishihara, H. Tanabe, S. Nozuma, Y. Okamoto, E. Matsuura, R. Ohkubo, S. Inamizu, W. Shiraishi, R. Yamasaki, Y. Ohyagi, J. I. Kira, Y. Oya, H. Yabe, N. Nishikawa, S. Tobisawa, N. Matsuda, M. Masuda, C. Kugimoto, K. Fukushima, S. Yano, J. Yoshimura, K. Doi, M. Nakagawa, S. Morishita, S. Tsuji and H. Takashima, "Mutations in MME Cause an Autosomal-Recessive Charcot-Marie-Tooth Disease Type 2", *Annals of Neurology*, Vol. 79, No. 4, pp. 659–672, 2016.

128. Costa, C. and I. Fineza, "P3.19 Neonatal Presentation of Charcot-Marie-Tooth Disease: A New Mutation in Mitofusin 2 Gene", *Neuromuscular Disorders*, Vol. 21, p. 687, 2011.

129. Park, J. Y. J. H., M. Kwon, Y. Yamaguchi, B. L. Firestein, J. Y. J. H. Park, J. Yun, J. O. Yang and M. Inouye, "Preferential Use of Minor Codons in the Translation Initiation Region of Human Genes", *Human Genetics*, Vol. 136, No. 1, pp. 67–74, 2017.

130. Del Bo, R., C. Tiloca, V. Pensato, L. Corrado, A. Ratti, N. Ticozzi, S. Corti, B. Castellotti, L. Mazzini, G. Sorarù, C. Cereda, S. D'Alfonso, C. Gellera, G. P. Comi and V. Silani, "Novel Optineurin Mutations in Patients with Familial and Sporadic Amyotrophic Lateral Sclerosis", *Journal of Neurology, Neurosurgery and Psychiatry*, Vol. 82, No. 11, pp. 1239–1243, 2011.

131. Campuzano, V., L. Montermini, M. D. Moltò, L. Pianese, M. Cossée, F. Cavalcanti, E. Monros, F. Rodius, F. Duclos, A. Monticelli, F. Zara, J. Cañizares, H. Koutnikova, S. I. Bidichandani, C. Gellera, A. Brice, P. Trouillas, G. De Michele, A. Filla, R. De Frutos, F. Palau, P. I. Patel, S. Di Donato, J. L. Mandel, S. Cocozza, M. Koenig and M. Pandolfo, "Friedreich's Ataxia: Autosomal Recessive Disease Caused by an Intronic GAA Triplet Repeat Expansion", *Science*, Vol. 271, No. 5254, pp. 1423–1427, 1996.

132. Bidichandani, S. I., T. Ashizawa and P. I. Patel, "Atypical Friedreich Ataxia Caused by Compound Heterozygosity for a Novel Missense Mutation and the GAA Triplet-Repeat Expansion", *American Journal of Human Genetics*, Vol. 60, No. 5, pp. 1251–1256, 1997.

133. Cossée, M., A. Dürr, M. Schmitt, N. Dahl, P. Trouillas, P. Allinson, M. Kostrzewa, A. Nivelon-Chevallier, K. H. Gustavson, A. Kohlschütter, U. Müller, J. L. Mandel, A. Brice, M. Koenig, F. Cavalcanti, A. Tammaro, G. De Michele, A. Filla, S. Cocozza, M. Labuda, L. Montermini, J. Poirier and M. Pandolfo, "Friedreich's Ataxia: Point Mutations and Clinical Presentation of Compound Heterozygotes", *Annals of Neurology*, Vol. 45, No. 2, pp. 200–206, 1999.

134. Télot, L., E. Rousseau, E. Lesuisse, C. Garcia, B. Morlet, T. Léger, J. M. Camadro

and V. Serre, "Quantitative Proteomics in Friedreich's Ataxia B-Lymphocytes: A Valuable Approach to Decipher the Biochemical Events Responsible for Pathogenesis", *Biochimica et Biophysica Acta - Molecular Basis of Disease*, Vol. 1864, No. 4, pp. 997–1009, 2018.

135. Coleman, J. A., F. Quazi and R. S. Molday, "Mammalian P4-ATPases and ABC Transporters and Their Role in Phospholipid Transport", *Biochimica et Biophysica Acta - Molecular and Cell Biology of Lipids*, Vol. 1831, No. 3, pp. 555–574, 2013.

136. Lopez-Marques, R. L., L. Theorin, M. G. Palmgren and T. G. Pomorski, "P4-ATPases: Lipid Flippases in Cell Membranes", *Pflugers Archiv European Journal of Physiology*, Vol. 466, No. 7, pp. 1227–1240, 2014.

137. Andersen, J. P., A. L. Vestergaard, S. A. Mikkelsen, L. S. Mogensen, M. Chalat and R. S. Molday, "P4-ATPases as Phospholipid Flippases-Structure, Function, and Enigmas", *Frontiers in Physiology*, Vol. 7, No. JUL, pp. 1–23, 2016.

138. Balasubramanian, K. and A. J. Schroit, "Aminophospholipid Asymmetry: A Matter of Life and Death", *Annual Review of Physiology*, Vol. 65, pp. 701–734, 2003.

139. Folmer, D. E., R. P. Elferink and C. C. Paulusma, "P4 ATPases - Lipid Flippases and Their Role in Disease", *Biochimica et Biophysica Acta - Molecular and Cell Biology of Lipids*, Vol. 1791, No. 7, pp. 628–635, 2009.

140. Sebastian, T. T., R. D. Baldridge, P. Xu and T. R. Graham, "Phospholipid Flippases: Building Asymmetric Membranes and Transport Vesicles", *Biochimica et Biophysica Acta - Molecular and Cell Biology of Lipids*, Vol. 1821, No. 8, pp. 1068–1077, 2012.

141. Stapelbroek, J. M., T. A. Peters, D. H. Van Beurden, J. H. Curfs, A. Joosten, A. J. Beynon, B. M. Van Leeuwen, L. M. Van Der Velden, L. Bull, R. P. Elferink,

B. A. Van Zanten, L. W. Klomp and R. H. Houwen, "ATP8B1 Is Essential for Maintaining Normal Hearing", *Proceedings of the National Academy of Sciences of the United States of America*, Vol. 106, No. 24, pp. 9709–9714, 2009.

142. Zhu, X., R. T. Libby, W. N. de Vries, R. S. Smith, D. L. Wright, R. T. Bronson, K. L. Seburn and S. W. John, "Mutations in a P-Type ATPase Gene Cause Axonal Degeneration", *PLoS Genetics*, Vol. 8, No. 8, 2012.

143. Coleman, J. A., X. Zhu, H. R. Djajadi, L. L. Molday, R. S. Smith, R. T. Libby, S. W. John and R. S. Molday, "Phospholipid Flippase ATP8A2 Is Required for Normal Visual and Auditory Function and Photoreceptor and Spiral Ganglion Cell Survival", *Journal of Cell Science*, Vol. 127, No. 5, pp. 1138–1149, 2014.

144. Gong, E. Y., E. Park, H. J. Lee and K. Lee, "Expression of Atp8b3 in Murine Testis and Its Characterization as a Testis Specific P-type ATPase", *Reproduction*, Vol. 137, No. 2, pp. 345–351, 2009.

145. Wang, L., C. Beserra and D. L. Garbers, "A Novel Aminophospholipid Transporter Exclusively Expressed in Spermatozoa Is Required for Membrane Lipid Asymmetry and Normal Fertilization", *Developmental Biology*, Vol. 267, No. 1, pp. 203–215, 2004.

146. Steinberg, K. M., B. Yu, D. C. Koboldt, E. R. Mardis and R. Pamphlett, "Exome Sequencing of Case-Unaffected-Parents Trios Reveals Recessive and De Novo Genetic Variants in Sporadic ALS", *Scientific Reports*, Vol. 5, pp. 1–8, 2015.

147. Bryde, S., H. Hennrich, P. M. Verhulst, P. F. Devaux, G. Lenoir and J. C. Holthuis, "CDC50 Proteins Are Critical Components of the Human Class-1 P4-ATPase Transport Machinery", *Journal of Biological Chemistry*, Vol. 285, No. 52, pp. 40562–40572, 2010.

148. Waterhouse, A., M. Bertoni, S. Bienert, G. Studer, G. Tauriello, R. Gumienny,

F. T. Heer, T. A. De Beer, C. Rempfer, L. Bordoli, R. Lepore and T. Schwede, "SWISS-MODEL: Homology Modelling of Protein Structures and Complexes", *Nucleic Acids Research*, Vol. 46, No. W1, pp. W296–W303, 2018.

149. Bienert, S., A. Waterhouse, T. A. De Beer, G. Tauriello, G. Studer, L. Bordoli and T. Schwede, "The SWISS-MODEL Repository-New Features and Functionality", *Nucleic Acids Research*, Vol. 45, No. D1, pp. D313–D319, 2017.

150. Humphrey, W., A. Dalke and S. Klaus, "VMD: Visual Molecular Dynamics", *Journal of Molecular Graphics*, Vol. 14, No. 1, pp. 33–38, 1996.

151. Lobanov, M. Y., N. S. Bogatyreva and O. V. Galzitskaya, "Radius of Gyration as an Indicator of Protein Structure Compactness", *Molecular Biology*, Vol. 42, No. 4, pp. 623–628, 2008.

152. Tada, T., A. Simonetta, M. Batterton, M. Kinoshita, D. Edbauer and M. Sheng, "Role of Septin Cytoskeleton in Spine Morphogenesis and Dendrite Development in Neurons", *Current Biology*, Vol. 17, No. 20, pp. 1752–1758, 2007.

153. Hanai, N., K. I. Nagata, A. Kawajiri, T. Shiromizu, N. Saitoh, Y. Hasegawa, S. Murakami and M. Inagaki, "Biochemical and Cell Biological Characterization of a Mammalian Septin, Sept11", *FEBS Letters*, Vol. 568, No. 1-3, pp. 83–88, 2004.

154. Nagata, K. I., T. Asano, Y. Nozawa and M. Inagaki, "Biochemical and Cell Biological Analyses of a Mammalian Septin Complex, Sept7/9b/11", *Journal of Biological Chemistry*, Vol. 279, No. 53, pp. 55895–55904, 2004.

155. Kinoshita, M., "Diversity of Septin Scaffolds", *Current Opinion in Cell Biology*, Vol. 18, No. 1, pp. 54–60, 2006.

156. Xie, Y., J. P. Vessey, A. Konecna, R. Dahm, P. Macchi and M. A. Kiebler, "The GTP-Binding Protein Septin 7 Is Critical for Dendrite Branching and Dendritic-

Spine Morphology", *Current Biology*, Vol. 17, No. 20, pp. 1746–1751, 2007.

157. Li, X., D. R. Serwanski, C. P. Miralles, K. I. Nagata and A. L. De Blas, "Septin 11 Is Present in GABAergic Synapses and Plays a Functional Role in the Cytoarchitecture of Neurons and GABAergic Synaptic Connectivity", *Journal of Biological Chemistry*, Vol. 284, No. 25, pp. 17253–17265, 2009.

158. Cho, S. J., H. Lee, S. Dutta, J. Song, R. Walikonis and I. S. Moon, "Septin 6 Regulates the Cytoarchitecture of Neurons Through Localization at Dendritic Branch Points and Bases of Protrusions", *Molecules and Cells*, Vol. 32, No. 1, pp. 89–98, 2011.

159. Buser, A. M., B. Erne, H. B. Werner, K. A. Nave and N. Schaeren-Wiemers, "The Septin Cytoskeleton in Myelinating Glia", *Molecular and Cellular Neuroscience*, Vol. 40, No. 2, pp. 156–166, 2009.

160. Sellin, M. E., L. Sandblad, S. Stenmark and M. Gullberg, "Deciphering the Rules Governing Assembly Order of Mammalian Septin Complexes", *Molecular Biology of the Cell*, Vol. 22, No. 17, pp. 3152–3164, 2011.

161. Hall, P. A. and S. E. Russell, "The Pathobiology of the Septin Gene Family", *Journal of Pathology*, Vol. 204, No. 4, pp. 489–505, 2004.

162. Martínez, C., M. a. Sanjuan, J. a. Dent, L. Karlsson and J. Ware, "Human Septin-Septin Interactions as a Prerequisite for Targeting Septin Complexes in the Cytosol.", *The Biochemical journal*, Vol. 382, No. Pt 3, pp. 783–91, 2004.

163. Mostowy, S. and P. Cossart, "Septins: The Fourth Component of the Cytoskeleton", *Nature Reviews Molecular Cell Biology*, Vol. 13, No. 3, pp. 183–194, 2012.

164. Ono, R., M. Ihara, H. Nakajima, K. Ozaki, Y. Kataoka-Fujiwara, T. Taki, K.-i. Nagata, M. Inagaki, N. Yoshida, T. Kitamura, Y. Hayashi, M. Kinoshita and T. Nosaka, "Disruption of Sept6, a Fusion Partner Gene of MLL, Does Not Affect

Ontogeny, Leukemogenesis Induced by MLL-SEPT6, or Phenotype Induced by the Loss of Sept4", *Molecular and Cellular Biology*, Vol. 25, No. 24, pp. 10965–10978, 2005.

165. Katsanis, N., "The Continuum of Causality in Human Genetic Disorders", *Genome Biology*, Vol. 17, No. 1, pp. 1–5, 2016.

166. Cady, J., P. Allred, T. Bali, A. Pestronk, A. Goate, T. M. Miller, R. Mitra, J. Ravits, M. B. Harms and R. H. Baloh, "ALS Onset Is Influenced by the Burden of Rare Variants in Known ALS Genes", *Annals of Neurology*, Vol. 77, No. 1, pp. 100–113, 2015.

167. Gonzaga-Jauregui, C., T. Harel, T. Gambin, M. Kousi, L. B. Griffin, L. Francescatto, B. Ozes, E. Karaca, S. N. Jhangiani, M. N. Bainbridge, K. S. Lawson, D. Pehlivan, Y. Okamoto, M. Withers, P. Mancias, A. Slavotinek, P. J. Reitnauer, M. T. Goksungur, M. Shy, T. O. Crawford, M. Koenig, J. Willer, B. N. Flores, I. Pediaditrakis, O. Us, W. Wiszniewski, Y. Parman, A. Antonellis, D. M. Muzny, N. Katsanis, E. Battaloglu, E. Boerwinkle, R. A. Gibbs and J. R. Lupski, "Exome Sequence Analysis Suggests that Genetic Burden Contributes to Phenotypic Variability and Complex Neuropathy", *Cell Reports*, Vol. 12, No. 7, pp. 1169–1183, 2015.

168. Lubbe, S. J., V. Escott-Price, J. R. Gibbs, M. A. Nalls, J. Bras, T. R. Price, A. Nicolas, I. E. Jansen, K. Y. Mok, A. M. Pittman, J. E. Tomkins, P. A. Lewis, A. J. Noyce, S. Lesage, M. Sharma, E. R. Schiff, A. P. Levine, A. Brice, T. Gasser, J. Hardy, P. Heutink, N. W. Wood, A. B. Singleton, N. M. Williams and H. R. Morris, "Additional Rare Variant Analysis in Parkinson's Disease Cases With and Without Known Pathogenic Mutations: Evidence for Oligogenic Inheritance", *Human Molecular Genetics*, Vol. 25, No. 24, pp. 5483–5489, 2016.

169. Hodapp, J. A., G. T. Carter, H. P. Lipe, S. J. Michelson, G. H. Kraft and T. D. Bird, "Double Trouble in Hereditary Neuropathy", *Archives of Neurology*, Vol. 63,

No. 1, p. 112, 2006.

170. Brusse, E., D. Majoor-Krakauer, B. M. De Graaf, G. H. Visser, S. Swagemakers, A. J. Boon, B. A. Oostra and A. M. Bertoli-Avella, "A Novel 16p Locus Associated With BSCL2 Hereditary Motor Neuronopathy: A Genetic Modifier?", *Neurogenetics*, Vol. 10, No. 4, pp. 289–297, 2009.

171. Drew, A. P., D. Zhu, A. Kidambi, C. Ly, S. Tey, M. H. Brewer, A. Ahmad-Annuar, G. A. Nicholson and M. L. Kennerson, "Improved Inherited Peripheral Neuropathy Genetic Diagnosis by Whole-Exome Sequencing", *Molecular Genetics and Genomic Medicine*, Vol. 3, No. 2, pp. 143–154, 2015.

172. Miressi, F., C. Magdelaine, P. Cintas, S. Bourthoumieux, A. Nizou, P. Derouault, F. Favreau, F. Sturtz, P.-A. Faye and A.-S. Lia, "One Multilocus Genomic Variation Is Responsible for a Severe Charcot–Marie–Tooth Axonal Form", *Brain Sciences*, Vol. 10, No. 12, p. 986, 2020.

173. Karaca, E., J. E. Posey, Z. Coban Akdemir, D. Pehlivan, T. Harel, S. N. Jhangiani, Y. Bayram, X. Song, V. Bahrambeigi, O. O. Yuregir, S. Bozdogan, G. Yesil, S. Isikay, D. Muzny, R. A. Gibbs and J. R. Lupski, "Phenotypic Expansion Illuminates Multilocus Pathogenic Variation", *Genetics in Medicine*, Vol. 20, No. 12, pp. 1528–1537, 2018.

174. Bao, R., L. Huang, J. Andrade, W. Tan, W. A. Kibbe, H. Jiang and G. Feng, "Review of Current Methods, Applications, and Data Management for the Bioinformatics Analysis of Whole Exome Sequencing", *Cancer Informatics*, Vol. 13, pp. 67–82, 2014.

175. Pareyson, D., P. Saveri and C. Pisciotta, "New Developments in Charcot-Marie-Tooth Neuropathy and Related Diseases", *Current Opinion in Neurology*, Vol. 30, No. 5, pp. 471–480, 2017.

176. Foo, J. N., J. J. Liu and E. K. Tan, "Whole-Genome and Whole-Exome Sequencing in Neurological Diseases", *Nature Reviews Neurology*, Vol. 8, No. 9, pp. 508–517, 2012.

177. Warman Chardon, J., C. Beaulieu, T. Hartley, K. M. Boycott and D. A. Dyment, "Axons to Exons: The Molecular Diagnosis of Rare Neurological Diseases by Next-Generation Sequencing", *Current Neurology and Neuroscience Reports*, Vol. 15, No. 9, pp. 1–8, 2015.

178. Matthijs, G., E. Souche, M. Alders, A. Corveleyn, S. Eck, I. Feenstra, V. Race, E. Sistermans, M. Sturm, M. Weiss, H. Yntema, E. Bakker, H. Scheffer and P. Bauer, "Guidelines for Diagnostic Next-Generation Sequencing", *European Journal of Human Genetics*, Vol. 24, No. 1, pp. 2–5, 2016.

179. Foley, A. R., S. Donkervoort and C. G. Bönnemann, "Next-Generation Sequencing Still Needs Our Generation's Clinicians", *Neurology: Genetics*, Vol. 1, No. 2, pp. 1–4, 2015.

180. Farwell, K. D., L. Shahmirzadi, D. El-Khechen, Z. Powis, E. C. Chao, B. Tippin Davis, R. M. Baxter, W. Zeng, C. Mroske, M. C. Parra, S. K. Gandomi, I. Lu, X. Li, H. Lu, H. M. Lu, D. Salvador, D. Ruble, M. Lao, S. Fischbach, J. Wen, S. Lee, A. Elliott, C. L. Dunlop and S. Tang, "Enhanced Utility of Family-Centered Diagnostic Exome Sequencing with Inheritance Model-Based Analysis: Results from 500 Unselected Families with Undiagnosed Genetic Conditions", *Genetics in Medicine*, Vol. 17, No. 7, pp. 578–586, 2015.

181. Dewey, F. E., M. E. Grove, C. Pan, B. A. Goldstein, J. A. Bernstein, H. Chaib, J. D. Merker, R. L. Goldfeder, G. M. Enns, S. P. David, N. Pakdaman, K. E. Ormond, C. Caleshu, K. Kingham, T. E. Klein, M. Whirl-Carrillo, K. Sakamoto, M. T. Wheeler, A. J. Butte, J. M. Ford, L. Boxer, J. P. Ioannidis, A. C. Yeung, R. B. Altman, T. L. Assimes, M. Snyder, E. A. Ashley and T. Quertermous, "Clinical Interpretation and Implications of Whole-Genome Sequencing", *JAMA*

- *Journal of the American Medical Association*, Vol. 311, No. 10, pp. 1035–1044, 2014.

182. Ankala, A., C. Da Silva, F. Gualandi, A. Ferlini, L. J. Bean, C. Collins, A. K. Tanner and M. R. Hegde, "A Comprehensive Genomic Approach for Neuromuscular Diseases Gives a High Diagnostic Yield", *Annals of Neurology*, Vol. 77, No. 2, pp. 206–214, 2015.

183. Shashi, V., A. McConkie-Rosell, B. Rosell, K. Schoch, K. Vellore, M. McDonald, Y. H. Jiang, P. Xie, A. Need and D. B. Goldstein, "The Utility of the Traditional Medical Genetics Diagnostic Evaluation in the Context of Next-Generation Sequencing for Undiagnosed Genetic Disorders", *Genetics in Medicine*, Vol. 16, No. 2, pp. 176–182, 2014.

184. Hirano, R., H. Takashima, F. Umehara, H. Arimura, K. Michizono, Y. Okamoto, M. Nakagawa, C. F. Boerkoel, J. R. Lupski, M. Osame and K. Arimura, "SET Binding Factor 2 (SBF2) Mutation Causes CMT4B with Juvenile Onset Glaucoma", *Neurology*, Vol. 63, No. 3, pp. 577–580, 2004.

185. Forrest, S. M., M. Knight, M. B. Delatycki, D. Paris, R. Williamson, J. King, L. Yeung, N. Nassif and G. A. Nicholson, "The Correlation of Clinical Phenotype in Friedreich Ataxia with the Site of Point Mutations in the FRDA Gene", *Neurogenetics*, Vol. 1, No. 4, pp. 253–257, 1998.

186. McCormack, M. L., R. P. Guttmann, M. Schumann, J. M. Farmer, C. A. Stolle, V. Campuzano, M. Koenig and D. R. Lynch, "Frataxin Point Mutations in Two Patients with Friedreich's Ataxia and Unusual Clinical Features", *Journal of Neurology Neurosurgery and Psychiatry*, Vol. 68, No. 5, pp. 661–664, 2000.

187. De Michele, G., A. Filla, F. Cavalcanti, A. Tammaro, A. Monticelli, L. Pianese, F. Di Salle, A. Perretti, L. Santoro, G. Caruso and S. Cocozza, "Atypical Friedreich Ataxia Phenotype Associated With a Novel Missense Mutation on the X25

Gene", *Neurology*, Vol. 54, No. 2, pp. 496–499, 2000.

188. Ygland, E., F. Taroni, C. Gellera, S. Caldarazzo, M. Duno, M. Soller and A. Puschmann, "Atypical Friedreich Ataxia in Patients with FXN p.R165P Point Mutation or Comorbid Hemochromatosis", *Parkinsonism and Related Disorders*, Vol. 20, No. 8, pp. 919–923, 2014.

189. Schmucker, S. and H. Puccio, "Understanding the Molecular Mechanisms of Friedreich's Ataxia to Develop Therapeutic Approaches", *Human Molecular Genetics*, Vol. 19, No. R1, pp. 103–110, 2010.

190. Clark, E., J. S. Butler, C. J. Isaacs, M. Napierala and D. R. Lynch, "Selected Missense Mutations Impair Frataxin Processing in Friedreich Ataxia", *Annals of Clinical and Translational Neurology*, Vol. 4, No. 8, pp. 575–584, 2017.

191. Bridwell-Rabb, J., A. M. Winn and D. P. Barondeau, "Structure-Function Analysis of Friedreich's Ataxia Mutants Reveals Determinants of Frataxin Binding and Activation of the Fe-S Assembly Complex", *Biochemistry*, Vol. 50, No. 33, pp. 7265–7274, 2011.

192. Candayan, A., G. Yunisova, A. Çakar, H. Durmuş, A. N. Başak, Y. Parman and E. Battaloğlu, "The First Biallelic Missense Mutation in the FXN Gene in a Consanguineous Turkish Family with Charcot-Marie-Tooth-Like Phenotype", *Neurogenetics*, Vol. 21, No. 1, pp. 73–78, 2020.

193. Harris, M. J. and I. M. Arias, "FIC1, A P-type ATPase Linked to Cholestatic Liver Disease, Has Homologues (ATP8B2 and ATP8B3) Expressed Throughout the Body", *Biochimica et Biophysica Acta - Molecular and Cell Biology of Lipids*, Vol. 1633, No. 2, pp. 127–131, 2003.

194. Kay, J. G. and G. D. Fairn, "Distribution, Dynamics and Functional Roles of Phosphatidylserine Within the Cell", *Cell Communication and Signaling*, Vol. 17,

No. 1, pp. 1–8, 2019.

195. Pizarro-Cerdá, J., R. Jonquières, E. Gouin, J. Vandekerckhove, J. Garin and P. Cossart, "Distinct Protein Patterns Associated with Listeria Monocytogenes InIA- or InIB-Phagosomes", *Cellular Microbiology*, Vol. 4, No. 2, pp. 101–115, 2002.

196. Van Nhieu, G. T., E. Caron, A. Hall and P. J. Sansonetti, "IpaC Induces Actin Polymerization and Filopodia Formation During Shigella Entry into Epithelial Cells", *EMBO Journal*, Vol. 18, No. 12, pp. 3249–3262, 1999.

197. Frischknecht, F. and M. Way, "Surfing Pathogens and the Lessons Learned for Actin Polymerization", *Trends in Cell Biology*, Vol. 11, No. 1, pp. 30–38, 2001.

198. Ihara, M., N. Yamasaki, A. Hagiwara, A. Tanigaki, A. Kitano, R. Hikawa, H. Tomimoto, M. Noda, M. Takanashi, H. Mori, N. Hattori, T. Miyakawa and M. Kinoshita, "Sept4, a Component of Presynaptic Scaffold and Lewy Bodies, Is Required for the Suppression of α-Synuclein Neurotoxicity", *Neuron*, Vol. 53, No. 4, pp. 519–533, 2007.

199. Kuhlenbäumer, G., M. C. Hannibal, E. Nelis, A. Schirmacher, N. Verpoorten, J. Meuleman, G. D. Watts, E. De Vriendt, P. Young, F. Stögbauer, H. Halfter, J. Irobi, D. Goossens, J. Del-Favero, B. G. Betz, H. Hor, G. Kurlemann, T. D. Bird, E. Airaksinen, T. Mononen, A. P. Serradell, J. M. Prats, C. Van Broeckhoven, P. De Jonghe, V. Timmerman, E. B. Ringelstein and P. F. Chance, "Mutations in SEPT9 Cause Hereditary Neuralgic Amyotrophy", *Nature Genetics*, Vol. 37, No. 10, pp. 1044–1046, 2005.

200. Honorat, J. A., A. Sebastian Lopez-Chiriboga, T. J. Kryzer, J. P. Fryer, M. Devine, A. Flores, V. A. Lennon, S. J. Pittock and A. McKeon, "Autoimmune Septin-5 Cerebellar Ataxia", *Neurology: Neuroimmunology and NeuroInflammation*, Vol. 5, No. 5, pp. 1–6, 2018.

201. Gozal, Y. M., N. T. Seyfried, M. Gearing, J. D. Glass, C. J. Heilman, J. Wuu, D. M. Duong, D. Cheng, Q. Xia, H. D. Rees, J. J. Fritz, D. S. Cooper, J. Peng, A. I. Levey and J. J. Lah, "Aberrant Septin 11 Is Associated with Sporadic Frontotemporal Lobar Degeneration", *Molecular Neurodegeneration*, Vol. 6, No. 1, pp. 1–13, 2011.

202. Röseler, S., K. Sandrock, I. Bartsch, A. Busse, H. Omran, N. T. Loges and B. Zieger, "Lethal Phenotype of Mice Carrying a Sept11 Null Mutation", *Biological Chemistry*, Vol. 392, No. 8-9, pp. 779–781, 2011.

APPENDIX A: CHROMATOGRAMS

Chromatograms pedigrees of genetically diagnosed families are given below.

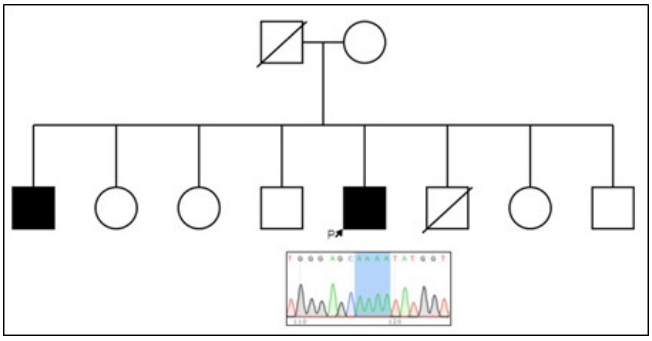

Figure A.1. Sanger chromatogram on pedigree of family P265 showing the novel homozygous c.531delA, p.Lys177Asnfs*15 variant in the *MME* gene.

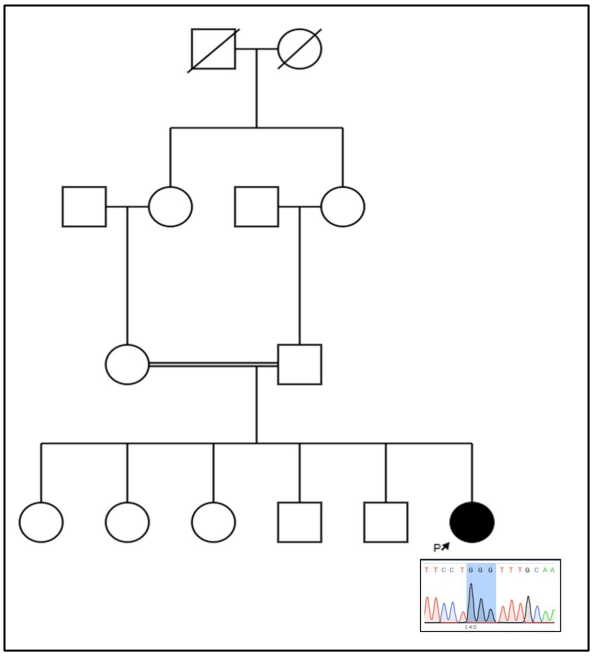

Figure A.2. Sanger chromatogram on pedigree of family P294 showing the recurrent homozygous c.786delG; p.Phe263Leufs*22 mutation in the *GDAP1* gene.

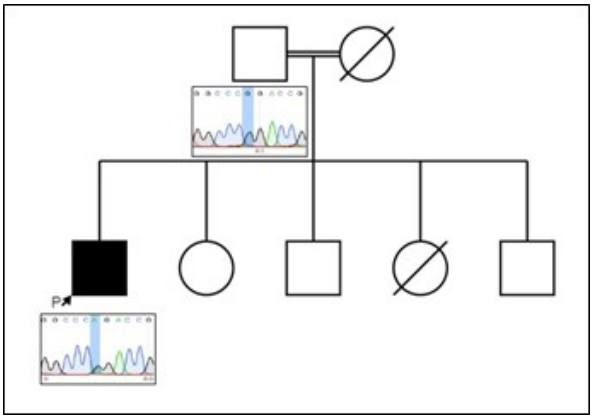

Figure A.3. Sanger chromatogram on pedigree of family P300 showing the recurrent heterozygous c.1090C>T, p.Arg364Trp mutation in the *MFN2* gene.

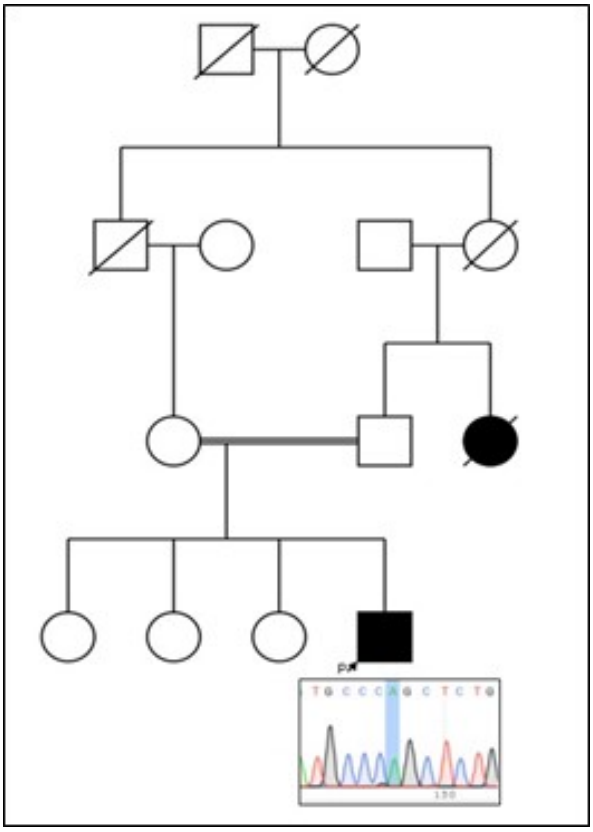

Figure A.4. Sanger chromatogram on pedigree of family P322 showing the novel homozygous c.1586G>A, p.Arg529His variant in the *SH3TC2* gene.

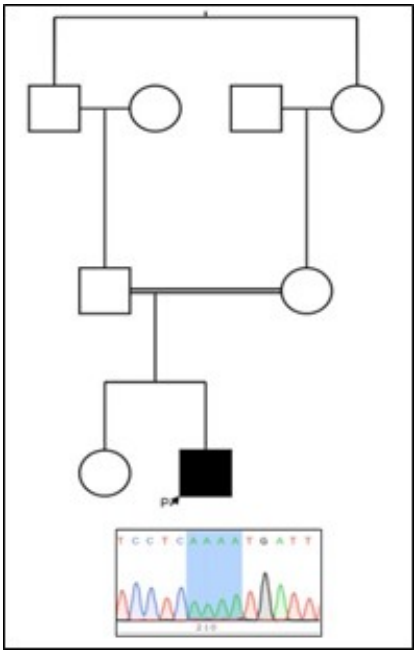

Figure A.5. Sanger chromatogram on pedigree of family P431 showing the novel homozygous c.99delT, p.Phe33Leufs*22 variant in the *HINT1* gene.

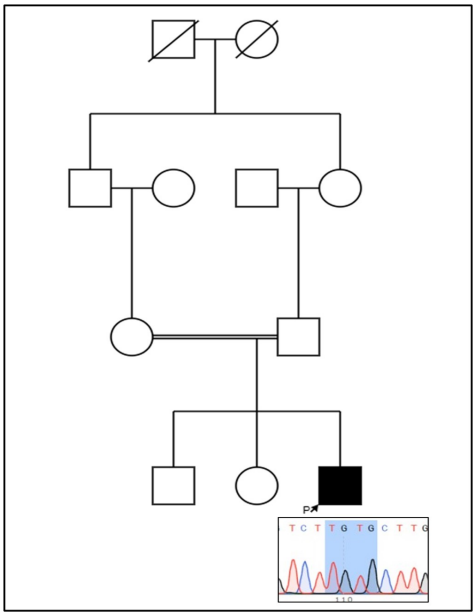

Figure A.6. Sanger chromatogram on pedigree of family P448 showing the recurrent homozygous c.174_176delinsTGTG; p.Pro59Valfs*4 mutation in the *GDAP1* gene.

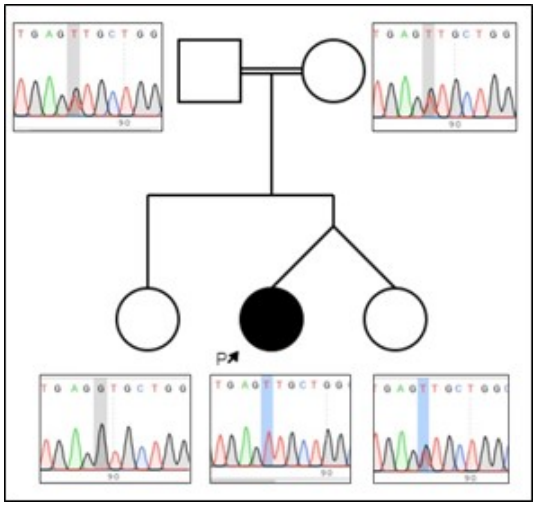

Figure A.7. Sanger chromatogram on pedigree of family P492 showing the novel homozygous c.271G>T, p.Val91Leu variant in the *MFN2* gene.

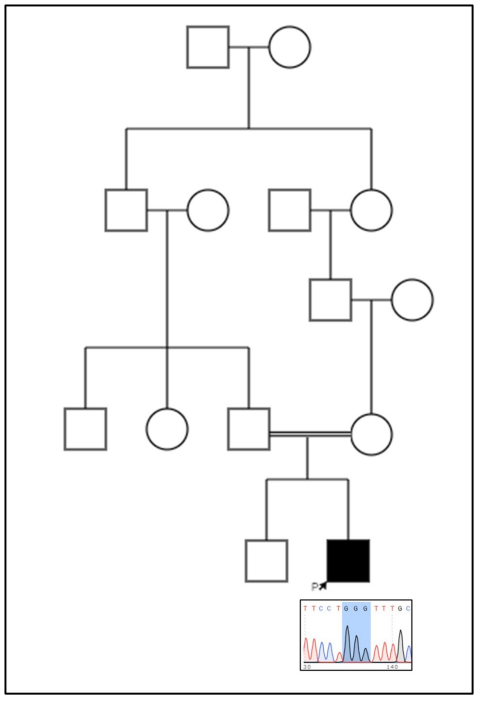

Figure A.8. Sanger chromatogram on pedigree of family P555 showing the recurrent homozygous c.786delG; p.Phe263Leufs*22 mutation in the *GDAP1* gene.

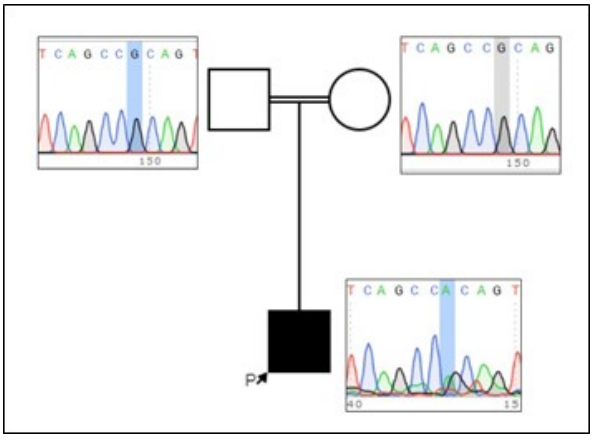

Figure A.9. Sanger chromatogram on pedigree of family P581 showing the recurrent heterozygous c.1142G>A, p.Arg381His mutation in *EGR2* gene.

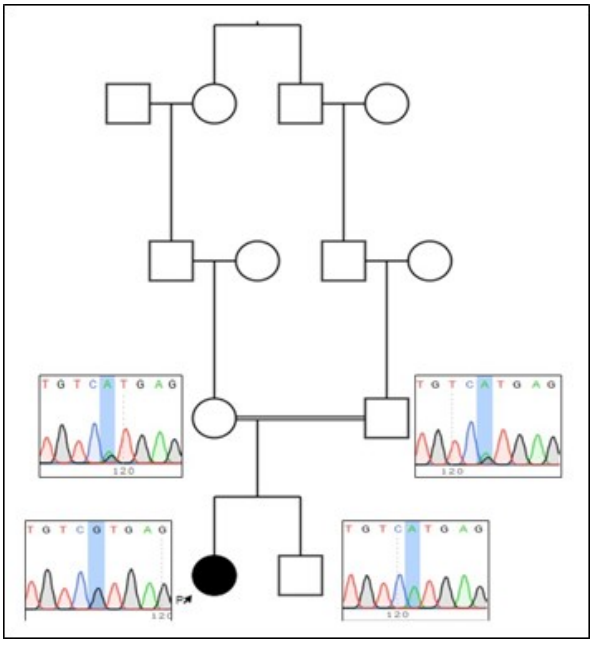

Figure A.10. Sanger chromatogram on pedigree of family P629 showing the novel homozygous c.454A>G, p.Met152Val variant in the *SPG7* gene.

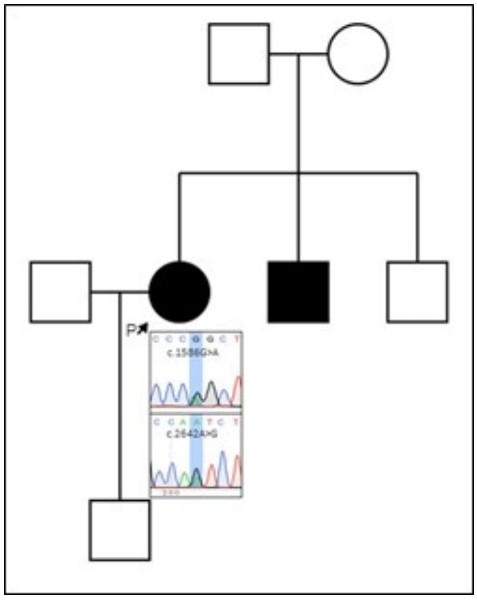

Figure A.11. Sanger chromatogram on pedigree of family P639 showing the recurrent heterozygous c.2642A>G, p.Asn881Ser and heterozygous c.1586G>A, p.Arg529His mutations in the *SH3TC2* gene.

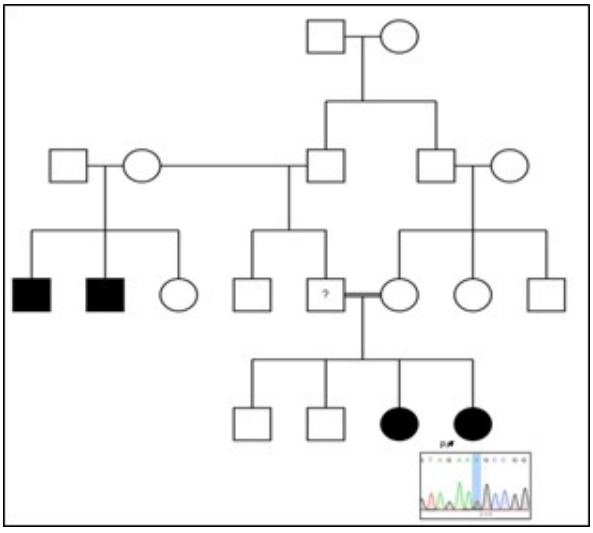

Figure A.12. Sanger chromatogram on pedigree of family P711 showing the recurrent heterozygous c.47A>T, p.His16Leu mutation in the *GJB1* gene.

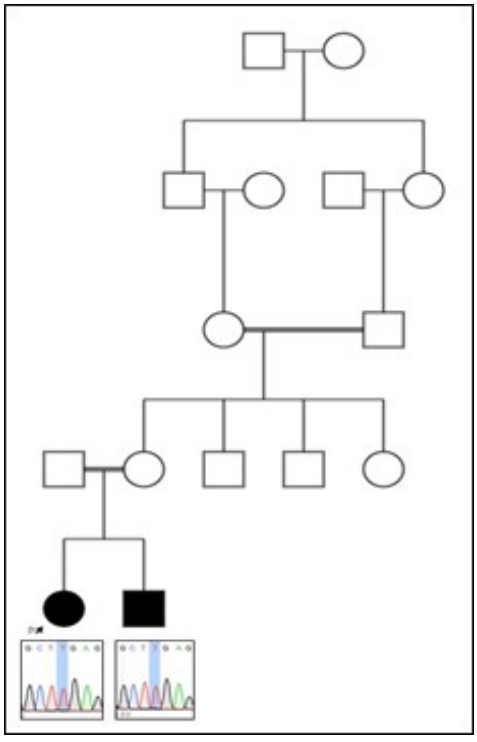

Figure A.13. Sanger chromatogram on pedigree of family P811 showing the recurrent homozygous c.1102C>T, p.Arg368Ter mutation in the *PRX* gene.

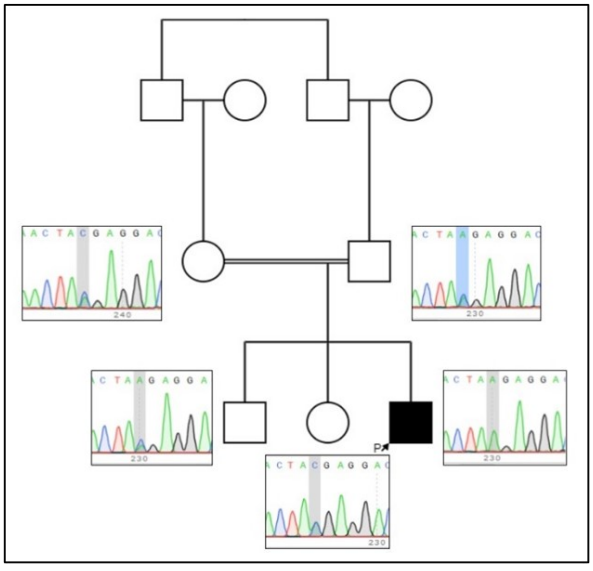

Figure A.14. Sanger chromatogram on pedigree of family P963 showing the novel homozygous c.237C>A, p.Tyr79Ter variant in the *NDRG1* gene.

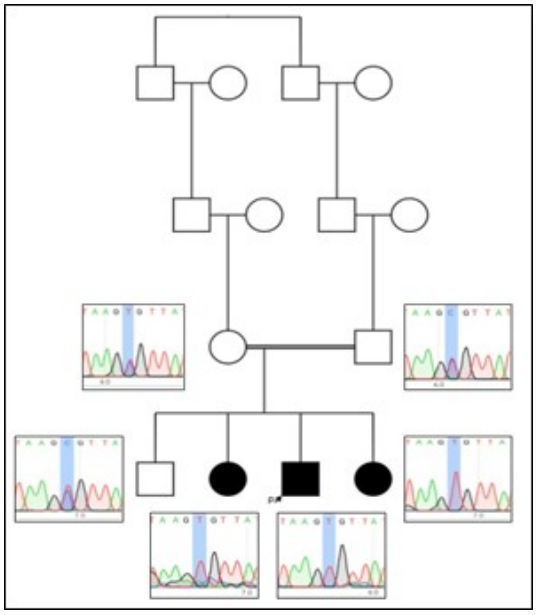

Figure A.15. Sanger chromatogram on pedigree of family P966 showing the homozygous c.493C>T, p.Arg165Cys mutation in the *FXN* gene.

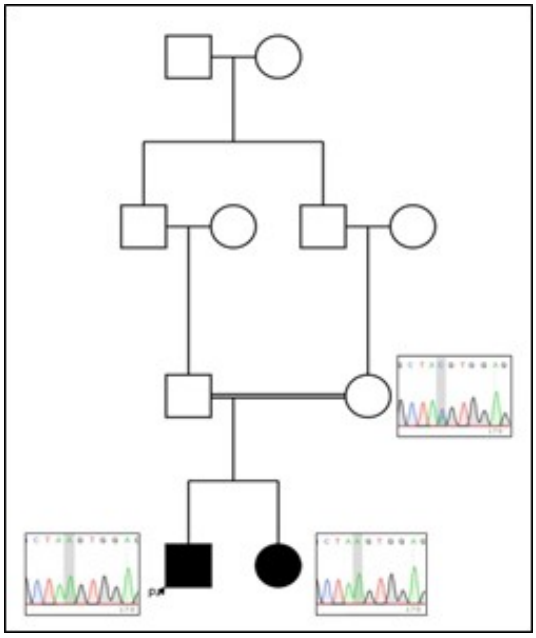

Figure A.16. Sanger chromatogram on pedigree of family P969 showing the novel homozygous c.54C>A, p.Tyr18Ter variant in the *NEFL* gene.

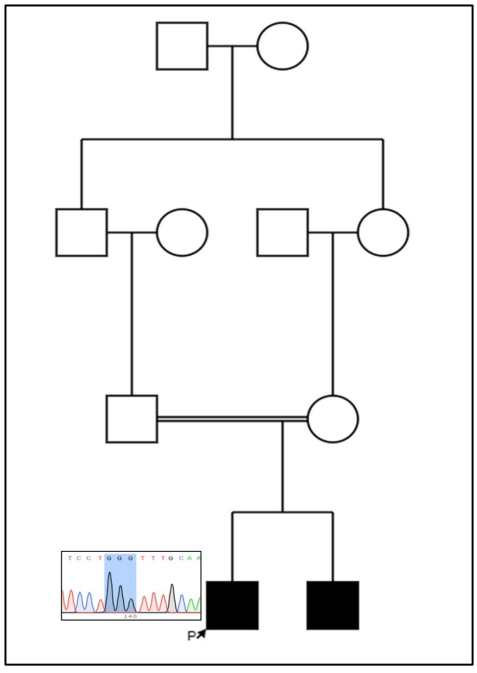

Figure A.17. Sanger chromatogram on pedigree of family P987 showing the recurrent homozygous c.786delG; p.Phe263Leufs*22 mutation in the *GDAP1* gene.

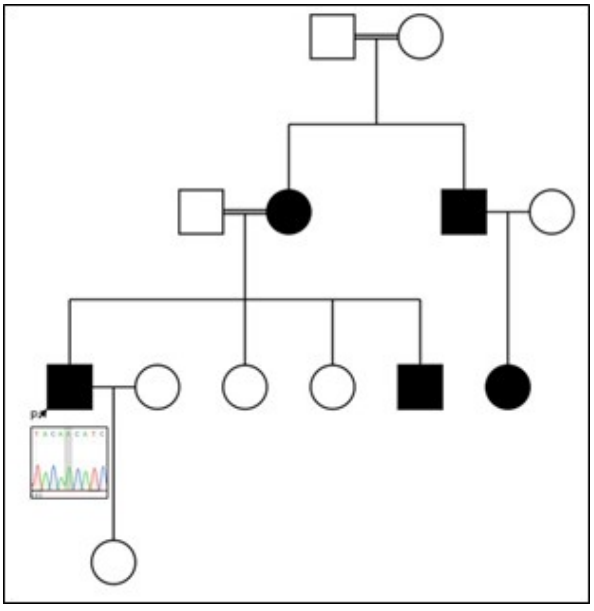

Figure A.18. Sanger chromatogram on pedigree of family P991 showing the recurrent homozygous c.1178-1G>A mutation in the *SH3TC2* gene.

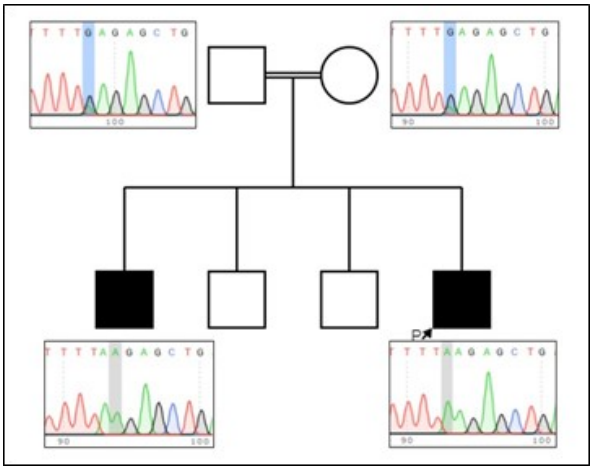

Figure A.19. Sanger chromatogram on pedigree of family P1130 showing the novel homozygous c.112C>T, p.Gln38Ter variant in the *GDAP1* gene.

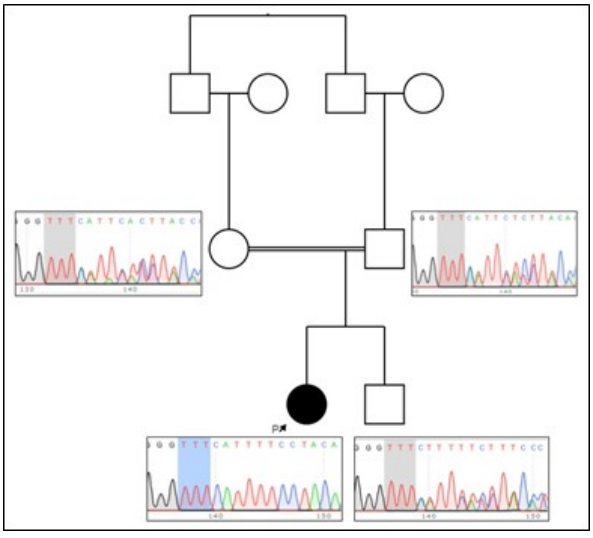

Figure A.20. Sanger chromatogram on pedigree of family P1142 showing the novel homozygous c.18_21delATTT, p.Leu6PhefsTer7 variant in the *C12ORF65* gene.

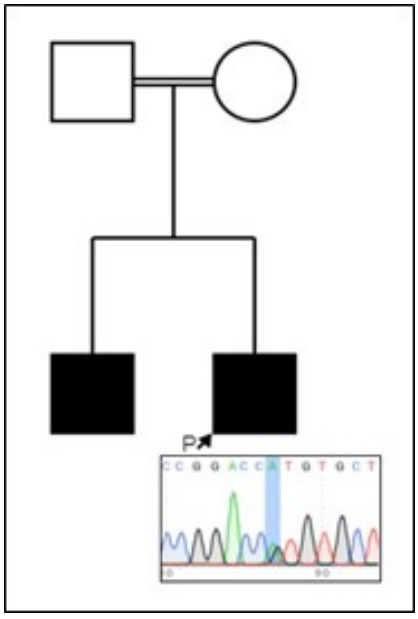

Figure A.21. Sanger chromatogram on pedigree of family P1148 showing the recurrent heterozygous c.1085C>T, p.Thr362Met mutation in the *MFN2* gene.

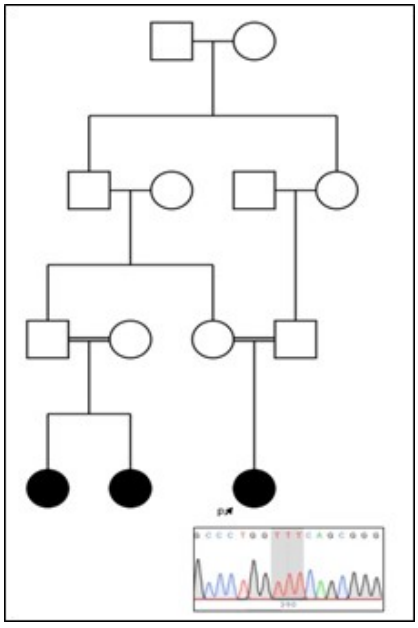

Figure A.22. Sanger chromatogram on pedigree of family P1152 showing the recurrent homozygous c.1894_1897delinsAAA, p.Glu632Lysfs*13 mutation in the *SH3TC2* gene.

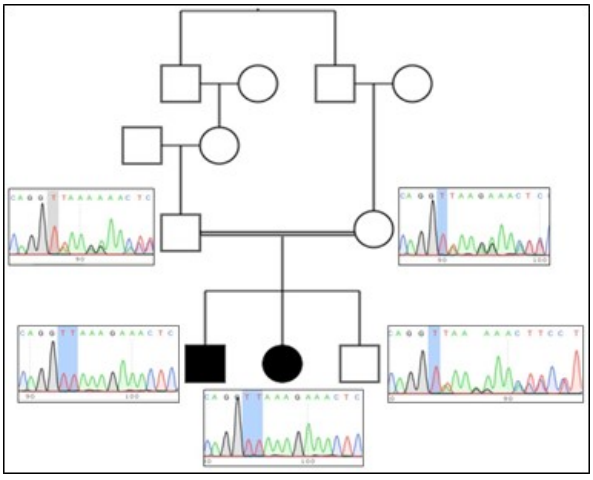

Figure A.23. Sanger chromatogram on pedigree of family P1180-4 showing the novel homozygous c.54dupT, p.Lys19Ter variant in the *SH3TC2* gene.

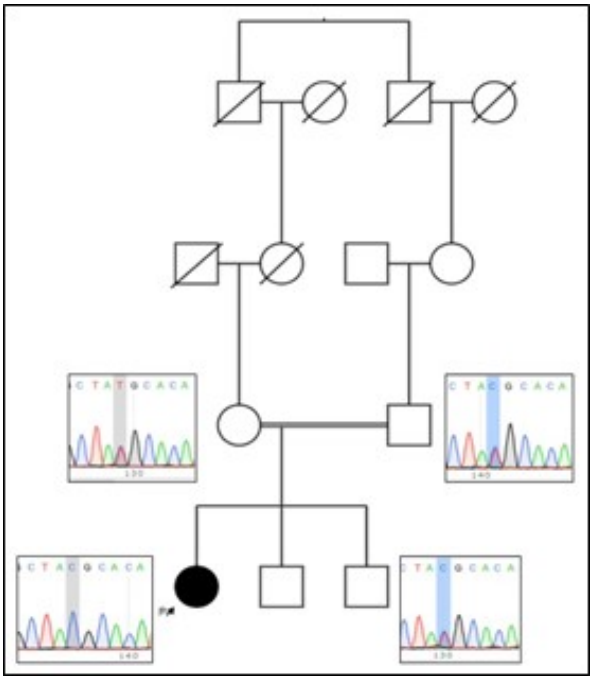

Figure A.24. Sanger chromatogram on pedigree of family P1188 showing the novel homozygous c.2549T>C, p.Met850Thr variant in the *SBF2* gene.

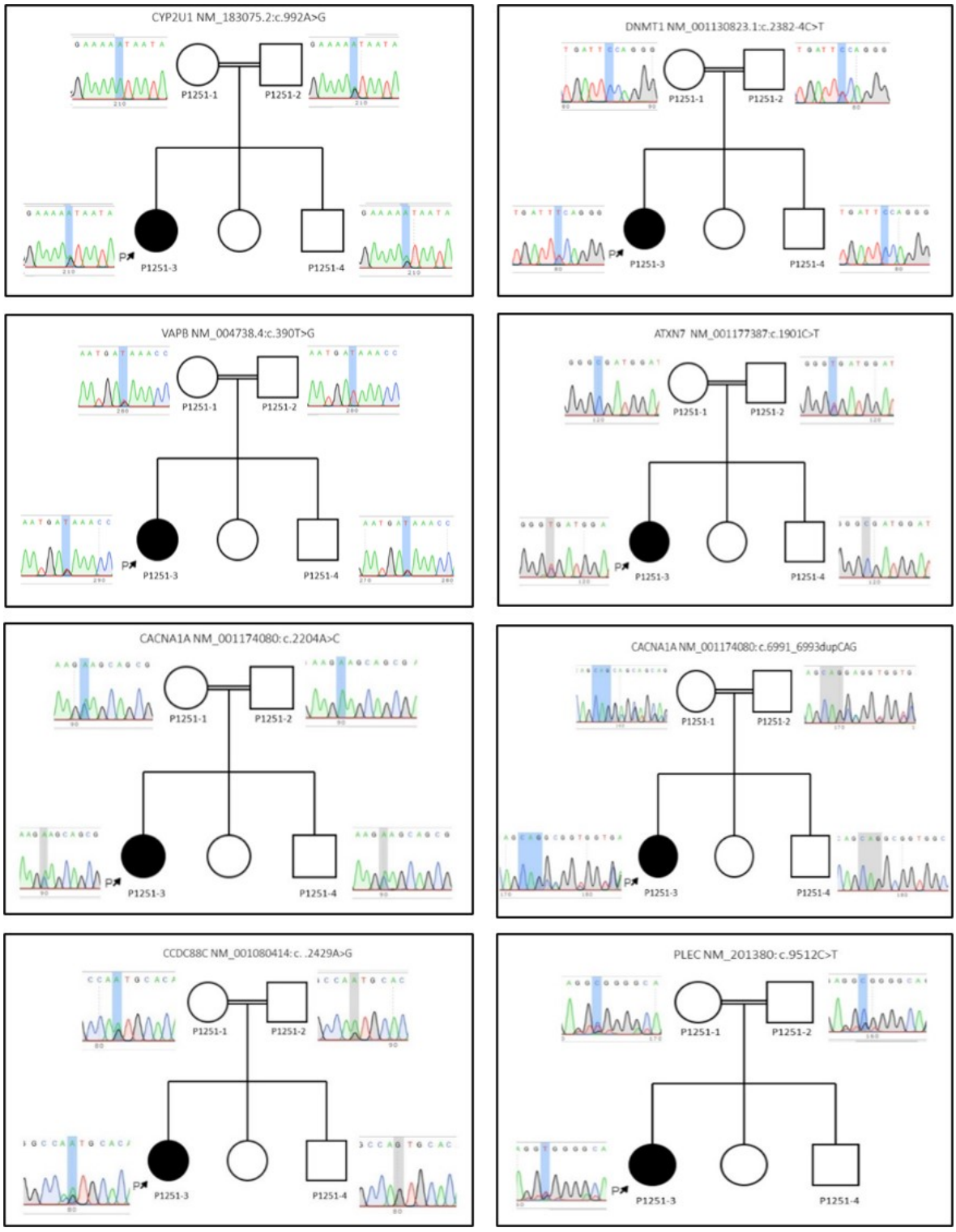

Figure A.25. Pedigree of family P1251 and Sanger chromatograms showing segregation of candidate novel variants in known IPN-related genes.

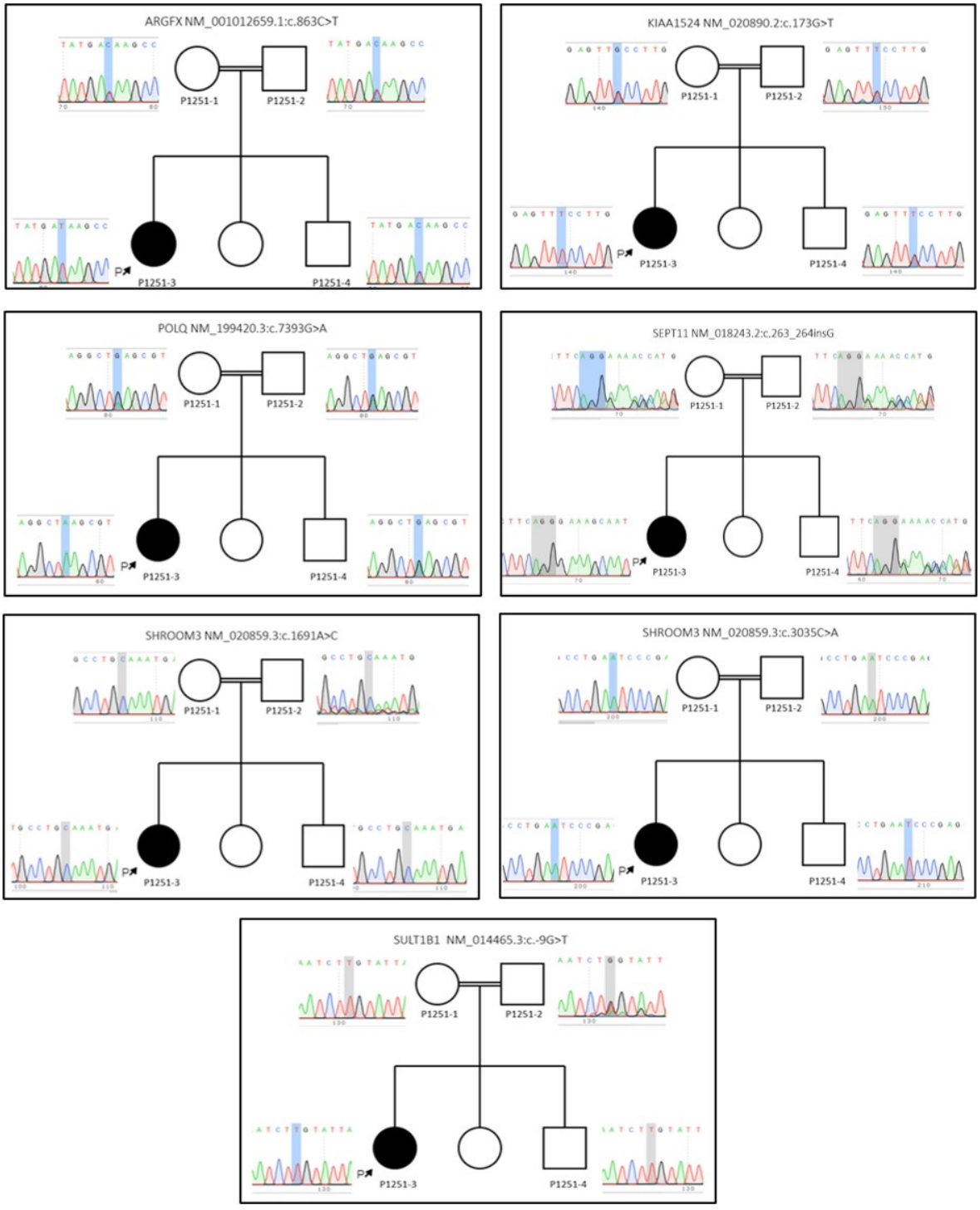

Figure A.26. Pedigree of family P1251 and Sanger chromatograms showing segregation of novel candidate gene variants.

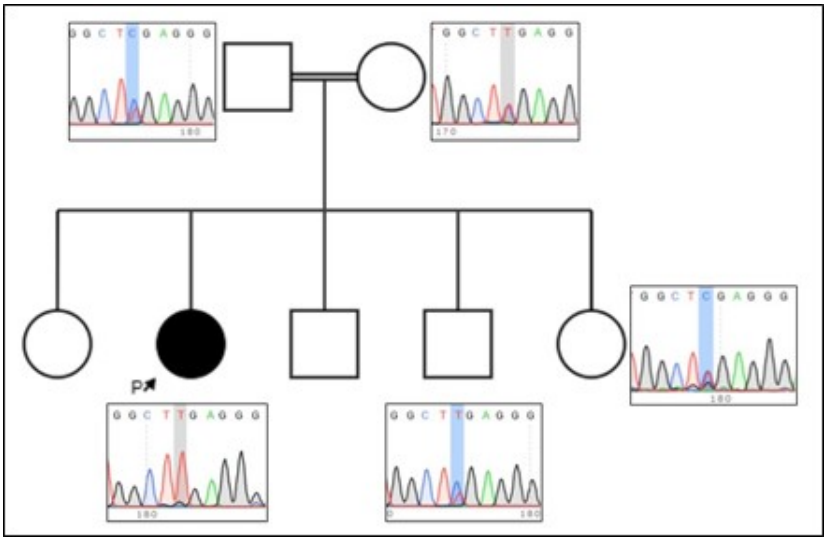

Figure A.27. Sanger chromatogram on pedigree of family P1255 showing the recurrent homozygous c.3208C>T, p.Arg1070Ter mutation in the *PRX* gene.

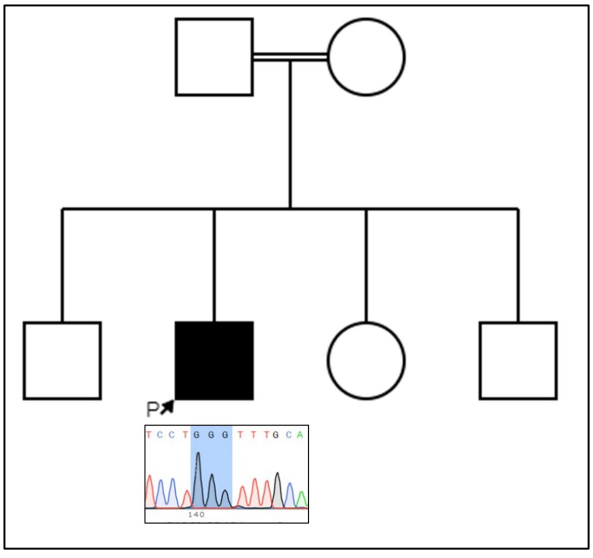

Figure A.28. Sanger chromatogram on pedigree of family P1262 showing the recurrent homozygous c.786delG; p.Phe263Leufs*22 mutation in the *GDAP1* gene.

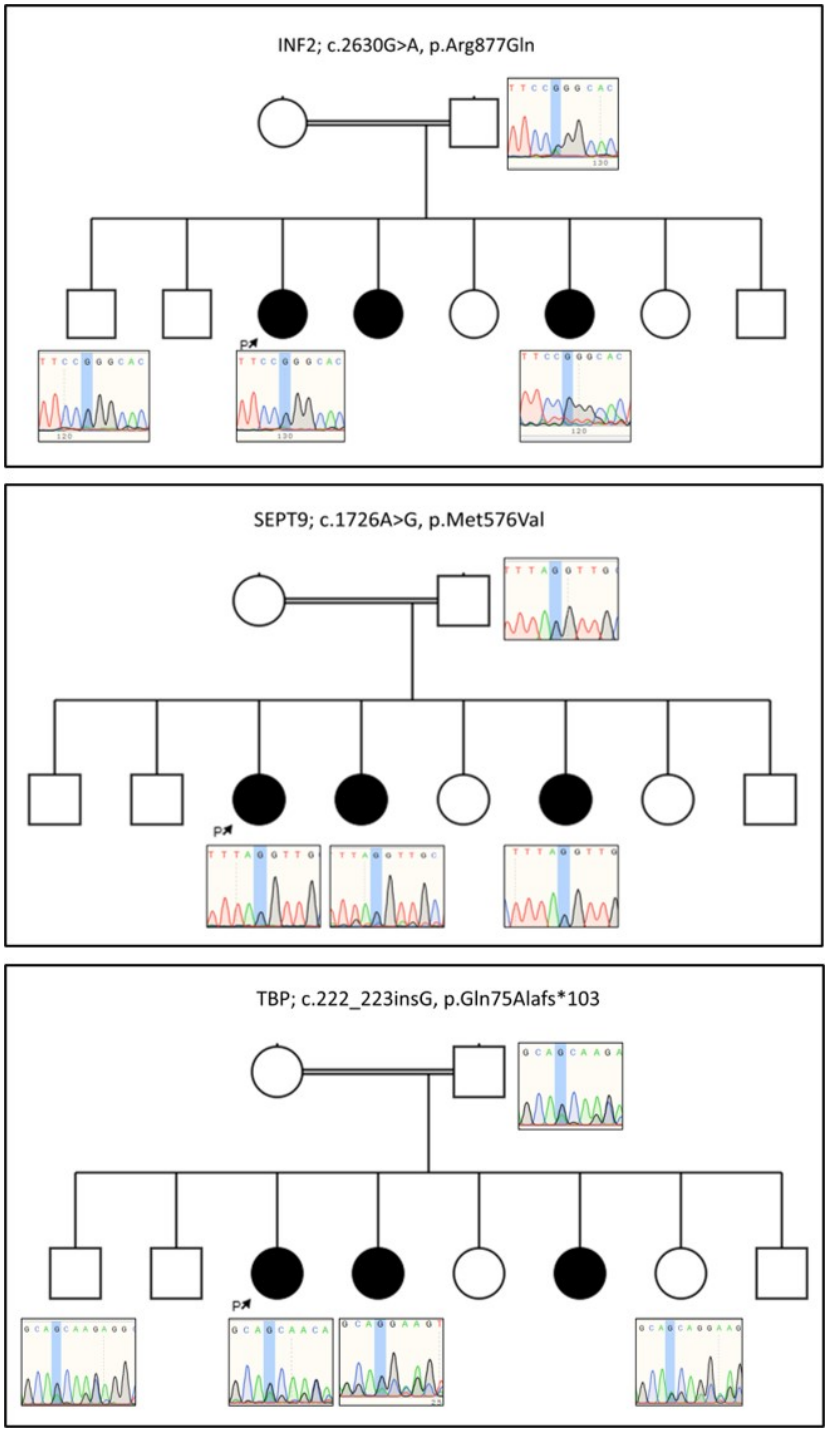

Figure A.29. Pedigree of family P1258 and Sanger chromatograms showing segregation of candidate novel variants in known IPN-related genes.

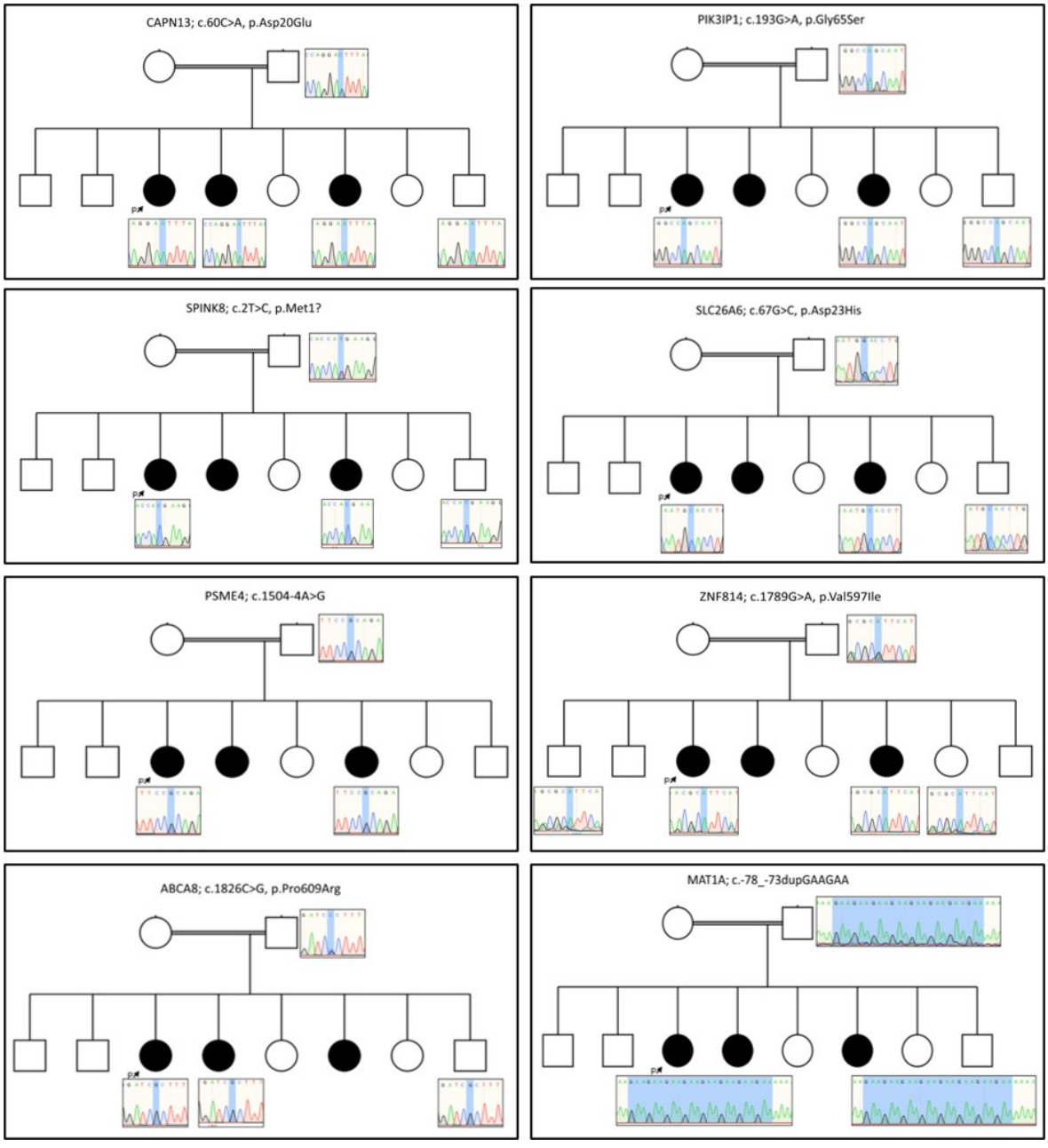

Figure A.30. Pedigree of family P1258 and Sanger chromatograms showing segregation of novel candidate gene variants.

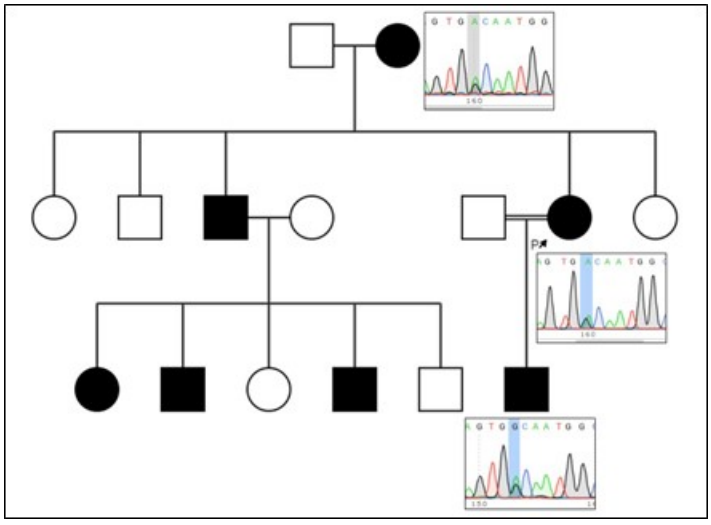

Figure A.31. Sanger chromatogram on pedigree of family P1267-3 showing the novel heterozygous c.362A>G, p.Asp121Gly variant in the *MPZ* gene.

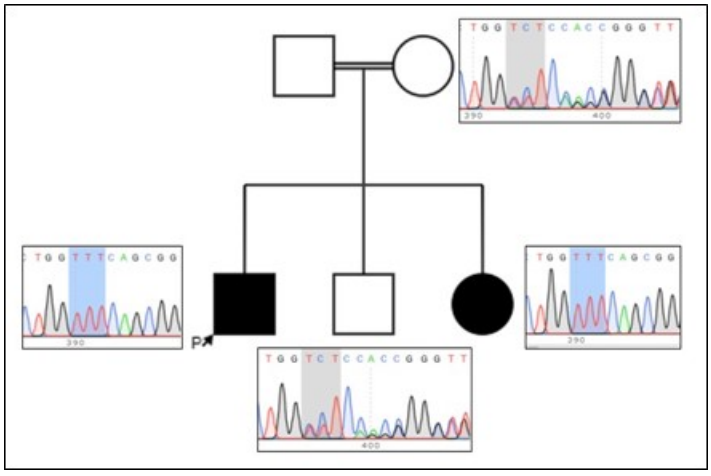

Figure A.32. Sanger chromatogram on pedigree of family P1289 showing the recurrent homozygous c.1894_1897delinsAAA, p.Glu632Lysfs*13 mutation in the *SH3TC2* gene.

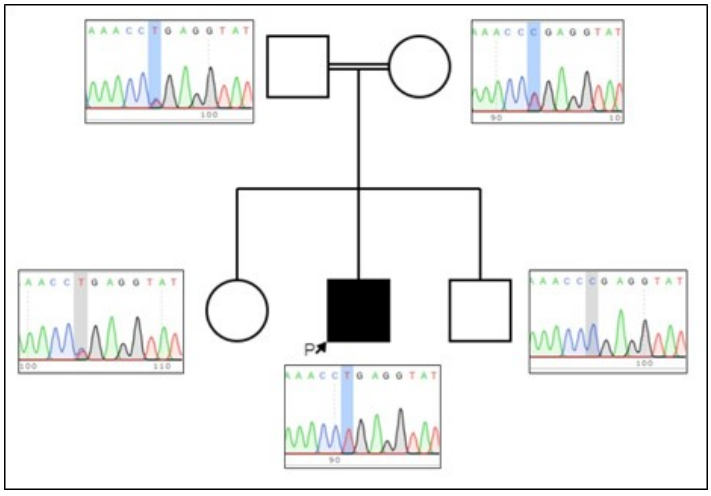

Figure A.33. Sanger chromatogram on pedigree of family P1291 showing the recurrent homozygous c.2182C>T, p.Arg728Ter mutation in the *SACS* gene.

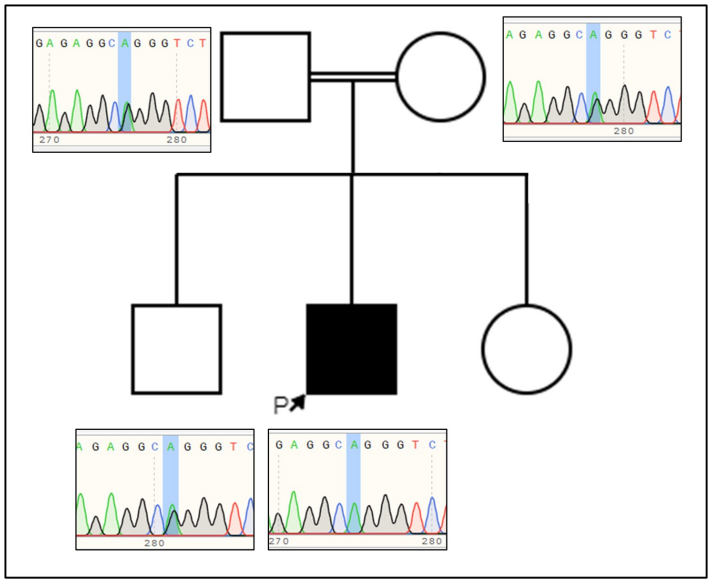

Figure A.34. Sanger chromatogram on pedigree of family P1306 showing the recurrent homozygous c.122G>A; p.Arg41Gln mutation in *MPV17* gene.

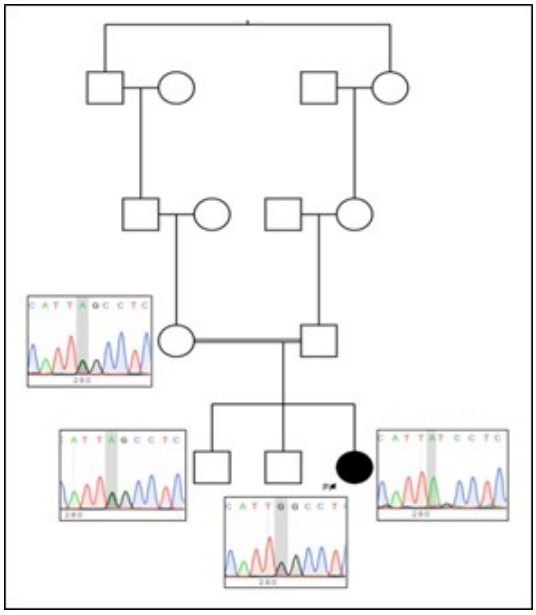

Figure A.35. Sanger chromatogram on pedigree of family P1319 showing the novel homozygous c.368G>A, p.Trp123Ter variant in the *HINT1* gene.

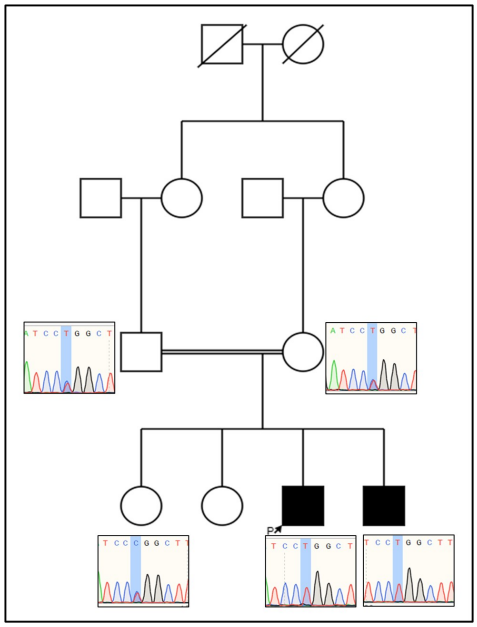

Figure A.36. Sanger chromatogram on pedigree of family P1325 showing the recurrent homozygous c.458C>T; p.Pro153Leu mutation in the *GDAP1* gene.

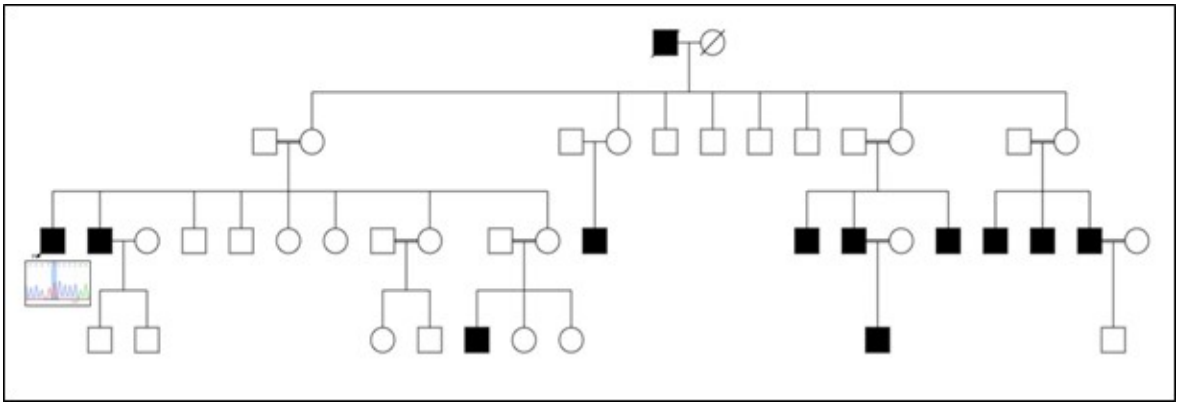

Figure A.37. Sanger chromatogram on pedigree of family P1330 showing the recurrent hemizygous c.518G>T, p.Cys173Phe mutation in the *GJB1* gene.

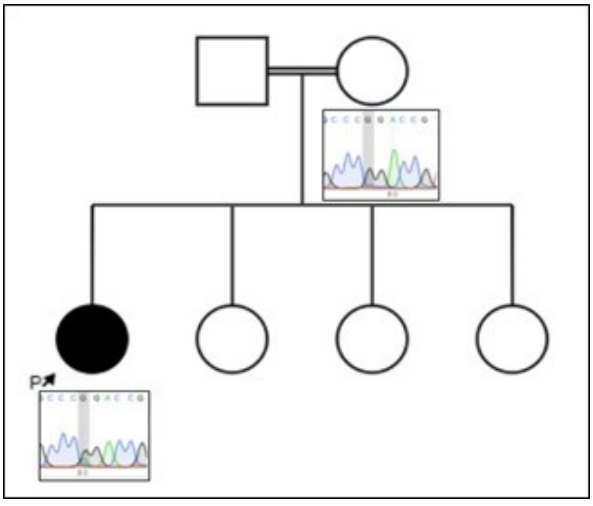

Figure A.38. Sanger chromatogram on pedigree of family P1331 showing the recurrent heterozygous c.1090C>T, p.Arg364Trp mutation in the *MFN2* gene.

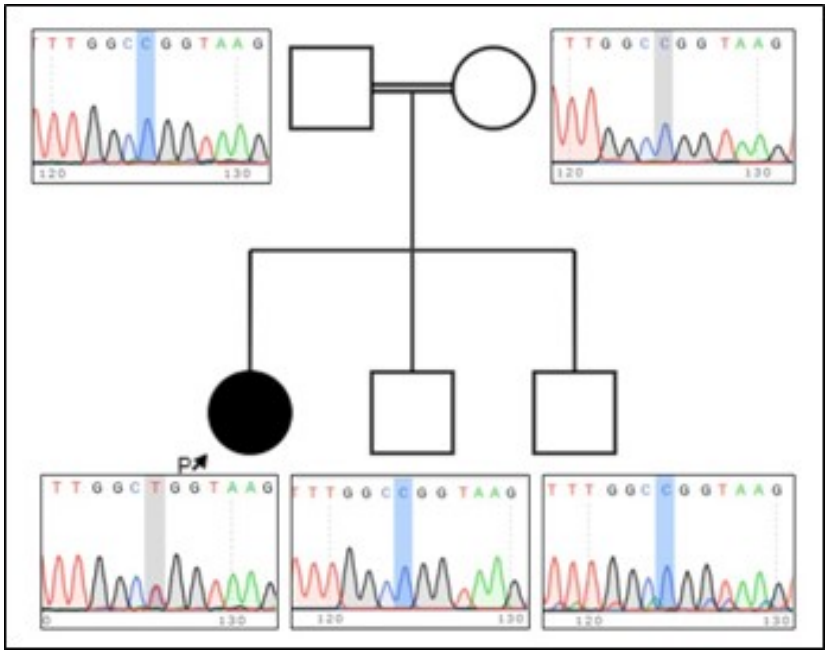

Figure A.39. Sanger chromatogram on pedigree of family P1333 showing the recurrent heterozygous c.310C>T, p.Arg104Trp mutation in the *MFN2* gene.

APPENDIX B: IN SILICO ANALYSES

Additional results of VMD analyses for the novel variant (c.3056G>A; p.Gly1019Asp) in *ATP8B3* gene in P1258 family are given below.

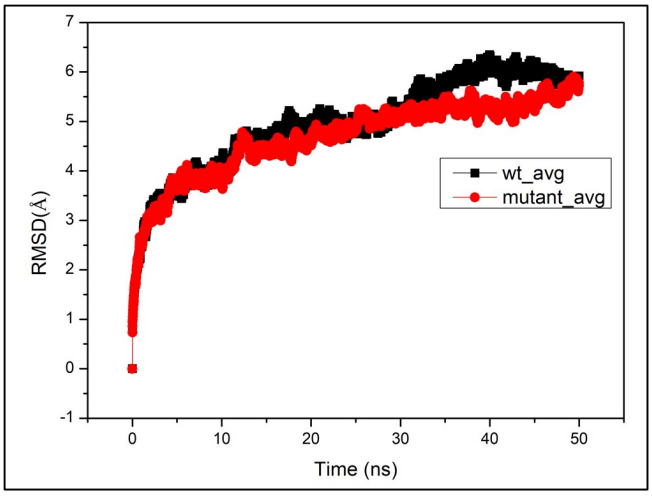

Figure B.1. Root-mean-square deviation of wild-type and mutant Atp8b3 for 50ns under normal cellular conditions indicating backbone mobility of the of the protein.

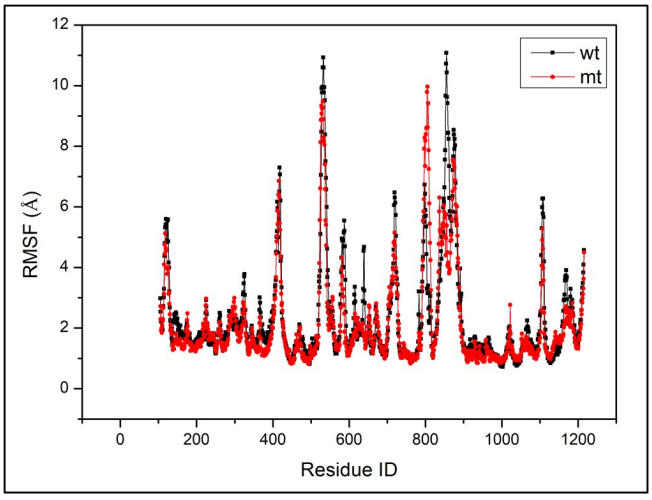

Figure B.2. Root mean square fluctuation of different amino acid residues in wild-type and mutant Atp8b3 indicating how much a residue contributes to molecular motion.

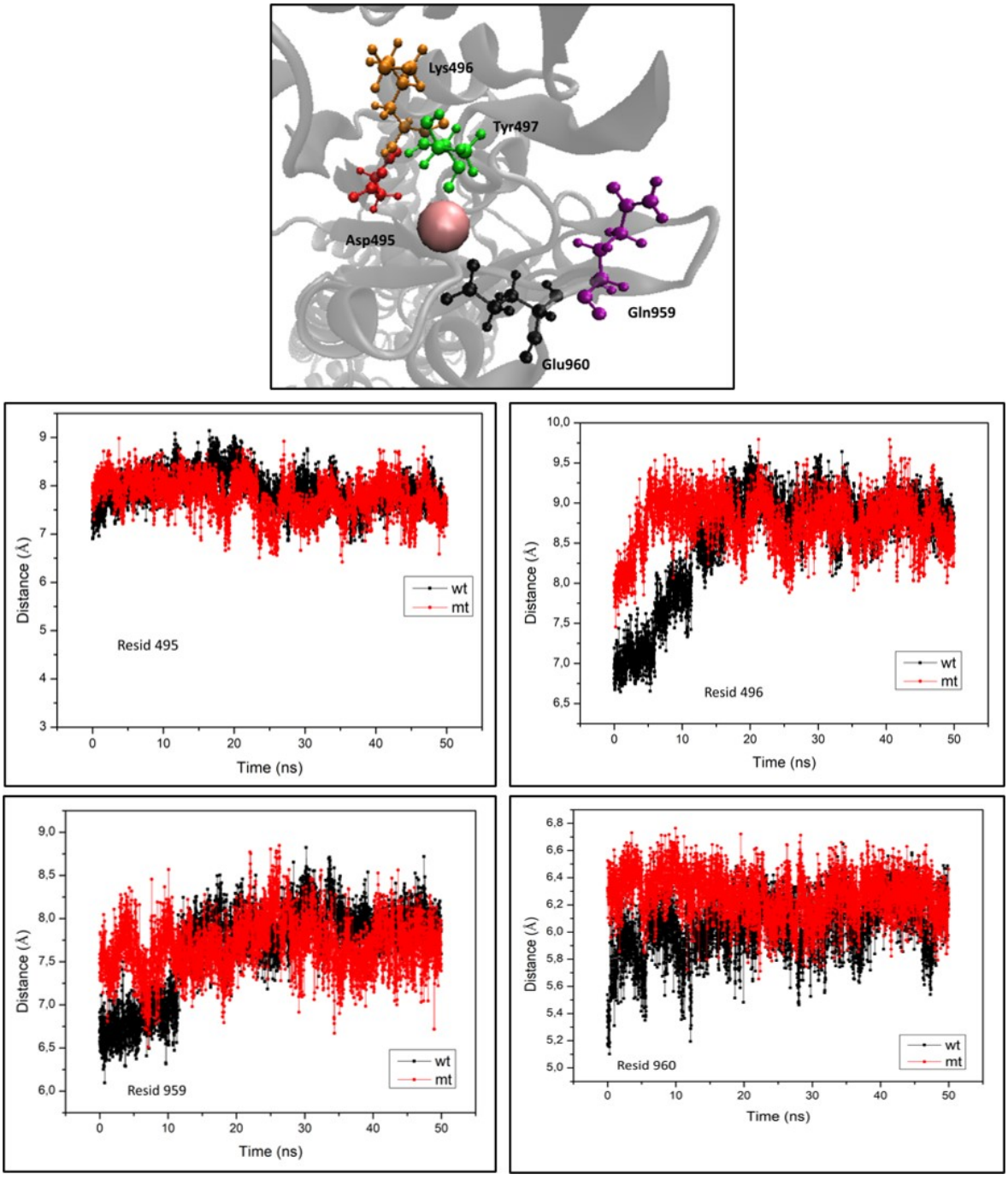

Figure B.3. The representative image for Mg^{+} coordinating residues in the protein structure (top panel) and individual investigation of these residues to the Mg^{+} atom in wild-type and mutant protein under normal cellular conditions (lower panels).

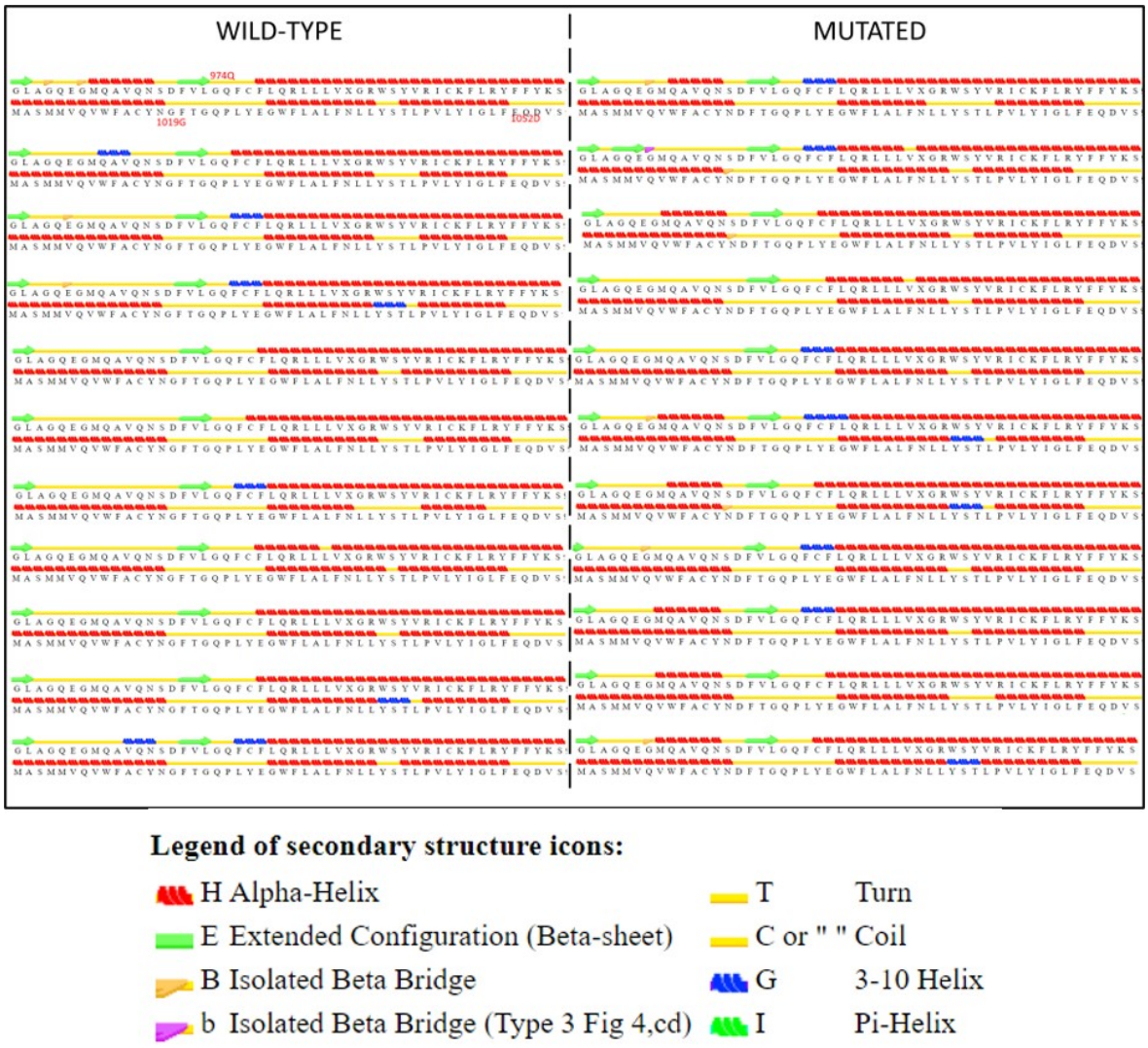

Figure B.4. STRIDE analysis for wild-type and mutant Atp8b3 for 50 ns under normal cellular conditions.

APPENDIX C: GENE PRIORITIZATION OUTCOMES

Candidate prioritization results from Endeavour algorithm are given below.

Table C.1. Gene prioritization analysis performed using the Endeavour algorithm.

Gene name	**SEPT11**	**KIAA1524**	**POLQ**	**ARGFX**
gene	ENSG0000-0138758	ENSG0000-0163507	ENSG0000-0051341	ENSG0000-0186103
rank	1	2	3	4
P-value	0.8222	0.9556	0.9778	1
Annotation UniProt	0.9333	0.8	0.9778	1
Text-mining	1	0.9767	0.9535	0
Annotation InterPro	0.7727	0.77275	0.7727	0.7727
Annotation Pfam	0.8837	0	0.8837	0.8837
Annotation SIMAP (localization)	0.3226	0.3226	0.3226	0
Annotation DrugBank	0	0	0	0
Annotation Stitch	0	0.8387	0.8387	0
Annotation RGD ChEBI	0.4091	0.3636	0.7273	0
Annotation Reactome	0	0	0	0
Annotation WikiPathways	0	0	0	0
Annotation RGD pathways	0	0	0	0
Annotation BioCarta	0	0	0	0

Table C.1. Gene prioritization analysis performed using the Endeavour algorithm. (cont.)

Gene name	**SEPT11**	**KIAA1524**	**POLQ**	**ARGFX**
Annotation CPDB	0.8519	0	0	0
Annotation hiPathDB	0	0	0.9474	0
Annotation GAD	0.7436	0	0.7436	0
Annotation OMIM	0	0	0	0
Annotation RGD MP	0	0.9091	0.9697	0
Annotation RGD RDO	0	0	0	0
Annotation PaGenBase	0.4667	0.4667	0.4667	1
Annotation CGAP	0.3182	0.9318	0.8182	0
Annotation GNF	0.2439	0.4146	0.3659	0.9512
Annotation eGenetics	0.3333	0.9524	0.8333	1
Annotation Aura	0.2727	0.0682	0.0227	0.9545
Annotation mirZ	0.1556	0.8222	0.8222	0.8222
Interaction String	0.9111	0.9111	0.8222	0.9111
Interaction BioGrid	0.9111	0.8889	0.9333	0.9778
Interaction I2D	0.8444	0.8222	0.9333	0.9333
Interaction IntAct	0.6667	0.6889	0.8444	0.8444
Interaction iRefIndex	0.8889	0.8889	0.9556	0.9556

Table C.1. Gene prioritization analysis performed using the Endeavour algorithm. (cont.)

Gene name	**SEPT11**	**KIAA1524**	**POLQ**	**ARGFX**
Interaction Mint	0.7556	0.7556	0.7556	0.7556
Interaction HPRD	0.8	0.8	0.8	0.8
Interaction MIPS	0.5778	0.5778	0.5778	0.5778
Interaction GeneRIF	0.9333	0.9111	0.9778	0.9778
Expression Su et al (2002)	0.7931	0	0	0
Expression Su et al (2004)	0.0833	0	0.4167	0
Expression CMAP	0.75	0	0.6944	0
Blast	0.9333	0.9778	0.9778	0.9778
Precalculated Ouzounis	0.5122	0.9024	0.4878	0
Precalculated Prospectr	0.0227	0.8864	0.6818	1
Precalculated HaploPred	0.5	0.7045	0.5455	1

Candidate prioritization results from ToppGene algorithm are given below.

Table C.2. Gene prioritization analysis performed using the ToppGene algorithm.

Gene Symbol	**KIAA1524**	**SEPT11**	**POLQ**	**ARGFX**
Rank	1	2	3	4
Overall p-Value	0.0313	0.0331	0.0643	0.3153
Average Score	0.2919	0.4653	0.1599	0.0413
GeneID	57650	55752	10721	503582
GO: Molecular Function Score	0	0	0.1183	0

Table C.2. Gene prioritization analysis performed using the ToppGene algorithm. (cont.)

Gene Symbol	**KIAA1524**	**SEPT11**	**POLQ**	**ARGFX**
GO: Molecular Function p-Value	0.5473	0.5473	0.0443	0.5473
GO: Biological Process Score	0.0194	0.2126	0.4202	0.01939
GO: Biological Process p-Value	0.1462	0.1071	0.0804	0.1462
GO: Cellular Component Score	0.3339	0.8052	0.2816	0.1459
GO: Cellular Component p-Value	0.1042	0.02905	0.14169	0.1824
Human Phenotype Score	-1	-1	-1	-1
Human Phenotype p-Value	0	0	0	0
Mouse Phenotype Score	0.01	-1	0.01	-1
Mouse Phenotype p-Value	0.0655	0	0.0655	0
Pathway Score	-1	0	0	-1
Pathway p-Value	0	0.5009	0.5009	0
Pubmed Score	0.9959	0.9867	0.2892	0
Pubmed p-Value	0.0292	0.0389	0.1787	0.6003
Disease Score	0.3921	0.7874	0	-1
Disease p-Value	0.06	0.0337	0.5445	0

APPENDIX D: QUANTITATIVE PCR RESULTS

Cq results of qPCR analysis for family P1251 is given below.

Table D.1. Cq values and calculations performed using the ΔΔCq method for the genes studied in qPCR analysis for family P1251.

	Gene name	Average Cq		Cq geometric mean		ΔΔCq	Fold change ($2^{-\Delta\Delta Cq}$)	Log2-fold change
		Control	P1251	Control	P1251			
Reference	ACTB	13,51	13,92	15,88	16,04			
	GAPDH	14,88	15,19	ΔCq				
	SDHA	19,94	19,54	Control	P1251			
Experiment	SEPT2	20,78	21,86	4,90	5,82	0,92	0,53	-0,92
	SEPT5	25,76	23,48	9,88	7,44	-2,44	5,43	2,44
	SEPT6	24,24	21,81	8,35	5,77	-2,58	6,00	2,58
	SEPT7	18,67	18,45	2,78	2,41	-0,37	1,30	0,37
	SEPT8	21,36	21,74	5,47	5,70	0,22	0,86	-0,22
	SEPT9	20,08	19,37	4,19	3,33	-0,86	1,82	0,86
	SEPT10	20,52	19,76	4,63	3,71	-0,92	1,89	0,92
	SEPT11	21,38	23,35	5,50	7,31	1,81	0,29	-1,81

APPENDIX E: ADDITIONAL CONFOCAL IMAGES

Additional confocal microscopy images for the candidate *SEPT11* gene expression are given below.

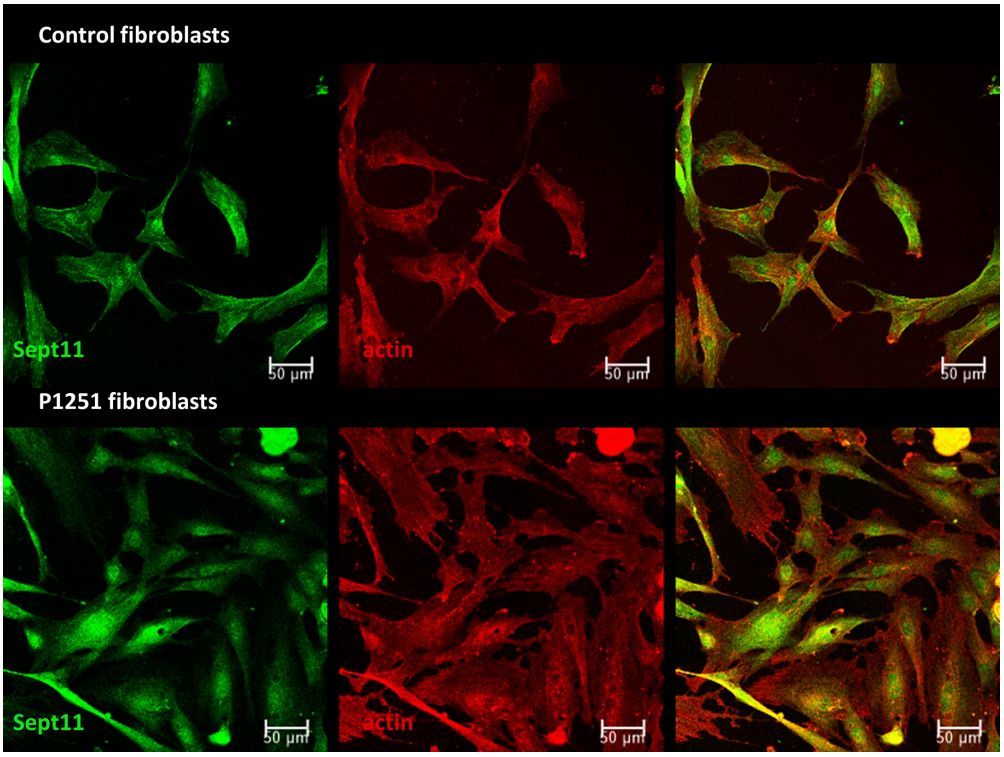

Figure E.1. Confocal microscopy images of control and P1251 primary fibroblasts after antibody staining of Sept11 and F-actin.

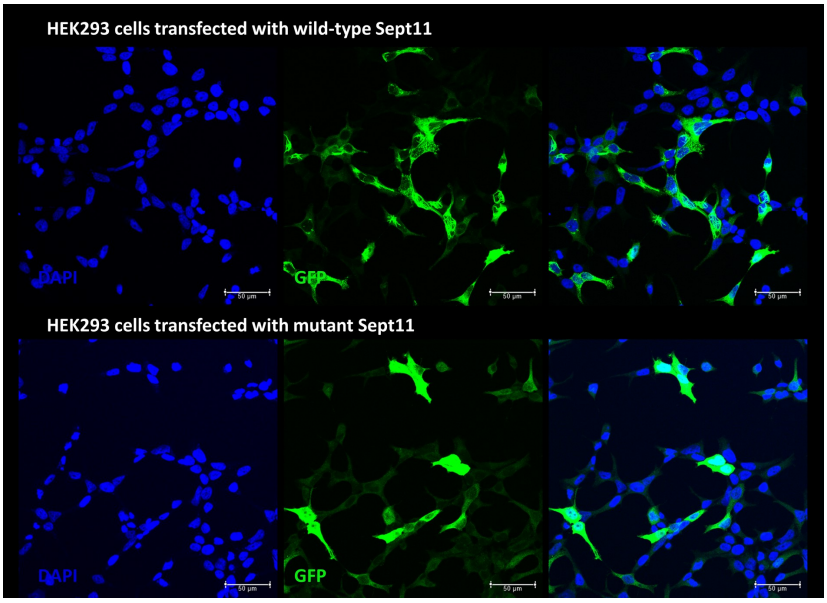

Figure E.2. Confocal microscopy images of HEK293 cells overexpressing wild-type and mutant Sept11 tagged with a GFP signal at the C-terminal.

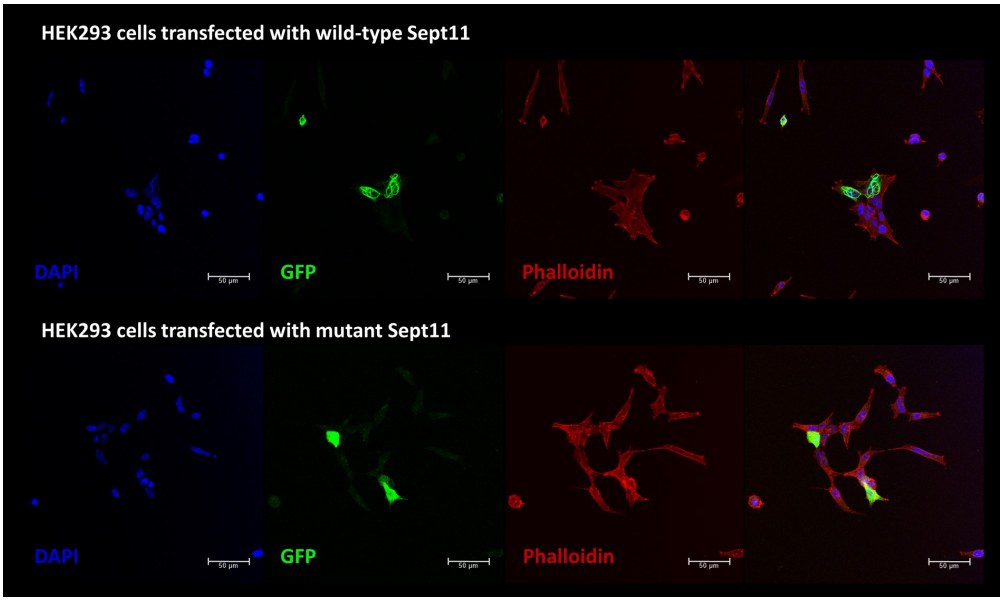

Figure E.3. Confocal microscopy images of HEK293 cells overexpressing wild-type and mutant Sept11 tagged with a GFP signal at the C-terminal. The cells are co-stained for F-actin.

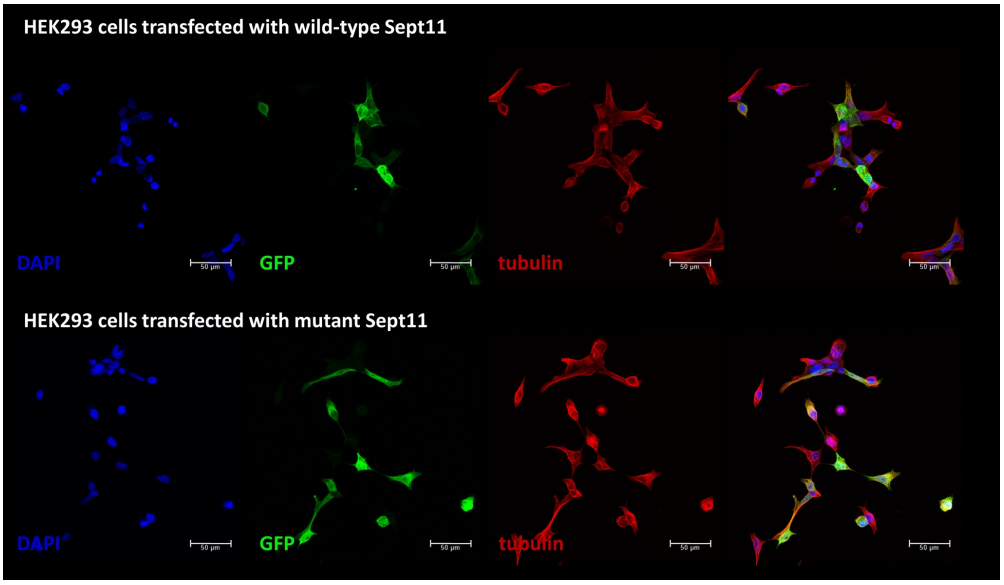

Figure E.4. Confocal microscopy images of HEK293 cells overexpressing wild-type and mutant Sept11 tagged with a GFP signal at the C-terminal. The cells are co-stained for α-tubulin.

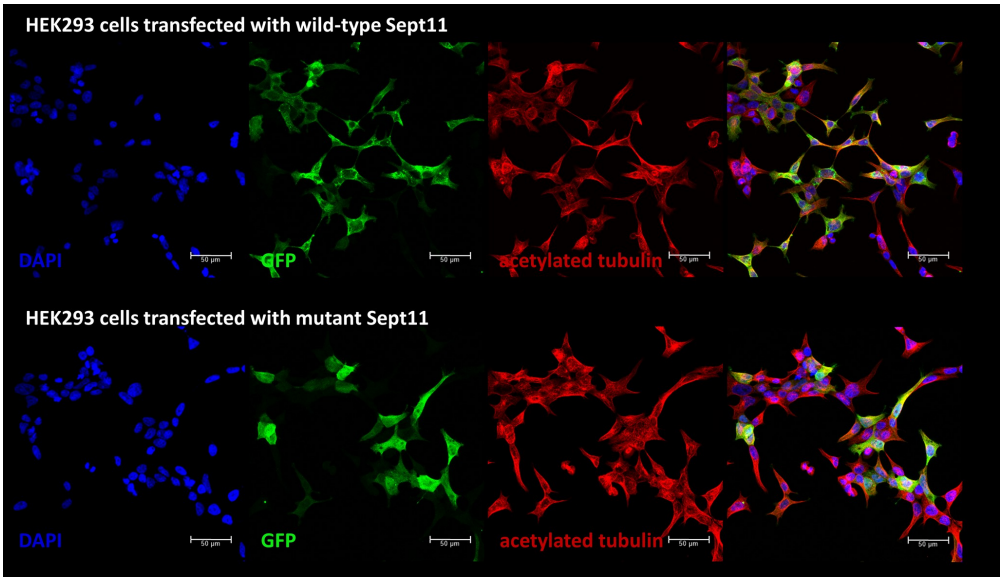

Figure E.5. Confocal microscopy images of HEK293 cells overexpressing wild-type and mutant Sept11 tagged with a GFP signal at the C-terminal. The cells are co-stained for acetylated tubulin.

APPENDIX F: PERMISSIONS FOR RE-USED FIGURES

Figure 1.2 and Figure 1.3 in this study have been re-used from publications in Nature Reviews Neurology Journal. Official permissions to reuse these images have been obtained from the publisher and the licencing documents are given below.

11.08.2021 RightsLink Printable License

SPRINGER NATURE LICENSE
TERMS AND CONDITIONS

Aug 11, 2021

This Agreement between Dr. Ayse Candayan ("You") and Springer Nature ("Springer Nature") consists of your license details and the terms and conditions provided by Springer Nature and Copyright Clearance Center.

License Number	5125810037247
License date	Aug 11, 2021
Licensed Content Publisher	Springer Nature
Licensed Content Publication	Nature Reviews Neurology
Licensed Content Title	Clinical implications of genetic advances in Charcot–Marie–Tooth disease
Licensed Content Author	Alexander M. Rossor et al
Licensed Content Date	Sep 10, 2013
Type of Use	Thesis/Dissertation
Requestor type	academic/university or research institute
Format	print and electronic
Portion	figures/tables/illustrations
Number of figures/tables/illustrations	1
High-res required	no
Will you be translating?	no
Circulation/distribution	1 - 29
Author of this Springer Nature content	no
Title	Investigation of novel recessive CMT genes/alleles
Institution name	Bogazici University
Expected presentation date	Aug 2021
Order reference number	rossor2013
Portions	Figure 3
Requestor Location	Dr. Ayse Candayan Bogazici Universitesi Molekuler Biyoloji ve Genetik Bolumu Bebek Istanbul, Turkey 34342 Turkey Attn: Bogazici University
Total	0.00 USD

Figure F.1. Permission obtained from the publisher for the re-use of a figure from Rossor *et al.*, 2013.

11.08.2021 RightsLink Printable License

SPRINGER NATURE LICENSE
TERMS AND CONDITIONS

Aug 11, 2021

This Agreement between Dr. Ayse Candayan ("You") and Springer Nature ("Springer Nature") consists of your license details and the terms and conditions provided by Springer Nature and Copyright Clearance Center.

License Number	5125810310995
License date	Aug 11, 2021
Licensed Content Publisher	Springer Nature
Licensed Content Publication	Nature Clinical Practice Neurology
Licensed Content Title	Mechanisms of Disease: inherited demyelinating neuropathies—from basic to clinical research
Licensed Content Author	Klaus-Armin Nave et al
Licensed Content Date	Dec 31, 1969
Type of Use	Thesis/Dissertation
Requestor type	academic/university or research institute
Format	print and electronic
Portion	figures/tables/illustrations
Number of figures/tables/illustrations	1
Will you be translating?	no
Circulation/distribution	1 - 29
Author of this Springer Nature content	no
Title	Investigation of novel recessive CMT genes/alleles
Institution name	Bogazici University
Expected presentation date	Aug 2021
Order reference number	nave2007
Portions	Figure 1
Requestor Location	Dr. Ayse Candayan Bogazici Universitesi Molekuler Biyoloji ve Genetik Bolumu Bebek Istanbul, Turkey 34342 Turkey Attn: Bogazici University
Total	0.00 USD

Figure F.2. Permission obtained from the publisher for the re-use of a figure from Nave *et al.*, 2007.